# Matrix models and eigenfunctions from the Topological String/Spectral Theory correspondence

Zakany, Szabolcs

Université de Genève
Section de Physique

Faculté des Sciences
Professeur Marcos Mariño Beiras

# Matrix models and eigenfunctions from the Topological String/Spectral Theory correspondence

Thèse

présentée à la Faculté des Sciences de l'Université de Genève
pour obtenir le grade de
Docteur ès sciences, mention physique

par

Szabolcs Zakany

de

Genève (GE)

Thèse N° 5303

Ateliers d'impression de l'Université de Genève
Février 2019

UNIVERSITÉ DE GENÈVE

FACULTÉ DES SCIENCES

DOCTORAT ÈS SCIENCES, MENTION PHYSIQUE

**Thèse de Monsieur Szabolcs ZAKANY**

intitulée :

**«Matrix Models and Eigenfunctions from the Topological String/Spectral Theory Correspondence»**

La Faculté des sciences, sur le préavis de Monsieur M. MARIÑO BEIRAS, professeur ordinaire et directeur de thèse (Département de physique théorique), Monsieur P. WITTWER, professeur titulaire (Département de physique théorique), Monsieur A.-K. KASHANI-POOR, professeur (Laboratoire de physique théorique, Ecole Normale Supérieure, Paris, France), autorise l'impression de la présente thèse, sans exprimer d'opinion sur les propositions qui y sont énoncées.

Genève, le 29 janvier 2019

**Thèse - 5303 -**

**Le Doyen**

N.B. - La thèse doit porter la déclaration précédente et remplir les conditions énumérées dans les "Informations relatives aux thèses de doctorat à l'Université de Genève".

## Abstract

The Topological String/Spectral Theory (TS/ST) correspondence was introduced as a sharp, non-perturbative relationship between topological strings on toric Calabi–Yau threefolds on one side, and the spectral theory of operators given by the quantized mirror curve on the other side. It predicts a non-trivial relationship between enumerative invariants of the toric Calabi–Yau threefold and spectral quantities of the corresponding operator. This work explores three consequences and extensions of the TS/ST correspondence. First, we show that the TS/ST correspondence implies a new realization of the topological string as convergent matrix models. Second, we propose an extension of the TS/ST correspondence involving the open sector of topological strings on the TS side and the eigenfunctions of the operator on the ST side. Third, we investigate how the TS/ST correspondence and its interpretation in terms of a non-interacting Fermi gas can help us defining a sensible notion of "quantum curve".

## Acknowledgements

No part of this work could have been possible without the incredible support and help of my doctoral advisor Marcos Mariño. Each and every meeting with him was for me a source of new motivation and intellectual progress, but also an extremely pleasant time.

I also address my many thanks to my PhD colleagues, who were there when I started this adventure. To Alba Grassi, who always had time for all the questions of a novice like me. To Santiago Codesido, who did never hesitate to embark in thrilling discussions, ranging from the most abstract ideas (related to physics or not) to the tiniest technicalities of a computation.

Many thanks also to Johan Källén, Yasuyuki Hatsuda, Massimiliano Ronzani, Yoan Emery and Tomas Reis, all my other colleagues during the years, with whom I had many interesting and helpful discussions.

I would like to extend my thanks to Kazumi Okuyama, Rinat Kashaev and Antonio Sciarappa, with whom I had the chance and pleasure to collaborate.

Finally I would like to thank my wonderful family and my loving wife for all the support during these years.

## Remerciements

Ce travail n'aurait aucunement été possible sans l'aide et le soutient extraordinaire de mon directeur de thèse Marcos Mariño. Chacune des réunions et discussions avec lui ont été pour moi une nouvelle source de motivation et de progrès intellectuel, mais aussi un très bon moment passé en sa compagnie.

J'adresse également mes remerciements à mes collègues de doctorat qui étaient présents lors du début de cette aventure. À Alba Grassi, qui avait toujours du temps pour les questions d'un novice comme moi. À Santiago Codesido, toujours prêt à s'embarquer dans des discussions passionnantes, allant des idées les plus abstraites (en lien avec la physique ou pas) aux détails techniques les plus pointues.

Mes remerciements également à Johan Källén, Yasuyuki Hatsuda, Massimiliano Ronzani, Yoan Emery et Tomas Reis, tous mes autres collègues pendant mes années de doctorats, qui ont pu m'aider et avec qui j'ai partagé de nombreuses discussions intéressantes.

Je souhaite remercier Kazumi Okuyama, Rinat Kashaev et Antonio Sciarappa, avec qui j'ai eu la chance et le plaisir de collaborer.

Finalement, j'aimerais remercier ma famille merveilleuse et ma tendre épouse pour tout le soutient pendant ces années.

## Résumé en français

La théorie des cordes est une construction en physique théorique qui a amené des idées fructueuses dans divers branches des mathématiques. Elle reste pourtant plutôt mal comprise à bien des égards. Une version simplifiée, appelée la théorie des cordes topologiques, est une arène de choix pour mieux comprendre certains aspects de la théorie des cordes.

Durant ces dernières années, une correspondance conjecturale a été formulée et étudiée, reliant la théorie des cordes topologiques et la théorie spectrale d'opérateurs agissant sur des fonctions $L^2(\mathbb{R})$. Elle a été proposée pour la première fois par Hatsuda, Grassi et Marino (2014), et est souvent nommée la correspondance TS/ST (Topological Strings / Spectral Theory). C'est une conjecture précise et testable, qui relie certaines fonctions génératrices d'invariants énumérgatifs associés à la géométrie $X$ à des invariants spectraux. Les fonctions génératrices sont les énergies libres de la théorie des cordes sur $X$, où $X$ est un Calabi–Yau torique. Les invariants spectraux quant à eux, sont encodés dans le déterminant spectral d'un opérateur $\rho$ de la classe trace, qui est directement construit à partir de la géometrie $X$ via la symmétrie miroir. Son inverse est un opérateur de différences finies. La conjecture TS/ST permet de calculer le spectre de $\rho$ en utilisant les invariants énumératifs données par les cordes topologiques. De plus, la théorie spectrale de l'opérateur fournit une définition non-perturbative de l'énergie libre de la corde topologique, qui était originellement définie perturbativement en $g_s$, la constant de couplage de la corde.

La présente thèse propose et investigue trois extensions et conséquences de la correspondance TS/ST, en fournissant de nombreux tests. Ces extensions jettent de la lumière à la fois sur le côté théorie des cordes topologiques et sur le côté théorie spectrale.

Le premier aspect étudié dans cette thèse est une conséquence de la correspondance TS/ST. Nous montrons en détail comment cette conjecture prédit l'existence d'une famille de modèles de matrices associés aux cordes topologiques sur les espaces de Calabi–Yau toriques. Ces modèles de matrices ont plusieures propriétés intéressantes : elles sont convergentes, la relation entre les modèles de matrices et les cordes topologiques est non-triviale, et les cordes topologiques émergent dans la limite des larges matrices, la taille $N$ des matrices étant directement reliée à un paramètre plat sur l'espace des moduli de la géometrie $X$. Concrètement, la série perturbative des énergies libre émerge des modèles de matrices dans une limite asymptotique similaire à la limite de 't Hooft. Nous performons des calculs détaillés dans plusieurs exemples concrets des deux côtés de le correspondance. Ces tests sont effectués d'abord dans la limite de faible couplage de 't Hooft par des calculs directs.

Ensuite, nous montrons comment résoudre le modèle de matrice exactement dans la limite planaire, ce qui permet d'effectuer des tests dans la limite de fort couplage de 't Hooft. Au passage, nous montrons dans plusieurs cas que la courbe spectrale du modèle de matrice est la courbe miroir de $X$.

Le deuxième aspect étudié dans cette thèse est une extension de la correspondance TS/ST. Nous proposons une extension de la conjecture, qui relie les amplitudes de la corde ouverte (du côté cordes topologiques) aux fonctions d'ondes de l'opérateur $\rho$ (du côté spectral). Plus précisément, nous conjecturons que les fonctions d'ondes généralisées de $\rho$ peuvent être construites à partir de la fonction d'onde WKB re-sommée, supplémentée de la "fonction d'onde topologique", qui est un cas particulier des amplitudes de la corde ouverte. Nous commençons par définir et étudier les fonctions d'ondes généralisées du côté de la théorie spectrale Le résultat permet de formuler la conjecture précise. Le calcul se focalise sur un cas particulier, duquel nous extrapolons la conjecture à tous les cas où $X$ est un Calabi–Yau toriques. La conjecture est ensuite vérifiée dans divers cas en comparant ses prédictions à des calculs directs, numériques et analytiques. En particulier, dans le cas nommé "auto-dual", les fonctions d'ondes généralisés peuvent être écrites exactement en forme close grâce à la conjecture. Ensuite, nous commentons un lien possible entre les caractéristiques analytiques de nos fonctions d'ondes généralisées, et la quantification de certains systèmes intégrables correspondants. Finalement, nous proposons une manière alternative de construire le sous-ensemble des fonctions d'ondes généralisées qui est appropriée dans le contexte de ces systèmes intégrables.

Le troisième aspect qui est commencé à être étudié dans ce travail est la notion de "courbe quantique" qui émerge de la correspondance TS/ST. Dans cette correspondance, l'opérateur $\rho$ est essentiellement construit en "quantifiant" d'une manière appropriée la courbe miroir de la géométrie $X$. Semi-classiquement, l'intuition physique pointe vers une notion de courbe quantique qui serait une distribution quantique avec les propriétés suivantes : son support se réduit à la courbe mirroir dans une limite classique appropriée, et elle présente des fluctuations quantiques dans le régime semi-classique. En utilisant l'interprétation de la conjecture TS/ST en terme de gaz de $N$ fermions non-interagissantes, nous proposons un observable statistique qui est une bonne notion de courbe quantique. Nous vérifions dans plusieurs cas que cette distribution de quasi-probabilité se réduit à une fonction "échelon" avec support à l'intérieur de la courbe miroir, et que les fluctuations semi-classiques ont une forme bien connue. Ici, la limite "classique" appropriée est une limite de double échelle, où la constante de Planck du gaz grandit avec le nombre $N$ de fermions. Ceci n'est pas la limite classique standard du point de vue du gaz.

# Contents


**1 Introduction** **1**

**2 From mirror symmetry to spectral problems** **7**

2.1 Topological strings . . . . . 7

2.2 The A–model . . . . . 13

2.3 The B–model and the mirror geometry . . . . . 17

2.4 Refinement and quantum periods . . . . . 21

**3 Quantized mirror curves and the TS/ST correspondence** **25**

3.1 Spectral theory of quantized mirror curves . . . . . 25

3.2 Direct numerical computations . . . . . 33

3.3 The TS/ST correspondence . . . . . 34

3.4 Explicit integral kernels . . . . . 38

**4 Matrix models and topological strings** **47**

4.1 Deriving the matrix models . . . . . 48

4.2 The TS/ST correspondence in the 't Hooft limit . . . . . 50

4.3 Checks at weak coupling . . . . . 55

4.4 Exact planar results, spectral curve and checks at strong coupling . . 77

**5 Eigenfunctions and the open topological string** **103**

5.1 Eigenfunctions from spectral theory . . . . . 105

5.2 An application: eigenfunctions for local $\mathbb{P}^1 \times \mathbb{P}^1$ with $m_{\mathbb{F}_0} = 1$ . . . . 112

5.3 The 't Hooft limit of the eigenfunctions . . . . . 118

5.4 TS/ST conjecture for eigenfunctions . . . . . 132

5.5 Checking the conjecture for the self-dual case . . . . . 136

5.6 A comment on integrability . . . . . 161

5.7 Partial checks away from the self-dual case . . . . . 167

5.8 Fully on-shell eigenfunctions from resummed WKB . . . . . 173

**6 Quantum curves as quantum distributions** **199**

6.1 Classical and quantum geometry in Fermi gases . . . . . 201

6.2 A simple example: the harmonic oscillator . . . . . 210

6.3 The quantum geometry for mirror curves . . . . . 217

6.4 Semiclassical distribution for symmetric local $\mathbb{P}^1 \times \mathbb{P}^1$ . . . . . 231

**7 Concluding remarks** **239**

**Bibliography** **243**

# Chapter 1

# Introduction

*Can one hear the shape of a drum?* This is the title of the famous 1966 paper [1], in which Mark Kac investigates the relationship between the eigenvalues of the two dimensional Laplacian with given boundary conditions (the tones that one hears) to the shape of the boundary (the shape of the drum). The answer to the question turns out to be "no" – many families of isospectral shapes have been since constructed. However, one can still hear several geometric and topological properties of the drum. That is, the spectrum of the Laplacian operator with the specific boundary conditions given by the drum contains much geometric and topological information about its shape. For example, as suggested by Kac in [1], the eigenvalues $\{\lambda_n\}_{n=0}^{\infty}$ of the Laplacian obey the following asymptotics at large auxiliary parameter $t$:

$$\sum_{n=0}^{\infty} \mathrm{e}^{-t\lambda_n} \sim \frac{A}{2\pi t} - \frac{P}{4}\frac{1}{\sqrt{2\pi t}} + \frac{1}{6}(1-h). \tag{1.1}$$

In this equation, $A$ is the area inside the shape, $P$ is its perimeter and $h$ is the number of holes in it. The first two quantities are geometric data about the shape, while the third is a topological property. They are entirely encoded in the spectrum of the operator, which is just a discrete set of numbers. The first two leading contributions of this asymptotic formula were actually rigourosly derived by mathematicians before Kac's paper. The first term is equivalent to Hermann Weyl's law for the asymptotics of the eigenvalues of the Laplacian, while the second term was obtained by Åke Pleijel, a former PhD student of T. Carleman. The last term was derived by Kac by approximating the shape by a polygon, and taking the smooth limit – quite a physicist's approach! What is the connection of this result with the present thesis? Not much, strictly speaking. Except maybe the following aspects: we will be interested in a sharp relationship between the spectral theory of a family of operators ($\sim$ the tones) and the topological invariants of a corresponding fam-

ily of geometries ($\sim$ the drums). Also, we will adopt a very physical approach to this rather mathematical problem. No theorems, only conjectures, and arguments on the physical level of rigour, accompanied with down-to-earth "experimental" – numerical or analytical – tests in a case-by-case approach.

Various interesting interplays between geometry and spectral theory have turned up in several areas of research. These range from the relatively simple problem stated above, through for example the Atiyah–Singer index theorem, and up to the very sophisticated idea of holography in quantum gravity. In its most popular incarnation called the AdS/CFT correspondence, the idea of holography posits that gravity in an asymptotically anti–De Sitter space-time (a very geometric theory) corresponds to a conformal quantum field theory on its boundary (which in some sense may be seen as a very complicated spectral theory), in a certain asymptotic limit. Physicists are led to speculate that the geometry of space-time may really "emerge" from a quantum theory without any immediate notion of geometry. This kind of idea would in some sense address the longstanding issue of quantizing gravity: there would be no gravity to quantize since it would emerge as an effective description of already quantum degrees of freedom. But this problem is way beyond our scope, except maybe to motivate the enterprise of investigating the relationship between geometry and spectral theory in a relatively simple but nevertheless interesting setup. Indeed, understanding toy models is most often a mandatory step before understanding the full fledged problems.

Let us set the stage, and present our setup. On the geometric side, we have the theory of topological strings computing enumerative, topological invariants of their target space called toric Calabi–Yau threefolds. On the spectral side, we have the spectral theory of their quantized mirror curves. The precise relationship between these two worlds is stated by what is often called the Topological String/Spectral Theory (or TS/ST) correspondence. It is a conjectural, though sharp and testable relationship between the free energies of the topological string encoding enumerative invariants of the toric Calabi–Yau threefold, and the spectral determinant of the corresponding trace class and self-adjoint operator $\rho$. The spectral determinant encodes the spectrum and traces of $\rho$, which therefore are conjecturally determined by the enumerative invariants of the underlying toric Calabi–Yau threefold.

The TS/ST conjecture was first stated in [2], building up from insights gathered by studying ABJ(M) theory matrix models [3–7], as well as from the results in [8, 9]. It strongly relies on *mirror symmetry*, which is a duality between pairs of Calabi–Yau manifolds, more precisely between two topological string theories living on them. The interest of the TS/ST conjecture is twofold. Firstly, it provides an exact solution for the spectrum and traces of $\rho$, which in some cases can be writ-

ten down explicitly, or at least with arbitrary precision. Such exact results for the eigenvalues of quantum operators are quite rare in general. So the TS/ST correspondence offers a framework for finding the exact solution of spectral problems. Secondly, on a more conceptual note, the conjecture implies that certain spectral quantities provide a non-perturbative realization of topological strings. By this, we mean that the free energies of the topological string, which are intrinsically perturbative in their definition, arise in a certain limit as coefficients of the asymptotic expansion of a set of spectral quantities, which are well defined non-perturbative objects. So the TS/ST correspondence is also inscribed in the larger quest of finding non-perturbative definitions of string theories. Since its first statement in 2014 in [2], the TS/ST correspondence enjoyed several extensions in the subsequent years, and many of its interesting consequences have been investigated. Some of these consequences and extensions are the topic of the present thesis.

The first idea that was developed in this thesis is a consequence of the TS/ST correspondence: a new relationship between a family of matrix models and topological strings on toric Calabi–Yau threefolds. This relationship is a direct consequence of the TS/ST conjecture, and was already pointed at in [2]. On the spectral theory side, the matrix models are a rewriting of the *fermionic spectral traces*, which are the coefficients of the Fredholm determinant of the operator $\rho$. Using technical results in [10], the matrix models could in some cases be written down very explicitly in

- [11] M. Marino and S. Zakany, *Matrix models from operators and topological strings*, *Annales Henri Poincare* **17** (2016) 1075 [1502.02958],

- [12] R. Kashaev, M. Marino and S. Zakany, *Matrix models from operators and topological strings, 2*, *Annales Henri Poincare* **17** (2016) 2741 [1505.02243].

In these papers, we showed how the free energies of the closed topological string emerge from the matrix models in the so called 't Hooft limit (by analogy with the 't Hooft limit of gauge theories), or large $N$ limit. This fact is expected from the TS/ST correspondence, and could be explicitly checked in several cases. The first of the two papers explained in detail how the TS/ST conjecture implies this new relationship between the matrix models and topological strings. Then, it focused on the matrix models related to the toric Calabi–Yau geometries called local $\mathbb{P}^2$ and a certain restriction of local $\mathbb{F}_2$. The emergence of the topological string free energies from the matrix models was checked in the weak coupling limit of the matrix models. The second paper extended the technical results of [10] and investigated the matrix model of local $\mathbb{P}^1 \times \mathbb{P}^1$ (as well as full local $\mathbb{F}_2$ which turns out to be closely related). Checks of the conjecture were then performed in the weak and strong coupling limit

of the matrix models. Also, a part of the discussion was dedicated to establish the relationship of our matrix model for local $\mathbb{P}^1 \times \mathbb{P}^1$ with the ABJ(M) matrix model. Later, exact solutions in the planar limit of the matrix models related to a family of Calabi–Yau threefolds (including those mentioned above) could be obtained in

- [13] S. Zakany, *Matrix models for topological strings: exact results in the planar limit*, 1810.08608

by adapting the technique of [14] used for the six-vertex model on a random lattice. In those cases, the relationship between the spectral curve of the matrix model and the mirror curve of the underlying toric geometry could be established. Many of these results on matrix models and topological strings are reviewed in chapter 4.

The second idea that we developed in this thesis is an extension of the TS/ST conjecture. On the TS side it is extended to the open string amplitudes, and on the ST side to the eigenfunctions of the operator. By looking at the concrete example of local $\mathbb{P}^1 \times \mathbb{P}^1$, we could show in

- [15] M. Marino and S. Zakany, *Exact eigenfunctions and the open topological string*, *J. Phys.* **A50** (2017) 325401 [1606.05297]

that a one parameter family of eigenfunctions of the operator corresponding to local $\mathbb{P}^1 \times \mathbb{P}^1$ can be written down using open string data, namely the *topological string wavefunction*, which non-perturbatively completes the resummed WKB wavefunction. This result was proposed in the above paper after a thorough study in the 't Hooft limit of some matrix model expectation values related to the eigenfunctions. After interpreting this computation, we were led to the formulation of the open sector TS/ST correspondence, which is an extension of the conjecture in [2] and [16]. This extended conjecture allowed us to write down *exactly* the one parameter family of eigenfunctions in a precise case, and thus perform analytical checks against results coming purely from the spectral theory side. The actual eigenfunctions of the quantized mirror curve operator are a discrete subset of this family. This conjecture was further checked in

- [17] M. Marino and S. Zakany, *Wavefunctions, integrability, and open strings*, 1706.07402,

including the study of a higher genus case, i.e. a case where the mirror curve of the underlying geometry has genus larger than one. The higher genus case we investigated is the resolved $\mathbb{C}^3/\mathbb{Z}_5$ geometry, with a mirror curve of genus two. For genus two, the conjecture provides a two parameter family of eigenfunctions, which we wrote down exactly for the $\mathbb{C}^3/\mathbb{Z}_5$ geometry in a special case. This example

allowed us to discuss interesting aspects in quantum integrable systems of the type studied in [18], and their solutions through the Baxter equation and the separation of variable method. The Baxter equation of the integrable system is related to the difference operator given by the quantized mirror curve, and the solution of the spectral problem associated to the integrable system is in some sense a subset of the spectral problem associated to the quantized mirror curve [16, 18]. This subset can be obtained through extra quantization conditions. We checked that in our example, the extra quantization condition corresponds to enhanced decaying of the eigenfunction we constructed through the extended TS/ST conjecture. In this case, the full set of the two quantization conditions selects a discrete subset of the two parameter family of generalized eigenfunctions, which we call in this work "fully on-shell". In

- [19] S. Zakany, *Quantized mirror curves and resummed WKB*, `1711.01099`,

we proposed another method to build these "fully on-shell" eigenfunctions, only using the resummed WKB data. This proposal is not strictly speaking a consequence of the extended TS/ST conjecture stated in [15]. It rather builds on results in [20], which in turn relies on the modular duality structure [21] of the corresponding quantum integrable systems. Many of these results on eigenfunctions and the extended TS/ST correspondence are reviewed in chapter 5.

The third idea that we started developing in this thesis is a precise notion of "quantum geometry" for the operators given by the quantized mirror curves. In

- [22] M. Marino and S. Zakany, *Quantum curves as quantum distributions*, `1804.05574`,

we argued that through the phase space formulation of quantum mechanics and the Fermi gas picture of topological strings arising from the TS/ST correspondence, one can define a quantum distribution whose support reduces to the classical mirror curve in the classical limit. Moreover, the quantum fluctuation patterns around the classical curve are given by the Balazs–Zipfel approximation [23], for which we proposed an improvement in the process.

Some papers written during the time of the thesis are not developed in the present work. In

- [24] K. Okuyama and S. Zakany, *TBA-like integral equations from quantized mirror curves*, *JHEP* **03** (2016) 101 [`1512.06904`],

we worked on an extension of the Zamolodchikov [25] and Tracy–Widom [26] approach to compute the resolvent of the operator $\rho$ arising from the quantum mirror

curve. This results in a new set of thermodynamical Bethe ansazt-like equations satisfied by the resolvent. We also contributed to the efforts of

- [27] Y. Hatsuda, A. Sciarappa and S. Zakany, *Exact quantization conditions for the elliptic Ruijsenaars-Schneider model*, 1809.10294,

in which the spectrum of the elliptic Ruijsenaars–Schneider quantum integrable system [28, 29] was studied using supersymmetric gauge theory. This resulted in an improved version of the Nekrasov–Shatashvili quantization conditions [30], taking into account the modular duality structure of the integrable system.

The outline of this thesis is the following. In chapter 2, we present some background on topological strings and mirror symmetry. In chapter 3, we perform the quantization of mirror curves yielding the operator $\rho$, and define various quantities of interest in the spectral theory of $\rho$. We then state the TS/ST correspondence of [2, 16]. We also show how to construct explicit expressions for the integral kernel of the operator $\rho$, which will be used throughout the thesis. The last three chapters contain the original material. In chapter 4, we present our results on matrix models and topological strings. In chapter 5 we derive our results on eigenfunctions and open topological strings, and state the extended TS/ST correspondence. In chapter 6, we discuss our results on quantum distributions for quantized mirror curves. We finally conclude in chapter 7.

# Chapter 2

# From mirror symmetry to spectral problems

The main idea behind this work is the Topological String/Spectral Theory (or TS/ST) correspondence, first stated in [2] and further developed in different directions in [15, 16, 18, 31]. It is a conjectural relationship between two distinct worlds: topological strings (TS), and the spectral theory of operators (ST). This purpose of this chapter is to set some background, or at least sufficient working knowledge, for the TS part of this proposal. As such, it presents absolutely no original material. The ST part and the original proposal of the TS/ST correspondence will be presented in the next chapter.

String theories can be seen as quantum theories of maps from Riemann surfaces – the two real-dimensional worldsheets of strings – to the target space – the physical world. The theory of topological strings is an interesting, albeit simplified version of string theory whose amplitudes encode various topological and geometrical properties of the target space. It is a good physical setup to study mirror symmetry. We present a brief narrative overview of this vast topic, in order to give an idea of the physical origin of the ingredients used in further sections, and perhaps give some motivation for the TS/ST correspondence.

Nice introductory reviews on topological sigma models and topological strings can be found in [32] and also in [33–35]. Mirror symmetry and its applications is presented in a rather didactic way in [32].

## 2.1 Topological strings

Topological sigma models were introduced in [36, 37]. Topological string theory can be realized by starting with a two real-dimensional non-linear sigma model (NLSM)

with $\mathcal{N} = (2,2)$ supersymmetry; in other words a quantum field theory with 4 fermionic supersymmetry generators, where the main bosonic fields $\phi_A$ are coordinates on a manifold $X$. The theory does not depend on the choice of coordinates, so the fields will be sometimes denoted without indices, and called the map $\phi$,

$$\phi : \Sigma_g \to X \tag{2.1}$$

which maps the genus $g$ Riemann surface $\Sigma_g$ (the worldsheet of the string) to $X$ (the target space). It is useful for the formulation of the theory if the target space has a key geometric property: we take $X$ to be a Kähler manifold[1], so that $\mathcal{N} = (2,2)$ supersymmetry is easily realized in the action of the theory via the $(2,2)$ superspace formalism. The kinetic term (or D–term) for the supersymmetric multiplet corresponding to the map $\phi$ is built from the Kähler potential, which is the only geometric data in the definition of the theory. If the target $X$ is non-compact, one can use a non trivial holomorphic function on $X$ to build an extra term in the action, called the superpotential term (or F–term). Finally, if the target space contains homological 2–cycles, one can define another extra term (the so called B–field term). All these terms in the action are supersymmetric by construction. Beside supersymmetry and the usual Poincaré symmetry in two dimensions, there are extra symmetries which correspond to $U(1)$ rotations in superspace. These are the two R–symmetries: one of them is called the "axial" and the other the "vector". We usually want these symmetries to be non-anomalous in the quantized theory. This gives a new constraint on the target space: since the anomaly for the axial R–symmetry is related to the first Chern class[2] $c_1$ of the target space, the anomaly free condition is satisfied if the first Chern class is trivial, $c_1 = 0$.[3] This is called the Calabi–Yau condition. So a well defined $\mathcal{N} = (2,2)$ quantum NLSM which is anomaly free has a target space $X$ obeying this condition, and thus called a Calabi–Yau (CY) manifold. The Calabi–Yau condition implies several properties. Most famously, as conjectured by Calabi and proved by Yau, the $c_1 = 0$ condition implies the existence of a unique Kähler metric on $X$ which is Ricci-flat. This is very important in full-fledged string theory with phenomenological ambitions, since it insures the flatness of the compactified part of space-time $X$, so that $X$ gives a "vacuum" (in the geometric sense) for the

[1] A complex manifold doted with a metric compatible with the complex structure, such that metric can be encoded in a closed $(1,1)$–form $\omega$, called the Kähler form. Then, the metric has a kind of "integrability" property: it is locally the second derivative of a scalar function called the Kähler potential.

[2] The Chern classes are objects related to topological invariants of the manifold, which basically measure how a bundle (here the holomorphic tangent space) fibrates over its base.

[3] If there is an F–term in the action, the anomaly free condition puts an extra requirement on the holomorphic function used to define the superpotential.

theory. More importantly for our context, the Calabi–Yau condition guarantees the existence of a nowhere holomorphic $(n, 0)$–form, where $n$ is the complex dimension of $X$. This is called the Calabi–Yau form $\Omega$.

A string theory is a sigma model coupled to gravity, that is, where the worldsheet metric is also considered as degrees of freedom, and is integrated over in the path integral. Therefore, the topological NLSM needs two major upgrades to become full fledged topological strings.

Firstly, the NLSM should make sense also for curved worldsheets. Because of the presence of the supersymmetric partners of $\phi$ which are fermionic degrees of freedom, preservation of some supersymmetry requires that the NLSM should be "twisted". This is called the topological twist, and it consists in replacing the Lorentz symmetry (rotation in physical euclidian space) by a mixture of Lorentz and one of the R–symmetries (rotation in superspace). This modified symmetry is the one which is "gauged" to obtain the gravity theory. There are two inequivalent ways of doing the twisting, which differ in which of the R–charges we choose. Choosing the so called vector R–charge gives the "A twist" leading to the *A–model*, whereas choosing the axial R–charge gives the "B twist" leading to the the *B–model*. In both models, a fermionic symmetry survives the twisting, with a corresponding fermionic charge $Q$ (different for the $A$– and the $B$–model) which squares to zero. The energy-momentum tensor $T_{\alpha\beta}$, given by the variation of the Lagrangian density with respect to the worldsheet metric, is $Q$–exact:

$$T_{\alpha\beta} = \{Q, G_{\alpha\beta}\} \tag{2.2}$$

for an operator $G_{\alpha\beta}$. The physical operators of each theory are defined to be the $Q$–cohomology classes, i.e. operators which are $Q$–closed modulo $Q$–exact operators. According to this definition and because of the exactness of $T_{\alpha\beta}$, the expectation values of physical operators do not depend on the worldsheet metric (at least formally). In this sense, they are *topological*. However, it turns out that there are not many non-trivial expectation values for such a theory.[4] This leads us to the second upgrade.

To obtain non-trivial expectation values of observables for worldsheets with arbitrary genus $g$, we need to integrate over the worldsheet metric. This is often called "coupling the sigma model to gravity". For target spaces with complex dimension $n = 3$, coupling the NLSM to gravity gives non-vanishing expectation values at all genera $g$. For this reason, the most interesting target spaces are CY threefolds, i.e.

[4]This comes from some selection rules related to the $R$–symmetries. A set of non-trivial expectation values are those of three operators from a certain subfamily, for a genus 0 worldsheet. They lead to the definition of the third derivatives of the genus zero free energy $F_0$.

manifolds of complex dimension three obeying the Calabi–Yau condition. We do not dwell on the precise technical way of performing the coupling to gravity; let us just mention that it involves appropriate insertions of the operator $G_{\alpha\beta}$ and an integration over the moduli-space $\overline{\mathcal{M}}_g$ of Riemann surfaces $\Sigma_g$ of fixed genus $g$ (at least for the closed string case; the open string case is appropriately modified and boundary conditions taken into account). This is quite similar to the quantization of the bosonic string, where the role of $Q$ is played by the BRST operator. In the end, we wish to sum over all worldsheet geometries, not just those at fixed genus. So to obtain a complete answer for an observable computed by the path integral, we perform a sum over all the observables computed for worldsheets $\Sigma_g$ with fixed genus $g$. In the sum, each amplitude at genus $g$ comes with a factor of $g_s$ at a certain power, where $g_s$ is called the *string coupling*. For example, the free energies at genus $g$ are noted $F_g$, and the full free energy is

$$F = \sum_{g=0}^{\infty} g_s^{2g-2} F_g. \tag{2.3}$$

In this way, we truly summed over all worldsheet geometries. However, we see that, as for all similar formulations of string theories, the construction is fundamentally perturbative in the string coupling.[5] It does not help that (2.3) is usually a divergent asymptotic series.

The outcome of the procedure outlined above is what is called topological string theory. As we said, it comes in two versions, the A–model and the B–model. Since the actual "physical" operators of each version is different, they correspond to different geometrical objects in the target space $X$. In particular, the amplitudes depend on a small set of geometrical data of the target. In the A–model these are the *Kähler parameters*, which parametrize the allowed deformations of CY threefold with fixed complex structure. In the B–model they are the *complex structure parameters*, which parametrize the allowed complex structure deformations of the CY threefold (these are identified with the possible deformations of the Calabi–Yau $(n,0)$–form $\Omega$). There is a very fruitful idea that relates the two versions of topological strings which is called *mirror symmetry*. Mirror symmetry is a duality which states that the A–model topological string amplitudes on a target space $X$ are equal to the B–model amplitudes on a different target $\widetilde{X}$. The geometry $\widetilde{X}$ is called the mirror of $X$. Since the A–model depends on the Kähler parameters of $X$ and the B–model depends on the complex structure parameters of $\widetilde{X}$, these two sets are

[5] The higher genus contributions correspond in some way to higher loop diagrams in the target space interpretation (as a quantum field theory). That is why we think of the expansion in $g_s$ as a perturbative expansion.

exchanged under mirror symmetry. Mirror symmetry is therefore a most interesting mathematical relationship between pairs of CY geometries, but also a most useful tool to carry out computations which can sometimes be difficult on one side of the duality, but easy on the other.

In the present work, our interest will be directed to the cases where the A–model target space $X$ is a *toric Calabi–Yau threefold*. Toric means that the geometry in question contains a torus as a dense subset, and this torus acts on the whole space as an abelian group. It turns out that toric Calabi–Yau threefolds are non-compact. This arguably lessens their interest in phenomenological applications (after all, the compactified dimensions should be compact). However, they are a very favourable arena to study mirror symmetry, which is comparatively well understood in their context.

The physical argument for mirror symmetry involving toric CY threefolds is presented in [38]. It relies on a useful realization of the NLSM for toric CY threefolds as the low energy limit of a *gauged linear sigma model* (GLSM). One neat feature of the GLSM formulation is that it has a global description, as opposed to the NLSM where the fields $\phi$ are local coordinates on the target space. The GLSM for the toric cases (amongst others) is constructed in [39]. In this setup, the fields $\phi$ are a map from the worldsheet to $\mathbb{C}^{3+m}$. The theory is an $\mathcal{N} = (2, 2)$ sigma model with this rather trivial target space. The novelty is that it also contains gauge fields. The gauge group is the abelian group $U(1)^m = U(1)_1 \times U(1)_2 \times ... \times U(1)_m$. The $3 + m$ coordinates $\phi_i$ of the map – or rather their supersymmetric multiplets $\Phi_i$ – have definite charges $Q_i^k$ under the various $U(1)_k$ components of the gauge group. The gauge couplings are denoted $e_k$. The supersymmetric action is built from the gauge invariant kinetic part for the chiral multiplets containing $\phi_i$, a kinetic part for the real vector multiplets containing the gauge fields, and finally an extra term (a twisted F–term) involving the superfield-strength of the vector multiplet, as well as $m$ parameters $t_k = r_k - \mathrm{i}\theta_k$ (the complexified Fayet–Iliopoulos parameters involving a theta term). In our case, there is no superpotential for $\Phi_i$. Integrating out the various auxiliary fields appearing in the superspace formalism, one ends up with an action containing a potential term for the $\phi_i$ which is

$$U = \sum_{k=1}^{m} \frac{e_k^2}{2} \left( \sum_{i=1}^{m+3} Q_i^k |\phi_i|^2 - r_k \right)^2 . \tag{2.4}$$

Classically, the vacuum configurations of the GLSM are given by gauge inequivalent configurations of fields $\phi_i$ satisfying $U = 0$. So the vacuum manifold is defined as

$$X = \left\{ (\phi_1, \ldots, \phi_{3+m}) \in \mathbb{C}^{3+m} : \sum_{i=1}^{3+m} Q_i^k |\phi_i|^2 = r_k \right\} \Big/ U(1)^m, \tag{2.5}$$

where $U(1)^m$ acts as

$$\phi_i \to \prod_{k=1}^{m} \mathrm{e}^{\mathrm{i}Q_i^k \lambda_k} \phi_i, \qquad i = 1, \dots 3+m. \tag{2.6}$$

This turns out to be a toric variety. It inherits the complex and the Kähler structure of the ambient $\mathbb{C}^{3+m}$ space (the formal mathematical setting to do this is called symplectic reduction). For the variety $X$ to be a toric Calabi–Yau manifold, the charges must satisfy the constraint

$$\sum_{i=1}^{3+m} Q_i^k = 0, \qquad k = 1, \dots 3, m. \tag{2.7}$$

The interest in this GLSM comes from the following: in the low energy (large gauge coupling) limit, the light modes describe a NLSM on the target space $X$. In brief, the modes of $\phi_i$ which are not tangential to the vacuum manifold (as well as some of their superpartners) acquire a mass. The potential is gauge invariant, but the choice of a vacuum breaks the gauge invariance, so, through the supersymmetric Higgs mechanism, the gauge fields freeze and they, as well as their superpartners also acquire a mass. The remaining light degrees of freedom essentially amount to the NLSM on $X$. The $t_k = r_k + \mathrm{i}\theta_k$ turn out to be the Kähler parameters, parametrizing the Kähler deformations of the target space $X$.

This construction is particularly useful to study the A–model, which will depend on the $t_k$. However, it is found that there is an equivalent – or dual – description of the GLSM in terms of a Landau–Ginzburg model, a cousin of the sigma model but with an extra twisted superpotential. This duality is explained in [38]. The relation between the two models is akin to T–duality[6], where one starts with a "generating theory" with auxiliary fields. The two dual descriptions are related to which precise fields one wants to integrate out. In the dual description, the charged chiral multiplet degrees of freedom are replaced by anti-chiral ones, and vector and axial R–symmetries are exchanged. Therefore, the corresponding Landau–Ginzburg model is a B–twisted topological model. It also has a low energy limit. In this limit, in terms of the anti-chiral superfields $Y_i$ which are dual to $\Phi_i$, and after taking into account non-perturbative effects [38], the twisted superpotential of the Landau–Ginzburg model reads

$$\widetilde{W} = \sum_{i=1}^{3+m} \mathrm{e}^{-Y_i}, \tag{2.8}$$

[6]The simplest version of $T$–dualty appears for a $1+1$ dimensional ($\mathbb{R} \times S^1$) free scalar field taking values in a circle of radius $R$ (so $x = x + 2\pi R$), i.e. a sigma model with the circle as target. The partition function of the quantum theory is invariant under $R \leftrightarrow R^{-1}$. Also, the full spectrum itself is invariant under $R \leftrightarrow R^{-1}$ provided that we exchange winding numbers and momentum numbers.

with additional constraints on $Y_i$:

$$\sum_{k=1}^{m} Q_i^k Y_i = t_k. \tag{2.9}$$

It can also be described by a (B–twisted) NLSM, but on a different target space [40]. This other Calabi–Yau manifold is precisely the mirror $\widetilde{X}$. The geometry of the mirror Calabi-Yau manifold is encoded in the above twisted superpotential.

Since the A–model NLSM on $X$ and the B–model NLSM on $\widetilde{X}$ eventually come from the same "generating theory", they should be equivalent. That is, the observables of these two theories should be the same (under the appropriate map). This is the physical motivation of mirror symmetry.

## 2.2 The A–model

In our setup, the target space $X$ for the A–model topological string is the toric CY threefold given by (2.5). But what does the A–model actually compute? A nice review of this is given in [34]. As we outlined in the previous section, the A–model is a twisted NLSM on $X$. Since the twisting allows for a remaining supersymmetry with charge $Q_A$, this can be used to localize the path integral on the "semi-classical configurations".[7] These turn out to correspond to *holomorphic maps* $\phi : \Sigma_g \to X$ from the worldsheet $\Sigma_g$ to the target $X$ [37]. Such holomorphic maps can be trivial (constant) maps, or they can "wrap" the worldsheet around non-trivial two cycles in the target $X$, in which case they can be seen as "worldsheet instantons". The action for each of the configurations contributing the amplitude is given by the "area" that the worldsheet spans in the target. Let us note by $[C_i] \in H_2(X)$, $i = 1, \ldots, b_2$ a homology basis for the two cycles in $X$. A holomorphic map wrapping the homological cycle $\beta = \sum_i d_i [C_i]$ comes with a factor whose exponent is the "area" of the wrapped cycle:

$$\mathrm{e}^{-\int_\beta \omega} = \mathrm{e}^{-\sum_i d_i t_i} = \mathrm{e}^{-\mathbf{d}\cdot\mathbf{t}}, \tag{2.10}$$

where $\omega$ is the Kähler form[8] and $t_i = \int_{[C_i]} \omega$ are the Kähler parameters. The numbers in $\mathbf{d} = (d_1, ..., d_{b_2})$ are referred to as the degrees of the holomorphic map. They are

[7] Supersymmetric localization relies on the fact that, due to supersymmetry, the path integral for expectations values of "physical" operators is invariant under a certain set of deformations. As usual for path integrals, they can be approximated semi-classically around the "classical" configurations (where the action is stationary, fixed by the action of $Q_A$). But it turns out that the deformation can be made such that the corrections to the semi-classical results vanish, and thus the semiclassical approximation to the path integral becomes exact.

[8] Actually, here $\omega$ is the "complexified" Kähler form, where the imaginary part is given by a so called $B$ field.

non-negative integers. For expectation values with (almost) no inserted operators, the path integral computes enumerative invariants which in some sense "count" the number of holomorphic maps from $\Sigma_g$ to $X$ with a certain degree $\mathbf{d}$. These are precisely the *Gromov–Witten* invariants $N_{g,\mathbf{d}}$ of $X$, in general rational numbers. The resulting amplitudes can be written in terms of the Gromov–Witten invariants as

$$\begin{aligned} F_0(\mathbf{t}) &= \frac{1}{3!}\sum_{i,j,k} a_{ijk}t_it_jt_k + \sum_{\mathbf{d}} N_{0,\mathbf{d}}\,\mathrm{e}^{-\mathbf{d}\cdot\mathbf{t}}, \\ F_1(\mathbf{t}) &= \sum_i b_it_i + \sum_{\mathbf{d}} N_{1,\mathbf{d}}\,\mathrm{e}^{-\mathbf{d}\cdot\mathbf{t}}, \\ F_g(\mathbf{t}) &= C_g + \sum_{\mathbf{d}} N_{g,\mathbf{d}}\,\mathrm{e}^{-\mathbf{d}\cdot\mathbf{t}}, \qquad\qquad g \geq 2. \end{aligned} \tag{2.11}$$

The $F_g$ are called the *topological string free energies*, and they depend on the Kähler parameters $\mathbf{t}$. We see that they are expansions at large $t_k$, which is called the *large radius* (LR) point in the moduli space of Kähler deformations. For $g \geq 2$, the non-instanton configurations are constant maps, which account for $C_g$. Because of the slightly different definition of the amplitudes at genus 0 and 1, the non-instanton sector encodes other invariants of $X$. The constants $a_{ijk}$ are triple intersection numbers $\sum_{i,j,k} a_{i,j,k}t^it^jt^k = \int_X \omega\wedge\omega\wedge\omega$, and the constants $b_i$ have a similar definition involving the second Chern class of the Calabi–Yau $X$. The full free energy of the string is a sum over all worldsheet topologies:

$$F(\mathbf{t}, g_s) = \sum_{g=0}^{\infty} g_s^{2g-2}F_g(\mathbf{t}), \tag{2.12}$$

where $g_s$ is the string coupling constant.

Actually, since the worldsheets we integrate over do not have punctures (or "boundaries"), we are dealing with the closed sector of the topological string, and (2.11) are the closed free energies at genus $g$. They can be generalized to the open sector as done in [41] (in which the open B–model is also considered, as well as a fruitful relationship between Chern–Simons theory and topological strings). For the open case, we consider worldsheets which have punctures. The amplitudes should involve an integration over the moduli space $\overline{\mathcal{M}}_{g,h}$ of Riemann surfaces $\Sigma_{g,h}$ of genus $g$ and $h$ punctures. We want the end-points of the strings to satisfy certain boundary conditions. Geometrically, this is done by introducing D–branes inside the target space. D–branes are the loci where the open strings can end, i.e. such that $\phi : \Sigma_{g,h} \to X$ maps the punctures of $\Sigma_{g,h}$ to the D–branes in $X$. This can be consistently done if these D–branes are Lagrangian submanifolds in $X$: submanifolds where the Kähler form, which is also a symplectic form, vanishes. Moreover, one can introduce $U(N)$ degrees of freedom on the D–branes (à la Chan-Paton), and insert

extra Wilson loop operators along these boundaries inside the expectation values for the amplitudes. In this setup, the localization computation can also be performed. Here we will assume that there is only one Lagrangian submanifold which is a cycle $\mathcal{L}$ wrapped by a D–brane. The relevant "semi-classical" configurations contributing to the amplitudes are holomorphic maps $\phi$ of degree $\mathbf{d}$ and whose $i^{\text{th}}$ boundary $(i = 1, \dots, h)$ wraps $\ell_i$ times the cycle $\mathcal{L}$. We put this data in a winding vector of positive integers $\boldsymbol{\ell} = (\ell_1, \dots, \ell_h)$. The amplitudes therefore compute enumerative invariants which in some sense "count" the number of these holomorphic maps from $\Sigma_{g,h}$ to $X$ with degree $\mathbf{d}$ (the relative homology class of the two cycle wrapped by the punctured worldsheet) and winding $\boldsymbol{\ell} = (\ell_1, \dots, \ell_h)$. These are the open versions of the Gromov–Witten invariants $N_{g,\mathbf{d},\boldsymbol{\ell}}$. The resulting amplitudes are the *open string amplitudes*. They formally depend on a matrix $V$ and are given by

$$F_{g,h}(V, \mathbf{t}) = \sum_{\mathbf{d}} \sum_{\boldsymbol{\ell}=(\ell_1,\dots\ell_h)} N_{g,\mathbf{d},\boldsymbol{\ell}} \operatorname{tr}(V^{\ell_1}) \cdots \operatorname{tr}(V^{\ell_h})\, \mathrm{e}^{-\mathbf{d}\cdot\mathbf{t}}. \tag{2.13}$$

They are assembled together by summing over all the topologies of the worldsheet, to form the full open string free energy:

$$F_{\text{open}}(V, \mathbf{t}, g_s) = \sum_{g=0}^{\infty} \sum_{h=1}^{\infty} \frac{1}{h!} (-\mathrm{i} g_s)^{2g-2+h} F_{g,h}(\mathbf{t}, V). \tag{2.14}$$

These results are intrinsically perturbative in the string coupling $g_s$. But, as found by Gopakumar and Vafa [42, 43], the $g_s$ dependence can be resummed. Their formula relies on considering M–theory on an 11 dimensional target space built from the initial Calabi–Yau threefold $X$, flat 4 dimensional space-time $\mathbb{R}^{1,3}$ and an extra circle $S^1$ (which is taken to be large, so effectively replaced by $\mathbb{R}$). This has an effective $\mathcal{N} = 2$ supersymmetric gauge theory description through Kaluza–Klein reduction to the five dimensional space-time. It is found that a so-called F–term in the effective gauge theory action is exactly given by the free energy $F(g_s, \mathbf{t})$ of the topological string on $X$, non-perturbatively in $g_s$. From the M–theory point of view, this term is generated by integrating out some degrees of freedom.[9] The relevant degrees of freedom are given by M2–branes wrapping two cycles in $X$. As such they are characterised by the degree $\mathbf{d}$ of the homology class of the wrapped two-cycle. These correspond to massive BPS states (preserving half of the supersymmetry) in the effective field theory, and are labelled by representations (or spin) $(j_L, j_R)$ of the little group $SO(4) = SU(2)_L \times SU(2)_R$ in five dimensional space-time. The

[9] A much simpler example of such an operation is Schwinger's computation of integrating out the charged scalar field from a gauged theory coupled to it, and obtain the effective theory in terms of the gauge field only.

computation of [42, 43] gives an expression for the topological free energy as a sum over these BPS states. The result is

$$F(\mathbf{t}, g_s) = g_s^{-2}\frac{1}{3!}\sum_{i,j,k} a_{ijk}t_i t_j t_k + \sum_i b_i t_i + \sum_{g=2}^{\infty} C_g g_s^{2g-2} + F_{\mathrm{GV}}(g_s, \mathbf{t}), \tag{2.15}$$

where $F_{\mathrm{GV}}$ is the Gopakumar–Vafa free energy:

$$F_{\mathrm{GV}}(\mathbf{t}, g_s) = \sum_{g=0}^{\infty}\sum_{\mathbf{d}}\sum_{w=1}^{\infty} n_g^{\mathbf{d}}\frac{1}{w}\left(2\sin\frac{wg_s}{2}\right)^{2g-2}\mathrm{e}^{-w\mathbf{d}\cdot\mathbf{t}}. \tag{2.16}$$

The integer numbers $n_g^{\mathbf{d}}$ are called *Gopakumar–Vafa invariants* and they are related to the number $\mathcal{N}^{\mathbf{d}}_{j_L,j_R}$ of BPS states of degree $\mathbf{d}$ and spin $(j_L, j_R)$, often called *BPS numbers*[10], through

$$\sum_{g=0}^{\infty}(-1)^g n_g^{\mathbf{d}}(q^{1/2}-q^{-1/2})^{2g} = \sum_{j_L,j_R}(-1)^{2j_L+2j_R}(2j_R+1)\,\mathcal{N}^{\mathbf{d}}_{j_L,j_R}\frac{q^{2j_L+1}-q^{-2j_L-1}}{q^1-q^{-1}}. \tag{2.17}$$

There is also a generalization to the open sector, obtained in [44, 45], using the relation between topological strings and large $N$ Chern–Simons theory as in [46] (where $N$ is the rank of the gauge group). It can be written as (see for example [47]):

$$\begin{aligned} F_{\mathrm{open}}(V, \mathbf{t}, g_s) = \sum_{g=0}^{\infty}\sum_{\mathbf{d}}\sum_{h=1}^{\infty}\sum_{\boldsymbol{\ell}=(\ell_1,\dots\ell_h)}\sum_{w=1}^{\infty}\frac{\mathrm{i}^h}{h!}n_g^{\mathbf{d},\boldsymbol{\ell}}\frac{1}{w}\left(2\sin\frac{wg_s}{2}\right)^{2g-2} \\ \times\left(\prod_{i=1}^{h}\frac{1}{\ell_i}\left(2\sin\frac{w\ell_i g_s}{2}\right)\mathrm{tr}V^{w\ell_i}\right)\mathrm{e}^{-w\mathbf{d}\cdot\mathbf{t}}. \end{aligned} \tag{2.18}$$

The numbers $n_g^{\mathbf{d},\boldsymbol{\ell}}$ are open equivalents to the Gopakumar-Vafa invariants. Expanding $F_{\mathrm{GV}}$ and $F_{\mathrm{open}}$ at small $g_s$, one obtains the closed and open Gromov–Witten invariants.

For toric Calabi–Yau threefolds, insight coming from Chern–Simons theory has allowed the authors of [48] to give an algorithmic and diagrammatic way of effectively computing the topological string partition function, and the open amplitudes. The only things required in this algorithm are the knowledge of all the amplitudes for the simplest toric case $X = \mathbb{C}^3$, also called the *topological vertex*, as well as a way of appropriately combining together several topological vertices to obtain the free energies and amplitudes for more complicated toric geometries. This relies on the fact that toric threefolds can be represented as $\mathbb{C}^3$ patches glued together.

[10] Sometimes, a multiplicative factor $(-1)^{2j_L+2j_R}$ is included in the definition of the BPS number. In the present work we do not include it, so that the BPS numbers remain positive integers.

## 2.3 The B–model and the mirror geometry

In our setup, mirror symmetry relates the A–model on a toric CY threefold $X$ to the B–model on its mirror geometry $\widetilde{X}$. The mirror geometry for toric CY threefolds is obtainable from (2.8-2.9) and is given in [38, 40] (see also [49]). It is completely defined using the charge vectors $Q_i^k$ of the initial toric CY threefold. Let us take $3+m$ complex variables $y_i$, and $(w_+, w_-) \in \mathbb{C}^2$. The mirror geometry is given by the relation

$$w_+ w_- = \sum_{i=1}^{3+m} \mathrm{e}^{y_i}, \tag{2.19}$$

with the additional constraints given by the charge vectors $Q_i^k$ of the initial toric CY manifold,

$$\sum_{k=1}^{m} Q_i^k y_i = \log z_k. \tag{2.20}$$

Using the constraints and the scaling freedom, the left hand side of (2.19) can be reduced to a function of two variables $x, y$:

$$\sum_{i=1}^{3+m} \mathrm{e}^{y_i} = W(\mathrm{e}^x, \mathrm{e}^y). \tag{2.21}$$

In the function on the right-hand side, the $z_k$ appear as parameters. The notation $W(\mathrm{e}^x, \mathrm{e}^y)$ stresses the fact that it is a polynomial in the variables $\mathrm{e}^x$ and $\mathrm{e}^y$.

What does the B–model compute? An introductory review for the B–model topological string can be found in [35]. It turns out that the "physical" operators are in one-to-one correspondence to (Dolbeault cohomology classes of) $(0,p)$–forms on $\widetilde{X}$, taking values in the $q^{th}$ exterior power of the holomorphic tangent bundle of $\widetilde{X}$. Moreover, by the supersymmetric localization argument using the symmetry generated by $Q_B$, it can be shown that only constant maps contribute to path integrals. So integration over the maps reduces to integration over the target manifold $\widetilde{X}$ itself. Moreover, because of selection rules, the only interesting expectation values for genus 0 worldsheets are three-point functions of the form $\langle \mathcal{O}_i \mathcal{O}_j \mathcal{O}_k \rangle$, where $\mathcal{O}_i$ are $(0,1)$–forms taking values in the holomorphic tangent bundle. These kind of objects actually correspond to possible deformations of the CY $(3,0)$–form $\Omega$, equivalently deformations of complex structure. Well known results state that the complex deformations of our manifold can be (redundantly) parametrized by period integrals of the Calabi–Yau form $\Omega$ over three-cycles of the geometry. Let us define $\mathcal{A}_i, \mathcal{B}_i \in H_3(\tilde{X})$ for $i = 0, \ldots, h_{2,1}$ to be a homological basis of three-cycles[11], which

[11] The number of independent three cycles is $b_3 = 2h_{2,1} + 2$ in our geometries.

intersect as $\mathcal{A}_i \cap \mathcal{B}_j = \delta_{ij}$. We have the periods

$$\tilde{t}_i = \int_{\mathcal{A}_i} \Omega, \qquad f_i = \int_{\mathcal{B}_i} \Omega. \tag{2.22}$$

The $\tilde{t}_i$ are projective coordinates on the moduli space of complex structure deformations.[12] So, for $\tilde{t}_0 \neq 0$, $t_i = \tilde{t}_i/\tilde{t}_0$ are local coordinates. It can be shown that $\partial_{\tilde{t}_i} f_j = \partial_{\tilde{t}_j} f_i$, so there exists a function $\mathcal{F}$ such that

$$\frac{\partial \mathcal{F}}{\partial \tilde{t}_i} = f_i. \tag{2.23}$$

This function $\mathcal{F}$ is called the *prepotential*. It turns out to be a homogeneous function of degree 2, so we can use the rescaled version $F_0(\mathbf{t}) = \tilde{t}_0^{-2}\mathcal{F}(\tilde{\mathbf{t}})$. In terms of the rescaled Calabi–Yau 3–form $\tilde{\Omega} = \tilde{t}_0^{-1}\Omega$, we obtain

$$t_i = \int_{\mathcal{A}_i} \tilde{\Omega}, \qquad \partial_{t_i} F_0 = \int_{\mathcal{B}_i} \tilde{\Omega}. \tag{2.24}$$

The importance of the function $F_0$ comes from the fact that the three-point functions $\langle \mathcal{O}_i \mathcal{O}_j \mathcal{O}_k \rangle$ are expressed in terms of it:

$$\langle \mathcal{O}_i \mathcal{O}_j \mathcal{O}_k \rangle = \frac{\partial F_0}{\partial t_i \partial t_j \partial t_k}. \tag{2.25}$$

The function $F_0$ is the genus 0 free energy. As can be seen from this construction, the free energy thus defined will depend on the actual choice of the symplectic basis $\mathcal{A}_i, \mathcal{B}_i$. A change of basis is given by an $\mathrm{Sp}(b_3, \mathbb{Z})$ transformation. Choosing a basis corresponds to choosing a "frame" for the topological string free energy. If the frame chosen is the so called "large radius" frame, the flat coordinates $t_i$ for the complex structure deformation of the mirror $\widetilde{X}$ correspond to the Kähler parameters of the toric Calabi–Yau $X$, and $F_0(\mathbf{t})$ equals the A–model free energy by mirror symmetry. But other frames can be chosen. For example, the so called "conifold point" in moduli space of the mirror geometry is characterised by the pinching of some of its cycles[13]. If those cycles are chosen as $A$–periods, then we say that the free energy is in the "conifold frame". In each case, the dependence on the local coordinates $t_i$ is through the $A$–period integrals in (2.24), which gives a map between the flat coordinates and the parameters $z_k$ entering explicitly the mirror curve. This map is called the *mirror map*.

[12] The projective nature of these coordinates can be seen from the fact that $\Omega$ is defined up to an overall scale.

[13] Then, the toric Calabi–Yau threefold develops a singularity which locally looks like the conifold singularity given by $XY - UV = 0$ in $\mathbb{C}^4$.

For the mirrors of toric CY threefolds given by

$$w_+ w_- = W(\mathrm{e}^x, \mathrm{e}^y), \tag{2.26}$$

the CY $(3,0)$–form is given by

$$\Omega = \frac{\mathrm{d}w \wedge \mathrm{d}x \wedge \mathrm{d}y}{w}. \tag{2.27}$$

($w$ equals either $w_+$ or $w_-$). This particular form for the mirror geometry has the following consequence: all the periods of the form (2.24) reduce to one dimensional periods over the curve in $\mathbb{C}^* \times \mathbb{C}^*$ given by

$$W(\mathrm{e}^x, \mathrm{e}^y) = 0, \tag{2.28}$$

which is called the *mirror curve*. The three-cycles $\mathcal{A}_i, \mathcal{B}_i$ descend to one-cycles in the mirror curve, which we will also call $\mathcal{A}_i, \mathcal{B}_i$ (this should not pose any problem since from now on we will only deal with the one-cycles). The expressions (2.24) become period integrals on the mirror curve given by

$$t_i \propto \int_{\mathcal{A}_i} y \, \mathrm{d}x, \qquad \partial_{t_i} F_0 \propto \int_{\mathcal{B}_i} y \, \mathrm{d}x, \tag{2.29}$$

up to multiplicative constants. The integrals over the $\mathcal{A}_i$ one-cycles give the mirror map, i.e. a relationship between the $t_i$ and the parameters $z_k$ appearing explicitly in the mirror curve. Inverting this, we obtain the mirror maps $z_k(\mathbf{t})$, which can be plugged in the second expression of (2.29) in order to get the derivatives of the genus 0 free energy.

As is well known, periods such as (2.24) (and thus (2.29)) obey specific differential equations in terms of the parameters $z_i$, called the *Picard–Fuchs* equations. In our case, the differential operators can be written down explicitly in terms of the charges $Q_i^k$. The Picard–Fuchs equations can be very useful to compute the periods, and thus obtain the mirror map and the genus 0 free energy.

As we mentioned earlier, to get non-trivial correlations functions at higher genus $g$, we need to couple the sigma model to gravity. An effective way of computing recursively the higher genus free energies $F_g$ is the so called holomorphic anomaly equation [50]. The holomorphic equation strongly constrains the free energies (up to the so called holomorphic ambiguity). For mirrors of toric CY threefolds, the holomorphic anomaly equation can be used to completely fix the $F_g$ [51]. This approach depends on the choice of frame, i.e. the choice of the basis of cycles in the mirror geometry. It was shown in [52] that changing the frame for the free energies amounts to a formal integral transform, which is consistent with the claim that the closed string partition function behaves as a wavefunction [53].

As we saw for the A–model, open string amplitudes can be defined if we introduce D–branes (that is, specific boundary conditions for the maps $\phi$). This construction has a mirror dual in the B–model: branes in the A–model given by Lagrangian submanifolds of $X$ are dual to complex submanifolds in $\widetilde{X}$. For example, as shown in [54, 55], the B–model equivalent of the *disk amplitude*, which is $F_{0,1}(\mathbf{t}, V)$ in (2.13), reduces to an integral on the mirror curve. If one replaces $\mathrm{tr}V$ by a formal variable $X$ in (2.14), $F_{0,1}(\mathbf{t}, X)$ essentially corresponds to[14]

$$\int^x y(x')\mathrm{d}x'. \tag{2.30}$$

The map between the two quantities is through the mirror map $z_k(\mathbf{t})$, and a so called open mirror map relating $\mathrm{e}^x$ to $X$.

Quite naturally, one would expect that all the amplitudes $F_{g,h}(\mathbf{t}, V)$ in eq. (2.14) should be obtainable from the mirror curve in an explicit way, as was done for the disk amplitude $F_{0,1}$. This is what is advocated in the BKMP approach (or "remodelling" approach) initiated in [56] and fully stated in [57]. The proposal is essentially the following. Let us define

$$F_{g,h}(\mathbf{t}, X_1, \ldots, X_h) \tag{2.31}$$

by performing in (2.13) the following substitution:

$$\mathrm{tr}V^{n_1} \cdots \mathrm{tr}V^{n_h} \quad \longleftrightarrow \quad \frac{1}{h!}\left(X_1^{n_1} \cdots X_h^{n_h} + \text{permutations}\right). \tag{2.32}$$

Using as input data only the mirror curve $W(\mathrm{e}^x, \mathrm{e}^y) = 0$ and the so called *Bergmann kernel* of this curve[15], one can define a set of invariants $\mathcal{W}_{g,h}(x_1, ..., x_h)$ associated to it using what is called the *topological recursion*. The BKMP proposal is that the quantities

$$\int^{x_1} \mathrm{d}x_1' \cdots \int^{x_h} \mathrm{d}x_h' \, \mathcal{W}_{g,h}(x_1', ..., x_h') \tag{2.33}$$

correspond to $F_{g,h}(X_1, ..., X_h)$ after application of the mirror maps. Also, the closed free energies $F_g$ can be obtained from $\mathcal{W}_{g,1}(x)$ by taking an appropriate residue (and application of the mirror map). The precise formulas for the topological recursion in the context of mirror curves for toric CY threefolds are given in [57]. A proof for the BKMP proposal was given in [58], and further formalised in [59, 60].

Why does this work? The full artillery of topological recursion was introduced by Eynard, Chekhov and Orentin in [61–63]. It can be applied quite abstractly to any

[14] This result is valid for a D–brane on a non-compact cycle of $X$.

[15] The Bergmann kernel $B(q,p)\mathrm{d}q\mathrm{d}p$ is a meromorphic differential on the curve with a unique double pole at $q = p$ and vanishing residue. Here $q, p$ are local coordinates of two points on the curve.

curve, but it was at first introduced in order to solve loop equations giving $n$–point correlators of large $N$ matrix models. The appearance of matrix models in the game does not seem to be fortuitous. Indeed, the B–model topological strings have been related to large $N$ matrix models quite before the BKMP proposal. An example is the Dijkgraaf–Vafa proposal in [64], relating the B–model topological strings on a certain family of targets, to large $N$ hermitian matrix models. Another example closer to our setup is a family of matrix models associated to Chern–Simons theory [65, 66], which was related to topological strings on $A_n$ fibrations over $\mathbb{P}^1$ through Gopakumar–Vafa large $N$ duality [46].

The behaviour of the open string aptitudes under symplectic frame transformation has been established in [47], which generalizes the results of [52] of the open sector.

## 2.4 Refinement and quantum periods

One aspect of topological strings which we did not mention yet, is that of refinement. To understand the refined topological string, let us go back to the Gopakumar–Vafa expansion of the free energies (2.16), and their relation to the BPS numbers $\mathcal{N}^{\mathbf{d}}_{j_L,j_R}$. The expression (2.16) can be seen as a generating function for the Gopakumar–Vafa invariants $n^{\mathbf{d}}_g$. But the BPS numbers themselves are topological invariants of our toric CY threefolds[16], so we may expect that there exists a refined version of (2.16) which encodes $\mathcal{N}^{\mathbf{d}}_{j_L,j_R}$ themselves, not only their combination giving $n^{\mathbf{d}}_g$. Moreover, some sort of refinement is also expected from a sort of gauge theory–topological string correspondence. Indeed, for specific families of local CY threefolds (usually resolutions of singularities modelled by toric geometries), the topological free energy is related to the instanton partition function of a corresponding $\mathcal{N} = 2$ gauge theory. This is the "geometric engineering" approach to gauge theories [67]. However, the instanton partition function of the gauge theory (on the so called $\Omega$–background) found by Nekrasov [68] has more parameters than the topological string. In particular it has two "equivariant rotation parameters" $\epsilon_1, \epsilon_2$, and the topological string partition function is obtained when setting $\epsilon_1 = -\epsilon_2 = \mathrm{i}g_s$. Keeping $\epsilon_1$ and $\epsilon_2$ independent thus looks like a "refinement" of the free energy from the topological string perspective. This refinement was first proposed in [69]. In terms of the BPS numbers $\mathcal{N}^{\mathbf{d}}_{j_L,j_R}$, the refined topological string free energy (or rather its instanton

[16] This is not true for compact CY manifolds, only for local (non-compact) ones as our toric cases.

part generalizing (2.16)) reads

$$F_{\text{ref}}(\epsilon_1,\epsilon_2,\mathbf{t}) = \sum_{\mathbf{d}}\sum_{w=1}^{\infty}\sum_{j_L,j_R}(-1)^{2j_L+2j_R}\mathcal{N}^{\mathbf{d}}_{j_L,j_R} \cdot\frac{1}{w}\frac{\chi_{j_L}\left(\mathrm{e}^{w\frac{\epsilon_1-\epsilon_2}{2}}\right)\chi_{j_R}\left(\mathrm{e}^{w\frac{\epsilon_1+\epsilon_2}{2}}\right)}{(\mathrm{e}^{w\epsilon_1/2}-\mathrm{e}^{-w\epsilon_1/2})(\mathrm{e}^{w\epsilon_2/2}-\mathrm{e}^{-w\epsilon_2/2})}\mathrm{e}^{-w\mathbf{d}\cdot\mathbf{t}}, \tag{2.34}$$

where

$$\chi_j(q) = \frac{q^{2j+1}-q^{-2j-1}}{q^1-q^{-1}}. \tag{2.35}$$

This refinement was also incorporated into the topological vertex approach in [70], which results in the *refined topological vertex*, allowing for an efficient computation of (2.34) in many cases. Indeed, as defined in [70], it can be used for toric Calabi–Yau manifolds which engineer gauge theories. Other toric cases can be obtained from these by "blowdown" procedures.[17]

As already mentioned, taking the limit

$$\epsilon_1 \to \mathrm{i}g_s, \qquad \epsilon_2 \to -\mathrm{i}g_s, \tag{2.36}$$

in (2.34), we recover the Gopakumar–Vafa representation of the standard, unrefined topological string partition function. There is another limit which will be of interest to us: the *Nekrasov–Shatashvili limit* (or NS limit). On the gauge theory side, the NS limit is very interesting: it is proposed in [30] that in the NS limit, 4 or 5 dimensional $\mathcal{N}=2$ gauge theory partition functions (as well as other gauge theoretic quantities) can be used to write down exact quantization conditions (and other spectral quantities) for various quantum integrable systems.[18] We therefore conclude that the NS limit of the refined topological string free energy will have something to say about the corresponding quantum integrable systems. This limit can be taken as multiplying (2.34) by $\mathrm{i}\epsilon_2$ and taking

$$\epsilon_1 \to \mathrm{i}\hbar, \qquad \epsilon_2 \to 0. \tag{2.37}$$

[17] This is the case for the example where the toric Calabi-Yau is local $\mathbb{P}^2$. However, this case (and other related cases) can also be computed with a modified version of the refined topological vertex algorithm [71].

[18] The 4 dimensional case was well understood in [30], but the 5 dimensional case, related to "relativistic" integrable systems, was better elucidated by various authors in the following years. For example, the exact quantization conditions for the relativistic Toda lattice are given in [72], and they contain an extra non-perturbative part (in $\hbar$) not predicted in [30]. This extra part guarantees the "modular double structure" [21] expected in such relativistic integrable systems [73].

The parameter $\hbar$ is the "Planck constant" in the quantum integrable system. In this limit, we obtain:

$$F_{\rm NS}^{\rm inst}(\mathbf{t},\hbar)=\sum_{\mathbf{d}}\sum_{w=1}^{\infty}\sum_{j_L,j_R}(-1)^{2j_L+2j_R}\mathcal{N}^{\mathbf{d}}_{j_L,j_R}\frac{1}{2w^2}\frac{\sin\frac{(2j_L+1)w\hbar}{2}\sin\frac{(2j_R+1)w\hbar}{2}}{\sin^3\frac{w\hbar}{2}}\mathrm{e}^{-w\mathbf{d}\cdot\mathbf{t}}. \tag{2.38}$$

This will be an important function in later sections. The full *Nekrasov–Shatashvili (NS) free energy* is

$$F_{\rm NS}(\mathbf{t},\hbar)=F_{\rm NS}^{\rm pert}(\mathbf{t},\hbar)+F_{\rm NS}^{\rm inst}(\mathbf{t},\hbar)\ , \tag{2.39}$$

where

$$F_{\rm NS}^{\rm pert}(\mathbf{t},\hbar)=\frac{1}{6\hbar}\sum_{i,j,k=1}^{n_\Sigma}a_{ijk}t_it_jt_k+\left(\hbar+\frac{4\pi^2}{\hbar}\right)\sum_{i=1}^{n_\Sigma}b_i^{\rm NS}t_i. \tag{2.40}$$

The $a_{ijk}$ are the same as in (2.11), and $b_i^{\rm NS}$ are geometry dependent constants which can be obtained by other means. The NS free energy can also be expanded in powers of $\hbar$, to get an expansion similar to the standard free energy:

$$F_{\rm NS}(\mathbf{t},\hbar)=\sum_{n=0}^{\infty}F_g^{\rm NS}(\mathbf{t})\hbar^{2g-1}. \tag{2.41}$$

An interesting aspect of topological strings in the NS limit is the following. It was found in [74] that the small $\hbar$ expansion (2.41) can be obtained quite directly from the mirror curve itself. Their method (partially motivated by an argument involving deformed matrix models) consists in taking the mirror curve $W(\mathrm{e}^x,\mathrm{e}^y)$ and replacing $y\to-\mathrm{i}\hbar\partial_x$. Then, one can consider formal solutions $\Phi(x)$ of

$$W(\mathrm{e}^x,\mathrm{e}^{-\mathrm{i}\hbar\partial_x})\Phi(x)=0 \tag{2.42}$$

in the small $\hbar$ expansion. Since in our cases $W(\mathrm{e}^x,\mathrm{e}^y)$ is a polynomial in $\mathrm{e}^x$ and $\mathrm{e}^y$, the above equation yields a difference equation for $\Phi(x)$. As for Schrödinger equations in stationary quantum mechanics, the WKB ansatz can be used to construct formal solutions

$$\Phi(x)=\exp\left(\frac{1}{-\mathrm{i}\hbar}\int^x p(x',\hbar)\mathrm{d}x'\right), \tag{2.43}$$

where

$$p(x,\hbar)=\sum_{n\geq0}(-\mathrm{i}\hbar)^n p_n(x). \tag{2.44}$$

is a formal series in $\hbar$. The $p_n(x)$ are solved recursively by plugging (2.43) in (2.42). It is easily seen that $p_0(x)$ is nothing but the function $y(x)$ on the mirror curve $W(\mathrm{e}^x,\mathrm{e}^y)=0$. So the $p_n(x)$ for $n>0$ can be seen as "quantum corrections" of it. Then, the periods

$$t_i(\hbar)\propto\int_{\mathcal{A}_i}p(x,\hbar)\,\mathrm{d}x,\qquad\qquad\partial_{t_i}F(\hbar)\propto\int_{\mathcal{B}_i}p(x,\hbar)\,\mathrm{d}x, \tag{2.45}$$

are interpreted as "quantum corrections" of the periods in (2.29). The quantum period over the $\mathcal{A}_i$ one-cycles is interpreted as a *quantum mirror map* which can be inverted to yield $z_k = z_k(\mathbf{t}, \hbar)$. Through this procedure, we get a quantum corrected version $F(\mathbf{t}, \hbar)$ of the genus zero free energy $F_0(\mathbf{t})$. The point is that $F(\hbar)$ is precisely the small $\hbar$ expansion of the NS free energy (2.38)![19] Interestingly, if we work using an expansion in another variable (which is a combination of the $z_k$), this procedure can be made exact in $\hbar$ [6, 74]. In this case, we retrieve the form (2.38).

This relationship between the NS topological free energy and quantum periods is quite suggestive. It sharply suggests to quantize the spectral curve (doing basically $y \to -\mathrm{i}\hbar\partial_x$), and take the resulting spectral operator seriously. This is basically the philosophy underlying the TS/ST correspondence, which will be the topic of the next section. The idea that the quantum mirror curve should be related to topological strings was already put forward in [75]. Here, we already learned that the small $\hbar$ limit of the spectral operator contains information about the NS limit in topological strings. But what about, for example, the large $\hbar$ limit (if it exists)? Also, exact spectral quantities for finite $\hbar$ cannot be straightforwardly obtained from their small $\hbar$ expansions, which are asymptotic and often non Borel-resummable as many examples in quantum mechanics teach us. Could topological strings help us in obtaining exact results at finite $\hbar$ for, say, traces or eigenvalues of the quantized mirror curve – or some associated operator? Or its eigenfunctions? These questions are best approached in the context of the TS/ST correspondence.

[19] For this, the choice of the symplectic basis for the homological cycles $\mathcal{A}_i, \mathcal{B}_i$ should correspond to the "large radius" frame, as discussed after eq. (2.25).

# Chapter 3

# Quantized mirror curves and the TS/ST correspondence

The Topological String/Spectral Theory (TS/ST) correspondence, or GHM (Grassi-Hatsuda-Mariño) conjecture, relates the spectral quantities of a trace class operator acting $L^2(\mathbb{R})$, to quantities appearing naturally in the context of topological strings.

In this chapter, we first define the operator, as well as the various interesting spectral quantities associated to it. Then we state the TS/ST correspondence of [2] and its higher genus version [16]. In the end, we provide a useful representation of the trace class operator in terms of an explicit integral kernel. Except for some details in the last section, nothing presented here is original material.

## 3.1 Spectral theory of quantized mirror curves

As seen in the previous section, to every toric CY threefold $X$ there corresponds a mirror curve. It is defined in $\mathbb{C}^* \times \mathbb{C}^*$ by the vanishing locus of a function $W(\mathrm{e}^x, \mathrm{e}^y)$, which is polynomial in $\mathrm{e}^x$ and $\mathrm{e}^y$. It also contains the parameters $z_k$, which appear in the constraints (2.20). Combinations of these will appear in the function $W(\mathrm{e}^x, \mathrm{e}^y)$ as coefficients in front of the monomials. These coefficients come in two categories. There are $g_W$ of them which we call the "true" moduli

$$\kappa_i, \qquad i = 1, \dots, g_W, \tag{3.1}$$

where $g_W$ is the genus of the mirror curve. The remaining $r_W$ ones are called the mass parameters

$$m_k, \qquad k = 1, \dots, r_W. \tag{3.2}$$

We will see below how to distinguish them. The total number of moduli is

$$n_W = g_W + r_W. \tag{3.3}$$

Let us first focus on the case where we have $g_W = 1$, that is, when the mirror curve has genus one. This is the case when the toric CY threefold $X$ is a local (almost) del Pezzo CY threefold, which is defined as the total space of the anti-canonical bundle on a toric (almost) del Pezzo surface $S$. In this case, we call the geometry "local $S$". The important aspect is that we only have one true modulus $\kappa$. By overall rescaling the relation $W(\mathrm{e}^x, \mathrm{e}^y) = 0$ and shifting $x, y$ by constant terms, we can put it in the following canonical form:

$$\mathcal{O}(\mathrm{e}^x, \mathrm{e}^y) + \kappa = 0. \tag{3.4}$$

Generically, $\mathcal{O}(\mathrm{e}^x, \mathrm{e}^y)$ is written as

$$\mathcal{O}(\mathrm{e}^x, \mathrm{e}^y) = \sum_{i=1}^{m+3} \exp\left(\nu_1^{(i)} x + \nu_2^{(i)} y + f_i(m_1, \ldots, m_{r_W})\right), \tag{3.5}$$

where the vectors $\boldsymbol{\nu}^{(i)} = (\nu_1^{(i)}, \nu_2^{(i)})$ satisfy

$$\sum_{i=1}^{m+3} Q_i^k \boldsymbol{\nu}^{(i)} = 0, \qquad k = 1, \ldots, m, \tag{3.6}$$

and $f_i$ are appropriate functions of the mass parameters. Several sets of vectors $\boldsymbol{\nu}^{(i)}$ can be found that satisfy the condition (3.6) for fixed charge vectors $Q_i^k$. These different sets correspond to different parametrizations of the mirror curve. We will privilege the parameterization where both the monomials $\mathrm{e}^x$ and $\mathrm{e}^y$ appear, and are not multiplied by any mass parameter (this is arbitrary but will prove useful). Here are some examples which will be relevant later on:

| | |
|---|---|
| local $\mathbb{P}^2$: | $\mathcal{O}_{\mathbb{P}^2}(\mathrm{e}^x, \mathrm{e}^y) = \mathrm{e}^x + \mathrm{e}^y + \mathrm{e}^{-x-y}$ |
| local $\mathbb{P}^1 \times \mathbb{P}^1 = \mathbb{F}_0$: | $\mathcal{O}_{\mathbb{P}^1\times\mathbb{P}^1}(\mathrm{e}^x, \mathrm{e}^y) = \mathrm{e}^x + \mathrm{e}^y + m_{\mathbb{F}_0}\mathrm{e}^{-x} + \mathrm{e}^{-y}$ |
| local $\mathbb{F}_2$: | $\mathcal{O}_{\mathbb{F}_2}(\mathrm{e}^x, \mathrm{e}^y) = \mathrm{e}^x + \mathrm{e}^y + m_{\mathbb{F}_2}\mathrm{e}^{-x} + \mathrm{e}^{-2x-y}$ |

**Table 3.1:** Functions $\mathcal{O}(\mathrm{e}^x, \mathrm{e}^y)$ defining the mirror curve of some toric CY threefolds.

The first example has no mass parameter, whereas the to other examples have one mass parameter.

Let us look in more details at the example of local $\mathbb{P}^1 \times \mathbb{P}^1$. The toric geometry is defined by two charge vectors $Q^1 = (1, 0, 1, 0, -2)$ and $Q^2 = (0, 1, 0, 1, -2)$. So

$m = 2$ in (2.19-2.21). The mirror curve is given by $0 = \sum_i \mathrm{e}^{y_i}$ with the constraints

$$\begin{aligned} \log z_1 &= \sum_{i=1}^{5} Q_i^1 y_i = y_1 + y_3 - 2y_5, \\ \log z_2 &= \sum_{i=1}^{5} Q_i^2 y_i = y_2 + y_4 - 2y_5. \end{aligned} \tag{3.7}$$

This can by used to express $y_3$ and $y_4$ in terms of the other $y_i$. By defining

$$x = y_1 - y_5 - \frac{1}{2}\log z_2, \qquad y = y_2 - y_5 - \frac{1}{2}\log z_2, \tag{3.8}$$

we obtain

$$0 = \sum_{i}^{5} \mathrm{e}^{y_i} = z_2^{1/2}\mathrm{e}^{y_5}\left(\mathrm{e}^{x} + \mathrm{e}^{y} + \frac{z_1}{z_2}\mathrm{e}^{-x} + \mathrm{e}^{-y} + \frac{1}{z_2^{1/2}}\right). \tag{3.9}$$

The vanishing of this expression gives the mirror curve. The vectors $\boldsymbol{\nu}^{(i)}$ in this case are

$$\boldsymbol{\nu}^{(1)} = \begin{pmatrix} 1 \\ 0 \end{pmatrix}, \quad \boldsymbol{\nu}^{(2)} = \begin{pmatrix} 0 \\ 1 \end{pmatrix}, \quad \boldsymbol{\nu}^{(3)} = \begin{pmatrix} -1 \\ 0 \end{pmatrix}, \quad \boldsymbol{\nu}^{(4)} = \begin{pmatrix} 0 \\ -1 \end{pmatrix}. \tag{3.10}$$

There is an easy way of identifying which parameters are "true" moduli. Each monomial $\mathrm{e}^{n_1 x + n_2 y}$ appearing in the relation $W(\mathrm{e}^x, \mathrm{e}^y) = 0$ defines a point in $(n_1, n_2) \in \mathbb{Z}^2$. These points form the Newton polytope of the mirror curve in $\mathbb{Z}^2$. Moduli multiplying monomials lying strictly inside the convex hull of the Newton polytope are "true" moduli, whereas those multiplying monomials on the border of it are mass parameters. So in this example, we identify the "true" modulus $\kappa = z_2^{-1/2}$ and the mass parameter $m_{\mathbb{F}_0} = z_1/z_2$.

We are ready to quantize the mirror curve. We promote $x$ and $y$ to self-adjoint Heisenberg operators $\mathsf{x}, \mathsf{y}$ which satisfy the commutation relation

$$[\mathsf{x}, \mathsf{y}] = \mathrm{i}\hbar. \tag{3.11}$$

The operator $\mathsf{O}$ is given by replacing $x$ and $y$ in $\mathcal{O}(\mathrm{e}^x, \mathrm{e}^y)$ by their corresponding operators:

$$\mathsf{O} = \mathcal{O}(\mathrm{e}^{\mathsf{x}}, \mathrm{e}^{\mathsf{y}}). \tag{3.12}$$

Ordering ambiguities are resolved by requiring the resulting operator to be self-adjoint (more precisely, we use the Weyl prescription). For example, $\mathrm{e}^{n_1 x + n_2 y}$ becomes

$$\mathrm{e}^{n_1 \mathsf{x} + n_2 \mathsf{y}} = \mathrm{e}^{\frac{\mathrm{i} n_1 n_2 \hbar}{2}} \mathrm{e}^{n_1 \mathsf{x}} \mathrm{e}^{n_2 \mathsf{y}} = \mathrm{e}^{-\frac{\mathrm{i} n_1 n_2 \hbar}{2}} \mathrm{e}^{n_2 \mathsf{y}} \mathrm{e}^{n_1 \mathsf{x}}, \tag{3.13}$$

where we used the Baker–Campbell–Hausdorff formula to obtain the last two expressions. The most important operator turns out not to be $\mathsf{O}$ itself, but its inverse

$$\rho = \mathsf{O}^{-1}. \tag{3.14}$$

As conjectured in [2] and proved in many cases in [10] (see also [76]), $\rho$ is an operator acting on $L^2(\mathbb{R})$ which is positive self-adjoint and trace class for appropriate values of the mass parameters. Therefore, we have for all integers $n \geq 1$ that

$$\mathrm{Tr}\rho^n < \infty. \tag{3.15}$$

This is a stronger condition than what we have for Hilbert–Schmidt operators, where this condition needs only to be satisfied for $n \geq 2$. The nice feature of positive self-adjoint trace class operators is that they have a discrete positive spectrum. In bra-ket notation,

$$\rho|\psi_n\rangle = \mathrm{e}^{-E_n}|\psi_n\rangle, \qquad n = 0, 1, 2, \ldots \tag{3.16}$$

Here $\mathrm{e}^{-E_n}$ are the eigenvalues of $\rho$ and $|\psi_n\rangle$ the corresponding normalized eigenfunctions, which form a normalized orthogonal basis of $L^2(\mathbb{R})$. The eigenfunctions can be represented in the $|x\rangle$ basis satisfying $\mathsf{x}|x\rangle = x|x\rangle$, as

$$\psi_n(x) = \langle x|\psi_n\rangle. \tag{3.17}$$

It can of course be represented in other bases, for example in the eigenbasis of any linear combination of $\mathsf{x}$ and $\mathsf{y}$.[1] By denoting $\kappa_n = -\mathrm{e}^{E_n}$, the inverse of the eigenvalue equation is

$$(\mathsf{O} + \kappa_n)|\psi_n\rangle = 0. \tag{3.18}$$

In other terms, it is a kind of "quantum equivalent" for the definition of the mirror curve (3.4). On functions of $x$ the operator $\mathsf{y}$ can be represented as $-\mathrm{i}\hbar\partial_x$. Supposing that $\psi(x)$ can be expanded in Taylor series, the exponentiated derivative acts as a shift operator. Therefore, we can write the equation $(\mathsf{O} + \kappa)|\psi\rangle = 0$ as a difference equation for the function $\psi(x)$:

$$\begin{aligned} -\kappa\psi(x) &= \sum_{i=1}^{m+3} \mathrm{e}^{f_i(m_1,\ldots,m_{r_W}) - \frac{\mathrm{i}\hbar}{2}\nu_1^{(i)}\nu_2^{(i)}} \mathrm{e}^{\nu_1^{(i)}x} \mathrm{e}^{-\mathrm{i}\hbar\nu_2^{(i)}\partial_x}\psi\,(x) \\ &= \sum_{i=1}^{m+3} \mathrm{e}^{f_i(m_1,\ldots,m_{r_W}) - \frac{\mathrm{i}\hbar}{2}\nu_1^{(i)}\nu_2^{(i)}} \mathrm{e}^{\nu_1^{(i)}x} \psi\left(x - \mathrm{i}\hbar\nu_2^{(i)}\right). \end{aligned} \tag{3.19}$$

[1] For example, the eigenfunction $\tilde{\psi}_n(y) = \langle y|\psi_n\rangle$ represented in the basis $|y\rangle$ of $\mathsf{y}$ is the Fourier transform of $\psi_n(x)$.

When going from the first to the second line, we assumed that the Taylor expansion of $\psi(x)$ exists and converges to the function. That is, we assumed analyticity of the function $\psi(x)$ in the appropriate strip around the real line.

An important spectral quantity associated to trace class operators is the *Fredholm determinant*. The Fredholm determinant of $\rho$ is given by

$$\Xi(\kappa) = \det(1 + \kappa\rho). \tag{3.20}$$

It is an entire function of $\kappa$ and, by evaluating the determinant in the eigenbasis, it can be given by the eigenvalues of $\rho$ as

$$\Xi(\kappa) = \prod_{n=0}^{\infty}(1 + \kappa \mathrm{e}^{-E_n}). \tag{3.21}$$

We see that it vanishes when $\kappa = -\mathrm{e}^{E_n}$. So its vanishing locus gives the spectrum of $\rho$. Since it is an entire function, it can be given as a series near $\kappa = 0$ as

$$\Xi(\kappa) = 1 + \sum_{N=1}^{\infty} \kappa^N Z(N). \tag{3.22}$$

We will call $Z(N)$ the *fermionic spectral traces*. A famous result by Fredholm expresses the quantities $Z(N)$ in terms of the integral kernel $\rho(x_1, x_2) = \langle x_1|\rho|x_2\rangle$:

$$Z(N) = \frac{1}{N!}\int_{\mathbb{R}^N} \rho \begin{pmatrix} x_1 & x_2 & \dots & x_N \\ x_1 & x_2 & \dots & x_N \end{pmatrix} \mathrm{d}x_1 \cdots \mathrm{d}x_N, \tag{3.23}$$

where we use the notation

$$\rho \begin{pmatrix} x_1 & x_2 & \dots & x_N \\ y_1 & y_2 & \dots & y_N \end{pmatrix} = \det_{i,j=1,\dots,N} \rho(x_i, y_j). \tag{3.24}$$

As for the eigenfunction, we can use other bases than $|x\rangle$ to write down these formulas. In a basis which is unitarily equivalent to $|x\rangle$ (like the eigenbasis related to linear combinations of $\mathsf{x}$ and $\mathsf{y}$), these formulas do not change. Of course, the traces themselves can be represented as integrals of $\rho(x_1, x_2)$:

$$\mathrm{Tr}\rho^n = \int_{\mathbb{R}^N} \rho(x_1, x_2)\rho(x_2, x_3)\cdots\rho(x_N, x_1)\mathrm{d}x_1 \cdots \mathrm{d}x_N. \tag{3.25}$$

Another interesting quantity in spectral theory is the *resolvent* operator

$$\mathsf{R} = \frac{1}{\kappa + \mathsf{O}} = \frac{\rho}{1 + \kappa\rho}. \tag{3.26}$$

Its trace is a generating function of the traces of $\rho$

$$\mathrm{Tr}\,\mathsf{R} = \sum_{n=0}^{\infty}(-1)^n \kappa^n \mathrm{Tr}\rho^{n+1} \tag{3.27}$$

and it is related to the Fredholm determinant:

$$\int_0^\kappa \mathrm{Tr}\,\mathsf{R} = \mathrm{Tr}\log(1+\kappa\rho) = \log\det(1+\kappa\rho) = \log\Xi(\kappa). \tag{3.28}$$

Equating the small $\kappa$ expansions on both sides yields a relation between $Z(N)$ and the traces $\mathrm{Tr}\rho^n$:

$$Z(N) = \sum_{\boldsymbol{\ell}\,|\,\sum_i i\ell_i = N} (-1)^N \prod_i \frac{(-1)^{\ell_i}(\mathrm{Tr}\rho^i)^{\ell_i}}{\ell_i!\, i^{\ell_i}}. \tag{3.29}$$

The sum is over the partitions of $N$ in frequency representation. In the normalized eigenbasis of $\rho$, the resolvent can be expanded as a sum of projectors:

$$\mathsf{R} = \sum_{n=0}^{\infty} \frac{|\psi_n\rangle\langle\psi_n|}{\kappa + \mathrm{e}^{E_n}}. \tag{3.30}$$

The resolvent kernel is

$$R(x_1, x_2; \kappa) = \langle x_1|\mathsf{R}|x_2\rangle = \sum_{n=0}^{\infty} \frac{\psi^*(x_2)\psi(x_1)}{\kappa + \mathrm{e}^{E_n}}. \tag{3.31}$$

Another important result in Fredholm theory is an expression for $R(x_1, x_2; \kappa)$ in terms of the integral kernel $\rho(x_1, x_2)$:

$$D(x, t; \kappa) = \Xi(\kappa) R(x, t; \kappa) = \sum_{N=0}^{\infty} \kappa^N B_N(x, t), \tag{3.32}$$

where

$$B_N(x, t) = \frac{1}{N!} \int_{\mathbb{R}^N} \rho \begin{pmatrix} x & x_1 & x_2 & \dots & x_N \\ t & x_1 & x_2 & \dots & x_N \end{pmatrix} \mathrm{d}x_1 \cdots \mathrm{d}x_N. \tag{3.33}$$

The integrand is an $(N+1) \times (N+1)$ determinant of the form (3.24). The quantity $D(x, t; \kappa)$ contains information on the eigenfunctions. Supposing that the $n^{\text{th}}$ eigenvalue is non-degenerate, we obtain from (3.31):

$$\psi_n(x)\psi_n^*(t) = \lim_{\kappa \to -\mathrm{e}^{E_n}} (\kappa + \mathrm{e}^{E_n}) \frac{D(x, t; \kappa)}{\Xi(\kappa)} = \frac{1}{\Xi'(-\mathrm{e}^{E_n})} D(x, t; -\mathrm{e}^{E_n}). \tag{3.34}$$

So, an unnormalized eigenfunction can be obtained using only $D(x, t; \kappa)$:

$$\frac{\psi_n(x)}{\psi_n(x_0)} = \frac{D(x, t_0; -\mathrm{e}^{E_n})}{D(x_0, t_0; -\mathrm{e}^{E_n})}. \tag{3.35}$$

This is Fredholm's expression for the eigenfunctions in terms of the determinant $D(x, t; \kappa)$. It requires prior knowledge of the integral kernel $\rho(x_1, x_2)$ and of the spectrum.

Until now, we focused on the quantization of mirror curves of genus $g_W = 1$, containing one "true" modulus. We now extend this construction to the case of higher genus mirror curves. This was done in [16], providing a formulation of the TS/ST conjecture at higher genus. In the higher genus case, the quantization procedure itself is the same; the difference lies in the presence of $g_W$ "true" moduli $\kappa_i$, corresponding to $g_W$ canonical forms for the mirror curve:

$$\mathcal{O}_i(\mathrm{e}^x, \mathrm{e}^y) + \kappa_i = 0, \qquad i = 1, ..., g_W. \tag{3.36}$$

We can write

$$\mathcal{O}_i(\mathrm{e}^x, \mathrm{e}^y) + \kappa_i = \mathcal{O}_i^{(0)}(\mathrm{e}^x, \mathrm{e}^y) + \sum_{j=1}^{g_W} \mathcal{P}_{ij}(\mathrm{e}^x, \mathrm{e}^y)\kappa_j, \tag{3.37}$$

where $\mathcal{P}_{ii}(\mathrm{e}^x, \mathrm{e}^y) = 1$, and $\mathcal{O}_i^{(0)}(\mathrm{e}^x, \mathrm{e}^y)$ contains the terms with mass parameters. The $\mathcal{P}_{ii}(\mathrm{e}^x, \mathrm{e}^y) = 1$ are precisely the overall multiplicative factors to go from one canonical form to another:

$$\mathcal{O}_i(\mathrm{e}^x, \mathrm{e}^y) + \kappa_i = \mathcal{P}_{ij}(\mathrm{e}^x, \mathrm{e}^y)\left(\mathcal{O}_j(\mathrm{e}^x, \mathrm{e}^y) + \kappa_j\right), \tag{3.38}$$

for $i, j = 1, \ldots, g_W$ (no summation over repeated indices!).

To illustrate this, let us look at the geometry which will be our prime example for the higher genus case: the resolution of $\mathbb{C}^3/\mathbb{Z}_5$. The charge vectors of this toric CY threefold are given by $Q^1 = (-3, 1, 1, 1, 0)$ and $Q^1 = (0, 1, 1, -2, 1)$. The constraints are

$$\begin{aligned} \log z_1 &= \sum_{i=1}^{5} Q_i^1 y_i = -3y_1 + y_2 + y_3 + y_4, \\ \log z_2 &= \sum_{i=1}^{5} Q_i^2 y_i = y_1 - 2y_2 + y_5. \end{aligned} \tag{3.39}$$

We use this to express $y_3$ and $y_5$ in terms of the other coordinates. By defining

$$\begin{aligned} x &= -y_1 + y_4 - \frac{1}{5}\log z_1 + \frac{2}{5}\log z_2, \\ y &= 3y_1 - 2y_4 - y_3 + \frac{4}{5}\log z_1 - \frac{3}{5}\log z_2, \end{aligned} \tag{3.40}$$

we obtain

$$0 = \sum_i^5 \mathrm{e}^{y_i} = z_1^{1/5} z_2^{3/5} \mathrm{e}^{y_4} \left( \mathrm{e}^x + \mathrm{e}^y + \mathrm{e}^{-3x-y} + \frac{1}{z_1^{2/5} z_2^{1/5}} \mathrm{e}^{-x} + \frac{1}{z_1^{1/5} z_2^{3/5}} \right). \tag{3.41}$$

The vanishing of the bracket gives the mirror curve. By the Newton polytope argument, we deduce that the two combinations of $z_i$ appearing in the bracket are "true"

moduli. So we call them $\kappa_1 = z_1^{-2/5} z_2^{-1/5}$ and $\kappa_2 = z_1^{-1/5} z_2^{-3/5}$. The two canonical forms of the curve are:

$$\begin{aligned} 0 &= \mathcal{O}_1(\mathrm{e}^x, \mathrm{e}^y) + \kappa_1 = \mathrm{e}^{2x} + \mathrm{e}^{x+y} + \mathrm{e}^{-2x-y} + \mathrm{e}^x \kappa_2 + \kappa_1, \\ 0 &= \mathcal{O}_2(\mathrm{e}^x, \mathrm{e}^y) + \kappa_2 = \mathrm{e}^x + \mathrm{e}^y + \mathrm{e}^{-3x-y} + \mathrm{e}^{-x} \kappa_1 + \kappa_2. \end{aligned} \tag{3.42}$$

Also, $\mathcal{P}_{12}(\mathrm{e}^x, \mathrm{e}^y) = \mathrm{e}^x, \mathcal{P}_{21}(\mathrm{e}^x, \mathrm{e}^y) = \mathrm{e}^{-x}$. It is sometimes useful to perform a linear change of variables for the first parametrization using

$$\begin{pmatrix} x \\ y \end{pmatrix} = \begin{pmatrix} -1 & -1 \\ 2 & 1 \end{pmatrix} \begin{pmatrix} x' \\ y' \end{pmatrix}, \tag{3.43}$$

such that the first canonical form is written as

$$0 = \tilde{\mathcal{O}}_1(\mathrm{e}^{x'}, \mathrm{e}^{y'}) + \kappa_1 = \mathrm{e}^{x'} + \mathrm{e}^{y'} + \mathrm{e}^{-2x'-2y'} + \mathrm{e}^{-x'-y'} \kappa_2 + \kappa_1. \tag{3.44}$$

As we will see later, the usefulness of this new parametrization comes from the fact that the first three terms have the form $\mathrm{e}^{x'} + \mathrm{e}^{y'} + \mathrm{e}^{-mx'-ny'}$ (this is already the case for the second parametrization).

Quantization by promoting $x, y$ to the usual self-adjoint Heisenberg operators $\mathsf{x}, \mathsf{y}$ yields $g_W$ different operators

$$\mathsf{O}_i = \mathcal{O}_i(\mathrm{e}^{\mathsf{x}}, \mathrm{e}^{\mathsf{y}}). \tag{3.45}$$

Each of these operators corresponds to the "quantization" of its corresponding modulus $\kappa_i$ (which takes the role of the "quantized energy" in stationary quantum mechanics), whereas the other $\kappa_j$ behave as parameters. Again, if the mass parameters and the other "true" moduli satisfy certain positivity conditions, the operators

$$\rho_i = \mathsf{O}_i^{-1} \tag{3.46}$$

acting on $L^2(\mathbb{R})$ are expected to be trace class operators (the proof for many known cases are covered by [10, 76]). Each of these operators has a discrete spectrum $\mathrm{e}^{-E_n^{(i)}}$ with $n = 0, 1, 2, \ldots$ The corresponding eigenfunctions $|\psi_n^{(i)}\rangle$ satisfy for $i = 1, \ldots, g_W$:

$$\left(\mathsf{O}_i + \kappa_i^{(n)}\right) |\psi_n^{(i)}\rangle = 0. \tag{3.47}$$

The operator counterpart of (3.38) is

$$\mathsf{O}_i + \kappa_i = \mathsf{P}_{ij}^{1/2} \left(\mathsf{O}_j + \kappa_j\right) \mathsf{P}_{ij}^{1/2}, \qquad i, j = 1, \ldots, g_W, \tag{3.48}$$

where $\mathsf{P}_{ij} = \mathcal{P}_{ij}(\mathrm{e}^{\mathsf{x}}, \mathrm{e}^{\mathsf{y}})$. This implies the following relation between the eigenfunctions of the different operators:

$$|\psi_n^{(j)}\rangle = \mathsf{P}_{ij}^{1/2} |\psi_n^{(i)}\rangle. \tag{3.49}$$

The most important spectral quantity for the genus one case was the Fredholm determinant. We need to find an appropriate generalization for it for the higher genus case. It was proposed in [16] that the following generalization is the good quantity to consider (at least in the context of the TS/ST correspondence). Define the operators $\mathsf{A}_{ij}$ through

$$\mathsf{O}_i + \kappa_i = \mathsf{O}_i^{(0)} \left( 1 + \sum_{j=1}^{g_W} \kappa_j \mathsf{A}_{ij} \right). \tag{3.50}$$

The operator $\mathsf{O}_i^{(0)}$ is the quantum version of $\mathcal{O}_i^{(0)}$ appearing in (3.37). The generalized Fredholm determinant is

$$\Xi(\boldsymbol{\kappa}) = \det \left( 1 + \sum_{j=1}^{g_W} \kappa_j \mathsf{A}_{ij} \right). \tag{3.51}$$

It would seem that this definition depends on which operator $\mathsf{O}_i$ we singled out in (3.50), but actually it turns out that it is independent of this choice [16]. So the generalized Fredholm determinant $\Xi(\boldsymbol{\kappa})$ really depends on the curve itself and not on its particular parametrization related to $\mathsf{O}_i$. The zero locus of $\Xi(\boldsymbol{\kappa})$ defines a codimension one submanifold in the $g_W$ dimensional space of "true" moduli $\kappa_i$. This submanifold gives the spectrum of all the operators $\mathsf{O}_i$ for $i = 1, \ldots, g_W$. For example, if we fix concrete values for $\kappa_j$, $j \neq i$ and let $\kappa_i$ vary, the intersection of this line with the zero locus submanifold gives the spectrum $\kappa_i^{(n)}$, $n = 0, 1, 2, \ldots$ of the operator $\mathsf{O}_i$ (where the $\kappa_j$ take the given numerical values). Similarly to the genus one case, the generalized spectral determinant can also be expanded at small $\boldsymbol{\kappa}$:

$$\Xi(\boldsymbol{\kappa}) = \sum_{N_1 \geq 0} \cdots \sum_{N_{g_W} \geq 0} Z(\boldsymbol{N}) \kappa_1^{N_1} \cdots \kappa_{g_W}^{N_{g_W}}, \tag{3.52}$$

with $Z(0, \ldots, 0) = 1$. The expression of $Z(\boldsymbol{N})$ in terms of the integral kernels $A_{ij}(x_1, x_2) = \langle x_1 | \mathsf{A}_{ij} | x_2 \rangle$ can be found in [16].

## 3.2 Direct numerical computations

It will be very useful to have purely numerical techniques to obtain the eigenvalues and the eigenfunctions of the operator $\mathsf{O}$. We will use the Rayleigh–Ritz method with the basis of the harmonic oscillator with frequency $\omega$ and centred at $x_0$. This is a very convenient orthonormal basis of $L^2(\mathbb{R})$. We denote it by $|c_k^{(\omega, x_0)}\rangle$ for $k = 0, 1, 2, \ldots$:

$$c_k^{(\omega, x_0)}(x) = \langle x | c_k^{(\omega, x_0)} \rangle = \frac{\omega^{1/4}}{\pi^{1/4} \sqrt{2^k k!}} \mathrm{e}^{-\frac{\omega}{2}(x - x_0)^2} H_k(\omega^{1/2}(x - x_0)). \tag{3.53}$$

For each operator, the optimal values for $\omega$ and $x_0$ can be chosen using various variational arguments. A normalizable eigenfunction can be expanded in this basis:

$$|\psi\rangle = \sum_{k\geq 0} v_k |c_k^{(\omega,x_0)}\rangle. \tag{3.54}$$

We truncate the basis to the first $N$ elements: $k = 0, 1, \ldots, N-1$. For an operator $\mathsf{O}$, we have the eigenvalue equation

$$\mathsf{O}|\psi\rangle = -\kappa|\psi\rangle. \tag{3.55}$$

Projecting this on the truncated basis, we obtain

$$\sum_{\ell=0}^{N-1} O_{k\ell} v_\ell = -\kappa v_k, \qquad\qquad k = 0, 1, \ldots, N-1, \tag{3.56}$$

where the matrix elements $O_{k\ell}$ of the $N \times N$ matrix $O$ are

$$O_{k\ell} = \langle c_k^{(\omega,x_0)} | \mathsf{O} | c_\ell^{(\omega,x_0)} \rangle. \tag{3.57}$$

This is an eigenvalue equation for a finite matrix which can be solved by numerical methods. To compute exact matrix elements for quantized mirror curves, we use (see for example [9, 20]):

$$\langle c_k^{(\omega,x_0)} | \mathrm{e}^{a\mathsf{x}} \mathrm{e}^{b\mathsf{y}} | c_\ell^{(\omega,x_0)} \rangle = \mathrm{e}^{ax_0} \sqrt{2^{k+\ell} k! \ell!}\, \mathrm{e}^{|\zeta|^2 + \frac{\mathrm{i}\hbar}{2} ab} \zeta^k \bar{\zeta}^\ell \sum_{n=0}^{\min(k,\ell)} \frac{2^n}{(k-n)!(\ell-n)! n!} \frac{1}{(2|\zeta|)^{2n}}, \tag{3.58}$$

with

$$\zeta = \frac{1}{2\sqrt{\omega}}(a + \mathrm{i}\hbar\omega b), \qquad\qquad a, b \in \mathbb{R}. \tag{3.59}$$

To find an approximation for the optimal parameters $\omega, x_0$, we can use various variational principles, for example the one proposed in [77] (which proposes to fix the parameters by requiring the extremization of the trace $\sum_{k=0}^{N-1} O_{kk}$).

This gives a quick and efficient way of approximating numerically the eigenvalues $-\kappa_n = \mathrm{e}^{E_n}$ and the eigenfunctions $|\psi_n\rangle$ which are built from the solutions of the eigenvalue equation (3.56). Convergence can be checked, and an approximate estimation of the error can be obtained by varying the size $N$ of the matrix $O_{k\ell}$. All the numerical diagonalizations are performed using the built-in algorithms of *Mathematica 11*.

## 3.3 The TS/ST correspondence

The Topological String/Spectral Theory (TS/ST) correspondence is a precise conjectural proposal which expresses some of the spectral quantities defined in the previous

section in terms of topological string quantities defined in chapter 2. The "core" proposal was put forward in [2] ($g_W = 1$) and in [16] ($g_W > 1$) and gives an expression for the Fredholm determinant $\Xi(\boldsymbol{\kappa})$ of the quantized mirror curve operator in terms of the refined topological string free energy in the standard and in the NS limit. This means that the spectral data related to the Fredholm determinant (such as the traces or eigenvalues of the operators) are essentially encoded in the BPS invariants $\mathcal{N}^{\mathbf{d}}_{j_L,j_R}$ of the corresponding geometry. The origin of the idea of TS/ST goes back to the study of non-perturbative aspects of ABJ(M) theory [5–7, 78, 79], which was previously found to be related to topological string on local $\mathbb{P}^1 \times \mathbb{P}^1$ [3, 80]. Inspired by the insights of [6] and the early partial proposal of [8], it was brought to its final form in [2, 16]. Let us state the correspondence.

We introduce the "chemical potentials" $\mu_i$, given by

$$\kappa_i = \mathrm{e}^{\mu_i}, \qquad i = 1, \ldots, g_W. \tag{3.60}$$

As we saw in the above examples, their relation to the parameters $z_i$ is geometry dependent. We write it as

$$-\log z_i = \sum_{j=1}^{g_W} C_{ij}\mu_j - \sum_{k=1}^{r_W} \alpha_{ik} \log m_k, \qquad i = 1, \ldots, n_W. \tag{3.61}$$

One can choose the parameters $z_i$ in such a way that they correspond to the "true" moduli for $i = 1, \ldots, g_W$ and to mass parameters for $i = g_W + 1, \ldots, n_W$. In this case, the first $g_W$ rows of the matrix $C_{ij}$ form an invertible square matrix. As we saw around eq. (2.3), the mirror map relates the parameters $z_i$ to the Kähler parameters $t_i$ of the CY threefold, and it is given by period integrals on the mirror curve. It has the form[2]

$$-t_i = \log z_i + \tilde{\Pi}_i(\boldsymbol{z}), \qquad i = 1, \ldots, n_W, \tag{3.62}$$

where $\tilde{\Pi}_i(\boldsymbol{z})$ is a power series in $z_i$. What we will actually need is the *quantum mirror map* [74]. This has the form

$$-t_i(\hbar) = \log z_i + \tilde{\Pi}_i(\boldsymbol{z}, \hbar), \qquad i = 1, \ldots, n_W, \tag{3.63}$$

As we mentioned around eq. (2.45), it can be obtained exactly in $\hbar$ if we work in a small $\boldsymbol{z}$ expansion. Of course, $\tilde{\Pi}_i(\boldsymbol{z}, \hbar)$ reduces to $\tilde{\Pi}_i(\boldsymbol{z})$ for $\hbar = 0$. In terms of $\mu_i$, this relation can be written as

$$t_i(\boldsymbol{\mu}, \hbar) = \sum_{j=1}^{g_W} C_{ij}\mu_j - \sum_{k=1}^{r_W} \alpha_{ik} \log m_k + \mathcal{O}(\mathrm{e}^{-\mu}), \tag{3.64}$$

[2] This form is expected, since the "large radius" frame is precisely the frame where the $A$–periods have this behaviour for small $z_i$.

where $\mathcal{O}(\mathrm{e}^{-\mu})$ is $\hbar$ dependent, but exponentially suppressed in the $\mu_i$. We now define the *modified grand potential* $J(\boldsymbol{\mu},\hbar)$. It also depends on the mass parameters $m_i$, but we do not write this dependence explicitly. It is made of two pieces,

$$J(\boldsymbol{\mu},\hbar) = J^{\mathrm{WKB}}(\boldsymbol{\mu},\hbar) + J^{\mathrm{WS}}(\boldsymbol{\mu},\hbar), \tag{3.65}$$

which we will now define. Firstly, let us recall the NS free energy $F_{\mathrm{NS}}(\mathbf{t},\hbar)$ given in eq. (2.39):

$$F_{\mathrm{NS}}(\mathbf{t},\hbar) = F^{\mathrm{pert}}_{\mathrm{NS}}(\mathbf{t},\hbar) + F^{\mathrm{inst}}_{\mathrm{NS}}(\mathbf{t},\hbar)\ , \tag{3.66}$$

where

$$\begin{aligned} F^{\mathrm{inst}}_{\mathrm{NS}}(\mathbf{t},\hbar) &= \sum_{\mathbf{d}}\sum_{w=1}^{\infty}\sum_{j_L,j_R}(-1)^{2j_L+2j_R}\mathcal{N}^{\mathbf{d}}_{j_L,j_R}\frac{1}{2w^2}\frac{\sin\frac{(2j_L+1)w\hbar}{2}\sin\frac{(2j_R+1)w\hbar}{2}}{\sin^3\frac{w\hbar}{2}}\mathrm{e}^{-w\mathbf{d}\cdot\mathbf{t}}, \\ F^{\mathrm{pert}}_{\mathrm{NS}}(\mathbf{t},\hbar) &= \frac{1}{6\hbar}\sum_{i,j,k=1}^{n_\Sigma}a_{ijk}t_it_jt_k + \left(\hbar+\frac{4\pi^2}{\hbar}\right)\sum_{i=1}^{n_\Sigma}b_i^{\mathrm{NS}}t_i. \end{aligned} \tag{3.67}$$

The WKB part of the modified grand potential is given by

$$\begin{aligned} J^{\mathrm{WKB}}(\boldsymbol{\mu},\hbar) = \Bigg(&\sum_{i=1}^{n_W}\frac{t_i}{2\pi}\frac{\partial F_{\mathrm{NS}}(\mathbf{t},\hbar)}{\partial t_i} + \frac{\hbar^2}{2\pi}\frac{\partial}{\partial\hbar}\left(\frac{F_{\mathrm{NS}}(\mathbf{t},\hbar)}{\hbar}\right) \\ &+\frac{2\pi}{\hbar}\sum_{i=1}^{n_W}(b_i+b_i^{\mathrm{NS}})t_i + A(\boldsymbol{m},\hbar)\Bigg)\Bigg|_{\mathbf{t}=\mathbf{t}(\mu,\hbar)}. \end{aligned} \tag{3.68}$$

In the above, $b_i$ are the numbers appearing in the genus 1 topological string free energy (2.11), and $b_i^{\mathrm{NS}}$ are similar quantities for the NS limit. The constant $A(\boldsymbol{m},\hbar)$ is geometry dependent. It is only known in closed form for some simple geometries, but this is not too problematic as we will see later on. Secondly, let us define

$$F_{\mathrm{GV}}(\mathbf{t},g_s) = \sum_{g=0}^{\infty}\sum_{\mathbf{d}}\sum_{w=1}^{\infty}n_g^{\mathbf{d}}\frac{1}{w}\left(2\sin\frac{wg_s}{2}\right)^{2g-2}\mathrm{e}^{-w\mathbf{d}\cdot\mathbf{t}}. \tag{3.69}$$

This is precisely the Gopakumar–Vafa free energy (2.16) for the standard topological string. We recall that the Gopakumar–Vafa invariants $n_g^{\mathbf{d}}$ can be built from the BPS invariants $\mathcal{N}^{\mathbf{d}}_{j_L,j_R}$ through (2.17). The WS (worldsheet) part of the modified grand potential is given by

$$J^{\mathrm{WS}}(\boldsymbol{\mu},\hbar) = F_{\mathrm{GV}}\left(\frac{2\pi}{\hbar}\mathbf{t}(\hbar) + \mathrm{i}\pi\mathbf{B}, \frac{4\pi^2}{\hbar}\right). \tag{3.70}$$

The vector $\mathbf{B}$ is the so called "B field", which depends on the geometry under consideration. It is a vector of integers satisfying

$$(-1)^{2j_L+2j_R+1} = (-1)^{\mathbf{B}\cdot\mathbf{d}}. \tag{3.71}$$

for all $j_L, j_R$ and $\mathbf{d}$ such that $\mathcal{N}^{\mathbf{d}}_{j_L,j_R}$ do not vanish. We see that the almost only essential data used to build the modified grand potential $J(\boldsymbol{\mu}, \hbar)$ are enumerative invariants of CY threefolds in the form of the $\mathcal{N}^{\mathbf{d}}_{j_L,j_R}$.

Let us mention that this construction applies for any value of $\hbar \geq 0$.[3] However, care must be taken in the case where

$$\frac{\hbar}{2\pi} \in \mathbb{Q}. \tag{3.72}$$

In this case, both $J^{\mathrm{WKB}}(\boldsymbol{\mu}, \hbar)$ and $J^{\mathrm{WS}}(\boldsymbol{\mu}, \hbar)$ have poles. But the polar behaviours are exactly of opposite signs, so the sum $J(\boldsymbol{\mu}, \hbar)$ is well defined even in the rational case. This is the topological string equivalent of the HMO cancellation mechanism first noticed in the context of ABJM theory [5].

Now that we introduced all the ingredients, we are ready to state the TS/ST conjecture. The Fredholm determinant of the operator(s) associated to the mirror curve $W(\mathrm{e}^x, \mathrm{e}^y) = 0$ defining the geometry $\widetilde{X}$ is given by the modified grand potential built using the enumerative invariants of $X$, as:

$$\Xi(\boldsymbol{\kappa}) = \sum_{\mathbf{n} \in \mathbb{Z}^{g_W}} \mathrm{e}^{J(\boldsymbol{\mu} + 2\pi \mathrm{i} \mathbf{n}, \hbar)}. \tag{3.73}$$

Let us remark that the contribution $J^{\mathrm{WS}}(\boldsymbol{\mu}, \hbar)$ in the modified grand-potential is non-perturbative in small $\hbar$. So in some sense, the TS/ST conjecture claims that in the spectral theory of our operators, the quantum mechanical non-perturbative completion of the WKB quantities is controlled by the topological strings.

We saw that the vanishing locus of the Fredholm determinant $\Xi(\boldsymbol{\kappa})$ gives the spectrum of our operators. So the conjecture solves for the spectrum. This can be implemented very concretely for example numerically, and was checked in many examples. In some cases, the expression for $\Xi(\boldsymbol{\kappa})$ can even be written down exactly, as for example in the so called "self-dual" case where $\hbar = 2\pi$ [2, 7, 16, 82]. Also, the small $\kappa$ expansion of the Fredholm determinant gives the fermionic spectral traces. So the conjecture gives a prediction for the spectral traces, which have been verified in many cases, both numerically and exactly [2, 7, 16, 82, 83]. Again, exact results were mostly obtained for the self-dual case. But the conjecture could be checked to high numerical precision in many settings.

By giving an explicit formula for the Fredholm determinant, the TS/ST correspondence sorts out the eigenvalue part of the eigenproblem related to our operators. One obvious question is, can the TS/ST correspondence say something about the eigenfunctions? The answer to this is the topic of chapter 5, and it will have something to do with open string amplitudes. But before that, we will investigate that

[3] There is also very strong evidence that this is also valid for complex $\hbar$ [81].

large $\hbar$ limit of the proposal. More precisely, we will see that the fermionic traces $Z(N)$ can be written down as convergent matrix models, and their free energy in the limit $N, \hbar \to \infty$ precisely reproduces the closed string free energy of the (standard) topological string. Thus, the TS/ST conjecture predicts a new family of matrix models for the topological string on toric CY threefolds.

Let us also mention that there is a different, though related conjecture which expresses the quantization condition for the spectrum. It was proposed first in [31]. Then, it was generalized in [18, 72] to the higher genus cases, and the relation between the generalized quantizations conditions and some quantum integrable systems were clarified. That proposal is close in spirit to the Nekrasov-Shatashvili quantization conditions [30], and it only involves the refined topological string free energy in the NS limit (or equivalently, the quantum periods of the mirror curve). It can also be seen as part of the TS/ST correspondence scheme, although the spectral problem which it solves is not the same. Indeed, as we will elaborate more in section 5.6, those quantization conditions actually give the spectrum of an underlying integrable system. In particular, the spectrum obtained from those quantization conditions is a subset of the solutions given by $\Xi(\boldsymbol{\kappa}) = 0$. For the genus one case, the two proposals give the same spectrum. Indeed, it was shown in [84] that the formulations of [2] and [31] are equivalent for the genus one cases, and consistent for higher genus cases (see also [85, 86] for further work along this direction). Let us mention though that the spectral determinant gives more spectral data than just the eigenvalues. It also gives exact expressions for the fermionic spectral traces $Z(\boldsymbol{N})$.

To go further, we should have a better characterization of the operator $\rho$ in (3.14) (or $\rho_i$ and $\mathsf{A}_{ij}$ for the higher genus case). We will see in the next section that an exact integral kernel $\rho(x_1, x_2)$ can be written down in many cases.

## 3.4 Explicit integral kernels

To write down explicit kernels for $\rho$ or $\mathsf{A}_{ij}$, we need a function called the *Faddeev quantum dilogarithm* $\Phi_b(u)$ (also called modular quantum dilogarithm). It was introduced by Faddeev in [21], and was used by Kashaev and Mariño to invert quantum mirror curves in [10]. The results of [10] were extended in [12] and [83]. Here we give a further generalization of this construction (see [13]).

But first, let us define $\Phi_b(u)$ and give some of its main properties. Let $b$ be a complex number such that $\mathrm{Re}(b) > 0$. The Faddeev quantum dilogarithm can be defined through the integral formula

$$\Phi_b(u) = \exp\left(\int_{\mathbb{R}+\mathrm{i}0} \frac{\mathrm{e}^{-2\mathrm{i}yu}}{4\sinh(by)\sinh(y/b)} \frac{\mathrm{d}y}{y}\right). \tag{3.74}$$

The integration path is along the real axis and avoids the pole at $y = 0$ by going above it. This integral definition converges in the strip

$$|\mathrm{Im}(u)| < \mathrm{Re}\left(\frac{b+b^{-1}}{2}\right), \tag{3.75}$$

but it can be analytically continued to a meromorphic function on the complex plane. It has manifestly the following property:

$$\Phi_b(u) = \Phi_{b^{-1}}(u). \tag{3.76}$$

Also, for real or unitary $b$, we have

$$\overline{\Phi_b(u)} = \frac{1}{\Phi_b(\bar{u})}. \tag{3.77}$$

By deforming the path of integration and picking up the residue at $y = 0$, it is easy to obtain the following formula:

$$\Phi_b(-u) = \mathrm{e}^{\mathrm{i}\pi u^2 + \frac{\mathrm{i}\pi}{12}\left(b^2+b^{-2}\right)} \frac{1}{\Phi_b(u)}. \tag{3.78}$$

Its asymptotic behaviour is [87]

$$\begin{aligned} &\Phi_b(u) \sim 1, && \text{when} \quad \mathrm{Re}(u) \ll 0, \\ &\Phi_b(u) \sim \mathrm{e}^{\mathrm{i}\pi u^2 + \frac{\mathrm{i}\pi}{12}\left(b^2+b^{-2}\right)}, && \text{when} \quad \mathrm{Re}(u) \gg 0. \end{aligned} \tag{3.79}$$

It obeys the following difference equation

$$\frac{\Phi_b\left(u - \frac{\mathrm{i}b}{2}\right)}{\Phi_b\left(u + \frac{\mathrm{i}b}{2}\right)} = 1 + \mathrm{e}^{2\pi b u}, \tag{3.80}$$

which can be obtained from the definition, using that

$$\int_{\mathbb{R}+\mathrm{i}0} \frac{\mathrm{e}^{-2\mathrm{i}uy}}{2\sinh(y/b)} \frac{\mathrm{d}y}{y} = -\log(1 + \mathrm{e}^{2\pi b u}). \tag{3.81}$$

Similarly, using property (3.76), we have the dual difference equation

$$\frac{\Phi_b\left(u - \frac{\mathrm{i}}{2b}\right)}{\Phi_b\left(u + \frac{\mathrm{i}}{2b}\right)} = 1 + \mathrm{e}^{\frac{2\pi u}{b}}. \tag{3.82}$$

The poles and the zeros of the Faddeev quantum dilogarithm $\Phi_b(u)$ are located at

$$\begin{aligned} &\text{poles}: && u = \mathrm{i}\frac{b+b^{-1}}{2} + mib + nib^{-1}, \\ &\text{zeros}: && u = -\mathrm{i}\frac{b+b^{-1}}{2} - mib - nib^{-1}, \end{aligned} \tag{3.83}$$

for $m, n \in \mathbb{Z}_{\geq 0}$.

The following small $b$ asymptotic expansion is also useful [87]:

$$\log \Phi_b\left(\frac{q}{2\pi b}\right) \sim \frac{1}{2\pi \mathrm{i}} \sum_{k=0}^{\infty} (-4\pi^2)^k b^{4k-2} \frac{(2^{-2k+1}-1)B_{2k}}{(2k)!} \mathrm{Li}_{2-2k}(-\mathrm{e}^q), \tag{3.84}$$

where $B_k$ are the Bernoulli numbers and $\mathrm{Li}_k(z)$ are the polylogarithms. Using property (3.76), there is the corresponding large $b$ expansion:

$$\log \Phi_b\left(\frac{bq}{2\pi}\right) \sim \frac{1}{2\pi \mathrm{i}} \sum_{k=0}^{\infty} (-4\pi^2)^k b^{-4k+2} \frac{(2^{-2k+1}-1)B_{2k}}{(2k)!} \mathrm{Li}_{2-2k}(-\mathrm{e}^q). \tag{3.85}$$

We now show how to factorize and invert some quantized mirror curves using $\Phi_b(u)$. Let us introduce canonically commuting hermitian operators $\mathsf{q}$ and $\mathsf{p}$ such that

$$[\mathsf{q}, \mathsf{p}] = \mathrm{i} \times 2\pi b^2. \tag{3.86}$$

with $b$ real. Suppose that $A, B$ are real numbers and $\epsilon < 0$. For any function $f(z)$ which is analytic over the strip $-2\pi b^2 A - \epsilon < \mathrm{Im}(z) < \epsilon$ if $A$ is positive, or $-\epsilon < \mathrm{Im}(z) < -2\pi b^2 A + \epsilon$ if $A$ is negative, we have

$$\mathrm{e}^{A\mathsf{p}} f(\mathsf{q}) \mathrm{e}^{-A\mathsf{p}} = f(\mathsf{q} - 2\pi \mathrm{i} b^2 A), \tag{3.87}$$

which follows from Taylor expanding $f(\mathsf{q})$.[4] Similarly, for any function $g(z)$ which is analytic on the strip $-\epsilon < \mathrm{Im}(z) < 2\pi b^2 B + \epsilon$ if $B$ is positive, or $2\pi b^2 B - \epsilon < \mathrm{Im}(z) < \epsilon$ if $B$ is negative, we have

$$\mathrm{e}^{B\mathsf{q}} g(\mathsf{p}) \mathrm{e}^{-B\mathsf{q}} = g(\mathsf{p} + 2\pi \mathrm{i} b^2 B). \tag{3.88}$$

Using these formulas, we can write the operator versions of the difference equations obeyed by the Faddeev quantum dilogarithm. From (3.80), we obtain

$$\begin{aligned} 1 + \mathrm{e}^{\mathsf{q}} &= \mathrm{e}^{\mathsf{p}/2} \Phi_b\left(\frac{1}{2\pi b}\mathsf{q}\right) \mathrm{e}^{-\mathsf{p}/2} \mathrm{e}^{-\mathsf{p}/2} \frac{1}{\Phi_b\left(\frac{1}{2\pi b}\mathsf{q}\right)} \mathrm{e}^{\mathsf{p}/2} \\ &= \mathrm{e}^{-\mathsf{p}/2} \frac{1}{\Phi_b\left(\frac{1}{2\pi b}\mathsf{q}\right)} \mathrm{e}^{\mathsf{p}/2} \mathrm{e}^{\mathsf{p}/2} \Phi_b\left(\frac{1}{2\pi b}\mathsf{q}\right) \mathrm{e}^{-\mathsf{p}/2}. \end{aligned} \tag{3.89}$$

From this, we obtain the formula for the conjugation of the exponentials by the unitary operator given by the dilogarithm:

$$\begin{aligned} \Phi_b\left(\frac{1}{2\pi b}\mathsf{q}\right) \mathrm{e}^{-\mathsf{p}} \frac{1}{\Phi_b\left(\frac{1}{2\pi b}\mathsf{q}\right)} &= \mathrm{e}^{-\mathsf{p}} + \mathrm{e}^{\mathsf{q}-\mathsf{p}}, \\ \frac{1}{\Phi_b\left(\frac{1}{2\pi b}\mathsf{q}\right)} \mathrm{e}^{\mathsf{p}} \Phi_b\left(\frac{1}{2\pi b}\mathsf{q}\right) &= \mathrm{e}^{\mathsf{p}} + \mathrm{e}^{\mathsf{q}+\mathsf{p}}. \end{aligned} \tag{3.90}$$

[4] Use that $\mathrm{e}^{A\mathsf{p}} \mathsf{q}^n \mathrm{e}^{-A\mathsf{p}} = (\mathsf{q} - 2\pi b^2 A)^n$, which is easily shown algebraically.

Repeated applications of these formulas on the operator $1+\mathrm{e}^{\mathsf{p}}$ yields the basic operator relations which we then map to the desired quantum curve using a linear canonical transformation. This provides a factorization of the quantum curve, in which form it is straightforward to invert. We remark that in this procedure the explicit use of the pentagon identity for the Faddeev quantum dilogarithm (as in for example [12]) is not needed. We also remark that this procedure in itself cannot yield all the genus one quantum curves (let alone higher genus quantum curves). Indeed, it can be seen that all the curves that we can reach with this method have a Newton polytope (in variables $\mathrm{e}^{\mathsf{x}}$ and $\mathrm{e}^{\mathsf{y}}$) which can be mapped by a linear canonical transformation to a trapezoid (a 4-gon with two parallel sides), or its degenerate case, the triangle.

The cases which interest us can be regrouped into the single formula obtain by three successive applications of (3.90). This provides a generalization of all the cases studied in [10, 12, 83]. Let us define

$$\begin{aligned} F(\mathsf{q}) &= \mathrm{e}^{-\frac{1}{2(m+n+1)}\mathsf{q}} \frac{\Phi_b\left(\frac{\mathsf{q}+\alpha}{2\pi b} - \frac{n}{2(m+n+1)}\mathrm{i}b\right)\Phi_b\left(\frac{\mathsf{q}+\beta}{2\pi b} - \frac{n}{2(m+n+1)}\mathrm{i}b\right)}{\Phi_b\left(\frac{\mathsf{q}+\gamma}{2\pi b} + \frac{m+1}{2(m+n+1)}\mathrm{i}b\right)}, \\ F^*(\mathsf{q}) &= \mathrm{e}^{-\frac{1}{2(m+n+1)}\mathsf{q}} \frac{\Phi_b\left(\frac{\mathsf{q}+\gamma}{2\pi b} - \frac{m+1}{2(m+n+1)}\mathrm{i}b\right)}{\Phi_b\left(\frac{\mathsf{q}+\alpha}{2\pi b} + \frac{n}{2(m+n+1)}\mathrm{i}b\right)\Phi_b\left(\frac{\mathsf{q}+\beta}{2\pi b} + \frac{n}{2(m+n+1)}\mathrm{i}b\right)}, \end{aligned} \tag{3.91}$$

where $\alpha, \beta, \gamma, m, n$ are real numbers. Then, we have the following factorization:

$$\begin{aligned} F(\mathsf{q})\mathrm{e}^{\frac{n}{m+n+1}\mathsf{p}}(1+\mathrm{e}^{\mathsf{p}})F^*(\mathsf{q}) &= \mathrm{e}^{\mathsf{x}} + \mathrm{e}^{\mathsf{y}} + \mathrm{e}^{\gamma}\mathrm{e}^{-m\mathsf{x}-n\mathsf{y}} \\ &\quad + (\mathrm{e}^{\alpha}+\mathrm{e}^{\beta})\mathrm{e}^{-(m+1)\mathsf{x}-(n-1)\mathsf{y}} + \mathrm{e}^{\alpha+\beta}\mathrm{e}^{-2(m+1)\mathsf{x}-(2n-1)\mathsf{y}}. \end{aligned} \tag{3.92}$$

The relation between $\mathsf{q}, \mathsf{p}$ and $\mathsf{x}, \mathsf{y}$ is

$$\begin{pmatrix} \mathsf{q} \\ \mathsf{p} \end{pmatrix} = \begin{pmatrix} -(m+1) & -n \\ 1 & -1 \end{pmatrix} \begin{pmatrix} \mathsf{x} \\ \mathsf{y} \end{pmatrix}, \tag{3.93}$$

so

$$[\mathsf{x}, \mathsf{y}] = \mathrm{i}\hbar, \qquad \hbar = \frac{2\pi b^2}{m+n+1}. \tag{3.94}$$

The advantage of the factorized form (3.92) is that it is easily inverted:

$$\begin{aligned} \rho &\equiv \left[\mathrm{e}^{\mathsf{x}} + \mathrm{e}^{\mathsf{y}} + \mathrm{e}^{\gamma}\mathrm{e}^{-m\mathsf{x}-n\mathsf{y}} + (\mathrm{e}^{\alpha}+\mathrm{e}^{\beta})\mathrm{e}^{-(m+1)\mathsf{x}-(n-1)\mathsf{y}} + \mathrm{e}^{\alpha+\beta}\mathrm{e}^{-2(m+1)\mathsf{x}-(2n-1)\mathsf{y}}\right]^{-1} \\ &= \frac{1}{F^*(\mathsf{q})}\left(\frac{\mathrm{e}^{\frac{m+1}{m+n+1}\mathsf{p}}}{1+\mathrm{e}^{\mathsf{p}}}\right)\frac{1}{F(\mathsf{q})}. \end{aligned} \tag{3.95}$$

The three-term family of [10] is recovered in the limit $\alpha, \beta \to -\infty$ and $\gamma = 0$. From (3.79), we see that the limit on $\alpha, \beta$ "kills" some of the $\Phi_b$, and we obtain:

$$\begin{aligned}\rho_{m,n} &= \left[\mathrm{e}^{\mathsf{x}} + \mathrm{e}^{\mathsf{y}} + \mathrm{e}^{-m\mathsf{x}-n\mathsf{y}}\right]^{-1} \\ &= \frac{\mathrm{e}^{\frac{1}{2(m+n+1)}\mathsf{q}}}{\Phi_b\left(\frac{\mathsf{q}}{2\pi b} - \frac{m+1}{2(m+n+1)}\mathrm{i}b\right)} \left(\frac{\mathrm{e}^{\frac{m+1}{m+n+1}\mathsf{p}}}{1+\mathrm{e}^{\mathsf{p}}}\right) \Phi_b\left(\frac{\mathsf{q}}{2\pi b} + \frac{m+1}{2(m+n+1)}\mathrm{i}b\right) \mathrm{e}^{\frac{1}{2(m+n+1)}\mathsf{q}}.\end{aligned} \tag{3.96}$$

The particular case where $(m, n) = (1, 1)$ gives the local $\mathbb{P}^2$ operator, see Table 3.1.

The four term family of [83] is recovered when $\beta \to -\infty$ and $\gamma = 0$:

$$\begin{aligned}\rho_{m,n;\alpha} &= \left[\mathrm{e}^{\mathsf{x}} + \mathrm{e}^{\mathsf{y}} + \mathrm{e}^{-m\mathsf{x}-n\mathsf{y}} + \mathrm{e}^{\alpha}\mathrm{e}^{-(m+1)\mathsf{x}-(n-1)\mathsf{y}}\right]^{-1} \\ &= \mathrm{e}^{\frac{1}{2(m+n+1)}\mathsf{q}} \frac{\Phi_b\left(\frac{\mathsf{q}+\alpha}{2\pi b} + \frac{n}{2(m+n+1)}\mathrm{i}b\right)}{\Phi_b\left(\frac{\mathsf{q}}{2\pi b} - \frac{m+1}{2(m+n+1)}\mathrm{i}b\right)} \left(\frac{\mathrm{e}^{\frac{m+1}{m+n+1}\mathsf{p}}}{1+\mathrm{e}^{\mathsf{p}}}\right) \\ &\qquad \times \frac{\Phi_b\left(\frac{\mathsf{q}}{2\pi b} + \frac{m+1}{2(m+n+1)}\mathrm{i}b\right)}{\Phi_b\left(\frac{\mathsf{q}+\alpha}{2\pi b} - \frac{n}{2(m+n+1)}\mathrm{i}b\right)} \mathrm{e}^{\frac{1}{2(m+n+1)}\mathsf{q}}.\end{aligned} \tag{3.97}$$

It is a perturbation of the three term operator. The particular case where $(m, n) = (0, 1)$ and $\mathrm{e}^{\alpha} = m_{\mathbb{F}_0}$ gives the local $\mathbb{F}_0$ (= local $\mathbb{P}^1 \times \mathbb{P}^1$) operator studied in [12], see Table 3.1.

A third subfamily of four term operators can be extracted from the general case. Let us set $\beta = -\alpha$ and send $\gamma \to -\infty$. We obtain

$$\begin{aligned}\tilde{\rho}_{m,n;\alpha} &= \left[\mathrm{e}^{\mathsf{x}} + \mathrm{e}^{\mathsf{y}} + \mathrm{e}^{-2(m+1)\mathsf{x}-(2n-1)\mathsf{y}} + 2\cosh(\alpha)\mathrm{e}^{-(m+1)\mathsf{x}-(n-1)\mathsf{y}}\right]^{-1} \\ &= \mathrm{e}^{\frac{1}{2(m+n+1)}\mathsf{q}} \Phi_b\left(\frac{\mathsf{q}+\alpha}{2\pi b} + \frac{n}{2(m+n+1)}\mathrm{i}b\right) \Phi_b\left(\frac{\mathsf{q}-\alpha}{2\pi b} + \frac{n}{2(m+n+1)}\mathrm{i}b\right) \\ &\qquad \times \left(\frac{\mathrm{e}^{\frac{m+1}{m+n+1}\mathsf{p}}}{1+\mathrm{e}^{\mathsf{p}}}\right) \\ &\qquad \times \frac{1}{\Phi_b\left(\frac{\mathsf{q}+\alpha}{2\pi b} - \frac{n}{2(m+n+1)}\mathrm{i}b\right) \Phi_b\left(\frac{\mathsf{q}-\alpha}{2\pi b} - \frac{n}{2(m+n+1)}\mathrm{i}b\right)} \mathrm{e}^{\frac{1}{2(m+n+1)}\mathsf{q}}.\end{aligned} \tag{3.98}$$

The special case with $(m, n) = (0, 1)$ and $2\cosh(\alpha) = m_{\mathbb{F}_2}$ gives the local $\mathbb{F}_2$ operator, see Table 3.1. There is a relationship between the two families of four term operators: one of the families can be retrieved from the other by a unitary conjugation, a constant shift of $\mathsf{q}$ and an overall rescaling:

$$\mathrm{e}^{\frac{\alpha}{m+n+1}} \rho_{m,n;2\alpha}\Big|_{\mathsf{q}\to\mathsf{q}-\alpha} = \mathsf{U}^{-1}\, \tilde{\rho}_{m,n;\alpha}\, \mathsf{U}, \tag{3.99}$$

with

$$\mathsf{U} = \Phi_b\left(\frac{\mathsf{q}-\alpha}{2\pi b} + \frac{m+1}{2(m+n+1)}\mathrm{i}b\right)\Phi_b\left(\frac{\mathsf{q}-\alpha}{2\pi b} - \frac{n}{2(m+n+1)}\mathrm{i}b\right). \tag{3.100}$$

Unitarity of the operator $\mathsf{U}$ is a consequence of the operator version of (3.77) (we recall that $m, n, \alpha, b$ are real numbers). A particular case of the above relation is that the operators of local $\mathbb{P}^1\times\mathbb{P}^1$ and local $\mathbb{F}_2$ are unitarily equivalent. This mirrors the fact that the corresponding CY threefolds (and their BPS numbers) are known to be intimately related [82].

For appropriate restrictions on the values of $\alpha, \beta, \gamma$ and $m, n$, the operator $\rho$ is of trace class. This can be shown rigorously along the lines of [10], where the proof is given for the family of three-term operators and the local $\mathbb{F}_0$ operator. The essential point to prove this is that the functions $1/F^*(q)$ and $1/F(q)$ in (3.95) decrease fast enough when $q \to \pm\infty$ for the appropriate restrictions on the values of $\alpha, \beta, \gamma$ and $m, n$.

The factorized form of our operator allows us to obtain the integral kernel of the inverse operator (3.95). Let us introduce the basis $|q\rangle$ diagonalising the operator $\mathsf{q}$,

$$\mathsf{q}|q\rangle = q|q\rangle. \tag{3.101}$$

and the $|p\rangle$ basis diagonalising $\mathsf{p}$:

$$\mathsf{p}|p) = p|p). \tag{3.102}$$

We have

$$\langle q|p) = \frac{1}{2\pi b}\mathrm{e}^{\mathrm{i}\frac{qp}{2\pi b^2}}. \tag{3.103}$$

In the $q$ basis, the integral kernel of (3.95) can be obtained for $0 < \frac{m+1}{m+n+1} < 1$. It is given by

$$\begin{aligned}\rho(q_1,q_2) &= \langle q_1|\frac{1}{F^*(\mathsf{q})}\left(\frac{\mathrm{e}^{\frac{m+1}{m+n+1}\mathsf{p}}}{1+\mathrm{e}^{\mathsf{p}}}\right)\frac{1}{F(\mathsf{q})}|q_2\rangle \\ &= \frac{1}{F^*(q_1)}\frac{1}{F(q_2)}\frac{1}{4\pi^2b^2}\int_{-\infty}^{\infty}\mathrm{d}p\,\mathrm{e}^{\frac{i}{2\pi b^2}p(q_1-q_2)}\frac{\mathrm{e}^{\frac{m+1}{m+n+1}p}}{1+\mathrm{e}^{p}} \\ &= \frac{1}{F^*(q_1)}\frac{1}{4\pi b^2\cosh\left(\frac{q_1-q_2}{2b^2}-\mathrm{i}\pi C\right)}\frac{1}{F(q_2)},\end{aligned} \tag{3.104}$$

where

$$C = \frac{m-n+1}{2(m+n+1)}. \tag{3.105}$$

This is the explicit form of the integral kernel of $\rho$, in variables which are related by (3.93) to the initial mirror curve variables.

For later use, it is convenient to perform a rescaling of the our variables by defining

$$\nu_i = b^{-2} q_i, \tag{3.106}$$

as well as

$$\alpha = b^2 \tilde{\alpha}, \qquad \beta = b^2 \tilde{\beta}, \qquad \gamma = b^2 \tilde{\gamma}. \tag{3.107}$$

The integral kernel of $\rho$ transforms as a density:

$$\rho(\nu_1, \nu_2) \mathrm{d}\nu_2 = \rho(q_1, q_2) \mathrm{d}q_2. \tag{3.108}$$

It is of the form

$$\rho(\nu_1, \nu_2) = \frac{1}{2\pi} \frac{\mathrm{e}^{-\frac{\hbar}{2} V(\nu_1)} \mathrm{e}^{-\frac{\hbar}{2} \overline{V(\nu_2)}}}{2 \cosh\left(\frac{\nu_1 - \nu_2}{2} - \mathrm{i}\pi C\right)}, \tag{3.109}$$

where

$$V(\nu) = -\frac{1}{2\pi}\nu - \frac{2}{\hbar} \log \frac{\Phi_b\left(\frac{b}{2\pi}\left[\nu + \tilde{\alpha} + \frac{\mathrm{i}\pi n}{m+n+1}\right]\right) \Phi_b\left(\frac{b}{2\pi}\left[\nu + \tilde{\beta} + \frac{\mathrm{i}\pi n}{m+n+1}\right]\right)}{\Phi_b\left(\frac{b}{2\pi}\left[\nu + \tilde{\gamma} - \frac{\mathrm{i}\pi(m+1)}{m+n+1}\right]\right)}. \tag{3.110}$$

We recall that the parameters $b$ and $\hbar$ are related through $\hbar = \frac{2\pi b^2}{m+n+1}$.

The knowledge of the integral kernel $\rho(\nu_1, \nu_2)$ allows us to compute traces and fermionic traces. If $\hbar \in 2\pi\mathbb{Q}$, the integral kernel becomes a rational function of exponentials (one uses repeatedly the difference equations satisfied by $\Phi_b(u)$ to obtain them). Then, the integrals for traces (3.25) and fermionic traces (3.23) can be computed for low $N$. See examples in [10, 12, 83]. Such a computation can be organized very efficiently using the Tracy–Widom lemma in [26] for $C = 0$, and its generalization in [24] for rational $C$. In this way, we can do precision checks of the TS/ST conjecture at finite $\hbar$, by comparing the exact results obtained from the integral kernel $\rho(\nu_1, \nu_2)$ to the conjectural expressions obtained from (3.73).[5] We contributed in [24] to such high precision checks. But let us rather turn our attention to the limit $\hbar \to \infty$. The large $\hbar$ limit of the potential can be easily obtained using the large $b$ asymptotic expansion (3.85). Keeping $\nu, \tilde{\alpha}, \tilde{\beta}, \tilde{\gamma}$ fixed, we find

$$V(\nu) = \sum_{k=0}^{\infty} \hbar^{-2k} V_k(\nu), \tag{3.111}$$

[5] A very efficient method to extract the fermionic traces from the conjecture as a fast converging series is the "Airy method" (so called since it involves Airy functions), see for example [7].

with

$$V_0(\nu) = -\frac{1}{2\pi}\nu + \frac{m+n+1}{2\pi^2\mathrm{i}}\left( -\mathrm{Li}_2\left(-\mathrm{e}^{\nu+\tilde{\alpha}+\frac{\mathrm{i}\pi n}{m+n+1}}\right) - \mathrm{Li}_2\left(-\mathrm{e}^{\nu+\tilde{\beta}+\frac{\mathrm{i}\pi n}{m+n+1}}\right) + \mathrm{Li}_2\left(-\mathrm{e}^{\nu+\tilde{\gamma}-\mathrm{i}\pi\frac{m+1}{m+n+1}}\right)\right), \tag{3.112}$$

and

$$V_k(\nu) = \frac{(-16\pi^4)^k}{2\pi^2\mathrm{i}}(m+n+1)^{1-2k}\frac{(2^{-2k+1}-1)B_{2k}}{(2k)!}\left( -\mathrm{Li}_{2-2k}\left(-\mathrm{e}^{\nu+\tilde{\alpha}+\frac{\mathrm{i}\pi n}{m+n+1}}\right) - \mathrm{Li}_{2-2k}\left(-\mathrm{e}^{\nu+\tilde{\beta}+\frac{\mathrm{i}\pi n}{m+n+1}}\right) + \mathrm{Li}_{2-2k}\left(-\mathrm{e}^{\nu+\tilde{\gamma}-\mathrm{i}\pi\frac{m+1}{m+n+1}}\right)\right) \tag{3.113}$$

for $k > 0$. This asymptotic expression will be most useful in the next section.

# Chapter 4

# Matrix models and topological strings

In this chapter, we derive a matrix model representation of the fermionic spectral traces $Z(N,\hbar)$ given in eq. (3.23) by using the explicit form of $\rho(\nu_1,\nu_2)$. We work out what the TS/ST correspondence predicts for the $Z(N,\hbar)$ in the so called *'t Hooft limit*

$$N,\hbar \longrightarrow \infty, \qquad \frac{N}{\hbar} = \lambda \quad \text{fixed.} \tag{4.1}$$

The quantity $\lambda$ which is fixed in the limit is called the *'t Hooft coupling*. As a consequence of the TS/ST correspondence, our matrix models provide a non-perturbative realization of the topological string partition function, and the genus expansion of the topological string corresponds to the 't Hooft expansion of the matrix model. As we will see, from the point of view of the matrix model, the natural frame for the topological string free energies is the so called *conifold frame*, and $\lambda$ is a flat coordinate in moduli space around the conifold point. We check this prediction for different geometries. The matrix model can be easily tackled in the weak 't Hooft coupling limit, so we start by checking this regime. We also show how the matrix model can be solved exactly in $\lambda$ in the planar limit, i.e. we find the leading terms of the free energy, the one-point and two-point functions in the 't Hooft limit. This also allows us to perform checks in the strong 't Hooft coupling regime. Another exact check in the planar limit is the identification of the spectral curve of the matrix model with the mirror curve itself. We restrict the analysis to those genus one cases where we know the explicit form of the integral kernel $\rho(\nu_1,\nu_2)$, which was given in the previous chapter.

A different matrix model representation for topological strings on toric CY threefolds has been proposed in [88, 89]. Those matrix models are rather different in spirit,

with their own advantages and disadvantages. They are formal but explicit matrix models constructed for arbitrary CY threefolds (up to "flops" and "blow-downs"), which are tailored to reproduce the topological string partition function as built from the topological vertex, and written as sums over partitions. So they are a kind of rewriting of the topological vertex result in the language of matrix model; in particular, the size of the matrices seems to play just an auxiliary role. The matrix models presented here are only explicitly given (as of now) for a subset of toric CY threefolds, but they are convergent (so non-perturbative) matrix models[1] with a precise meaning in the spectral theory of the underlying operator. They therefore provide a non-perturbative realization of topological strings. Also, the fact that they reproduce the topological string partition function is a non-trivial consequence of the TS/ST conjecture, and the size $N$ of the matrices is directly connected with a flat coordinate in moduli space.

In this chapter, we focus on genus one cases. Higher genus cases were considered in the weak 't Hooft coupling limit in [16, 83], and also in [90] where the so called "dual 4D limit" of the TS/ST correspondence is considered. This chapter is based on [11–13].

## 4.1 Deriving the matrix models

The fermionc spectral traces $Z(N)$ are the coefficients of the Fredholm determinant:

$$\Xi(\kappa,\hbar) = \det(1+\kappa\rho) = 1 + \sum_{N=1}^{\infty} \kappa^N Z(N,\hbar), \tag{4.2}$$

where

$$Z(N,\hbar) = \frac{1}{N!}\int_{\mathbb{R}^N} \mathrm{d}^N\nu \det_{i,j=1,\ldots,N} \rho(\nu_i,\nu_j). \tag{4.3}$$

[1] for an appropriate range of mass parameters

Since the integral kernel has the form (3.109), the integrand can be rewritten using the Cauchy determinant formula[2]

$$\det_{i,j=1,\dots,N} \frac{1}{2\cosh\left(\frac{\mu_i-\nu_j}{2}\right)} = \frac{\prod_{i>j} 2\sinh\frac{\mu_i-\mu_j}{2} 2\sinh\frac{\nu_i-\nu_j}{2}}{\prod_{i,j} 2\cosh\frac{\mu_i-\nu_j}{2}}. \tag{4.5}$$

We obtain:

$$Z(N,\hbar) = \frac{1}{N!}\int_{\mathbb{R}^N} \frac{\mathrm{d}^N\nu}{(2\pi)^N} \mathrm{e}^{-\hbar\sum_{k=1}^N \mathrm{Re}\, V(\nu_k)} \frac{\prod_{i<j}\left[2\sinh\left(\frac{\nu_i-\nu_j}{2}\right)\right]^2}{\prod_{i,j} 2\cosh\left(\frac{\nu_i-\nu_j}{2} - \mathrm{i}\pi C\right)}. \tag{4.6}$$

Notice that this is valid for any function $V(\nu)$. Those who are familiar with matrix models may perhaps recognize (4.6): it is the deformed version of the $O(n)$ matrix model for $n = 2$, introduced by Kostov in [14] in order to study the statistical model known as the "six-vertex model" on a random lattice. The matrix model for the $O(n)$ model itself was formulated by Kostov earlier in [91]. The convergent version of the deformed $O(2)$ matrix model can be written as

$$\hat{\mathcal{Z}}(N,\beta,\hbar) = \int \mathrm{d}A \int \mathrm{d}M^\dagger \mathrm{d}M \exp\left[-\mathrm{Tr}\left(\mathrm{i}\mathrm{e}^{-\mathrm{i}\frac{\beta}{2}} AMM^\dagger - \mathrm{i}\mathrm{e}^{\mathrm{i}\frac{\beta}{2}} AM^\dagger M + \hbar\mathcal{W}(A)\right)\right], \tag{4.7}$$

where the integral over $A$ is an integral over all $N \times N$ hermitian matrices with *positive* eigenvalues, with measure $\mathrm{d}A = \prod_{i=1}^N \mathrm{dRe}A_{ii} \prod_{i<j} \mathrm{dRe}A_{ij}\mathrm{dIm}A_{ij}$. The integral over $M$ is an integral over all $N \times N$ complex matrices with measure $\mathrm{d}M^\dagger\mathrm{d}M = \prod_{i,j=1}^N \mathrm{dRe}M_{ij}\mathrm{dIm}M_{ij}$. The parameter $\hbar$ is positive, and the function $\mathcal{W}(z)$ is bounded from below on the positive real line and goes to $+\infty$ when $z \to 0, \infty$. To recover the form given before, we integrate over the complex matrix $M$ and reduce the integration over $A$ to an integration over its eigenvalues $\mathrm{e}^{x_i}$ using the usual techniques [92, 93]. After a change of variables, we find that

$$Z(N,\hbar) = \frac{G(N+1)}{2^N \pi^{\frac{N(N+1)}{2}+N^2}} \hat{\mathcal{Z}}(N,\beta), \qquad \beta = 2\pi\left(\frac{1}{2} - C\right), \tag{4.8}$$

where $\mathcal{W}(\mathrm{e}^\nu) = \mathrm{Re}\, V(\nu)$, which in our case has the appropriate behaviour. Some examples for the planar potential $\mathrm{Re}\, V_0(\nu)$ can be seen in Fig 4.1. The function $G(N)$ is the Barnes $G$ function defined by $G(N+1) = \Gamma(N)G(N)$, $\Gamma(1) = 1$.

[2] This relation is more commonly written

$$\det_{i,j} \frac{1}{x_i + y_j} = \frac{\prod_{i>j}(x_i - x_j)(y_i - y_j)}{\prod_{i,j}(x_i + y_j)}, \tag{4.4}$$

which is the more convenient form for its proof. Indeed, one way to prove this is the following: the denominator is fixed since it is the common denominator of the determinant expression; the numerator has to appear as a factor since when $x_i = x_j$ or $y_i = y_j$, the determinant vanishes; no more factor can appear in the numerator by power counting; and finally the overall constant is fixed to 1 by comparing a limit case on both sides, for example $x_N \to \infty$, $y_N = 1 - x_N$.

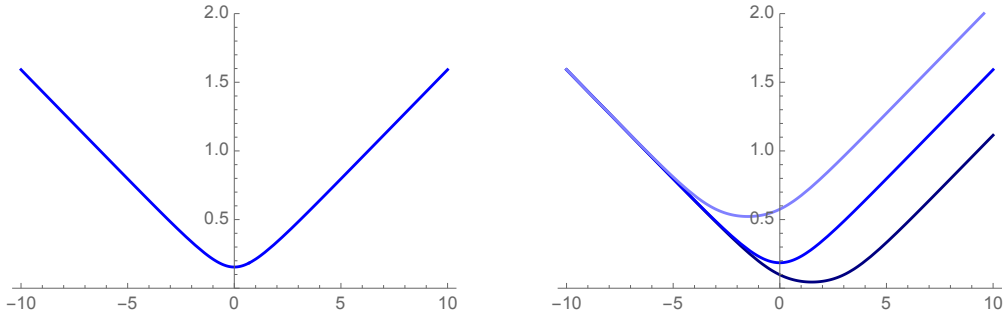


**Figure 4.1:** The planar potentials of the matrix model $\operatorname{Re} V_0(\nu)$ as a function of $\nu$ for some cases. On the left, the local $\mathbb{P}^2$ case and on the right the local $\mathbb{P}^1 \times \mathbb{P}^1$ case with parameter $\tilde{\alpha} = -3, 0, 3$.

The advantage of the matrix model representation of the fermionic spectral traces $Z(N)$ is that the whole technology of matrix models is now available, especially those techniques which are used for the large $N$ limit.

## 4.2 The TS/ST correspondence in the 't Hooft limit

What happens with $Z(N, \hbar)$ in the 't Hooft limit from the point of view of the TS/ST correspondence? The TS/ST conjectures that

$$\Xi(\kappa, \hbar) = \sum_{n \in \mathbb{Z}} \mathrm{e}^{J(\mu + 2\pi \mathrm{i} n, \hbar)}, \tag{4.9}$$

where

$$\kappa = \mathrm{e}^{\mu}. \tag{4.10}$$

The fermionic spectral traces $Z(N, \hbar)$ are the $N^{\text{th}}$ coefficients of $\Xi(\kappa, \hbar)$, so they can be extracted by a contour integration around $\kappa = 0$:

$$Z(N, \hbar) = \frac{1}{2\pi \mathrm{i}} \oint \frac{\mathrm{d}\kappa}{\kappa} \kappa^{-N} \Xi(\kappa, \hbar). \tag{4.11}$$

Plugging in the conjecture, we find

$$\begin{aligned} Z(N, \hbar) &= \frac{1}{2\pi \mathrm{i}} \int_{-\mathrm{i}\pi}^{\mathrm{i}\pi} \mathrm{d}\mu \, \mathrm{e}^{-N\mu} \sum_{n \in \mathbb{Z}} \mathrm{e}^{J(\mu + 2\pi \mathrm{i} n, \hbar)} \\ &= \frac{1}{2\pi \mathrm{i}} \int_{\mathcal{C}} \mathrm{d}\mu \, \mathrm{e}^{J(\mu, \hbar) - N\mu}, \end{aligned} \tag{4.12}$$

where the contour $\mathcal{C}$ is along the imaginary axis, but can be deformed to correspond to the Airy contour of Fig. 4.2. Along this contour, the integral converges fastest,

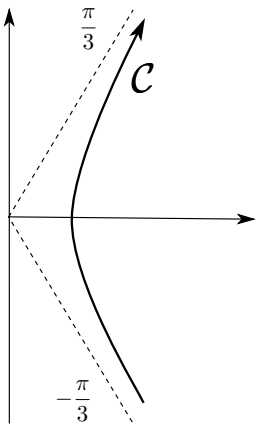


**Figure 4.2:** The deformed contour $\mathcal{C}$ in the complex plane of $\mu$.

since $J(\mu, \hbar)$ has a cubic behaviour at large $\mu$. To obtain the 't Hooft expansion of $Z(N, \hbar)$, we need to look at the behaviour of $J(\mu, \hbar)$ at large $\hbar$. We will scale $\mu$ with $\hbar$. So let us introduce

$$\zeta = \frac{\mu}{\hbar}, \qquad \mu, \hbar \longrightarrow \infty, \tag{4.13}$$

and

$$\log m_k = \frac{\hbar}{2\pi}\xi_k \tag{4.14}$$

(so the mass parameters also scale with $\hbar$). In the genus one case, the rescaled quantum mirror map (3.64) becomes

$$\frac{1}{\hbar}t_i(\hbar) = c_i\zeta - \frac{1}{2\pi}\sum_{k=1}^{r_W}\alpha_{ik}\xi_k + \mathcal{O}\left(\frac{1}{\hbar}\mathrm{e}^{-\hbar\zeta}\right), \tag{4.15}$$

and we neglect the exponentially small corrections at large $\hbar$. In this regime, $t(\hbar)$ scales like $\hbar$, so all the instanton corrections coming from $F_{\mathrm{NS}}^{\mathrm{inst}}$ in $J^{\mathrm{WKB}}(\mu, \hbar)$ in eq. (3.68) vanish non-perturbatively. Only the perturbative part remains, as well as $J^{\mathrm{WS}}(\mu, \hbar)$. In a sense, our limit isolates the "worldsheet" part of the modified grand potential. To write down what remains, we introduce

$$T_i(\zeta) = \frac{2\pi}{\hbar}t_i(\hbar) = 2\pi c_i\zeta - \sum_k \alpha_{ik}\xi_k. \tag{4.16}$$

Since we are in the genus one case, we can choose the definition of $t_i$ such that, say,

$$c_i = c\delta_{i1}. \tag{4.17}$$

Then, we call $T = T_1$ the rescaled Kähler parameter corresponding to the one "true" modulus. The "worldsheet" part is given by the Gopakumar–Vafa free energy:

$$\begin{aligned} J^{\mathrm{WS}}(\mu,\hbar) &= F_{\mathrm{GV}}\left(\mathbf{T}(\zeta) + \mathrm{i}\pi\mathbf{B}, \frac{4\pi^2}{\hbar}\right) \\ &= \sum_{g=0}^{\infty}\sum_{\mathbf{d}}\sum_{w=1}^{\infty} n_g^{\mathbf{d}} \frac{1}{w}\left(2\sin\frac{w}{2}\frac{4\pi^2}{\hbar}\right)^{2g-2} (-1)^{w\mathbf{d}\cdot\mathbf{B}} \mathrm{e}^{-w\mathbf{d}\cdot\mathbf{t}} \end{aligned} \tag{4.18}$$

In the large $\hbar$ limit, its asymptotic expansion is precisely given by the topological string free energies (2.11) (the generating functions of the Gromov–Witten invariants), with additional signs introduced by the $\mathbf{B}$ field:

$$\begin{aligned} J^{\mathrm{WS}}(\mu,\hbar) &= \sum_{g=0}^{\infty}\left(\frac{4\pi^2}{\hbar}\right)^{2g-2} F_g^{\mathrm{inst}}(\mathbf{T}(\zeta) + \mathrm{i}\pi\mathbf{B}), \\ &= \sum_{g=0}^{\infty}\left(\frac{4\pi^2}{\hbar}\right)^{2g-2} \widehat{F}_g^{\mathrm{inst}}(\mathbf{T}(\zeta)), \end{aligned} \tag{4.19}$$

where

$$\widehat{F}_g^{\mathrm{inst}}(\mathbf{T}(\zeta)) = \sum_{\mathbf{d}} N_{g,\mathbf{d}}\,(-1)^{\mathbf{d}\cdot\mathbf{B}} \mathrm{e}^{-\mathbf{d}\cdot\mathbf{t}}. \tag{4.20}$$

The WKB modified grand potential reduces to the part given only by the pertrubative NS free energy $F_{\mathrm{NS}}^{\mathrm{pert}}$, and becomes

$$J^{\mathrm{WKB}}(\mu,\hbar) = \frac{\hbar^2}{(2\pi)^4}\left(\widehat{F}_0^{\mathrm{p}}(\mathbf{T}(\zeta)) + (2\pi)^2\sum_i b_i^{\mathrm{NS}} T_i\right) + \widehat{F}_1^{\mathrm{p}}(\mathbf{T}(\zeta)) + A(\boldsymbol{\xi},\hbar), \tag{4.21}$$

where we defined

$$\widehat{F}_0^{\mathrm{p}}(\mathbf{T}) = \frac{1}{6}\sum_{i,j,k} a_{ijk} T_i T_j T_k, \qquad \widehat{F}_1^{\mathrm{p}}(\mathbf{T}) = \sum_i b_i T_i. \tag{4.22}$$

Assuming that the function $A(\boldsymbol{\xi},\hbar)$ has an asymptotic expansion in small $\hbar^{-2}$,

$$A(\boldsymbol{\xi},\hbar) = \sum_{g=0}^{\infty} A_g \hbar^{2-2g}, \tag{4.23}$$

we find

$$J(\mu,\hbar) = \sum_{g=0}^{\infty} J_g(\zeta)\hbar^{2-2g}, \tag{4.24}$$

with

$$\begin{aligned} J_0(\zeta) &= \frac{1}{(2\pi)^4}\left(\widehat{F}_0(\mathbf{T}(\zeta)) + (2\pi)^2\sum_i b_i^{\mathrm{NS}} T_i(\zeta)\right) + A_0, \\ J_1(\zeta) &= \widehat{F}_1(\mathbf{T}(\zeta)) + A_1, \\ J_g(\zeta) &= (4\pi^2)^{2g-2}(\widehat{F}_g(\mathbf{T}(\zeta)) - C_g) + A_g, \qquad g \geq 2, \end{aligned} \tag{4.25}$$

where

$$\begin{aligned}\widehat{F}_0(\mathbf{T}) &= \widehat{F}_0^{\mathrm{p}}(\mathbf{T}) + \widehat{F}_0^{\mathrm{inst}}(\mathbf{T}),\\ \widehat{F}_1(\mathbf{T}) &= \widehat{F}_1^{\mathrm{p}}(\mathbf{T}) + \widehat{F}_1^{\mathrm{inst}}(\mathbf{T}),\\ \widehat{F}_g(\mathbf{T}) &= C_g + \widehat{F}_g^{\mathrm{inst}}(\mathbf{T}), \qquad\qquad g \geq 2.\end{aligned} \tag{4.26}$$

Here, the $C_g$ are the constant map contributions in (2.11). Of course, (4.24) should be understood as an asymptotic expansion. Taking all this into account, the expression for $Z(N,\hbar)$ in the 't Hooft limit is

$$\begin{aligned}Z(N,\hbar) &= \frac{1}{2\pi\mathrm{i}}\int_{\mathcal{C}} \mathrm{d}\mu\, \mathrm{e}^{J(\mu,\hbar)-N\mu}\\ &= \frac{\hbar}{2\pi\mathrm{i}}\int_{\mathcal{C}} \mathrm{d}\zeta \exp\left[\hbar^2\left(J_0(\zeta) - \lambda\zeta + \sum_{g=1}^{\infty} J_g(\zeta)\hbar^{-2g}\right)\right].\end{aligned} \tag{4.27}$$

This integral can be evaluated using the saddle point expansion for large $\hbar$. We expand around the critical point $\zeta^* = \zeta^*(\lambda)$ defined by

$$J_0'(\zeta^*) = \lambda. \tag{4.28}$$

By a change of variables, we find

$$\begin{aligned}Z(N,\hbar) = \mathrm{e}^{\hbar^2(J_0(\zeta^*)-\lambda\zeta^*)+J_1(\zeta^*)}\sqrt{\frac{1}{2\pi^2 J_0''(\zeta^*)}}\\ \int_{-\infty}^{\infty}\mathrm{d}t\,\mathrm{e}^{-t^2}\exp\left(\sum_{g,n}{}' \frac{\mathrm{i}^n}{n!}J_g^{(n)}(\zeta^*)\left(\frac{2}{J_0''(\zeta^*)}\right)^{n/2} t^n\hbar^{2-2g-n}\right).\end{aligned} \tag{4.29}$$

The sum is over all positive $(n,g)$ except $(0,0),(0,1),(0,2),(1,0)$. One can now expand the last exponential in large $\hbar$ and perform the integration term by term. The outcome is an expansion for

$$\mathcal{F} = \log Z(N,\hbar) \tag{4.30}$$

which has the form

$$\mathcal{F} = \sum_{g=0}^{\infty}\hbar^{2-2g}\mathcal{F}_g(\lambda). \tag{4.31}$$

We find

$$\begin{aligned}
\mathcal{F}_0(\lambda) &= J_0(\zeta^*(\lambda)) - \lambda\zeta^*(\lambda), \\
\mathcal{F}_1(\lambda) &= J_1(\zeta^*(\lambda)) - \frac{1}{2}\log\left(2\pi J_0''(\zeta^*)\right), \\
\mathcal{F}_2(\lambda) &= J_2(\zeta^*(\lambda)) - \frac{1}{2}\frac{J_1''(\zeta*(\lambda))}{J_0''(\zeta^*)} - \frac{1}{2}\frac{(J_1'(\zeta*(\lambda)))^2}{J_0''(\zeta^*)} + \frac{1}{2}\frac{J_0^{(3)}(\zeta^*)J_1'(\zeta*(\lambda))}{(J_0''(\zeta^*))^2} \\
&\quad + \frac{1}{8}\frac{J_0^{(4)}(\zeta^*)}{(J_0''(\zeta^*))^2} - \frac{5}{24}\frac{(J_0^{(3)}(\zeta^*))^2}{(J_0''(\zeta^*))^3}, \\
&\cdots
\end{aligned} \tag{4.32}$$

Differentiating the first line, we find

$$\begin{aligned}
\mathcal{F}_0'(\lambda) &= -\zeta^*, \\
J_0'(\zeta^*) &= \lambda,
\end{aligned} \tag{4.33}$$

(we also reported relation (4.28)). The saddle point expansion we performed is precisely the implementation of the symplectic transformation of [52] for the changing of frames of the topological string free energies. The $J_g(\zeta)$ are essentially the free energies of the topological string in the *large radius frame* (with their enumerative interpretation in terms of Gromow–Witten invariants), and the relations (4.33) imply that the symplectic transformation we have implemented is to the *conifold frame*. Indeed, using (4.16), we can rewrite (4.33) as

$$\begin{aligned}
\partial_\lambda \mathcal{F}_0 &= -\frac{1}{2\pi c}T - \frac{1}{2\pi c}\sum_k \alpha_{1k}\xi_k, \\
\frac{(2\pi)^3}{c}\lambda &= \partial_T \widehat{F}_0 + (2\pi)^2 b_1^{\mathrm{NS}}.
\end{aligned} \tag{4.34}$$

This is (up to some constants) the symplectic $S$ transformation, i.e. the exchange of $A$–periods ($T$ or $\lambda$) and $B$–periods ($\partial_T\widehat{F}_0$ or $\partial_\lambda\mathcal{F}_0$) typical for the large radius to conifold change of frame. Therefore, we conclude that *the functions $\mathcal{F}_g(\lambda)$ appearing in the 't Hooft expansion of the fermionic traces, i.e. the 't Hooft expansion of our matrix models, are the genus g free energies of the topological string in the conifold frame*. This is an appealing idea: we have a well defined, non-perturbative quantity $Z(N,\hbar)$ which in this limit has an asymptotic expansion giving the topological string free energies; in other words, a non-perturbative realization of the topological string free energies. The construction leading to this result is summarized in Fig. 4.3.

We will now perform some checks of this proposal, which consists in expanding the $Z(N)$ of eq. (4.6) in the 't Hooft limit, and compare it to known results for topological string free energies in the conifold frame. We will focus on two examples, the local $\mathbb{P}^2$ case and the $\mathbb{P}^1 \times \mathbb{P}^1$ case.

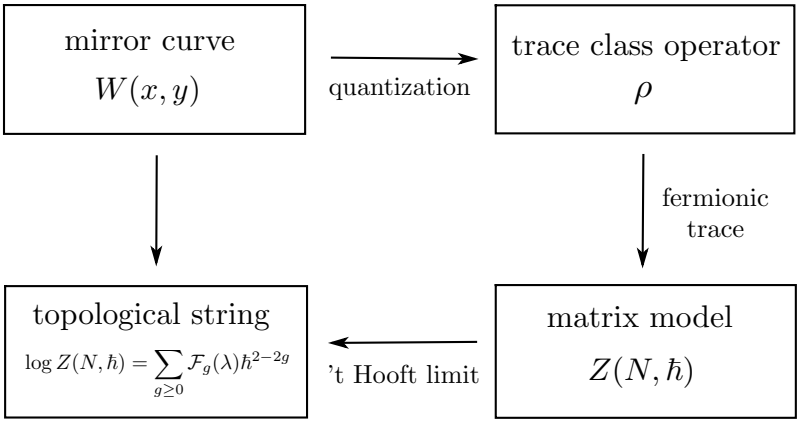


**Figure 4.3:** The emergence of matrix models for topological strings in CY threefolds: given a geometry, the quantization of its mirror curve leads to a trace class operator $\rho$; the standard topological string free energy is obtained as the 't Hooft expansion of its fermionic traces $Z(N,\hbar)$.

## 4.3 Checks at weak coupling

We first want to compute $Z(N,\hbar)$ from the matrix model expression (4.6), in the 't Hooft limit $N,\hbar\to\infty$, $N/\hbar=\lambda$ fixed. The easiest regime to consider is the small $\lambda$ expansion that we call the weak coupling expansion. In this limit, the "coupling" $\hbar$ is much larger than $N$, therefore the 't Hooft expansion of the matrix model for small $\lambda$ can be inferred from the large $\hbar$ expansion of $Z(N,\hbar)$ for finite values of $N$. We basically perform a saddle point expansion at large $\hbar$, and the integrations reduce to gaussian ones. Physically, the potential term $-\hbar\sum_i \mathrm{Re}V(\nu_i)$ dominates in (4.6), and eigenvalues $\nu_i$ condense around the critical point of the leading part of the potential. In our case, it can be checked that the potential $\mathrm{Re}V(\nu)$ has a unique critical point.

We start with $Z(N,\hbar)$, with $N$ fixed:

$$\begin{aligned} Z(N,\hbar) &= \frac{1}{N!}\int_{\mathbb{R}^N}\frac{\mathrm{d}^N\nu}{(2\pi)^N}\mathrm{e}^{-\hbar\sum_{k=1}^N \mathrm{Re}\,V(\nu_k)}\frac{\prod_{i<j}\left[2\sinh\left(\frac{x_i-x_j}{2}\right)\right]^2}{\prod_{i,j}2\cosh\left(\frac{x_i-x_j}{2}-\mathrm{i}\pi C\right)} \\ &= \frac{\mathrm{e}^{-N^2\log 2\cos(\pi C)}}{N!(2\pi)^N}\int_{\mathbb{R}^N}\mathrm{d}^N\nu\ \ \mathrm{e}^{-\hbar\sum_{k=1}^N \mathrm{Re}\,V(\nu_k)}\prod_{i<j}D(\nu_i-\nu_j), \end{aligned} \tag{4.35}$$

where

$$D(\nu_i-\nu_j)=\frac{4\cos(\pi C)^2\sinh^2(\frac{\nu_i-\nu_j}{2})}{\cosh(\frac{\nu_i-\nu_j}{2}+\mathrm{i}\pi C)\cosh(\frac{\nu_i-\nu_j}{2}-\mathrm{i}\pi C)}=(\nu_i-\nu_j)^2\left(1+O(\nu_i-\nu_j)^2\right) \tag{4.36}$$

gives a perturbed Vandermonde determinant[3]. The potential has a large $\hbar$ expansion which in our case is given in eq. (3.111-3.113). It can be expanded around the minimum $\nu_{\min}$ of its leading part $\mathrm{Re}V_0'(\nu_{\min})=0$:

$$\begin{aligned}\mathrm{Re}\,V(\nu)=\mathrm{Re}\,V_0(\nu_{\min})+\frac{1}{2}\mathrm{Re}\,V_0''(\nu_{\min})(\nu-\nu_{\min})^2\\ +{\sum_{g\geq 0,k\geq 0}}'\frac{1}{k!}\mathrm{Re}\,V_g^{(k)}(\nu_{\min})\hbar^{-2g}(\nu-\nu_{\min})^k,\end{aligned} \tag{4.37}$$

where the prime on the sum means that we omit the terms $(g,k)=(0,0),(0,1),(0,2)$. We perform the change of variables $\nu_i=\tilde{\nu}_i\hbar^{-1/2}+\nu_{\min}$, and expand everything in large $\hbar$. The outcome has the form

$$\begin{aligned}Z(N,\hbar)\sim \mathrm{e}^{-N^2\log 2\cos(\pi C)-\log\Gamma(N+1)-\frac{N(N+1)}{2}\log\hbar-N\log 2\pi-\hbar N\,\mathrm{Re}\,V_0(\nu_{\min})}\\ \times\sum_{k\geq 0}\hbar^{-k/2}\sum_{\boldsymbol{\ell}}c_{k,\boldsymbol{\ell}}(N)\prod_{j=1}^{N}\int_{\mathbb{R}}\mathrm{d}\tilde{\nu}_j\mathrm{e}^{-\frac{1}{2}\mathrm{Re}\,V_0''(\nu_{\min})}\tilde{\nu}_j^{\ell_j}.\end{aligned} \tag{4.38}$$

where $\boldsymbol{\ell}=(\ell_1,\dots,\ell_N)$ is a vector of positive integers, and the coefficients $c_{k,\boldsymbol{\ell}}(N)$ are obtained by putting together the large $\hbar$ expansions of the different pieces. All the one dimensional gaussian integrals are straightforwardly performed using that for $a>0$ and $\ell$ a positive integer,

$$\int_{\mathbb{R}}\mathrm{d}\nu\,\mathrm{e}^{-\frac{1}{2}a\nu^2}\,\nu^\ell=\frac{1+(-1)^\ell}{2}\Gamma\left(\frac{\ell+1}{2}\right)\left(\frac{2}{a}\right)^{\frac{\ell+1}{2}}. \tag{4.39}$$

When $k$ is odd in (4.38), it can be seen that some of the $\ell_j$ are odd integers, so those terms vanish. The result looks like

$$\begin{aligned}Z(N,\hbar)\sim \mathrm{e}^{-N^2\log 2\cos(\pi C)-\log\Gamma(N+1)-\frac{N(N+1)}{2}\log\hbar-\hbar N\,\mathrm{Re}\,V_0(\nu_{\min})-\frac{N}{2}\log\left(2\pi^2\mathrm{Re}\,V_0''(\nu_{\min})\right)}\\ \times\sum_{k\geq 0}\hbar^{-k}\tilde{C}_k(N).\end{aligned} \tag{4.40}$$

Taking the logarithm gives the large $\hbar$ asymptotic expansion of the free energy. Since we expect that it admits a 't Hooft expansion of the form[4] (4.31), we can reorganize

[3] Of course, this expansion works for more general kinds of perturbations of the Vandermonde determinant.

[4] This is a consequence from the matrix model interpretation of $Z(N,\hbar)$, and its expansion using "fat-graphs". The combinatorics involved predict the form (4.31) of the 't Hooft expansion.

the large $\hbar$ series accordingly. The exponentiated prefactor is part of the gaussian contribution, which is well known,

$$\begin{aligned} Z^{\text{gaussian}}(N,\hbar) &= \frac{\mathrm{e}^{-N^2\log 2\cos(\pi C)-\hbar N \operatorname{Re} V_0(\nu_{\min})}}{\hbar^{\frac{N(N+1)}{2}}(2\pi)^N N!} \\ &\qquad \times \int_{\mathbb{R}^N} \mathrm{d}^N\tilde{\nu}\ \mathrm{e}^{-\frac{1}{2}\operatorname{Re} V_0''(\nu_{\min})\sum_{j=1}^N \tilde{\nu}_j^2} \prod_{i<j}(\tilde{\nu}_i-\tilde{\nu}_j)^2 \\ &= \mathrm{e}^{-\hbar N \operatorname{Re} V_0(\nu_{\min})} \frac{\mathrm{e}^{-\frac{N^2}{2}\log\left(4\cos^2(\pi C)\operatorname{Re} V_0''(\nu_{\min})\right)}}{\hbar^{\frac{N(N+1)}{2}}(2\pi)^{N/2}} G(N+1) \end{aligned} \tag{4.41}$$

and which we factor out. In the above, $G(N)$ is the Barnes function. Its logarithm has a well known large $N$ expansion. At each order in large $\hbar$, the coefficient of $\log Z_N - \log Z_N^{\text{gaussian}}$ has to have a precise polynomial dependence in $N$ (otherwise it cannot be converted into a 't Hooft expansion):

$$\begin{aligned} \log Z(N,\hbar) - \log Z^{\text{gaussian}}(N,\hbar) &\sim \sum_{k\geq 1} \hbar^{-k} C_k(N) \\ &\sim \frac{C_{1,3}N^3 + C_{1,1}N}{\hbar} + \frac{C_{2,4}N^4 + C_{2,2}N^2}{\hbar^2} \\ &\quad + \frac{C_{3,5}N^5 + C_{3,3}N^3 + C_{3,1}N}{\hbar^3} + \dots \end{aligned} \tag{4.42}$$

By fitting the finite $N$ values of $C_k(N) = \sum_g C_{k,g} N^g$ to the expected polynomial behaviour, we find the values of $C_{k,g}$. After using $N = \lambda\hbar$, plugging in the large $N$ asymptotic series of $Z^{\text{gaussian}}(N,\hbar)$, and reorganizing the series, we obtain the 't Hooft expansion at small coupling $\lambda$:

$$\begin{aligned} \log Z(N,\hbar) &\sim \log Z^{\text{gaussian}}(N,\hbar) + \hbar^2\left(C_{1,3}\lambda^3 + C_{2,4}\lambda^4 + C_{3,5}\lambda^5 + \dots\right) \\ &\qquad + (C_{1,1}\lambda + C_{2,2}\lambda^2 + C_{3,3}\lambda^3 + \dots) \\ &\qquad + \hbar^{-2}(C_{3,1}\lambda + \dots) + \dots \\ &\sim \sum_{g=0}^{\infty} \hbar^{2-2g}\mathcal{F}_g(\lambda), \end{aligned} \tag{4.43}$$

where

$$\begin{aligned} \log Z^{\text{gaussian}}(N,\hbar) \sim \hbar^2 &\left(\frac{\lambda^2}{2}\log\frac{\lambda}{4\cos^2(\pi C)\operatorname{Re} V_0''(\nu_{\min})} - \frac{3\lambda^2}{4} - \lambda \operatorname{Re} V_0(\nu_{\min})\right) \\ &+ \left(-\frac{1}{12}\log\lambda + \zeta'(-1)\right) + \sum_{g=2}^{\infty} \hbar^{2-2g}\frac{B_{2g}}{2g(2g-1)}\lambda^{2-2g} \\ &- \frac{1}{12}\log\hbar. \end{aligned} \tag{4.44}$$

In the above, $\zeta(z)$ is the Riemann zeta function, $\zeta'(-1) \approx -0.1654$. We will usually drop the $-\frac{1}{12}\log\hbar$ in the last line when writing the results. This procedure can be performed in the general case given by the potential (3.111-3.113). But for the sake of simplicity[5], let us focus on two special cases.

**Three term operators and local $\mathbb{P}^2$.** For $\tilde{\alpha}, \tilde{\beta} \to -\infty$, $\tilde{\gamma} = 0$ and general $m, n$, we have the "three term" operator case. The $m = n = 1$ case is the local $\mathbb{P}^2$ matrix model. We find the following result:

$$\begin{aligned}
\mathcal{F}_0(\lambda) &= \frac{\lambda^2}{2}\left(\log\frac{\lambda}{4\cos^2(\pi C)\mathrm{Re}V_0''(\nu_{\min})} - \frac{3}{2}\right) - \mathrm{Re}V_0(\nu_{\min})\lambda + \sum_{k=3}^{\infty} f_{0,k}\lambda^k, \\
\mathcal{F}_1(\lambda) &= -\frac{1}{12}\log(\lambda) + \zeta'(-1) + \sum_{k=1}^{\infty} f_{1,k}\lambda^k, \\
\mathcal{F}_g(\lambda) &= \frac{B_{2g}}{2g(2g-2)}\lambda^{2-2g} + \sum_{k=1}^{\infty} f_{g,k}\lambda^k, \qquad g \geq 2.
\end{aligned} \tag{4.45}$$

In this equation, we have

$$\begin{aligned}
\cos(\pi C) &= \sin\left(\frac{\pi n}{m+n+1}\right), \\
\mathrm{Re}V_0''(\nu_{\min}) &= \frac{m+n+1}{2\pi^2}\frac{\sin\left(\frac{\pi m}{m+n+1}\right)\sin\left(\frac{\pi}{m+n+1}\right)}{\sin\left(\frac{\pi n}{m+n+1}\right)}, \\
\mathrm{Re}V_0(\nu_{\min}) &= -\frac{1}{2\pi}\log\frac{\sin\frac{\pi}{m+n+1}}{\sin\frac{m\pi}{m+n+1}} - \frac{m+n+1}{2\pi^2}\mathrm{Im}\,\mathrm{Li}_2\left(\mathrm{e}^{-\frac{\mathrm{i}\pi n}{m+n+1}}\frac{\sin\frac{\pi}{m+n+1}}{\sin\frac{m\pi}{m+n+1}}\right).
\end{aligned} \tag{4.46}$$

[5]Indeed, the complication for the general case comes from the fact that the minimum of the leading potential $\mathrm{Re}V_0(\nu)$ is a very non-trivial function of the parameters $\tilde{\alpha}$, $\tilde{\beta}$, $\tilde{\gamma}$.

The first coefficients $f_{0,k}$, are given by

$$f_{0,3} = -\frac{\pi^2}{12(m+n+1)} \frac{\sum_{\alpha\in\{1,m,n\}} \cos\frac{2\pi\alpha}{m+n+1} + 3}{\prod_{\alpha\in\{1,m,n\}} \sin\frac{\pi\alpha}{m+n+1}},$$

$$\begin{aligned} f_{0,4} = {} & \frac{\pi^4}{576(m+n+1)^2} \\ & \times \frac{\sum_{\alpha\in\{1,m,n\}} \left(110\cos\frac{2\pi\alpha}{m+n+1} + \cos\frac{4\pi\alpha}{m+n+1}\right) + 5\sum_{\alpha,\beta\in\{1,m,n\}} \cos\frac{2\pi(\alpha-\beta)}{m+n+1} + 126}{\prod_{\alpha\in\{1,m,n\}} \sin^2\frac{\pi\alpha}{m+n+1}}, \end{aligned}$$

$$\begin{aligned} f_{0,5} = {} & -\frac{\pi^6}{480(m+n+1)^3} \frac{1}{\prod_{\alpha\in\{1,m,n\}} \sin^3\frac{\pi\alpha}{m+n+1}} \\ & \times \Big[ \sum_{\alpha\in\{1,m,n\}} \Big(283\cos\frac{2\pi\alpha}{m+n+1} + 23\cos\frac{4\pi\alpha}{m+n+1}\Big) \\ & \qquad + \sum_{\alpha,\beta\in\{1,m,n\}} \Big(30\cos\frac{2\pi(\alpha-\beta)}{m+n+1} + \cos\frac{2\pi(2\alpha-\beta)}{m+n+1}\Big) + 183\Big]. \end{aligned} \tag{4.47}$$

For genus one, one has

$$\begin{aligned} f_{1,1} = {} & -\frac{1}{2} f_{0,3} + \frac{\pi^2}{4(m+n+1)} \frac{1}{\prod_{\alpha\in\{1,m,n\}} \sin\frac{\pi\alpha}{m+n+1}}, \\ f_{1,2} = {} & -f_{0,4}, \\ f_{1,3} = {} & \frac{\pi^6}{288(m+n+1)^3} \frac{1}{\prod_{\alpha\in\{1,m,n\}} \sin^3\frac{\pi\alpha}{m+n+1}} \\ & \times \Big[ \sum_{\alpha\in\{1,m,n\}} \Big(175\cos\frac{2\pi\alpha}{m+n+1} + 11\cos\frac{4\pi\alpha}{m+n+1}\Big) \\ & \qquad + \sum_{\alpha,\beta\in\{1,m,n\}} \Big(18\cos\frac{2\pi(\alpha-\beta)}{m+n+1} + \cos\frac{2\pi(2\alpha-\beta)}{m+n+1}\Big) + 99\Big]. \end{aligned} \tag{4.48}$$

Finally, for genus two, we obtain:

$$\begin{aligned} f_{2,1} = {} & -\frac{\pi^6}{960(m+n+1)^3} \frac{1}{\prod_{\alpha\in\{1,m,n\}} \sin^3\frac{\pi\alpha}{m+n+1}} \\ & \times \Big[ \sum_{\alpha\in\{1,m,n\}} \Big(13\cos\frac{2\pi\alpha}{m+n+1} - 7\cos\frac{4\pi\alpha}{m+n+1}\Big) \\ & \qquad + \sum_{\alpha,\beta\in\{1,m,n\}} \cos\frac{2\pi(2\alpha-\beta)}{m+n+1} - 27\Big]. \end{aligned} \tag{4.49}$$

We now list some results in the case of $m = n = 1$, relevant for local $\mathbb{P}^2$. We find,

$$\begin{aligned}
\mathcal{F}_0(\lambda) &= \frac{\lambda^2}{2}\left(\log\left(\frac{4\pi^2\lambda}{9\sqrt{3}}\right) - \frac{3}{2}\right) - \frac{3\mathrm{Im}\,\mathrm{Li}_2(\mathrm{e}^{\frac{\mathrm{i}\pi}{3}})}{2\pi^2}\lambda - \frac{\pi^2}{9\sqrt{3}}\lambda^3 + \frac{\pi^4}{486}\lambda^4 + \frac{56\pi^6}{10935\sqrt{3}}\lambda^5 \\
&\quad - \frac{1058\pi^8}{492075}\lambda^6 + \frac{3392\pi^{10}}{2066715\sqrt{3}}\lambda^7 + \mathcal{O}(\lambda^8), \\
\mathcal{F}_1(\lambda) &= -\frac{1}{12}\log(\lambda) + \zeta'(-1) + \frac{5\pi^2}{18\sqrt{3}}\lambda - \frac{\pi^4}{486}\lambda^2 - \frac{40\pi^6}{2187\sqrt{3}}\lambda^3 \\
&\quad + \frac{283\pi^8}{32805}\lambda^4 - \frac{1376\pi^{10}}{177147\sqrt{3}}\lambda^5 + \mathcal{O}(\lambda^6), \\
\mathcal{F}_2(\lambda) &= -\frac{1}{240}\lambda^{-2} + \frac{4\pi^6}{405\sqrt{3}}\lambda - \frac{3187\pi^8}{492075}\lambda^2 + \frac{7648\pi^{10}}{885735\sqrt{3}}\lambda^3 + \mathcal{O}(\lambda^4), \\
\mathcal{F}_3(\lambda) &= \frac{1}{1008}\lambda^{-4} - \frac{32\pi^{10}}{15309\sqrt{3}}\lambda + \mathcal{O}(\lambda^2).
\end{aligned} \tag{4.50}$$

This should be compared with the topological string free energies in the conifold frame.

**Local** $\mathbb{P}^1 \times \mathbb{P}^1$. We take $\tilde{\beta} \to \infty$, $\tilde{\gamma} = 0$ and $(m, n) = (0, 1)$. This is the local $\mathbb{P}^1 \times \mathbb{P}^1$ case, with mass parameter $m_{\mathbb{F}_0} = \mathrm{e}^{\alpha} = \mathrm{e}^{\frac{\hbar}{\pi}\tilde{\alpha}}$. We find the following result:

$$\begin{aligned}
\mathcal{F}_0(\lambda, \xi) &= \frac{\lambda^2}{2}\left(\log\left(\frac{\pi^2\lambda\cosh\frac{\tilde{\alpha}}{2}}{4}\right) - \frac{3}{2}\right) - \frac{2}{\pi^2}\mathrm{Im}\left(\mathrm{Li}_2(\mathrm{i}\,\mathrm{e}^{\tilde{\alpha}/2})\right)\lambda + \sum_{k\geq 3} f_{0,k}\lambda^k, \\
\mathcal{F}_1(\lambda, \xi) &= -\frac{1}{12}\log\hbar - \frac{1}{12}\log\lambda + \zeta'(-1) + \sum_{k\geq 1} f_{1,k}\lambda^k, \\
\mathcal{F}_g(\lambda, \xi) &= \frac{B_{2g}}{2g(2g-2)}\lambda^{2-2g} + \sum_{k\geq 1} f_{g,k}\lambda^k, \qquad g \geq 2.
\end{aligned} \tag{4.51}$$

The coefficients $f_{g,k}$ are themselves non-trivial functions of the parameter $\xi$. For $g = 0$, one finds, at the very first orders,

$$\begin{aligned}
f_{0,3} &= \pi^2\frac{1 - 3\cosh(\tilde{\alpha})}{24\cosh(\tilde{\alpha}/2)}, \\
f_{0,4} &= \pi^4\frac{-73 + 68\cosh(\tilde{\alpha}) + 45\cosh(2\tilde{\alpha})}{2304\cosh^2(\tilde{\alpha}/2)}, \\
f_{0,5} &= \pi^6\frac{534 - 203\cosh(\tilde{\alpha}) - 390\cosh(2\tilde{\alpha}) - 165\cosh(3\tilde{\alpha})}{30720\cosh^3(\tilde{\alpha}/2)}, \\
f_{0,6} &= \frac{\pi^8(472\cosh(\tilde{\alpha}) + 126508\cosh(2\tilde{\alpha}) + 9(15400\cosh(3\tilde{\alpha}) + 4725\cosh(4\tilde{\alpha}) - 23809))}{22118400\cosh^4(\tilde{\alpha}/2)}, \\
f_{0,7} &= \frac{\pi^{10}}{41287680\cosh^5(\tilde{\alpha}/2)}(225994 + 66446\cosh(\tilde{\alpha}) - 49880\cosh(2\tilde{\alpha}) - 191709\cosh(3\tilde{\alpha}) \\
&\qquad - 137970\cosh(4\tilde{\alpha}) - 33201\cosh(5\tilde{\alpha})),
\end{aligned} \tag{4.52}$$

for $g = 1$ one finds,

$$
\begin{aligned}
f_{1,1} &= \pi^2 \frac{-1+3\cosh(\tilde{\alpha})}{48\cosh(\tilde{\alpha}/2)},\\
f_{1,2} &= \pi^4 \frac{127+4\cosh(\tilde{\alpha})-27\cosh(2\tilde{\alpha})}{2304\cosh^2(\tilde{\alpha}/2)},\\
f_{1,3} &= \pi^6 \frac{-750-265\cosh(\tilde{\alpha})+30\cosh(2\tilde{\alpha})+57\cosh(3\tilde{\alpha})}{18432\cosh^3(\tilde{\alpha}/2)},\\
f_{1,4} &= \frac{\pi^8(8408\cosh(\tilde{\alpha})+5492\cosh(2\tilde{\alpha})+9(40\cosh(3\tilde{\alpha})-45\cosh(4\tilde{\alpha})+1689))}{552960\cosh^4(\tilde{\alpha}/2)},\\
f_{1,5} &= -\frac{\pi^{10}}{11796480\cosh^5(\tilde{\alpha}/2)}(203134+126026\cosh(\tilde{\alpha})+204280\cosh(2\tilde{\alpha})+107001\cosh(3\tilde{\alpha})\\
&\qquad +22410\cosh(4\tilde{\alpha})+189\cosh(5\tilde{\alpha})),
\end{aligned}
\tag{4.53}
$$

and for $g=2$ one finds,

$$
\begin{aligned}
f_{2,1} &= \pi^6 \frac{894+577\cosh(\tilde{\alpha})+210\cosh(2\tilde{\alpha})+15\cosh(3\tilde{\alpha})}{61440\cosh^3(\tilde{\alpha}/2)},\\
f_{2,2} &= -\frac{\pi^8(72664\cosh(\tilde{\alpha})+66796\cosh(2\tilde{\alpha})+9(2600\cosh(3\tilde{\alpha})+325\cosh(4\tilde{\alpha})+13167))}{7372800\cosh^4(\tilde{\alpha}/2)},\\
f_{2,3} &= \frac{\pi^{10}}{2949120\cosh^5(\tilde{\alpha}/2)}(39166+6914\cosh(\tilde{\alpha})+32440\cosh(2\tilde{\alpha})+22389\cosh(3\tilde{\alpha})\\
&\qquad +8010\cosh(4\tilde{\alpha})+1161\cosh(5\tilde{\alpha})),
\end{aligned}
\tag{4.54}
$$

and for $g=3$ one finds,

$$
\begin{aligned}
f_{3,1} &= \frac{\pi^{10}}{99090432\cosh^5(\tilde{\alpha}/2)}(-200114+242714\cosh(\tilde{\alpha})+91192\cosh(2\tilde{\alpha})+56385\cosh(3\tilde{\alpha})\\
&\qquad +16506\cosh(4\tilde{\alpha})+1701\cosh(5\tilde{\alpha})).
\end{aligned}
\tag{4.55}
$$

For diagonal the $\mathbb{P}^1\times\mathbb{P}^1$ ($m=1$, equivalently $\tilde{\alpha}=0$), we obtain

$$
\begin{aligned}
\mathcal{F}_0(\lambda) &= \frac{\lambda^2}{2}\left(\log\left(\frac{\pi^2\lambda}{4}\right)-\frac{3}{2}\right)-\frac{2\mathcal{G}}{\pi^2}\lambda-\frac{\pi^2}{12}\lambda^3+\frac{5\pi^4}{288}\lambda^4-\frac{7\pi^6}{960}\lambda^5\\
&\qquad +\frac{733\pi^8}{172800}\lambda^6-\frac{47\pi^{10}}{16128}\lambda^7+\mathcal{O}(\lambda^8),\\
\mathcal{F}_1(\lambda) &= -\frac{1}{12}\log(\lambda)+\zeta'(-1)+\frac{\pi^2}{24}\lambda+\frac{13\pi^4}{288}\lambda^2-\frac{29\pi^6}{576}\lambda^3+\frac{227\pi^8}{4320}\lambda^4\\
&\qquad -\frac{259\pi^{10}}{4608}\lambda^5+\mathcal{O}(\lambda^6),\\
\mathcal{F}_2(\lambda) &= -\frac{1}{240}\lambda^{-2}+\frac{53\pi^6}{1920}\lambda-\frac{2221\pi^8}{57600}\lambda^2+\frac{43\pi^{10}}{1152}\lambda^3+\mathcal{O}(\lambda^4),\\
\mathcal{F}_3(\lambda) &= \frac{1}{1008}\lambda^{-4}+\frac{407\pi^{10}}{193536}\lambda+\mathcal{O}(\lambda^2).
\end{aligned}
\tag{4.56}
$$

Here, $\mathcal{G}\approx 0.915966$ is Catalan's constant.

Now, let us check if these expressions can be obtained from the topological string side. They should correspond to the free energies of the topological strings in the conifold frame. Before looking closer at our two examples, we can make the following general remark. Topological string theory in the conifold frame is known to

have a universal structure: when the free energies are expanded around the conifold point in moduli space, the leading singularities are of the form $t_c^{2-2g}$, where $t_c$ is the flat coordinate around the conifold point and is proportional to $\lambda$. The coefficients of these singularities are determined by the $c = 1$ string free energy [94]. There is in addition a "gap" condition, [95], which says that the corrections to this leading singularity involve only non-negative powers of $t_c$. This structure is precisely what is found in the weak 't Hooft coupling expansion of a perturbed gaussian hermitian matrix model such as we have here. Indeed, we clearly see this structure in eq. (4.43-4.44). We now examine the special cases of local $\mathbb{P}^2$ and local $\mathbb{P}^1 \times \mathbb{P}^1$.

**Local** $\mathbb{P}^2$. We need the expressions of the free energies of local $\mathbb{P}^2$ in the conifold frame. In order to write down results for local $\mathbb{P}^2$, let us recall some well known facts about its special geometry, relevant for our calculation. The mirror geometry of local $\mathbb{P}^2$ has only one modulus and no mass parameters: $g_W = 1$, $r_W = 0$. We only have one Kähler parameter

$$t \equiv T. \tag{4.57}$$

It is related to $\zeta$ through

$$t = 6\pi\zeta, \tag{4.58}$$

since $c = 3$ in this geometry. The Picard–Fuchs equation determining the periods is well known. It can be obtained directly from the charge vectors of local $\mathbb{P}^2$, and is given by

$$\left(\theta^3 - 3z(3\theta + 2)(3\theta + 1)\theta\right)\Pi = 0, \tag{4.59}$$

where

$$\theta = z\frac{\mathrm{d}}{\mathrm{d}z}, \tag{4.60}$$

and $z$ parametrizes the moduli space. The moduli space has three special points: $z = 0$ is the large radius point, $z = 1/27$ is the conifold point, and $z = \infty$ is the orbifold point (see Fig. 4.4). A basis of solutions around the large radius point $z = 0$ is given by

$$\begin{aligned}
\omega_1(z) &= \log(z) + 6z + 45z^2 + 560z^3 + \mathcal{O}(z^4), \\
\omega_2(z) &= \frac{\log^2(z)}{6} + \frac{\log(z)}{3}\left(6z + 45z^2 + 560z^3 + \mathcal{O}(z^4)\right) + 3z + \frac{141}{4}z^2 + \mathcal{O}(z^3),
\end{aligned} \tag{4.61}$$

which can be found by solving (4.59) using the appropriate ansatz. For this case,

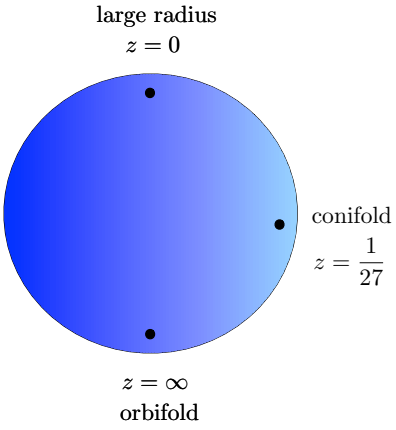


**Figure 4.4:** The moduli space of local $\mathbb{P}^2$ can be parametrized by a single complex variable $z$, and it has three special points: the large radius point at $z = 0$, the conifold point at $z = 1/27$, and the orbifold point at $z = \infty$.

closed formulas also exist in terms of hypergeometric functions and Meijer $G$ functions:

$$\begin{aligned}\omega_1(z) &= \log z + 6z\,{}_4F_3\left(1,1,\frac{4}{3},\frac{5}{3};2,2,2;27z\right),\\ \omega_2(z) &= \frac{1}{2\pi\sqrt{3}}G^{3,2}_{3,3}\left(\begin{array}{c}\frac{1}{3},\frac{2}{3},1\\ 0,0,0\end{array}\middle|\,27z\right)-\frac{5\pi^2}{18}.\end{aligned} \tag{4.62}$$

These periods determine the large radius, genus zero free energy $\widehat{F}_0(t)$ as

$$\begin{aligned}-t &= \omega_1(z),\\ \frac{\partial\widehat{F}_0}{\partial t} &= \omega_2(z),\end{aligned} \tag{4.63}$$

which gives

$$\widehat{F}_0(t) = \frac{t^3}{18} - 3\mathrm{e}^{-t} - \frac{45}{8}\mathrm{e}^{-2t} - \frac{244}{9}\mathrm{e}^{-3t} + \mathcal{O}(\mathrm{e}^{-4t}). \tag{4.64}$$

Note that the signs are not the standard ones. This is due to a non-trivial $B$ field which has to be turned on in (4.18) in order to obtain a consistent modified grand potential, as first noted in [6]. We can now write down the 't Hooft limit of the modified grand potential. The various constants appearing in the free energies are

$$a_{111} = \frac{1}{3}, \qquad b_1^{\mathrm{NS}} = -\frac{1}{24}, \qquad b_1 = \frac{1}{12}. \tag{4.65}$$

In the case of local $\mathbb{P}^2$, the function $A(\hbar)$ is known. It is given by

$$A(\hbar) = \frac{3A_{\mathrm{c}}(\hbar/\pi) - A_{\mathrm{c}}(3\hbar/\pi)}{4}, \tag{4.66}$$

where [96] (see also [97])

$$A_{\rm c}(k) = \frac{2\zeta(3)}{\pi^2 k}\left(1-\frac{k^3}{16}\right) + \frac{k^2}{\pi^2}\int_0^\infty \frac{x}{{\rm e}^{kx}-1}\log(1-{\rm e}^{-2x}){\rm d}x. \tag{4.67}$$

This function has a large $k$ expansion of the form,

$$\begin{aligned} A_{\rm c}(k) = &-\frac{k^2}{8\pi^2}\zeta(3) + \frac{1}{2}\log(2) + 2\zeta'(-1) + \frac{1}{6}\log\left(\frac{\pi}{2k}\right) \\ &+ \sum_{g\geq 2}\left(\frac{2\pi}{k}\right)^{2g-2} 4^g(-1)^{g-1}\frac{B_{2g}B_{2g-2}}{(4g)(2g-2)(2g-2)!}. \end{aligned} \tag{4.68}$$

We conclude that

$$\begin{aligned} A_0 &= \frac{3\zeta(3)}{16\pi^4}, \\ A_1 &= -\frac{1}{12}\log(\hbar) + \zeta'(-1) + \frac{1}{6}\log(2\pi) + \frac{1}{24}\log(3), \\ A_g &= (4\pi^2)^{2g-2}\left(3-3^{2-2g}\right)(-1)^{g-1}\frac{B_{2g}B_{2g-2}}{(4g)(2g-2)(2g-2)!}, \qquad g\geq 2, \end{aligned} \tag{4.69}$$

The function $J_0(\zeta)$ is

$$J_0(\zeta) = \frac{1}{16\pi^4}\left(\widehat{F}_0(t) + 3\zeta(3) - \frac{\pi^2 t}{6}\right). \tag{4.70}$$

The 't Hooft parameter is now given by the second line of (4.34), which reads in this case,

$$\begin{aligned} \frac{8\pi^3}{3}\lambda &= \frac{\partial\widehat{F}_0}{\partial t} - \frac{\pi^2}{6} \\ &= \omega_2(z) - \frac{\pi^2}{6}. \end{aligned} \tag{4.71}$$

The second line of this equation is nothing but the vanishing period at the conifold point, since $\omega_2(1/27) = \frac{\pi^2}{6}$.[6] Therefore, the 't Hooft parameter varies between 0 and $\infty$ as $z$ varies between $1/27$ and 0. The region around the large radius point $z = 0$ in CY moduli space corresponds to strong 't Hooft coupling, while the region around $z = 1/27$, the conifold point, corresponds to the weakly coupled theory. Since we are interested in expanding the free energies around $\lambda = 0$, we have to analyze the theory around the conifold point. To do this, we define the variable

$$y = 1 - 27z. \tag{4.72}$$

We now solve the Picard–Fuchs equation near the conifold point, i.e. near $y = 0$. There are again two independent periods. One of them, which we will denote by

[6] The easiest way to check this is numerically.

$t_c(y)$, is a flat coordinate near the conifold point. It is given by the power series expansion

$$t_c(y) = y + \frac{11y^2}{18} + \frac{109y^3}{243} + \frac{9389y^4}{26244} + \frac{88351y^5}{295245} + \frac{823187y^6}{3188646} + \mathcal{O}\left(y^7\right), \tag{4.73}$$

and is related to the 't Hooft parameter as

$$\lambda = \frac{\sqrt{3}}{12\pi^2} t_c(y). \tag{4.74}$$

Therefore, as announced above, the 't Hooft parameter defined by the fermionic traces is a flat coordinate at the conifold point, proportional to $t_c(y)$. The inverse series yields

$$y = \lambda - \frac{11}{18}\lambda^2 + \frac{145}{486}\lambda^3 - \frac{6733}{52488}\lambda^4 + \mathcal{O}(\lambda^5). \tag{4.75}$$

The period $\omega_1(z)$ defines the genus zero free energy $\mathcal{F}_0(\lambda)$. Indeed, from the first line of (4.34) and (4.63), we find

$$\frac{\partial \mathcal{F}_0}{\partial \lambda} = -\frac{t}{6\pi} = \frac{\omega_1(z)}{6\pi}. \tag{4.76}$$

This function is, up to normalizations and integration constants, the genus zero free energy of local $\mathbb{P}^2$ in the conifold frame, and it has been computed in [51] for example. In order to expand it around $\lambda = 0$, we need the expansion of the period $\omega_1(z)$ around the conifold point. This is a standard exercise in special geometry and one finds,

$$\omega_1(z) = -c_0 + \frac{\sqrt{3}}{2\pi}\left(t_c(y)\log\left(\frac{y}{3\log(3)+1}\right) + s\left(y\right)\right), \tag{4.77}$$

where

$$s(y) = \frac{7y^2}{12} + \frac{877y^3}{1458} + \frac{176015y^4}{314928} + \frac{9065753y^5}{17714700} + \frac{17960917y^6}{38263752} + \mathcal{O}\left(y^7\right), \tag{4.78}$$

and the constant $c_0$ is given in terms of a hypergeometric function at the conifold point $z = 1/27$:

$$\begin{aligned} c_0 &= -\frac{2}{9}\,{}_4F_3\left(1,1,\frac{4}{3},\frac{5}{3};2,2,2;1\right) + 3\log(3) \\ &\approx 2.90759 \end{aligned} \tag{4.79}$$

The relationship (4.76) can be integrated to obtain the genus zero free energy, up to an integration constant. This constant can be determined as follows. The value of $\mathcal{F}_0(\lambda)$ at $\lambda = 0$ is given by

$$\mathcal{F}_0(0) = J_0(\zeta(0)) = \frac{1}{16\pi^4}\left(\widehat{F}_0(c_0) - \frac{\pi^2 c_0}{6} + 3\zeta(3)\right), \tag{4.80}$$

where we used that

$$t\left(z=\frac{1}{27}\right)=c_0. \tag{4.81}$$

The value of $J_0(\zeta(0))$ can be obtained numerically with high precision and we find that $\mathcal{F}_0(0)$ *vanishes* (as expected from the conjecture), i.e. we find that

$$\widehat{F}_0(c_0)-\frac{\pi^2 c_0}{6}=-3\zeta(3). \tag{4.82}$$

When all this is taken into account, we find the expansion,

$$\begin{aligned}\mathcal{F}_0(\lambda)=&-\frac{c_0}{6\pi}\lambda+\frac{\lambda^2}{2}\left(\log\left(\frac{4\pi^2\lambda}{9\sqrt{3}}\right)-\frac{3}{2}\right)-\frac{\pi^2\lambda^3}{9\sqrt{3}}+\frac{\pi^4\lambda^4}{486}+\frac{56\pi^6\lambda^5}{10935\sqrt{3}}\\&-\frac{1058\pi^8\lambda^6}{492075}+\frac{3392\pi^{10}\lambda^7}{2066715\sqrt{3}}-\frac{208744\pi^{12}\lambda^8}{1171827405}+\mathcal{O}\left(\lambda^9\right).\end{aligned} \tag{4.83}$$

This expansion exactly agrees with the matrix model calculation (4.50), provided the number $c_0$ given in (4.79) satisfies

$$c_0=\frac{9}{\pi}\mathrm{Im}\,\mathrm{Li}_2(\mathrm{e}^{\mathrm{i}\pi/3}). \tag{4.84}$$

This is a true identity [98, 99] (see also [100]). This encapsulates the power of the TS/ST conjecture: the constant $c_0$ comes from the world of topological string theory, and it gives the value of the Kähler parameter $t$ at the conifold point. The constant $\frac{9}{\pi}\mathrm{Im}\,\mathrm{Li}_2(\mathrm{e}^{\mathrm{i}\pi/3})$ comes from the world of trace class operators arising from mirror curves, and their strong relationship with quantum dilogarithms. For the TS/ST conjecture to work, the two numbers coming from these two different worlds have to agree, which they do.

Let us now consider the genus one free energy. By using well-known results for the B–model of local $\mathbb{P}^2$, one finds (or see for example [51])

$$\begin{aligned}J_1(\zeta)&=\widehat{F}_1(t)+A_1\\&=\frac{1}{2}\log\left(-\frac{\mathrm{d}z}{\mathrm{d}t}\right)-\frac{1}{12}\log\left(z^7\left(1-27z\right)\right)+A_1.\end{aligned} \tag{4.85}$$

Using the second line of (4.32), as well as

$$\begin{aligned}2\pi\frac{\partial^2 J_0}{\partial\zeta^2}&=\frac{9}{2\pi}\frac{\partial^2\widehat{F}_0}{\partial t^2}\\&=\sqrt{3}\frac{\mathrm{d}t_c}{\mathrm{d}t},\end{aligned} \tag{4.86}$$

one obtains the following expansion for the genus 1 conifold free energy of local $\mathbb{P}^2$,

$$\begin{aligned}\mathcal{F}_1(\lambda)=&-\frac{1}{12}\log\left(\lambda\right)+\zeta'(-1)+\frac{5\pi^2\lambda}{18\sqrt{3}}-\frac{\pi^4\lambda^2}{486}-\frac{40\pi^6\lambda^3}{2187\sqrt{3}}+\frac{283\pi^8\lambda^4}{32805}-\frac{1376\pi^{10}\lambda^5}{177147\sqrt{3}}\\&+\frac{72272\pi^{12}\lambda^6}{55801305}+\frac{7936\pi^{14}\lambda^7}{14348907\sqrt{3}}+\mathcal{O}\left(\lambda^8\right),\end{aligned} \tag{4.87}$$

which again is in precise agreement with what was found in (4.50).

We can also test the conjecture for the higher genus free energies higher genus by using the results of [51]. Let us denote by $\hat{F}_g(t)$ the higher genus free energy of local $\mathbb{P}^2$, as computed in [51], with an extra sign $(-1)^{g-1}$. Then, one has from (4.25) and the known values of $A_g$ (4.69):

$$J_g(\zeta) = (4\pi^2)^{2g-2} \left\{ \hat{F}_g(t) - 3^{2-2g}(-1)^{g-1} \frac{B_{2g}B_{2g-2}}{(4g)(2g-2)(2g-2)!} \right\}, \qquad g \geq 2. \tag{4.88}$$

The genus $g$ free energy appearing here, $\widehat{F}_g(t)$, includes the so-called constant map contribution $C_g$, whose expression is well known:

$$\begin{aligned} \hat{F}_g(t) &= C_g + \mathcal{O}\left(\mathrm{e}^{-t}\right), \\ C_g &= 3(-1)^{g-1} \frac{B_{2g}B_{2g-2}}{(4g)(2g-2)(2g-2)!}. \end{aligned} \tag{4.89}$$

In our formalism, this contribution comes from the first term on the r.h.s. of (4.69), while the second term leads to an additional constant in (4.88). As mentioned above, the higher genus functions $\mathcal{F}_g(\lambda)$ should be given by the symplectic transformation of the (4.88) to the conifold frame. This was done for $\widehat{F}_g(t)$ (without the last constant term in (4.88)) in [51]. The resulting quantities, when expanded around the conifold point, display the singular term in $\lambda^{2-2g}$ appearing in (4.45), plus a constant, and a series starting in $\lambda$, i.e.

$$F_g^{\mathrm{con}}(t_c) = \frac{3^{g-1}B_{2g}}{2g(2g-2)} t_c^{2-2g} + 3^{2-2g}(-1)^{g-1} \frac{B_{2g}B_{2g-2}}{(4g)(2g-2)(2g-2)!} + \mathcal{O}(t_c). \tag{4.90}$$

This exhibits a "weak gap" condition, since the constant term is not 0. However, its value is such that it *cancels* exactly the second term on the r.h.s. of (4.88), as required by (4.45). In other words, the function $A(\hbar)$, which was conjectured in (4.66) in order to reproduce the spectral properties of $\rho$ for local $\mathbb{P}^2$, is precisely what is needed to guarantee the matrix model behavior of $\mathcal{F}_g(\lambda)$ near $\lambda = 0$, which exhibits a "strong gap" condition (after the pole, the expansion starts at first order in $\lambda$ and not the zeroth order). It is also easy to verify that, after taking into account the appropriate normalizations, the expansion of $\mathcal{F}_2(\lambda)$ and $\mathcal{F}_3(\lambda)$ in (4.50) agree with the higher genus topological string free energy at the conifold point given in [51] (eq. (4.49) of that reference). This concludes our checks for local $\mathbb{P}^2$.

**Local $\mathbb{P}^1 \times \mathbb{P}^1$.** Let us turn our attention to the local $\mathbb{P}^1 \times \mathbb{P}^1$ case. We want to obtain its free energies in the conifold frame. Again, let us recall some well known facts about its special geometry, relevant for our calculation. The mirror geometry of local $\mathbb{P}^1 \times \mathbb{P}^1$ has one "true" modulus and one mass parameter: $g_W = 1$,

$r_W = 1$. In terms of the two parameters $z_1, z_2$ defining the mirror curve, we have the "true" modulus $z = z_2$ and the mass parameter $m = z_1/z_2$. The Kähler parameter corresponding to the "true" modulus is related to $\zeta$ through

$$t \equiv T_2 = 4\pi\zeta, \tag{4.91}$$

since $c = 2$ in this geometry, whereas the one corresponding to pure mass is

$$T_m \equiv T_2 - T_1 = -\log m = -\frac{2\pi}{\hbar}\log m_{\mathbb{F}_0}. \tag{4.92}$$

The periods will be obtained as solutions to a single Picard–Fuchs equation [101]:

$$\begin{aligned}\Big[\Big(8(1-m)^2z^2 - 4(1+m)z + \frac{1}{2}\Big)\theta^3 + \Big(16(1-m)^2z^2 - 4(1+m)z\Big)\,\theta^2 \\ + \Big(6(1-m)^2z^2 - (1+m)z\Big)\theta\Big]\,\Pi = 0,\end{aligned} \tag{4.93}$$

where

$$\theta = z\frac{\mathrm{d}}{\mathrm{d}z}. \tag{4.94}$$

This is the form of the operator which is appropriate for the large radius point $z = 0$. As usual in local mirror symmetry, there will be a constant solution 1, a logarithmic solution,

$$\omega_1(z) = \log(z) + \sigma_1(z), \tag{4.95}$$

and a double logarithmic solution,

$$\omega_2(z) = \log^2(z) + 2\log(z)\sigma_1(z) + \sigma_2(z). \tag{4.96}$$

In these equations, $\sigma_{1,2}(z)$ are power series around $z = 0$, whose coefficients depend on $m$. The very first orders read,

$$\begin{aligned}\sigma_1(z) &= 2(m^{\frac{1}{2}} + m^{-\frac{1}{2}})m^{\frac{1}{2}}z + 3\Big((m + m^{-1}) + 4\Big)mz^2 \\ &\quad + \frac{20}{3}\Big((m^{\frac{3}{2}} + m^{-\frac{3}{2}}) + 9(m^{\frac{1}{2}} + m^{-\frac{1}{2}})\Big)m^{\frac{3}{2}}z^3 + \mathcal{O}(z^4), \\ \sigma_2(z) &= 4(m^{\frac{1}{2}} + m^{-\frac{1}{2}})m^{\frac{1}{2}}z + \Big(13(m + m^{-1}) + 40\Big)mz^2 \\ &\quad + \frac{8}{9}\Big(41(m^{\frac{3}{2}} + m^{-\frac{3}{2}}) + 279(m^{\frac{1}{2}} + m^{-\frac{1}{2}})\Big)m^{\frac{3}{2}}z^3 + \mathcal{O}(z^4).\end{aligned} \tag{4.97}$$

Let us now consider the following linear combinations of the basic periods,

$$\Pi_A^{(\mathrm{lr})}(z) = \begin{pmatrix}0 & 1 & 0\end{pmatrix} \cdot \begin{pmatrix}1 \\ \omega_1(z) \\ \omega_2(z)\end{pmatrix}, \tag{4.98}$$

$$\Pi_B^{(\mathrm{lr})}(z) = \begin{pmatrix}0 & \frac{\log m}{2} & \frac{1}{2}\end{pmatrix} \cdot \begin{pmatrix}1 \\ \omega_1(z) \\ \omega_2(z)\end{pmatrix}. \tag{4.99}$$

The first is the $A$–period and determines the flat coordinate $t$ through the mirror map, while the second, the $B$–period, determines the genus zero free energy $F_0(t,m)$ at large radius,

$$-t = \Pi_A^{(\mathrm{lr})}, \qquad \frac{\partial F_0}{\partial t} = \Pi_B^{(\mathrm{lr})}. \tag{4.100}$$

After integration we get,

$$F_0(t,m) = \frac{t^3}{6} - \frac{\log m}{4} t^2 - 2(m^{\frac{1}{2}} + m^{-\frac{1}{2}}) m^{\frac{1}{2}} \mathrm{e}^{-t} - \frac{1}{4}\Big((m+m^{-1}) + 16\Big) m \mathrm{e}^{-2t} \tag{4.101}$$

$$- \frac{2}{27}\Big((m^{\frac{3}{2}} + m^{-\frac{3}{2}}) + 81(m^{\frac{1}{2}} + m^{-\frac{1}{2}})\Big) m^{\frac{3}{2}} \mathrm{e}^{-3t} + \mathcal{O}(\mathrm{e}^{-4t}). \tag{4.102}$$

We omitted the hat over $F_0$ since the $B$ field is trivial in the local $\mathbb{P}^1 \times \mathbb{P}^1$ case, so $F_g$ and $\widehat{F}_g$ coincide. Equivalently, one can obtain the same information from the equations

$$\frac{\partial t}{\partial z} = -\frac{2}{\pi z \sqrt{1 - 4(\sqrt{m}+1)^2 z}} \mathrm{K}\left(\frac{16\sqrt{m} z}{4(\sqrt{m}+1)^2 z - 1}\right), \tag{4.103}$$

$$\frac{\partial^2 F_0}{\partial t \partial z} = -\frac{2}{z \sqrt{1 - 4(\sqrt{m}-1)^2 z}} \mathrm{K}\left(\frac{4(\sqrt{m}+1)^2 z - 1}{4(\sqrt{m}-1)^2 z - 1}\right), \tag{4.104}$$

which can be obtained from the results of [102] for local $\mathbb{F}_2$, together with the dictionary relating the moduli of local $\mathbb{F}_2$ to those of local $\mathbb{P}^1 \times \mathbb{P}^1$ (see discussion around eq. (3.99)). In the above, $\mathrm{K}(m) = \frac{\pi}{2} + \frac{\pi}{8} m + \mathcal{O}(m^2)$ is the elliptic integral of the first kind. We now analyze the theory near the conifold locus given by the vanishing of the discriminant (the factor in front of $\theta^3$ in the Picard–Fuchs equation):

$$\Delta = 1 - 8(m+1)z + 16(m-1)^2 z^2 = \Big(4(1+\sqrt{m})^2 z - 1\Big)\Big(4(1-\sqrt{m})^2 z - 1\Big). \tag{4.105}$$

Note that there are two different branches of the conifold locus, related to the two square roots of $m$. For each value of $m$, we have a different conifold point in each of the branches of the conifold locus, and we have to analyze the topological string near an arbitrary point, as a function of $m$. We will pick for convenience the branch of positive roots, and introduce the local variable,

$$y = 1 - 4(1+\sqrt{m})^2 z, \tag{4.106}$$

which vanishes at the conifold point

$$z_c = \frac{1}{4(1+\sqrt{m})^2}. \tag{4.107}$$

In the variables appropriate to the conifold point, the Picard–Fuchs equation becomes

$$\tilde{\mathcal{L}}\Pi = 0, \tag{4.108}$$

where

$$\begin{aligned}\tilde{\mathcal{L}} = {} & 4(y-1)^2\Big(y(\sqrt{m}-1)^2+4\sqrt{m}\Big)\theta_y^3 \\ & + 4(y-1)\Big(2y^2(\sqrt{m}-1)^2+y(1+\sqrt{m})^2+8\sqrt{m}\Big)\theta_y^2 \\ & + \Big(3y^3(\sqrt{m}-1)^2+4y^2\sqrt{m}+y(m-6\sqrt{m}+1)+16\sqrt{m}\Big)\theta_y.\end{aligned} \tag{4.109}$$

There is a basis of solutions given by a constant solution 1, a vanishing solution

$$f_1(y) = y + \mathcal{O}(y^2), \tag{4.110}$$

and a logarithmic solution

$$f_2(y) = \log(y) f_1(y) + s(y), \qquad s(y) = y + \mathcal{O}(y^2). \tag{4.111}$$

Solving for $f_1(y)$ and $s(y)$ as power series in $y$, we obtain:

$$\begin{aligned} f_1(y) &= y - \frac{\cosh(\tilde{\alpha})-11}{16}y^2 + \frac{9\cosh(2\tilde{\alpha})-124\cosh(\tilde{\alpha})+827}{1536}y^3 + \mathcal{O}(y^4), \\ s(y) &= y - \frac{7\cosh(\tilde{\alpha})-45}{32}y^2 + \frac{27\cosh(2\tilde{\alpha})-380\cosh(\tilde{\alpha})+1561}{1152}y^3 + \mathcal{O}(y^4), \end{aligned} \tag{4.112}$$

where we expressed the results in terms of the variable $\tilde{\alpha}$, related to the mass parameter $m$ by $m = \mathrm{e}^{2\tilde{\alpha}}$. The analytic continuation of the large radius periods to the conifold point must be a linear combination of the two solutions $f_1(y)$, $f_2(y)$ found above. By expanding the exact results (4.103-4.104) around the conifold locus, one finds

$$\Pi_A^{(\mathrm{lr})}(z) = \Big(C_1(\tilde{\alpha}) \qquad \frac{\cosh\tilde{\alpha}/2}{\pi}\Big(\log\Big(\frac{\cosh^2\tilde{\alpha}/2}{16}\Big)-2\Big) \qquad \frac{\cosh\tilde{\alpha}/2}{\pi}\Big)\cdot\begin{pmatrix}1\\ f_1(y)\\ f_2(y)\end{pmatrix}, \tag{4.113}$$

$$\Pi_B^{(\mathrm{lr})}(z) = \Big(C_2(\tilde{\alpha}) \qquad \pi\cosh\tilde{\alpha}/2 \qquad 0\Big)\cdot\begin{pmatrix}1\\ f_1(y)\\ f_2(y)\end{pmatrix}, \tag{4.114}$$

where $C_1(\tilde{\alpha})$, $C_2(\tilde{\alpha})$ are a priori $\tilde{\alpha}$–dependent constants which have to be obtained by other means since the exact results (4.103-4.104) are derivatives of periods. These constants are given by the values of the large radius periods at the conifold point:

$$C_1(\tilde{\alpha}) = \Pi_A^{(\mathrm{lr})}(z_c), \qquad C_2 = \Pi_B^{(\mathrm{lr})}(z_c). \tag{4.115}$$

The constant $C_1(\tilde{\alpha})$ can be computed analytically (see Appendix B of [12]). The constant $C_2(\tilde{\alpha})$ can be calculated numerically, by evaluating the series (4.97) at the conifold point (where the series still converges). However, as we will see in the next section, the value of these constants is *predicted* by the TS/ST conjecture, and we will find a precise agreement with the analytical and numerical evaluations of $C_{1,2}$, respectively. We will use the above results to determine the genus zero free energy at large radius $F_0(t,m)$. The genus one free energy can be obtained, for example, from the result for local $\mathbb{F}_2$ in [102], by using the map of moduli. One finds,

$$F_1(t,m) = -\frac{1}{12}\log\left(m^{\frac{1}{2}}z^7[16(m-1)^2z^2-8(m+1)z+1]\right) - \frac{1}{2}\log\left(-\frac{\partial t}{\partial z}\right), \quad (4.116)$$

with the large radius expansion

$$F_1(t,m) = -\frac{1}{24}\log(m) + \frac{t}{12} - \frac{1}{6}(1+m)\mathrm{e}^{-t} + \dots \quad (4.117)$$

The higher genus free energies near the conifold point can be obtained by integrating the holomorphic anomaly equation.

We need some data to state the conjecture. For this geometry, we have

$$\begin{aligned} \frac{1}{6}\sum_{ijk} a_{ijk}T_iT_jT_k &= \frac{1}{6}t^3 - \frac{1}{4}t^2\log m, \\ \sum_i b_iT_i &= \frac{1}{12}t - \frac{1}{24}\log(m), \\ \sum_i b_i^{\mathrm{NS}}T_i &= -\frac{1}{12}t. \end{aligned} \quad (4.118)$$

We also need an expression for the constant $A(m_{\mathbb{F}_0},\hbar)$. For our geometry, it has been determined by Y. Hatsuda[7] thanks to its close relation with ABJ(M) theory:

$$A(m_{\mathbb{F}_0},\hbar) = \frac{\log^3 m_{\mathbb{F}_0}}{48\pi\hbar} - \frac{\log m_{\mathbb{F}_0}}{4}\left(\frac{\pi}{3\hbar} - \frac{\hbar}{12\pi}\right) + A_{\mathrm{c}}\left(\frac{\hbar}{\pi}\right) - F_{\mathrm{CS}}\left(\frac{\hbar}{\pi}, M\right). \quad (4.119)$$

The function $A_{\mathrm{c}}(k)$ was introduced in [4] in the Fermi gas approach to ABJ(M) theory. It was determined explicitly in [96] and further simplified in [97]. It reads,

$$A_{\mathrm{c}}(k) = \frac{2\zeta(3)}{\pi^2 k}\left(1-\frac{k^3}{16}\right) + \frac{k^2}{\pi^2}\int_0^\infty \frac{x}{\mathrm{e}^{kx}-1}\log(1-\mathrm{e}^{-2x})\mathrm{d}x. \quad (4.120)$$

In (4.119), $F_{\mathrm{CS}}(k,M)$ is an analytic continuation of the Chern–Simons free energy on the three-sphere for the gauge group $U(M)$ and level $k$,

$$F_{\mathrm{CS}}(k,M) = \log\, Z_{\mathrm{CS}}(k,M), \quad (4.121)$$

[7] in an unpublished communication

where $M$ is related to the parameters of our problem through

$$M = \frac{\hbar + \mathrm{i}\log m_{\mathbb{F}_0}}{2\pi} = \frac{\hbar}{2\pi^2\mathrm{i}}\left(\mathrm{i}\pi - \frac{1}{2}\log m\right). \tag{4.122}$$

As it is well-known, the Chern–Simons partition function for integer $M$ is given by [103]

$$Z_{\mathrm{CS}}(k, M) = k^{-M/2}\prod_{j=1}^{M}\left(2\sin\frac{\pi j}{k}\right)^{M-j}, \tag{4.123}$$

but in view of (4.122) we have to extend it to arbitrary complex $M$. This can be done in various equivalent ways, but in this paper we will not need the precise form of this extension, only an asymptotic expansion at large $k, M$. The expansion of $A(m_{\mathbb{F}_0}, \hbar)$ in the 't Hooft limit can be easily worked out. The function $A_{\mathrm{c}}(k)$ has the large $k$ expansion [96]:

$$\begin{aligned} A_{\mathrm{c}}(k) = &-\frac{k^2}{8\pi^2}\zeta(3) + \frac{1}{2}\log(2) + 2\zeta'(-1) + \frac{1}{6}\log\left(\frac{\pi}{2k}\right) \\ &+ \sum_{g\geq 2}\left(\frac{2\pi}{k}\right)^{2g-2} 4^g(-1)^{g-1}\frac{B_{2g}B_{2g-2}}{(4g)(2g-2)(2g-2)!}, \end{aligned} \tag{4.124}$$

On the other hand, in the limit we are considering, $M \to \infty$ but

$$\frac{2\pi^2\mathrm{i}}{\hbar}M = \pi\mathrm{i} - \tilde{\alpha} \tag{4.125}$$

is fixed. This is the standard 't Hooft expansion of $F_{\mathrm{CS}}(\hbar/\pi, M)$, worked out at all genus in [46], and with 't Hooft parameter (4.125). One then finds an expansion of the form

$$A(m_{\mathbb{F}_0}, \hbar) = \sum_{g\geq 0} A_g(\tilde{\alpha})\hbar^{2-2g}, \tag{4.126}$$

where

$$\begin{aligned} A_0(\tilde{\alpha}) &= \frac{\zeta(3) - 2\mathrm{Li}_3(-\mathrm{e}^{\tilde{\alpha}})}{8\pi^4}, \\ A_1(\tilde{\alpha}) &= -\frac{\tilde{\alpha}}{12} + \frac{1}{12}\log\left(16\pi^2\cosh\frac{\tilde{\alpha}}{2}\right) - \frac{1}{12}\log\hbar + \zeta'(-1), \\ A_g(\tilde{\alpha}) &= (2\pi^2)^{2g-2}(-1)^{g-1} \\ &\quad \times\left\{(4^g-2)\frac{B_{2g}B_{2g-2}}{(4g)(2g-2)(2g-2)!} - \frac{B_{2g}}{2g(2g-2)!}\mathrm{Li}_{3-2g}\left(-\mathrm{e}^{\tilde{\alpha}}\right)\right\}. \end{aligned} \tag{4.127}$$

In the following, we drop the logarithmic dependence on $\hbar$ (the usual $\frac{1}{12}\log\hbar$ factor) in $A_1(\tilde{\alpha})$. Also, on the first line, $\zeta(3)$ is the value of the Riemann zeta function at 3.

The restriction $\tilde{\alpha} = 0$ agrees with the results in [2]. We conclude that, in the 't Hooft limit, the modified grand potential has the asymptotic expansion

$$J(\zeta, \tilde{\alpha}, \hbar) = \sum_{g=0}^{\infty} J_g(\zeta, \tilde{\alpha}) \hbar^{2-2g}, \tag{4.128}$$

where

$$\begin{aligned} J_0(\zeta, \tilde{\alpha}) &= \frac{2}{3\pi}\zeta^3 - \frac{\tilde{\alpha}}{2\pi^2}\zeta^2 - \frac{1}{12\pi}\zeta + A_0(\tilde{\alpha}) + \frac{1}{16\pi^4} F_0^{\text{inst}}(t(\zeta), m), \\ J_1(\zeta, \tilde{\alpha}) &= \frac{\pi}{3}\zeta + A_1(\tilde{\alpha}) + F_1^{\text{inst}}(t(\zeta), m), \\ J_g(\zeta, \tilde{\alpha}) &= A_g(\tilde{\alpha}) + (4\pi^2)^{2g-2} F_g^{\text{inst}}\left(t(\zeta), m\right), \qquad g \geq 2, \end{aligned} \tag{4.129}$$

where $m = \mathrm{e}^{2\tilde{\alpha}}$ and $F_g^{\text{inst}}(t, m)$ are the instanton parts of the free energies, as in (4.20) (the $B$ field is trivial). The first line can be written as

$$J_0(\zeta, \tilde{\alpha}) = \frac{1}{(2\pi)^4}\left(F_0(t(\zeta), m) - \frac{\pi^2}{3} t(\zeta)\right) + A_0(\tilde{\alpha}). \tag{4.130}$$

Relations (4.34) therefore read (with $T$ replaced by $t$)

$$4\pi^3 \lambda = \frac{\partial F_0}{\partial t} - \frac{\pi^2}{3} = \Pi_B^{(\text{lr})} - \frac{\pi^2}{3}, \tag{4.131}$$

and

$$\frac{\partial \mathcal{F}_0}{\partial \lambda} = -\zeta = -\frac{1}{4\pi} t = \frac{1}{4\pi}\Pi_A^{(\text{lr})}. \tag{4.132}$$

First, from the matrix model behaviour, we expect that $\lambda$ vanishes on the conifold locus. This implies the relation

$$\Pi_B^{(\text{lr})}(z_c) = C_2(\tilde{\alpha}) = \frac{\pi^2}{3}. \tag{4.133}$$

This is a prediction of the conjecture: the value $C_2(\tilde{\alpha})$ is a pure constant. We have verified this by evaluating this constant numerically. This test involves doing a high precision numerical sum of the large radius expansion of $\Pi_B^{(\text{lr})}(z = z_c)$, for different values of $m = \mathrm{e}^{2\tilde{\alpha}}$. Now, using the expansions (4.113-4.114) around the conifold locus, we can integrate the second relation to

$$\begin{aligned} \mathcal{F}_0(\lambda) = {} & \frac{\lambda^2}{2}\left(\log\left(\frac{\pi^2 \lambda \cosh\tilde{\alpha}/2}{4}\right) - \frac{3}{2}\right) + \frac{C_1(\tilde{\alpha})}{4\pi}\lambda + \pi^2 \frac{1 - 3\cosh(\tilde{\alpha})}{24\cosh(\tilde{\alpha}/2)}\lambda^3 \\ & + \pi^4 \frac{-73 + 68\cosh(\tilde{\alpha}) + 45\cosh(2\tilde{\alpha})}{2304\cosh^2(\tilde{\alpha}/2)}\lambda^4 \\ & + \pi^6 \frac{534 - 203\cosh(\tilde{\alpha}) - 390\cosh(2\tilde{\alpha}) - 165\cosh(3\tilde{\alpha})}{30720\cosh^3(\tilde{\alpha}/2)}\lambda^5 + \mathcal{O}(\lambda^6). \end{aligned} \tag{4.134}$$

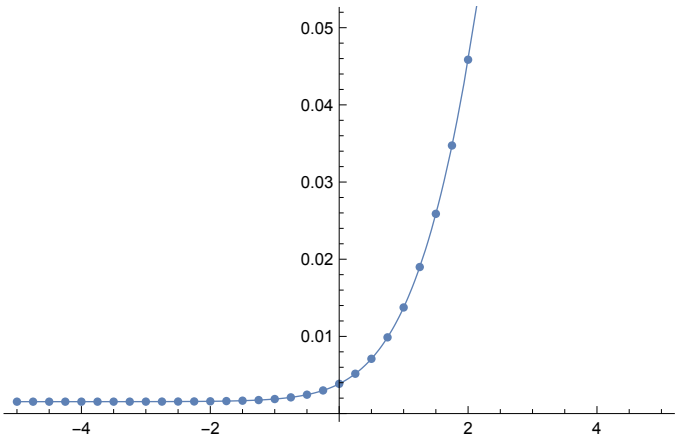


**Figure 4.5:** The continuous line shows the exact function $A_0(\xi/2)$, as given in (4.127), while the dots are numerical evaluations of the r.h.s. of (4.137) for some values of $\xi = 2\tilde{\alpha}$.

This result agrees with the results in (4.51-4.52) obtained in the matrix model (and higher orders can also be checked to match), provided that

$$C_1(\tilde{\alpha}) = -\frac{8}{\pi}\mathrm{Im}\left(\mathrm{Li}_2(\mathrm{i}\mathrm{e}^{\tilde{\alpha}/2})\right). \tag{4.135}$$

Again, this is a *prediction* of the TS/ST conjecture on the value of the $A$–period at the conifold point. This prediction comes from the explicit form of the potential in the matrix model (involving the quantum dilogarithms), which is in turn determined by the explicit form of the integral kernel for the quantized mirror curve. As shown in Appendix B of [12], the value (4.135) agrees precisely with the analytic evaluation of the $A$–period at the conifold point. As for the local $\mathbb{P}^2$ case, another neat identity can be obtained by noticing that the matrix model expression for $\mathcal{F}_0(\lambda)$ requires the vanishing of the constant term in $\lambda$. Therefore, we should have

$$0 = \mathcal{F}_0(\lambda = 0) = \Big(J_0(\zeta, \tilde{\alpha}) - \lambda\,\zeta\Big)\Big|_{\zeta=\zeta(\lambda=0)}. \tag{4.136}$$

Using (4.130) and the fact that $\zeta(\lambda = 0) = -\frac{1}{4\pi}\Pi_A^{(\mathrm{lr})}(z_c) = -\frac{1}{4\pi}C_1(\tilde{\alpha})$, this yields the following relation between the function $A_0(\tilde{\alpha})$ in (4.127) and the value of the genus zero free energy at the conifold point:

$$A_0(\tilde{\alpha}) = \frac{1}{16\pi^4}\Big(F_0(-C_1(\tilde{\alpha}), \tilde{\alpha}) + \frac{\pi^2}{3}C_1(\tilde{\alpha})\Big), \tag{4.137}$$

where we used that $t(z_c) = -C_1(\tilde{\alpha})$. This can be rewritten as

$$F_0\left(t\left(z_c\right), m\right) = 2\zeta(3) - 4\mathrm{Li}_3(-\sqrt{m}) + \frac{4\pi}{3\mathrm{i}}\left(\mathrm{Li}_2(\mathrm{i}m^{1/4}) - \mathrm{Li}_2(-\mathrm{i}m^{1/4})\right) \tag{4.138}$$

for $z_c = (2(1+\sqrt{m}))^{-2}$. This is yet another remarkable consequence of the TS/ST conjecture for the special geometry of the conifold point, and we have verified it numerically with high precision. To give a flavor of the validity of (4.137), in Fig. 4.5 we show the value of $A_0(\tilde{\alpha})$, as given in (4.127), against a numerical evaluation of the r.h.s. of (4.137) for some values of $\tilde{\alpha}$.

Let us now consider the genus one free energy. We have

$$J_1(\zeta,\tilde{\alpha}) = \frac{\pi}{3}\zeta + A_1(\tilde{\alpha}) + F_1^{\rm inst}(t,\tilde{\alpha}) = A_1(\tilde{\alpha}) + \frac{\tilde{\alpha}}{12} + F_1(t,m), \tag{4.139}$$

where we used (4.116) and the expansion (4.117). We now use (4.32)

$$\mathcal{F}_1(\lambda) = J_1(\zeta(\lambda)) - \frac{1}{2}\log\left(2\pi J_0''(\zeta(\lambda))\right) \tag{4.140}$$

and

$$\frac{\partial^2 J_0(\zeta)}{\partial\zeta^2} = 4\pi\frac{\partial\lambda}{\partial t}, \tag{4.141}$$

and obtain

$$\begin{aligned}\mathcal{F}_1(\lambda) = A_1(\xi) + \frac{\tilde{\alpha}}{12} - \frac{1}{24}\log m \\ - \frac{1}{12}\log\Big(m^{\frac{1}{2}} z^7(\lambda)(16(m-1)^2 z^2(\lambda) - 8(m+1)z(\lambda) + 1)\Big) \\ + \frac{1}{2}\log\Big(-\frac{1}{8\pi^2}\frac{\partial z(\lambda)}{\partial\lambda}\Big).\end{aligned} \tag{4.142}$$

By using the explicit expression for $A_1(\xi)$ in (4.127), we find that the small $\lambda$ expansion of this function is,

$$\begin{aligned}\mathcal{F}_1(\lambda) = -\frac{1}{12}\log\lambda - \frac{1}{12}\log\hbar + \zeta'(-1) \\ + \pi^2\frac{-1+3\cosh(\tilde{\alpha})}{48\cosh^2(\tilde{\alpha}/2)}\lambda + \pi^4\frac{127+4\cosh(\tilde{\alpha})-27\cosh(2\tilde{\alpha})}{2304\cosh^2(\tilde{\alpha}/2)}\lambda^2 + \mathcal{O}(\lambda^3),\end{aligned} \tag{4.143}$$

which is in precise agreement with what was found in (4.51-4.53). Higher order coefficients also match.

There are some non-trivial tests that can be done at higher genus, in the case $\tilde{\alpha} = 0$ (equivalently $m$=1), by using the results in [51, 80]. We recall that the topological string free energies in the conifold frame, when expanded around the conifold point in terms of a vanishing period, have a universal critical behavior characterized by a pole of order $2g-2$, for $g \geq 2$ as well as the "weak gap" condition, meaning that after the pole, the expansion starts at zeroth order (see previous example). However, in the matrix model free energies, as one can see in (4.51), the expansion around the conifold fulfills a "strong" gap condition, in the sense that the expansion in $\lambda$ after the pole starts at *first* order in $\lambda$ (and not at zeroth order). In

practice, this has the following consequence. Let us consider the instanton part of the large radius, genus $g$ free energies $F_g^{\rm inst}(t,m)$, and let us perform a symplectic transformation to the conifold frame. The "weak" gap condition of [95] implies that the expansion of the resulting quantities around the conifold point is of the form

$$\frac{B_{2g}}{2g(2g-2)}t_c^{2-2g}+b_g(\tilde{\alpha})+\mathcal{O}(t_c), \tag{4.144}$$

where $t_c=4\pi^2\lambda$ is a vanishing period at the conifold[8]. Then, it follows from the last line in (4.129) that

$$\mathcal{F}_g(\lambda)=\frac{B_{2g}}{2g(2g-2)}\lambda^{2-2g}+(4\pi^2)^{2g-2}b_g(\tilde{\alpha})+A_g(\tilde{\alpha})+\mathcal{O}(\lambda). \tag{4.145}$$

Therefore, consistency with the expansion (4.51), which satisfies a strong gap condition, requires that

$$b_g(\tilde{\alpha})=-\frac{A_g(\tilde{\alpha})}{(4\pi^2)^{2g-2}},\qquad g\geq 2. \tag{4.146}$$

This can be regarded as yet another prediction of spectral theory for the topological string (since the coefficients $A_g(\tilde{\alpha})$ have been fixed by consistency with studies of the spectrum). For $\tilde{\alpha}=0$, the constants $b_g(0)$ can be computed systematically from the holomorphic anomaly equations [51, 80]. One finds, for the very first genera (see for example eq. (5.22) in [51]),

$$b_2(0)=-\frac{1}{1152},\qquad b_3(0)=\frac{23}{5806080},\qquad b_4(0)=-\frac{19}{278691840}, \tag{4.147}$$

and by using (4.127), one verifies that (4.146) is indeed satisfied.

Finally, we note that the genus two and three free energy in the conifold frame is given by [51, 80]:

$$\begin{aligned} F_2^{\rm inst}(t_c,\tilde{\alpha}=0)&=-\frac{1}{240t_c^2}-\frac{1}{1152}+\frac{53t_c}{122880}-\frac{2221t_c^2}{14745600}+\ldots,\\ F_3^{\rm inst}(t_c,\tilde{\alpha}=0)&=\frac{1}{1008t_c^2}+\frac{23}{5806080}+\frac{407t_c}{198180864}+\ldots \end{aligned} \tag{4.148}$$

After taking into account the overall factor $(4\pi^2)^{2g-2}$ in (4.129), the third and fourth terms in $F_2^{\rm inst}$ and the third term in $F_3^{\rm inst}$ agree with the coefficients $f_{2,1}$, $f_{2,2}$ and $f_{3,1}$ in (4.56), for $\tilde{\alpha}=0$. This concludes our checks for local $\mathbb{P}^1\times\mathbb{P}^1$.

[8] We are considering just the instanton part of the large radius free energies, so we are not including the constant map contribution to these amplitudes. Note however that adding this contribution does not lead in general to a strong gap condition at the conifold. In other words, $-b_g$ is not the constant map contribution at large radius.

## 4.4 Exact planar results, spectral curve and checks at strong coupling

The results at weak 't Hooft coupling in the previous section provide rather convincing checks of the TS/ST correspondence in the 't Hooft limit. Nonetheless, obtaining exact results for the matrix model free energies $\mathcal{F}_g(\lambda)$ is quite desirable. This would allow us to perform checks of the TS/ST correspondence in the 't Hooft limit at strong coupling (large $\lambda$), or, taking the logic in reverse, to extract the Gromov–Witten invariants of the underlying CY threefold from the matrix model itself.

Exact results for the 't Hooft expansion of matrix models are known is several cases. The case which is close to our setup is the $O(n)$ matrix model. Indeed, whenever $C = \frac{m-n+1}{2(m+n+1)}$ in (4.6) is 0, our expression reduces to an $O(2)$ matrix model (although with non-polynomial, $\hbar$ dependent potential). This is for example the case for local $\mathbb{P}^1 \times \mathbb{P}^1$. The $O(n)$ matrix model in the planar limit[9] for any $n$ was solved by Eynard and Kristjansen in [104, 105] for a generic potential. Their results can be used for our matrix models when $C = 0$ (this was done in [12]).

However, for generic $C$, we have a *deformed* $O(2)$ matrix model, as given in (4.7). For example, the local $\mathbb{P}^2$ matrix model is a deformed $O(2)$ matrix model with $C = 1/6$. Exact planar results for the deformed case have, to our knowledge, not been obtained in full generality. For special forms of the potential, several results are available. The relevant case for the study of the statistical model known as the "six-vertex model" (or "ice model") has a precise polynomial potential (in the variable $\mathrm{e}^{\nu}$), and its planar limit was exactly solved by Kostov in [14]. Let us mention also that more general polynomial cases are solved in [106], and a rational case is solved in [107]. None of these solutions covers our cases, but we can adapt and extend the technique of [14] to tackle our matrix models. More precisely, we will derive exact results for the planar free energy, the planar one-point function and the planar two-point function, at least for our particular family of planar potentials $\mathrm{ReV}_0(\nu)$. Along the way, we will also obtain nice universal formulas for arbitrary potential. We will also see the emergence of the mirror curve itself in the matrix model.

Before starting the planar analysis of our model, let us make the following remark. The full solution of the matrix model in the 't Hooft limit would require the knowledge of all the $n$–point correlators at all orders in the 't Hooft expansion, or an algorithmic way to construct them. For many matrix models such as the

[9] By "planar", we mean genus 0 quantities, like $\mathcal{F}_0(\lambda)$.

hermitian matrix model or the $O(n)$ matrix model, this is given by the topological recursion [61–63]. The topological recursion is an algorithmic procedure, which, given a set of "initial conditions", generates the full set of the 't Hooft expanded $n$–point correlators recursively. The "initial conditions" are essentialy the spectral curve and the planar two point function. As we saw in chapter 2.3, the fact that the topological string amplitudes for all toric geometries obey the topological recursion is well known as the BKMP theorem. It was conjectured in [56, 57], first proved in [58], and the proof further formalized and extended in [59, 60]. It then appears that if we could manage to show that the matrix models considered in here were to satisfy the topological recursion with the right "initial conditions", the BKMP theorem would imply the proof of the relation between our matrix models and the topological string free energies. The planar results presented in this chapter can be considered as establishing the "initial condition" part of this program. The remainding task would be to show that these matrix models satisfy the topological recursion.

As usual for large $N$ matrix models, we perform a saddle point analysis of the multidimensional integral for the fermionic spectral traces $Z(N)$ given in (4.6). Let us write

$$Z(N) = \frac{1}{N!}\int_{\mathbb{R}^N} \mathrm{d}^N\nu\, \mathrm{e}^{-N^2 S_{\text{eff}}}. \tag{4.149}$$

Using the 't Hooft variable $\lambda = N/\hbar$, the effective action is given by

$$\begin{aligned} S_{\text{eff}} = \frac{1}{N\lambda}\sum_{k=1}^{N} \operatorname{Re} V(\nu_k) - \frac{1}{2N^2}\sum_{i\neq j}\log 4\sinh^2\left(\frac{\nu_i-\nu_j}{2}\right) \\ + \frac{1}{N^2}\sum_{i,j}\log 2\cosh\left(\frac{\nu_i-\nu_j}{2} - \mathrm{i}\pi C\right). \end{aligned} \tag{4.150}$$

In the large $N$ limit, $Z(N)$ is given by its value at the saddle point configuration given by $\nu^* = (\nu_1^*, \ldots, \nu_N^*)$ satisfying for all $k = 1, \ldots, N$:

$$\begin{aligned} 0 &= \left.\frac{\partial S_{\text{eff}}}{\partial \nu_k}\right|_{\nu=\nu^*} \\ &= \frac{1}{N\lambda}\frac{\partial}{\partial \nu_k^*}\mathrm{Re}V(\nu_k^*) - \frac{1}{2N^2}\sum_{i\neq k}\left[2\coth\left(\frac{\nu_k^*-\nu_i^*}{2}\right) - \tanh\left(\frac{\nu_k^*-\nu_i^*}{2} - \mathrm{i}\pi C\right)\right. \\ &\qquad \left. - \tanh\left(\frac{\nu_k^*-\nu_i^*}{2} + \mathrm{i}\pi C\right)\right]. \end{aligned} \tag{4.151}$$

It is convenient to use the exponential of $\nu_k^*$ as variables. Define

$$X_k = \mathrm{e}^{\nu_k^*}. \tag{4.152}$$

In the planar limit, only the leading part of the potential denoted $V_0(\nu)$ contributes, given by (3.112). Let us set

$$\mathcal{V}(X_k) = \mathrm{Re} V_0(\nu_k^*). \tag{4.153}$$

The explicit expression is

$$\begin{aligned}\mathcal{V}(X) = -\frac{1}{2\pi}\log X - \frac{m+n+1}{4\pi^2\mathrm{i}}\Big[&\mathrm{Li}_2\left(-X\mathrm{e}^{\tilde\alpha+\frac{\mathrm{i}\pi n}{m+n+1}}\right) - \mathrm{Li}_2\left(-X\mathrm{e}^{\tilde\alpha-\frac{\mathrm{i}\pi n}{m+n+1}}\right)\\ &+\mathrm{Li}_2\left(-X\mathrm{e}^{\tilde\beta+\frac{\mathrm{i}\pi n}{m+n+1}}\right) - \mathrm{Li}_2\left(-X\mathrm{e}^{\tilde\beta-\frac{\mathrm{i}\pi n}{m+n+1}}\right)\\ &+\mathrm{Li}_2\left(-X\mathrm{e}^{\tilde\gamma+\frac{\mathrm{i}\pi(m+1)}{m+n+1}}\right) - \mathrm{Li}_2\left(-X\mathrm{e}^{\tilde\gamma-\frac{\mathrm{i}\pi(m+1)}{m+n+1}}\right)\Big],\end{aligned} \tag{4.154}$$

where $(\tilde\alpha,\tilde\beta,\tilde\gamma) = \frac{2\pi}{m+n+1}\hbar^{-1}(\alpha,\beta,\gamma)$. The saddle point equation (4.151) at leading order in large $N$ can be rewritten as

$$\frac{1}{\lambda}\mathcal{V}'(X_k) = \frac{1}{N}\sum_{i\neq k}\left[\frac{2}{X_k-X_i} - \frac{\omega}{\omega X_k - X_i} - \frac{\omega^{-1}}{\omega^{-1}X_k - X_i}\right], \qquad k=1,\dots,N, \tag{4.155}$$

where

$$\omega = -\mathrm{e}^{2\pi\mathrm{i}C}. \tag{4.156}$$

The prime $'$ denotes derivation with respect to $X$. We will always suppose that $\omega$ is different from 1 (indeed, for $C=\pm 1/2$ the matrix model is not well behaved in the 't Hooft limit). In the 't Hooft limit, we expect the saddle point values $\nu_i^*$ to condense in a region $\mathcal{I}$ of the complex plane in such a way that they can be modelled by a distribution of a continuous variable. We work here with the variables $X=\mathrm{e}^\nu$, and use the normalized eigenvalue density $\rho(X)\mathrm{d}X$ satisfying

$$\int_{\mathcal{I}}\rho(X)\mathrm{d}X = 1. \tag{4.157}$$

Using this distribution, the sum in (4.155) can be rewritten as an integration over the region $\mathcal{I}$:

$$\frac{1}{\lambda}\mathcal{V}'(X) = 2\mathrm{P}\int_{\mathcal{I}}\frac{\rho(X')\mathrm{d}X'}{X-X'} - \omega\int_{\mathcal{I}}\frac{\rho(X')\mathrm{d}X'}{\omega X - X'} - \omega^{-1}\int_{\mathcal{I}}\frac{\rho(X')\mathrm{d}X'}{\omega^{-1}X - X'}, \qquad X\in\mathcal{I}, \tag{4.158}$$

where P denotes the Cauchy principal value. It can be checked that in our cases the potential has a single minimum, so we expect the saddle point configuration to condense inside a single interval on the positive real line

$$\mathcal{I} = [a,b], \qquad \text{with} \qquad a,b\in\mathbb{R}_+ \qquad \text{and} \qquad a<b. \tag{4.159}$$

We want to compute expectation values in our matrix model. We define the normalized expectation value

$$\langle f(\nu_1,\dots,\nu_N)\rangle = \frac{1}{Z(N)}\left(\frac{1}{N!}\int_{\mathbb{R}^N} \mathrm{d}^N\nu\, f(\nu_1,\dots,\nu_N)\mathrm{e}^{-N^2 S_{\text{eff}}}\right). \tag{4.160}$$

Let us define the following $n$–point correlators:

$$W_n(X_1,\dots,X_n) = \left\langle \prod_{k=1}^{n}\sum_{i_k=1}^{N}\left(\frac{1}{X_k-\mathrm{e}^{\nu_{i_k}}}-\frac{1}{X_k-\omega\mathrm{e}^{\nu_{i_k}}}\right)\right\rangle^{(c)}, \tag{4.161}$$

where $(c)$ means the connected correlator.[10] We will often find more useful the following, slightly different set of $n$–point correlators

$$\begin{aligned}\varpi_n(X_1,\dots,X_n) &= (\omega^{1/2}X_1)\cdots(\omega^{1/2}X_n)W_n(\omega^{1/2}X_1,\dots,\omega^{1/2}X_n)\\ &= \left\langle \prod_{k=1}^{n}\sum_{i_k=1}^{N}\left(\frac{\omega^{1/2}X_k}{\omega^{1/2}X_k-\mathrm{e}^{\nu_{i_k}}}-\frac{\omega^{-1/2}X_k}{\omega^{-1/2}X_k-\mathrm{e}^{\nu_{i_k}}}\right)\right\rangle^{(c)},\end{aligned} \tag{4.164}$$

which turn out to be more directly related to the spectral curve of the matrix integral. They will sometimes be called the *twisted correlators*. The $n$–point correlators have the following 't Hooft expansion[11]:

$$\begin{aligned}W_n(X_1,\dots,X_n) &= \sum_{g=0}^{\infty}\hbar^{2-2g-n}W_{n,g}(X_1,\dots,X_n),\\ \varpi_n(X_1,\dots,X_n) &= \sum_{g=0}^{\infty}\hbar^{2-2g-n}\varpi_{n,g}(X_1,\dots,X_n).\end{aligned} \tag{4.165}$$

Planar quantities are fully determined by the continuous eigenvalue saddle point distribution $\rho(X)\mathrm{d}X$. In particular, the one-point correlators in the large $N$ limit is

$$\varpi_{1,0}(X) = \lambda\int_{\mathcal{I}}\mathrm{d}X'\rho(X')\left(\frac{\omega^{1/2}X}{\omega^{1/2}X-X'}-\frac{\omega^{-1/2}X}{\omega^{-1/2}X-X'}\right). \tag{4.166}$$

[10] The connected correlators (or cumulants) of a set of random variables $X_n$ are defined through the equality of the two formal series in $\epsilon_n$:

$$\log\left\langle \mathrm{e}^{\sum_n \epsilon_n X_n}\right\rangle = \sum_{\mathbf{k}}\left(\prod_n\frac{\epsilon_n}{k_n!}\right)\left\langle\prod_n X_n^{k_n}\right\rangle^{(c)}. \tag{4.162}$$

where the sum is over all vectors $\mathbf{k}$ of non-negative integers of arbitrary size. The connected correlator is linear, therefore we can write

$$\left\langle \exp\sum_n \epsilon_n X_n\right\rangle = \exp\sum_{s=1}^{\infty}\frac{1}{s!}\left\langle\left(\sum_n\epsilon_n X_n\right)^s\right\rangle^{(c)}. \tag{4.163}$$

In the context of our matrix models, we take $X_n$ to be traces: $X_n = \sum_{i=1}^{N}\mathrm{e}^{n\nu_i}$.

[11] This is a consequence of the fatgraph expansion of the matrix model.

It is a function on the complex plane with branch cuts, which can be chosen to lie along the rotated intervals

$$\omega^{1/2}\mathcal{I} = [\omega^{1/2}a, \omega^{1/2}b] \qquad \text{and} \qquad \omega^{-1/2}\mathcal{I} = [\omega^{-1/2}a, \omega^{-1/2}b], \tag{4.167}$$

It is analytic everywhere else. The discontinuities along the branch cuts are given by the eigenvalue density $\rho(X)$: for $X \in \mathcal{I}$ we have

$$\varpi_{1,0}(\omega^{\mp 1/2}(X - \mathrm{i}0)) - \varpi_{1,0}(\omega^{\mp 1/2}(X + \mathrm{i}0)) = \pm 2\pi\mathrm{i}\lambda X\rho(X), \tag{4.168}$$

from which we immediately obtain the condition

$$\lambda = \pm\frac{1}{2\pi\mathrm{i}}\oint_{\omega^{\mp 1/2}\mathcal{I}} \varpi_{1,0}(X)\frac{\mathrm{d}X}{X}, \tag{4.169}$$

which is just the normalization of the eigenvalue density $\rho(X)$. Also, from its definition, we have the following small and large $X$ behaviour:

$$\begin{aligned} \varpi_{1,0}(X) &= O(X) \qquad && \text{for } X \to 0, \\ \varpi_{1,0}(X) &= O(X^{-1}) \qquad && \text{for } X \to \infty, \end{aligned} \tag{4.170}$$

The saddle point equation (4.158) can be written in terms of $\varpi_{1,0}(X)$ instead of the distribution $\rho(X)$. We obtain the following condition on $\varpi_{1,0}(X)$:

$$\varpi_{1,0}(\omega^{-1/2}(X \pm \mathrm{i}0)) - \varpi_{1,0}(\omega^{1/2}(X \mp \mathrm{i}0)) = X\mathcal{V}'(X), \qquad X \in \mathcal{I}, \tag{4.171}$$

The key argument is that these conditions together with the different analytic properties of $\varpi_{1,0}(X)$ fix it completely. To actually find what it is, we essentially use the technique of [14], adapted to our potential function $X\mathcal{V}'(X)$. In order for the technique of [14] to work for solving (4.171), we need $\mathcal{V}'(X)$ to be a meromorphic function of $X$. In the present situation this is not the case, since $\mathcal{V}(X)$ is built from dilogarithm functions $\mathrm{Li}_2(z)$, so $X\mathcal{V}'(X)$ has logarithmic singularities. Therefore, what we do is basically differentiate all involved functions another time and solve for the derivative of $\varpi_{1,0}(X)$. Indeed, the right hand side of (4.171) becomes a meromorphic function. Concretely, let us define $U(X)$ to be a meromorphic function satisfying

$$X(X\,\mathcal{V}'(X))' = U(\omega^{1/2}X) - U(\omega^{-1/2}X). \tag{4.172}$$

(an expression for $U(X)$ is given below). We also define

$$J(X) = U(X) + X\varpi'_{1,0}(X) \tag{4.173}$$

In terms of $J(X)$, by appropriate multiplication by $X$ and differentiation, we can rewrite (4.171) as

$$J(\omega^{\pm 1/2}(X + \mathrm{i}0)) - J(\omega^{\mp 1/2}(X - \mathrm{i}0)) = 0 \tag{4.174}$$

valid for $X \in \mathcal{I}$. So we learn that $J(X)$ is a function on the complex plane with two cuts along $\omega^{1/2}\mathcal{I}$ and $\omega^{-1/2}\mathcal{I}$, with a sort of "periodic" matching along the different sides of the two branch cuts as a consequence of (4.174). These branch points may be of the inverse square root type because of the extra differentiation. Apart from these points, $J(X)$ is meromorphic away from the cuts, all of whose poles are inherited exclusively from the potential part $U(X)$. Also, for large $X$,

$$J(X) = U_{\rm pol}(X) + O(X^{-1}), \tag{4.175}$$

where $U_{\rm pol}(X)$ is the polynomial part of $U(X)$ at large $X$. These properties of $J$ tell us that if we can find a conformal map $X(u)$ from the interior of the fundamental rectangle with side 1 and $\tau \in \mathrm{i}\mathbb{R}_{>0}$ to the complex plane minus the cuts, then the function

$$j(u) \equiv J(X(u)) \tag{4.176}$$

is an elliptic function. In other words, it is a doubly periodic meromorphic function in the complex plane, with fundamental domain given by the rectangle with sides 1 and $\tau$. An elliptic function is completely determined by its poles and its polar behaviour at those poles, up to an additive constant (a consequence of Liouville's theorem). Define the odd $\vartheta$ function as

$$\vartheta_1(u) = \frac{1}{\mathrm{i}} \sum_{n\in\mathbb{Z}} (-1)^n \mathrm{e}^{\mathrm{i}\pi(n+\frac{1}{2})^2\tau + 2\pi\mathrm{i}(n+\frac{1}{2})u}, \tag{4.177}$$

satisfying

$$\begin{aligned} \vartheta_1(u+1) &= \vartheta_1(-u) = -\vartheta_1(u), \\ \vartheta_1(u+\tau) &= -\mathrm{e}^{-\mathrm{i}\pi\tau - 2\pi\mathrm{i}u}\vartheta_1(u), \\ \vartheta_1(u) &= \vartheta_1'(0)u + O(u^3). \end{aligned} \tag{4.178}$$

An elliptic function with poles at $u = B_1, ..., B_k$ can be written as a ratio of $\vartheta_1$ functions:

$$f(u) = \text{const} \times \prod_{\ell=1}^{k} \frac{\vartheta_1(u - A_\ell)}{\vartheta_1(u - B_\ell)}, \tag{4.179}$$

provided that

$$A_1 + A_2 + \ldots + A_k = B_1 + B_2 + \ldots + B_k \mod 1. \tag{4.180}$$

Actually, all elliptic functions can be written in this way. The conformal mapping $X(u)$ has been found in [14, 108], and can also be written using the $\vartheta_1$ function. In our notation, it is given by

$$X(u) = \sqrt{ab}\frac{\vartheta_1(u_\infty + u)}{\vartheta_1(u_\infty - u)}. \tag{4.181}$$

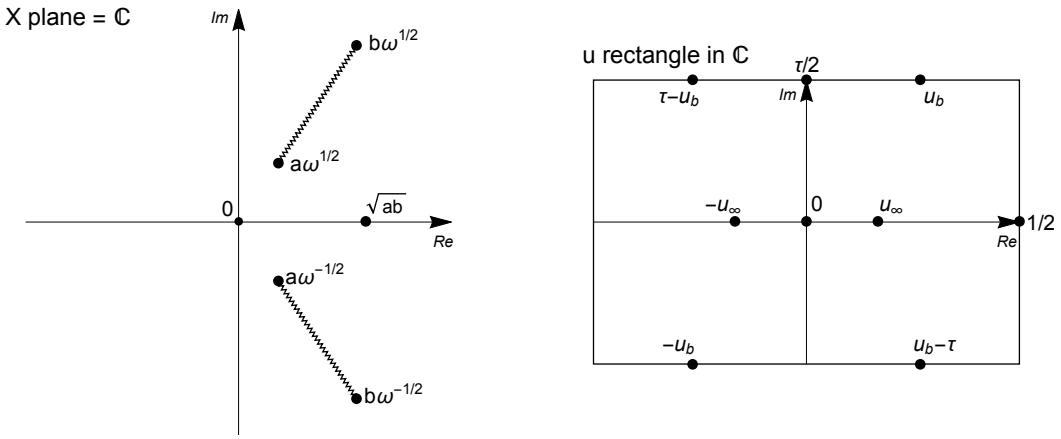


**Figure 4.6:** The various points of interest in the $X$ plane and their images in the $u$ rectangle under the conformal mapping $X(u)$. On the left, the wiggly lines denote the segments $\omega^{1/2}\mathcal{I} = [\omega^{1/2}a, \omega^{1/2}b]$ and $\omega^{-1/2}\mathcal{I} = [\omega^{-1/2}a, \omega^{-1/2}b]$, which are the branch cuts of $\varpi_{1,0}(X)$. These segments are mapped to the upper and lower sides of the $u$ rectangle. This conformal mapping is a mapping between a single sheet in the cut $X$ plane to a flat torus. On this flat torus $j(u) = J(X(u))$ is a well defined meromorphic function. So $j(u)$ is an elliptic function of $u$.

The values $a, b$ determine the interval $\mathcal{I}$ and $u_\infty$ is the point in the $u$ plane that is mapped to $\infty$. Correspondingly, the point $-u_\infty$ is mapped to $X = 0$ (cf. Fig. 4.6). We want to map the upper and lower sides of the fundamental rectangle centred at $u = 0$ to the cuts $\omega^{1/2}\mathcal{I}$ and $\omega^{-1/2}\mathcal{I}$ respectively. This is fulfilled if a shift by $\tau$ in the $u$ plane is equivalent to a multiplication by $\omega$ in the $X$ plane. This fixes the relation

$$\omega = \frac{X(u+\tau)}{X(u)} = \frac{\vartheta_1(u_\infty + u + \tau)\vartheta_1(u_\infty - u)}{\vartheta_1(u_\infty - u - \tau)\vartheta_1(u_\infty + u)} = \mathrm{e}^{-4\pi \mathrm{i} u_\infty}. \tag{4.182}$$

The map $X(u)$ has therefore only two yet unfixed parameters: $\sqrt{ab}$ and $\tau$. The branch points located at $\omega^{\pm 1/2}a$ and $\omega^{\pm 1/2}b$ in the $X$ plane are stationary points of the map $X(u)$. Let us define $u_b$ to be the stationary point corresponding to $\omega^{1/2}b$:

$$X(u_b) = \omega^{1/2}b, \qquad X'(u_b) = 0. \tag{4.183}$$

The second equation is equivalent to

$$0 = \frac{X'(u_b)}{X(u_b)} = \frac{\vartheta_1'}{\vartheta_1}(u_\infty + u_b) + \frac{\vartheta_1'}{\vartheta_1}(u_\infty - u_b). \tag{4.184}$$

So $-u_b$ is also stationary point, in fact it is the one corresponding to $\omega^{-1/2}a$. Since $X(-u) = ab/X(u)$, the value $u_b$ defined from the above relation determines the ratio

$$\frac{b}{a} = \omega^{-1}\left(\frac{\vartheta_1(u_\infty + u_b)}{\vartheta_1(u_\infty - u_b)}\right)^2, \tag{4.185}$$

which corresponds to the length of the cut.

To find the function $j(u)$ we will need the explicit form of the potential function $U(X)$. From (4.154) we have

$$\begin{aligned} X(X\mathcal{V}'(X))' = \frac{m+n+1}{4\pi^2\mathrm{i}}\Bigg(&\frac{\mathrm{e}^{\mathrm{i}\pi\frac{n}{m+n+1}}X}{\mathrm{e}^{-\tilde\alpha}+\mathrm{e}^{\mathrm{i}\pi\frac{n}{m+n+1}}X} - \frac{\mathrm{e}^{-\mathrm{i}\pi\frac{n}{m+n+1}}X}{\mathrm{e}^{-\tilde\alpha}+\mathrm{e}^{-\mathrm{i}\pi\frac{n}{m+n+1}}X} \\ &+\frac{\mathrm{e}^{\mathrm{i}\pi\frac{n}{m+n+1}}X}{\mathrm{e}^{-\tilde\beta}+\mathrm{e}^{\mathrm{i}\pi\frac{n}{m+n+1}}X} - \frac{\mathrm{e}^{-\mathrm{i}\pi\frac{n}{m+n+1}}X}{\mathrm{e}^{-\tilde\beta}+\mathrm{e}^{-\mathrm{i}\pi\frac{n}{m+n+1}}X} \\ &+\frac{\mathrm{e}^{\mathrm{i}\pi\frac{m+1}{m+n+1}}X}{\mathrm{e}^{-\tilde\gamma}+\mathrm{e}^{\mathrm{i}\pi\frac{m+1}{m+n+1}}X} - \frac{\mathrm{e}^{-\mathrm{i}\pi\frac{m+1}{m+n+1}}X}{\mathrm{e}^{-\tilde\gamma}+\mathrm{e}^{-\mathrm{i}\pi\frac{m+1}{m+n+1}}X}\Bigg). \end{aligned} \tag{4.186}$$

Since

$$\omega = \mathrm{e}^{2\pi\mathrm{i}\frac{m+1}{m+n+1}} = \mathrm{e}^{-2\pi\mathrm{i}\frac{n}{m+n+1}}, \tag{4.187}$$

a consistent choice for the branch of the square root gives

$$\omega^{1/2} = -\mathrm{e}^{-\mathrm{i}\pi\frac{n}{m+n+1}} = \mathrm{e}^{\mathrm{i}\pi\frac{m+1}{m+n+1}}, \qquad \omega^{-1/2} = -\mathrm{e}^{\mathrm{i}\pi\frac{n}{m+n+1}} = \mathrm{e}^{-\mathrm{i}\pi\frac{m+1}{m+n+1}}. \tag{4.188}$$

The function $U(X)$ is given by the relatively simple expression

$$U(X) = \frac{(m+n+1)}{4\pi^2\mathrm{i}}\left(\frac{X}{\mathrm{e}^{-\tilde\alpha}-X} + \frac{X}{\mathrm{e}^{-\tilde\beta}-X} + \frac{X}{\mathrm{e}^{-\tilde\gamma}+X}\right). \tag{4.189}$$

Its three poles are inherited by the $J(X)$ function. Let us list the points where $J(X)$ has a singular behaviour:

$$\begin{aligned} \text{single poles} \quad &: \quad X = \mathrm{e}^{-\tilde\alpha}, \quad X = \mathrm{e}^{-\tilde\beta}, \quad X = -\mathrm{e}^{-\tilde\gamma}, \\ \text{inverse square-roots} \quad &: \quad X = \omega^{1/2}a, \quad X = \omega^{1/2}b, \quad X = \omega^{-1/2}a, \quad X = \omega^{-1/2}b. \end{aligned} \tag{4.190}$$

In the fundamental rectangle in the $u$ plane, we define the corresponding points $u_{\alpha,\beta,\gamma}$.

$$X(u_\alpha) = \mathrm{e}^{-\tilde\alpha}, \qquad X(u_\beta) = \mathrm{e}^{-\tilde\beta}, \qquad X(u_\gamma) = -\mathrm{e}^{-\tilde\gamma}. \tag{4.191}$$

We also have the points $u_b, -u_b, u_b - \tau, -u_b + \tau$ corresponding to the branch points:

$$X(u_b) = \omega^{1/2}b, \quad X(-u_b) = \omega^{-1/2}a, \quad X(u_b - \tau) = \omega^{-1/2}b, \qquad X(-u_b + \tau) = \omega^{1/2}a. \tag{4.192}$$

The function $j(u)$ is an elliptic function which has poles at all these locations in the $u$ rectangle. As a ratio of $\vartheta_1$ functions, it can be given as

$$j(u) \propto \frac{\vartheta_1(u-v_1)\vartheta_1(u-v_2)\vartheta_1(u-v_3)\vartheta_1(u-v_4)\vartheta_1(u-v_5)}{\vartheta_1(u-u_\alpha)\vartheta_1(u-u_\beta)\vartheta_1(u-u_\gamma)\vartheta_1(u-u_b)\vartheta_1(u+u_b)}, \tag{4.193}$$

such that

$$v_5 = u_\alpha + u_\beta + u_\gamma - v_1 - v_2 - v_3 - v_4 \mod 1. \tag{4.194}$$

The constants $v_i$ for $i = 1, \ldots, 4$ and the overall multiplicative constant are yet undetermined (we will not need their actual values). From (4.173), the planar one-point correlator $\varpi_{1,0}(X)$ satisfies

$$\varpi_{1,0}(X) = \int \frac{J(X) - U(X)}{X} \mathrm{d}X = \left[ \int \frac{X'(u)}{X(u)} j(u) \mathrm{d}u \right]_{u=u(X)} - \int \frac{U(X)}{X} \mathrm{d}X. \tag{4.195}$$

The second integral gives a sum of logarithmic terms:

$$\int \frac{U(X)}{X} \mathrm{d}X = \frac{m+n+1}{4\pi^2 \mathrm{i}} \left( \log(\mathrm{e}^{-\tilde{\gamma}} + X) - \log(\mathrm{e}^{-\tilde{\alpha}} - X) - \log(\mathrm{e}^{-\tilde{\beta}} - X) \right), \tag{4.196}$$

whereas evaluating the first integral needs a bit more investigation. Firstly, we find that

$$\log X(u+1) = \log X(u), \qquad \log X(u+\tau) = \log X(u) + \log \omega. \tag{4.197}$$

So $\frac{X'(u)}{X(u)}$ is an elliptic function with poles at $\pm u_\infty$ and zeros at $\pm u_b$. It can be therefore given by

$$\frac{X'(u)}{X(u)} \propto \frac{\vartheta_1(u-u_b)\vartheta_1(u+u_b)}{\vartheta_1(u-u_\infty)\vartheta_1(u+u_\infty)}. \tag{4.198}$$

Then, we have

$$\frac{X'(u)}{X(u)} j(u) \propto \frac{\vartheta_1(u-v_1)\vartheta_1(u-v_2)\vartheta_1(u-v_3)\vartheta_1(u-v_4)\vartheta_1(u-v_5)}{\vartheta_1(u-u_\alpha)\vartheta_1(u-u_\beta)\vartheta_1(u-u_\gamma)\vartheta_1(u-u_\infty)\vartheta_1(u+u_\infty)}. \tag{4.199}$$

Let us now define

$$\begin{aligned} \xi(u) = {} & k_1 \log \vartheta_1(u+u_\infty) + k_2 \log \vartheta_1(u-u_\infty) + k_3 \log \vartheta_1(u-u_\alpha) \\ & + k_4 \log \vartheta_1(u-u_\beta) + k_5 \log \vartheta_1(u-u_\gamma), \end{aligned} \tag{4.200}$$

where $k_i$ are yet undetermined constants satisfying $\sum_{i=1}^5 k_i = 0$. Since

$$\xi(u+1) = \xi(u), \qquad \xi(u+\tau) = \xi(u) + \text{constant shift}, \tag{4.201}$$

the function $\xi'(u)$ is an elliptic function with single poles at $\pm u_\infty$ and $u_{\alpha,\beta,\gamma}$. Therefore, it can be written as

$$\xi'(u) = \frac{\vartheta_1(u-v_1)\vartheta_1(u-v_2)\vartheta_1(u-v_3)\vartheta_1(u-v_4)\vartheta_1(u-v_5)}{\vartheta_1(u-u_\alpha)\vartheta_1(u-u_\beta)\vartheta_1(u-u_\gamma)\vartheta_1(u-u_\infty)\vartheta_1(u+u_\infty)} + \text{const}. \tag{4.202}$$

for the appropriate $k_i$. From this, we obtain

$$\int \frac{X'(u)}{X(u)} j(u) \mathrm{d}u = \xi(u) + k_6 u + k_7. \tag{4.203}$$

So we find

$$\begin{aligned}\varpi_{1,0}(X) = {} & k_1 \log \vartheta_1(u(X) + u_\infty) + k_2 \log \vartheta_1(u(X) - u_\infty) + k_3 \log \vartheta_1(u(X) - u_\alpha) \\ & + k_4 \log \vartheta_1(u(X) - u_\beta) + k_5 \log \vartheta_1(u(X) - u_\gamma) + k_6 u(X) + k_7 \\ & + \frac{m+n+1}{4\pi^2 \mathrm{i}} \Big( \log(\mathrm{e}^{-\tilde{\alpha}} + X) + \log(\mathrm{e}^{-\tilde{\beta}} + X) - \log(\mathrm{e}^{-\tilde{\gamma}} - X) \Big).\end{aligned} \tag{4.204}$$

We now need to determine the seven constants $k_i$, $i = 1, \dots, 7$. These can be fixed by looking at the behaviour of $\varpi_{1,0}(X)$ at $X \to \infty, 0$ where it should vanish, as well as at $X = \mathrm{e}^{-\tilde{\alpha}}, \mathrm{e}^{-\tilde{\beta}}, -\mathrm{e}^{-\tilde{\gamma}}$ where it should be regular. We find seven equations which fully determine $k_i$. In the end, the twisted planar one-point correlator is

$$\begin{aligned}\varpi_{1,0}(X) = \frac{m+n+1}{4\pi^2 \mathrm{i}} \log \Bigg( & \frac{\vartheta_1(u_\infty + u_\alpha)\vartheta_1(u_\infty + u_\beta)}{\vartheta_1(2u_\infty)\vartheta_1(u_\infty + u_\gamma)} \frac{\vartheta_1(u(X) - u_\gamma)\vartheta_1(u(X) - u_\infty)}{\vartheta_1(u(X) - u_\alpha)\vartheta_1(u(X) - u_\beta)} \\ & \times \frac{(\mathrm{e}^{\tilde{\alpha}} X - 1)(\mathrm{e}^{\tilde{\beta}} X - 1)}{(\mathrm{e}^{\tilde{\gamma}} X + 1)} \Bigg).\end{aligned} \tag{4.205}$$

We derived $\varpi_{1,0}(X)$ (and thus $W_{1,0}(X) = \lambda^{-1} \varpi_{1,0}(\omega^{-1/2} X)/X$) only using the saddle point equation for the derivative function $J(X)$. In particular, we lost some information on the growth of the potential for $X \to \infty$. We need to consider the full condition (4.171). We use that if $X$ is in the interval $\mathcal{I}$, we have

$$u(\omega^{-1/2}(X \pm \mathrm{i}0)) + \tau = u(\omega^{1/2} X (X \mp \mathrm{i}0)). \tag{4.206}$$

From our expression for $\varpi_{1,0}(X)$, we find that

$$\begin{aligned}& \varpi_{1,0}(\omega^{-1/2}(X \pm \mathrm{i}0)) - \varpi_{1,0}(\omega^{1/2}(X \mp \mathrm{i}0)) - X \mathcal{V}'(X) \\ & \qquad = \frac{m+n+1}{4\pi^2 \mathrm{i}} \log \left( \mathrm{e}^{-2\pi \mathrm{i}(u_\gamma + u_\infty - u_\alpha - u_\beta - \frac{1}{m+n+1})} \right).\end{aligned} \tag{4.207}$$

So the saddle point equation for $\varpi_{1,0}(X)$ implies the extra relation

$$u_\gamma + u_\infty - u_\alpha - u_\beta = \frac{1}{m+n+1} \mod 1. \tag{4.208}$$

This should in principle define the relation between $\sqrt{ab}$ and $\tau$. At this stage, the only undetermined parameter is the imaginary side of the fundamental rectangle $\tau$. It is implicitly determined as a function of the 't Hooft coupling $\lambda$ from the normalization condition (4.169).

Let us define

$$q = \mathrm{e}^{\mathrm{i}\pi\tau}. \tag{4.209}$$

It is insightful to consider the small $q$ expansion of our result. Well known small expansions exist for the $\vartheta$ functions. Useful ones include

$$\begin{aligned}\log\frac{\vartheta_1(u)}{\vartheta_1(v)} &= \log\frac{\sin\pi u}{\sin\pi v} - 2\sum_{n=1}^{\infty}\frac{q^{2n}}{n(1-q^{2n})}\left(\cos 2\pi n u - \cos 2\pi n v\right),\\ \frac{\vartheta_1'}{\vartheta_1}(u) &= \pi\frac{\cos\pi u}{\sin\pi u} + 4\pi\sum_{n=1}^{\infty}\frac{q^{2n}}{1-q^{2n}}\sin 2\pi n u.\end{aligned} \tag{4.210}$$

Inverting functions can be done order by order in $q$. We find that $u_b = \frac{1}{4} + \frac{\tau}{2} + O(q)$, and the ratio $b/a$ given in eq. (4.185) and controlling the size of the eigenvalue support $\mathcal{I}$ is:

$$\frac{b}{a} = 1 + 8\sin(2\pi u_\infty)q + 32\sin(2\pi u_\infty)^2 q^2 + O(q^3). \tag{4.211}$$

So we deduce that the small $q$ expansion corresponds to the weak coupling expansion (small $\lambda$ expansion) of the matrix model. Indeed, when $q \to 0$, we have that $a \to b$ and the interval $\mathcal{I}$ collapses to a point, which is given by $a = b = \sqrt{ab}$. It can be checked that in the small $q$ limit, the value of $\sqrt{ab}$ goes to the minimum of the planar potential.

Usually, when studying large $N$ matrix models, the planar one-point correlator is expressed through the so called spectral curve, which is often an algebraic curve in $\mathbb{C}^2$. In our case, the elliptic parametrization used in the previous section hides the role of the spectral curve, but it can be made apparent and is expected to be algebraic when $m, n$ are rationals (which is the case when the matrix model is related to toric CY threefolds or their degenerations). We start by considering the following functions of $u$:

$$\begin{aligned}X(u) &= \sqrt{ab}\frac{\vartheta_1(u_\infty + u)}{\vartheta_1(u_\infty - u)},\\ Y(u) &= \exp\left(-\frac{4\pi^2\mathrm{i}}{m+n+1}\varpi_{1,0}(X(u)) - \log\left[-\frac{\mathrm{e}^{\tilde\gamma}X(u)+1}{(\mathrm{e}^{\tilde\alpha}X(u)-1)\left(\mathrm{e}^{\tilde\beta}X(u)-1\right)}\right]\right)\\ &= -\frac{\vartheta_1(2u_\infty)\vartheta_1(u_\infty+u_\gamma)}{\vartheta_1(u_\infty+u_\alpha)\vartheta_1(u_\infty+u_\beta)}\frac{\vartheta_1(u-u_\alpha)\vartheta_1(u-u_\beta)}{\vartheta_1(u-u_\infty)\vartheta_1(u-u_\gamma)}.\end{aligned} \tag{4.212}$$

Both functions satisfy $f(u+1) = f(u)$, and moreover

$$\begin{aligned}X(u+\tau) &= \mathrm{e}^{-4\pi\mathrm{i}u_\infty}X(u) = \mathrm{e}^{-2\pi\mathrm{i}\frac{n}{m+n+1}}X(u),\\ Y(u+\tau) &= \mathrm{e}^{2\pi\mathrm{i}(u_\alpha+u_\beta-u_\gamma-u_\infty)}Y(u) = \mathrm{e}^{-2\pi\mathrm{i}\frac{1}{m+n+1}}Y(u),\end{aligned} \tag{4.213}$$

where we used (4.182) and (4.208). Therefore, we can build elliptic functions by multiplying powers of $X$ and $Y$, and an appropriate linear combination of these functions can be chosen such that all the poles vanish. By the usual argument, this combination is then a constant, and the corresponding relation defines the spectral curve of the matrix model. To see how this works, let us take some concrete cases.

**The local $\mathbb{P}^2$ spectral curve.** We fix $m = n = 1$, $\tilde{\alpha}, \tilde{\beta} \to -\infty$, $\gamma = 0$. In this case, $\sqrt{ab} = 1$. The quantities $u_\infty$ and $u_\gamma$ take the special values

$$u_\infty = u_\alpha = u_\beta = \frac{1}{6}, \qquad u_\gamma = \frac{1}{2}. \tag{4.214}$$

The value of $\omega^{1/2}$ is

$$\omega^{1/2} = \mathrm{e}^{\frac{2\pi \mathrm{i}}{3}}. \tag{4.215}$$

We have

$$X = \frac{\vartheta_1(u_\infty + u)}{\vartheta_1(u_\infty - u)}, \tag{4.216}$$

and

$$-1 = X(u_\gamma). \tag{4.217}$$

Also, we have

$$X(u+\tau) = \mathrm{e}^{-\frac{2\pi \mathrm{i}}{3}} X(u), \qquad Y(u+\tau) = \mathrm{e}^{-\frac{2\pi \mathrm{i}}{3}} Y(u). \tag{4.218}$$

We conclude that the following three combinations are elliptic functions:

$$\begin{aligned} X(u)^3 &\propto \frac{\vartheta_1(u+u_\infty)^3}{\vartheta_1(u-u_\infty)^3}, \\ \frac{1}{Y(u)^3} &\propto \frac{\vartheta_1(u-u_\gamma)^3}{\vartheta_1(u-u_\infty)^3}, \\ \frac{X(u)}{Y(u)} &\propto \frac{\vartheta_1(u+u_\infty)\vartheta_1(u-u_\gamma)}{\vartheta_1(u-u_\infty)^2}. \end{aligned} \tag{4.219}$$

The linear combination

$$\frac{1}{Y^3} + c_1 X^3 + c_2 \frac{X}{Y} + c_3 \tag{4.220}$$

has poles of order up to three in the $u$ plane, located at $u_\infty$. By appropriately fixing the constants $c_i$ for $i = 1, 2$, we can make all the poles cancel each other, which implies that this elliptic function is a constant. By fixing $c_3$, this constant can be made to vanish. By looking at the polar behaviour at $u_\infty$, we find

$$\begin{aligned} c_1 &= 1, \\ c_2 &= \kappa, \\ c_3 &= 1, \end{aligned} \tag{4.221}$$

where

$$\kappa = 3\frac{\vartheta_1(2u_\infty)}{\vartheta_1'(0)}\left(\frac{\vartheta_1'}{\vartheta_1}(u_\infty - u_\gamma) - \frac{\vartheta_1'}{\vartheta_1}(2u_\infty)\right) = -6\frac{\vartheta_1'(\frac{1}{3})}{\vartheta_1'(0)}. \tag{4.222}$$

We find the relation

$$\frac{1}{Y^3} + X^3 + \kappa\frac{X}{Y} + 1 = 0. \tag{4.223}$$

We call this the spectral curve, characterising the planar limit of the matrix model. The appropriate branch of its solution $Y(X)$ yields $\varpi_{1,0}(X)$ which is the (twisted) planar one-point correlator:

$$\varpi_{1,0}(X) = -\frac{3}{4\pi^2\mathrm{i}}\left[\log Y(X) + \log(-X-1)\right]. \tag{4.224}$$

Setting

$$\mathrm{e}^{x'} = \frac{Y}{X}, \qquad \mathrm{e}^{y'} = \frac{1}{XY^2}, \tag{4.225}$$

the spectral curve (4.223) becomes

$$\mathrm{e}^{x'} + \mathrm{e}^{y'} + \mathrm{e}^{-x'-y'} + \kappa = 0, \tag{4.226}$$

which is indeed the mirror curve of the local $\mathbb{P}^2$ toric CY, cf. Table 3.1. The relation between the 't Hooft coupling $\lambda$ and the modulus of the spectral curve $\kappa$ is given by the normalization condition (4.169), which reduces to

$$\lambda = \frac{3}{8\pi^3}\oint_{\omega^{-1/2}\mathcal{I}}\frac{\mathrm{d}X}{X}\log Y(X). \tag{4.227}$$

This can be expressed using only the curve (4.226). Let us call the cycle of integration the $\mathcal{A}$ cycle. We define the variables $x, y$ where $X = \mathrm{e}^x$, $Y = \mathrm{e}^y$. The variables $x, y$ are linearly related to $x', y'$ through (4.225): $(x, y) = (-\frac{2}{3}x' - \frac{1}{3}y', \frac{1}{3}x' - \frac{1}{3}y')$. Our period integral in terms of $x'$ and $y'(x')$ solving (4.226) becomes

$$\begin{aligned}
\lambda &= \frac{3}{(2\pi)^3}\oint_{\mathcal{A}} y(x)\mathrm{d}x \\
&= \frac{3}{(2\pi)^3}\oint_{\mathcal{A}'}\left(\frac{1}{3}x' - \frac{1}{3}y'(x')\right)\left(-\frac{2}{3} - \frac{1}{3}\partial_{x'}y'(x')\right)\mathrm{d}x' \\
&= \frac{3}{(2\pi)^3}\left[-\frac{2}{9}\oint_{\mathcal{A}'} x'\mathrm{d}x' + \frac{2}{9}\oint_{\mathcal{A}'} y'(x')\mathrm{d}x' - \frac{1}{9}\oint_{\mathcal{A}'} x'\partial_{x'}y'(x')\mathrm{d}x'\right. \\
&\qquad\qquad \left. + \frac{1}{9}\oint_{\mathcal{A}'} y'(x')\partial_{x'}y'(x')\mathrm{d}x'\right] \\
&= \frac{1}{(2\pi)^3}\oint_{\mathcal{A}'} y'(x')\mathrm{d}x'.
\end{aligned} \tag{4.228}$$

where the $\mathcal{A}'$ cycle is the image of the $\mathcal{A}$ cycle under the linear map relating $(x, y)$ to $(x', y')$. We thus showed that $\lambda$ is indeed the period of the mirror curve whose

cycle is "pinched" in the small coupling limit (remember that $\mathcal{I}$ shrinks to a point when $q \to 0$), i.e. the conifold $\mathcal{A}$ cycle.

**The local $\mathbb{P}^1 \times \mathbb{P}^1$ spectral curve.** This is actually an $O(2)$ case. We fix $m = 0$, $n = 1$, $\tilde{\beta} \to -\infty$, $\gamma = 0$. The quantities $u_\infty, u_\beta$ and $u_\gamma$ take the special values

$$u_\infty = u_\beta = \frac{1}{4}, \qquad u_\gamma = u_\alpha + \frac{1}{2}, \tag{4.229}$$

while $u_\alpha$ is unfixed. The value of $\omega^{1/2}$ is

$$\omega^{1/2} = \mathrm{i}. \tag{4.230}$$

We have

$$\begin{aligned} \mathrm{e}^{-\tilde{\alpha}} = X(u_\alpha) &= \sqrt{ab}\frac{\vartheta_1(\frac{1}{4}+u_\alpha)}{\vartheta_1(\frac{1}{4}-u_\alpha)}, \\ -1 = X(u_\gamma) &= \sqrt{ab}\frac{\vartheta_1(\frac{1}{4}+u_\gamma)}{\vartheta_1(\frac{1}{4}-u_\gamma)} = -\sqrt{ab}\frac{\vartheta_1(\frac{1}{4}-u_\alpha)}{\vartheta_1(\frac{1}{4}+u_\alpha)}, \end{aligned} \tag{4.231}$$

from which we deduce

$$ab = \mathrm{e}^{-\tilde{\alpha}}. \tag{4.232}$$

Also, we have

$$X(u+\tau) = -X(u), \qquad Y(u+\tau) = -Y(u). \tag{4.233}$$

This implies that the following combinations are elliptic functions:

$$\begin{aligned} X^{-2} &\propto \frac{\vartheta_1(u-u_\infty)^2}{\vartheta_1(u+u_\infty)^2}, \\ Y^2 &\propto \frac{\vartheta_1(u-u_\alpha)^2}{\vartheta_1(u-u_\gamma)^2}, \\ YX^{-1} &\propto \frac{\vartheta_1(u-u_\alpha)\vartheta_1(u-u_\infty)}{\vartheta_1(u+u_\infty)\vartheta_1(u-u_\gamma)}, \\ Y^2X^{-2} &\propto \frac{\vartheta_1(u-u_\alpha)^2\vartheta_1(u-u_\infty)^2}{\vartheta_1(u+u_\infty)^2\vartheta_1(u-u_\gamma)^2}. \end{aligned} \tag{4.234}$$

The general combination

$$\frac{1}{X^2} + c_1 Y^2 + c_2 \frac{Y}{X} + c_3 \frac{Y^2}{X^2} + c_4 \tag{4.235}$$

has order two poles in the $u$ plane, located at $-u_\infty$ and $u_\gamma$. By appropriately fixing the constants $c_i$ for $i = 1, 2, 3$, we can make all the poles cancel each other, which implies that this elliptic function is a constant. By fixing $c_4$, this constant can be made to vanish. By looking at the polar behaviour at $-u_\infty$ and $u_\gamma$, we find

$$\begin{aligned} c_1 &= 1, \\ c_2 &= -\kappa, \\ c_3 &= -1, \\ c_4 &= -\mathrm{e}^{2\tilde{\alpha}}, \end{aligned} \tag{4.236}$$

where

$$\kappa = \mathrm{e}^{\tilde{\alpha}/2}\frac{2\vartheta_1(\frac{1}{2})}{\vartheta_1'(0)}\left(\frac{\vartheta_1'}{\vartheta_1}\left(u_\alpha+\frac{3}{4}\right)-\frac{\vartheta_1'}{\vartheta_1}\left(u_\alpha+\frac{1}{4}\right)\right). \tag{4.237}$$

We find the relation

$$\frac{1}{X^2}+Y^2-\kappa\frac{Y}{X}-\frac{Y^2}{X^2}-\mathrm{e}^{2\tilde{\alpha}}=0, \tag{4.238}$$

The appropriate branch $Y(X)$ of the solution of this algebraic relation gives us directly the twisted planar one-point correlator as a function of $X$:

$$\varpi_{1,0}(X) = -\frac{1}{2\pi^2\mathrm{i}}\left[\log Y(X)+\log\frac{1+X}{\mathrm{e}^{\tilde{\alpha}}X-1}\right]. \tag{4.239}$$

Setting

$$\mathrm{e}^{x'}=\frac{Y}{X}, \qquad \mathrm{e}^{y'}=-\frac{1}{XY}, \tag{4.240}$$

the spectral curve (4.238) becomes

$$\mathrm{e}^{x'}+\mathrm{e}^{2\tilde{\alpha}}\mathrm{e}^{-x'}+\mathrm{e}^{y'}+\mathrm{e}^{-y'}+\kappa=0, \tag{4.241}$$

which is indeed the mirror curve of the toric Calabi-Yau called local $\mathbb{P}^1\times\mathbb{P}^1$, with mass parameter $m=\mathrm{e}^{2\tilde{\alpha}}$, see Table 3.1. Of course, the integral determining $\lambda$ is again the conifold $A$–period of the mirror curve. We have restricted the discussion of the spectral curve to the local $\mathbb{P}^2$ and local $\mathbb{P}^1\times\mathbb{P}^1$ cases, but it should no doubt be generalizable to all the cases with $m,n$ rationals. We expect in general that the spectral curve of the matrix model is just the classical mirror curve in the appropriate variables.

The conformal mapping $X(u)$ to a fundamental rectangle with sides 1 and $\tau$ is very effective to obtain the planar one-point correlator. In particular, the mapping $X(u)$ is independent of the full potential $\mathcal{W}(X)$ of the deformed $O(2)$ matrix model (4.7), or its planar part $\mathcal{V}(X)$. It only depends on $\omega=-\mathrm{e}^{2\pi\mathrm{i}C}=\mathrm{e}^{-4\pi\mathrm{i}u_\infty}$, in other words on the eigenvalue interaction term. As for example for the hermitian matrix integrals or the standard $O(2)$ matrix model, it is possible to obtain a universal formula for the planar one-point correlator, in the sense that the potential does only enter in the formula through geometric parameters (for example the branch points). We will see that these parameters can be chosen to be the parameter $\tau$ of the conformal mapping and the midpoint $\sqrt{ab}$. Let us keep in mind that, in the following paragraphs, we deal with *generic* planar potential $\mathcal{V}(X)$ or $\mathrm{Re}V_0(\nu)$ (and not, as before, with the specific case (4.154)). The important observation for obtaining our universal formula is that differentiating (4.171) with respect to $\lambda$,[12] we get a potential independent equation for $\partial_\lambda\varpi_{1,0}(X)$:

$$\partial_\lambda\varpi_{1,0}(\omega^{-1/2}(X\pm\mathrm{i}0))-\partial_\lambda\varpi_{1,0}(\omega^{1/2}(X\mp\mathrm{i}0))=0. \tag{4.242}$$

[12] We keep $X$ fixed, which means the map $u(X)$ varies since $\tau$ depends on $\lambda$.

This is the same kind of equation as (4.171) but for a vanishing potential. So the function $\partial_\lambda \varpi_{1,0}(X)|_{X=X(u)}$ in the $u$ plane must be an elliptic function which does not have poles except at the points congruent to $\pm u_b$ (the stationary points of the conformal map $X(u)$ corresponding to the branch points). Since $\varpi_{1,0}(X)$ must vanish at $X \to 0$ and $\infty$, our elliptic function $\partial_\lambda \varpi_{1,0}(X)|_{X=X(u)}$ should vanish at $\pm u_\infty$. This determines almost completely our elliptic function:

$$\partial_\lambda \varpi_{1,0}(X)|_{X=X(u)} \propto \frac{\vartheta_1(u+u_\infty)\vartheta_1(u-u_\infty)}{\vartheta_1(u+u_b)\vartheta_1(u-u_b)}. \tag{4.243}$$

Comparing with (4.198), we see that this can be written exclusively in terms of the conformal map $X(u)$ itself:

$$\partial_\lambda \varpi_{1,0}(X)|_{X=X(u)} = c\frac{X(u)}{X'(u)}. \tag{4.244}$$

The constant $c$ can be determined in the following way. Differentiating the contour integral (4.169) with respect to $\lambda$ (keeping the contour fixed), we get

$$\begin{aligned} 1 &= \frac{1}{2\pi \mathrm{i}} \oint_{\omega^{-1/2}\mathcal{I}} \frac{\mathrm{d}X}{X} \partial_\lambda \varpi_{1,0}(X) \\ &= \frac{1}{2\pi \mathrm{i}} \int_{\frac{1}{2}-\tau}^{-\frac{1}{2}-\tau} \mathrm{d}u \frac{X'(u)}{X(u)} c \frac{X(u)}{X'(u)} \\ &= -\frac{1}{2\pi \mathrm{i}} c \end{aligned} \tag{4.245}$$

So the constant $c$ equals $-2\pi \mathrm{i}$. We conclude that the derivative of $\varpi_{1,0}$ with respect to $\lambda$ has a universal form

$$\begin{aligned} \partial_\lambda \varpi_{1,0}(X) &= -2\pi \mathrm{i} \frac{X(u)}{X'(u)}\bigg|_{u=u(X)} \\ &= -\frac{2\pi \mathrm{i}}{\frac{\vartheta_1'}{\vartheta_1}(u_\infty + u(X)) + \frac{\vartheta_1'}{\vartheta_1}(u_\infty - u(X))}. \end{aligned} \tag{4.246}$$

The quantity $u_\infty$ only depends on the interaction term through $\omega$, and not on the potential. The potential dependence only enters through the relation $q = \mathrm{e}^{\mathrm{i}\pi\tau}$ and $\sqrt{ab}$ as functions of $\lambda$. The functional dependence on $\sqrt{ab}$ enters as a scaling of $X$. Using the result (4.246), we can derive universal formulas for the planar free energy $\mathcal{F}_0(\lambda)$. At fixed $\hbar$, we have

$$\log Z(N+1) - \log Z(N) = \hbar \mathcal{F}_0'(\lambda) + \frac{1}{2}\mathcal{F}_0''(\lambda) + O(\hbar^{-1}), \tag{4.247}$$

which should be understood as a 't Hooft expansion. In the planar limit, the quantity $\log Z(N)$ is given by the value of the effective action $-N^2 S_{\text{eff}}$ in (4.150), evaluated

at the saddle point configuration given by $\nu_i^*$, $i = 1, \dots, N$. We now assume that when adding an extra eigenvalue (going from $N$ to $N+1$), the saddle point positions of the $N$ first eigenvalues are not changed at leading order in large $N$. The extra eigenvalue $\nu_{N+1}$ will have its saddle point position $\nu_{N+1}^*$. Let us define

$$g(\nu) = \frac{1}{N}\sum_{i=1}^{N}\left[\log\left(4\sinh^2\frac{\nu-\nu_i^*}{2}\right) - \log\left(2\cosh\left(\frac{\nu-\nu_i^*}{2} - \mathrm{i}\pi C\right)\right) - \log\left(2\cosh\left(\frac{\nu-\nu_i^*}{2} + \mathrm{i}\pi C\right)\right)\right]. \tag{4.248}$$

Then, in the large $N$ limit, we find from (4.247):

$$\mathcal{F}_0'(\lambda) = -\mathrm{Re}V_0(\nu_{N+1}^*) + \lambda g(\nu_{N+1}^*). \tag{4.249}$$

The saddle point equation in the large $N$ limit implies that, as a function of $\nu_{N+1}^*$, the right hand side is constant on the interval where the eigenvalues condense. So we can put $\nu_{N+1}^*$ anywhere on the cut, for example at the larger end point $\nu_{N+1}^* = \log b$. Since we have

$$g(\nu) \to 0 \qquad \text{when} \qquad \nu \to 0, \tag{4.250}$$

we can write

$$\mathcal{F}_0'(\lambda) = -\mathrm{Re}V_0(\nu_{N+1}^*) + \lambda\int_{\infty}^{\log b} g'(\nu). \tag{4.251}$$

But in the large $N$ limit, $g'(\nu)$ is actually known:

$$\begin{aligned} g'(\nu) &= \frac{1}{N}\sum_{i=1}^{N}\left(\frac{2\mathrm{e}^{\nu}}{\mathrm{e}^{\nu}-\mathrm{e}^{\nu_i^*}} - \frac{\omega\mathrm{e}^{\nu}}{\omega\mathrm{e}^{\nu}-\mathrm{e}^{\nu_i^*}} - \frac{\omega^{-1}\mathrm{e}^{\nu}}{\omega^{-1}\mathrm{e}^{\nu}-\mathrm{e}^{\nu_i^*}}\right) \\ &= \int_{\mathcal{I}}\mathrm{d}X'\rho(X')\left(\frac{2X}{X-X'} - \frac{\omega X}{\omega X - X'} - \frac{\omega^{-1}X}{\omega^{-1}X-X'}\right) + o(1) \\ &= \frac{1}{\lambda}\left(\varpi_{1,0}(\omega^{-1/2}X) - \varpi_{1,0}(\omega^{1/2}X)\right) + o(1). \end{aligned} \tag{4.252}$$

Inserting this into the previous expression and using $\mathrm{Re}V_0(\nu) = \mathcal{V}(X)$, we obtain

$$\mathcal{F}_0'(\lambda) = -\mathcal{V}(b) + \int_{\infty}^{b}\frac{\mathrm{d}X}{X}\left(\varpi_{1,0}(\omega^{-1/2}X) - \varpi_{1,0}(\omega^{1/2}X)\right). \tag{4.253}$$

By changing variables in the integrations, we end up with the following formula for the derivative of the planar free-energy:

$$\mathcal{F}_0'(\lambda) = -\mathcal{V}(b) + \int_{\omega^{1/2}b}^{\omega^{-1/2}b}\frac{\mathrm{d}X}{X}\varpi_{1,0}(X). \tag{4.254}$$

The path from $\omega^{1/2}b$ to $\omega^{-1/2}b$ is a part of the symplectic dual cycle to the $\mathcal{A}$ cycle (which is the cycle surrounding the cut $\omega^{-1/2}\mathcal{I}$). Let us call this contour joining the

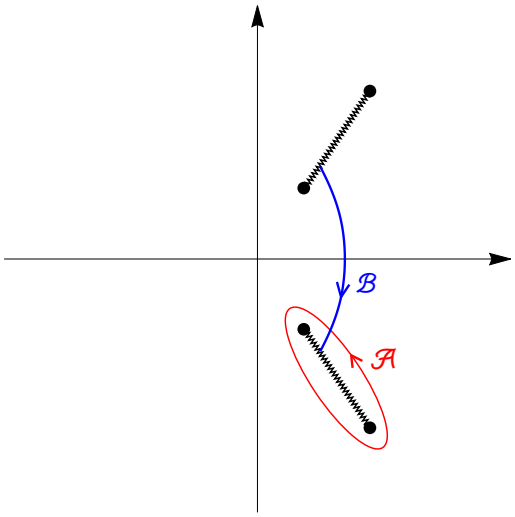


**Figure 4.7:** The $\mathcal{A}$ and $\mathcal{B}$ cycles in the $X$ plane.

cut $\omega^{1/2}\mathcal{I}$ to the cut $\omega^{-1/2}\mathcal{I}$ the $\mathcal{B}$ cycle (it is not an actual cycle in the $X$ plane but it is on the torus obtained by identifying the corresponding sides of the cuts), see Fig. 4.7. We then have the relations

$$\begin{aligned} \lambda &= \frac{1}{2\pi \mathrm{i}} \oint_{\mathcal{A}} \frac{\varpi_{1,0}(X)}{X} \mathrm{d}X, \\ \mathcal{F}_0'(\lambda) &= \int_{\mathcal{B}} \frac{\varpi_{1,0}(X)}{X} \mathrm{d}X - \mathcal{V}(b), \end{aligned} \tag{4.255}$$

typical of special geometry. As we saw in the example of local $\mathbb{P}^2$, the function $\varpi_{1,0}(X)$ can be substituted for $\log Y(X)$ on the spectral curve. So, as usual, the planar limit of the matrix integral is governed by the special geometry relations on the corresponding spectral curve.

Also, from this result, we can obtain a very useful relation for the second derivative of the planar free energy. Let us differentiate (4.254) with respect to $\lambda$. The endpoint of the integral can be chosen anywhere on the cut (not necessarily at $b$ which varies with $\lambda$), so we can keep it constant during differentiation and then set it back to the branch point $b$. We obtain

$$\mathcal{F}_0''(\lambda) = \int_{\omega^{1/2}b}^{\omega^{-1/2}b} \frac{\mathrm{d}X}{X} \partial_\lambda \varpi_{1,0}(X). \tag{4.256}$$

We use the universal result for $\partial_\lambda \varpi_{1,0}(X)$ in (4.246) and go to the $u$ plane to perform

the integration:

$$\begin{aligned}\mathcal{F}_0''(\lambda) &= \int_{u_b}^{u_b-\tau} \mathrm{d}u \frac{X'(u)}{X(u)} \partial_\lambda \varpi_{1,0}(X(u)) \\ &= \int_{u_b}^{u_b-\tau} \mathrm{d}u \frac{X'(u)}{X(u)} \left(\frac{-2\pi \mathrm{i} X(u)}{X'(u)}\right) \\ &= -2\pi\mathrm{i} \int_{u_b}^{u_b-\tau} \mathrm{d}u.\end{aligned} \tag{4.257}$$

We obtain a formula which is explicitly potential independent (the dependence enters implicitly through the relation $\tau(\lambda)$), and which is valid for all the deformed $O(2)$ cases:

$$\mathcal{F}_0''(\lambda) = 2\pi\mathrm{i}\tau. \tag{4.258}$$

The second derivative of the free energy with respect to the 't Hooft coupling is the modular parameter of our elliptic parametrization. This kind of result is standard in other families of matrix models.

We can find another formula involving the second derivative of the planar free energy and the $\mathcal{A}$ cycle instead of the $\mathcal{B}$ cycle. From the matrix model, it is easy to see that the derivative of the free energy with respect to $\hbar$ keeping $N$ fixed is

$$\begin{aligned}\partial_\hbar \log Z(N) &= -\Big\langle \sum_{k=1}^{N} \left( \mathrm{Re}V(\nu_k) + \hbar \frac{\partial}{\partial \hbar} \mathrm{Re}V(\nu_k) \right) \Big\rangle \\ &= -\Big\langle \sum_{k=1}^{N} \mathrm{Re}V_0(\nu_k) \Big\rangle + \mathcal{O}(N\hbar^{-2}).\end{aligned} \tag{4.259}$$

In the second line, we assumed that the generic ($\hbar$ dependent) potential $\mathrm{Re}V(\nu)$ behaves as $\mathrm{Re}V_0(\nu) + \mathcal{O}(\hbar^{-2})$. The generic ($\hbar$ independent) planar potential is $\mathrm{Re}V_0(\nu) = \mathcal{V}(X)$. In the large $N$ limit, we can use the continuous distribution of eigenvalues $\rho(X)$ and the fact that $\partial_\hbar = -N^{-1}\lambda^2\partial_\lambda$. The above relation becomes

$$\begin{aligned}\lambda^2 \partial_\lambda \lambda^{-2} \mathcal{F}_0(\lambda) &= \int_{\mathcal{I}} \mathrm{d}X \rho(X) \mathcal{V}(X) \\ &= \frac{1}{2\pi\mathrm{i}\lambda} \oint_{\omega^{-1/2}\mathcal{I}} \frac{\mathrm{d}X}{X} \varpi_{1,0}(X) \mathcal{V}(\omega^{1/2}X).\end{aligned} \tag{4.260}$$

Multiplying it by $\lambda$ and differentiating, we can use (4.246) to write

$$\begin{aligned}\partial_\lambda \lambda^3 \partial_\lambda \lambda^{-2} \mathcal{F}_0(\lambda) = \lambda \mathcal{F}_0''(\lambda) - \mathcal{F}_0'(\lambda) &= \frac{1}{2\pi\mathrm{i}} \oint_{\omega^{-1/2}\mathcal{I}} \frac{\mathrm{d}X}{X} \partial_\lambda \varpi_{1,0}(X) \mathcal{V}(\omega^{1/2}X), \\ &= \int_{-\frac{1}{2}-\frac{\tau}{2}}^{\frac{1}{2}-\frac{\tau}{2}} \mathcal{V}\left(\omega^{1/2} X\left(u\right)\right) \mathrm{d}u.\end{aligned} \tag{4.261}$$

Let us differentiate the left hand side of this formula with respect to $\tau$:

$$\begin{aligned}\frac{\mathrm{d}}{\mathrm{d}\tau}\left(\lambda\mathcal{F}_0''(\lambda)-\mathcal{F}_0'(\lambda)\right) &= \left(\mathcal{F}_0''(\lambda)+\mathcal{F}_0'''(\lambda)-\mathcal{F}_0''(\lambda)\right)\lambda'(\tau)\\ &= \lambda\frac{\mathcal{F}_0'''(\lambda)}{\frac{\mathrm{d}}{\mathrm{d}\lambda}\tau}\\ &= 2\pi\mathrm{i}\lambda.\end{aligned} \tag{4.262}$$

In the last line, we used the universal result (4.258). So we obtain another universal result, this time for $\lambda$:

$$\lambda = \frac{1}{2\pi\mathrm{i}}\frac{\mathrm{d}}{\mathrm{d}\tau}\int_{-\frac{1}{2}-\frac{\tau}{2}}^{\frac{1}{2}-\frac{\tau}{2}}\mathcal{V}\left(\omega^{1/2}X\left(u\right)\right)\mathrm{d}u. \tag{4.263}$$

In the above, not only the endpoints of the integral are functions of $\tau$, but also the map $X(u)$ (through $q$ and $\sqrt{ab}$ which is implicitly $q$ dependent). If $\sqrt{ab}$ is known (for example if the potential obeys $\mathcal{V}(X^{-1})=\mathcal{V}(X)$ we have $\sqrt{ab}=1$), then equations (4.258) and (4.263) determine $\mathcal{F}_0''(\lambda)$ completely, and also $\mathcal{F}_0(\lambda)$ up to two integration constants.

Let us go back to our particular family of potentials, for which we know the expression $\varpi_{0,1}(X)$ (4.205). Equation (4.258) gives a quite easy way of computing the planar free energy of our models in the small 't Hooft coupling limit, provided that we now the relation $\tau(\lambda)$. Extracting the part of $\varpi_{1,0}(X)$ which contributes non trivially to the contour integral, and then going to the $u$ variable, we find

$$\begin{aligned}\lambda = \frac{1}{2\pi\mathrm{i}}\left(\frac{m+n+1}{4\pi^2\mathrm{i}}\right)\int_{\frac{1}{2}-\frac{\tau}{2}}^{-\frac{1}{2}-\frac{\tau}{2}}\mathrm{d}u\left(\frac{\vartheta_1'}{\vartheta_1}(u_\infty+u)+\frac{\vartheta_1'}{\vartheta_1}(u_\infty-u)\right)\left(\log\frac{\vartheta_1(u-u_\infty)}{\vartheta_1(2u_\infty)}\right.\\ \left.+\log\frac{\vartheta_1(u-u_\gamma)}{\vartheta_1(u_\infty+u_\gamma)}-\log\frac{\vartheta_1(u-u_\alpha)}{\vartheta_1(u_\infty+u_\alpha)}-\log\frac{\vartheta_1(u-u_\beta)}{\vartheta_1(u_\infty+u_\beta)}\right).\end{aligned} \tag{4.264}$$

This can be rewritten as a different integral in the $u$ plane (see Appendix D in [13]):

$$\lambda = \frac{m+n+1}{4\pi^2\mathrm{i}}\left(\int_{u_\infty}^{u_\gamma}-\int_{u_\infty}^{u_\alpha}-\int_{u_\infty}^{u_\beta}\right)\mathrm{d}u\frac{\partial}{\partial\tau}\log X(u). \tag{4.265}$$

The differentiation should only be applied on the second variable of theta functions $\vartheta_1(u,\tau)$ which compose the map $X(u)$ (this means for example that here we consider $\sqrt{ab}$ to be independent of $\tau$ when differentiating). Expression (4.264) is very useful to obtain expansions of $\lambda(\tau)$ at weak and strong coupling. The weak coupling expansion corresponds to the small $q$ expansion. We find

$$\begin{aligned}\lambda = \frac{m+n+1}{\pi^2}\sum_{k=1}^{\infty}\frac{q^{2k}}{k(1-q^{2k})^2}\sin(2\pi k u_\infty)\left(\cos(2\pi k u_\alpha)+\cos(2\pi k u_\beta)\right.\\ \left.-\cos(2\pi k u_\gamma)-\cos(2\pi k u_\infty)\right).\end{aligned} \tag{4.266}$$

We need to express $u_{\alpha,\beta,\gamma}$ in terms of $\tilde{\alpha}, \tilde{\beta}$ and $\tilde{\gamma}$ since this relation may also be $q$–dependent. In general, we find that the expansion for $\lambda(q)$ looks like

$$\lambda = \sum_{k=1}^{\infty} a_k q^{2k}. \tag{4.267}$$

Since $q = \mathrm{e}^{\mathrm{i}\pi\tau} = \mathrm{e}^{\frac{1}{2}\mathcal{F}_0''}$, we can invert this series order by order in $q$. We find

$$\begin{aligned}\mathcal{F}_0(\lambda) = c_0 + c_1\lambda + \left[\frac{1}{2}\log\left(\frac{\lambda}{a_1}\right) - \frac{3}{4}\right]\lambda^2 - \frac{a_2}{6a_1^2}\lambda^3 \\ + \left(\frac{a_2^2}{8a_1^4} - \frac{a_3}{12a_1^3}\right)\lambda^4 + \left(-\frac{a_2^3}{6a_1^6} + \frac{a_2a_3}{5a_1^5} - \frac{a_4}{20a_1^4}\right)\lambda^5 \\ + \left(\frac{7a_2^4}{24a_1^8} - \frac{a_2^2a_3}{2a_1^7} + \frac{a_3^2}{12a_1^6} + \frac{a_2a_4}{6a_1^6} - \frac{a_5}{30a_1^5}\right)\lambda^6 + O(\lambda^7).\end{aligned} \tag{4.268}$$

As we saw in the previous section, the integration constants $c_0$ and $c_1$ can be obtained from the expansion of the matrix model around the minimum of the potential $\mathrm{Re}V_0(\nu)$. We obtain

$$c_0 = 0, \qquad c_1 = -\min_{\nu\in\mathbb{R}} \mathrm{Re}V_0(\nu). \tag{4.269}$$

In this way, we can easily get the small $\lambda$ expansion of the planar free energy $\mathcal{F}_0$. Let us look at our favourite examples.

**The three term operators and local $\mathbb{P}^2$.** In this case, we have $\tilde{\alpha}, \tilde{\beta} \to -\infty$, and $\tilde{\gamma} = 0$. Therefore, $u_\alpha = u_\beta = u_\infty = \frac{n}{2(m+n+1)}$, and we have $u_\gamma = \frac{1}{m+n+1} + u_\infty = \frac{n+2}{2(m+n+1)}$. Since none of the $u_{\alpha,\beta,\gamma}$ are $q$–dependent, the $a_k$ can be obtained at all orders:

$$a_k = 2\frac{m+n+1}{\pi^2} \sum_{d,\ell\in\mathbb{N}|d\ell=k} \frac{\ell}{d}(-1)^{d-1} \sin\frac{\pi d}{m+n+1} \sin\frac{\pi dm}{m+n+1} \sin\frac{\pi dn}{m+n+1}. \tag{4.270}$$

Inserting this in (4.268), we reproduce what we found in (4.45-4.47).

**Local $\mathbb{P}^1 \times \mathbb{P}^1$.** This is actually a standard $O(2)$ case, but our formulas work perfectly well. We have $(m,n) = (0,1)$, $\tilde{\beta} \to -\infty$, and $\tilde{\gamma} = 0$. The mass parameter of local $\mathbb{P}^1 \times \mathbb{P}^1$ is related to $\tilde{\alpha} = \frac{\pi}{\hbar}\alpha$ as $m_{\mathbb{F}_0} = \mathrm{e}^{\alpha}$. We have, $u_\infty = u_\beta = 1/4$, and $u_\gamma = 1/2 + u_\alpha$. The relation between $u_\alpha$ and $\tilde{\alpha}$ is obtained in the small $q$ expansion using that

$$-\mathrm{e}^{-\tilde{\alpha}} = \frac{X(u_\alpha)}{X(u_\gamma)} = -\frac{\vartheta_1(1/4+u_\alpha)^2}{\vartheta_1(1/4-u_\alpha)^2}, \tag{4.271}$$

which can be inverted in the small $q$ expansion:

$$\mathrm{e}^{2\pi\mathrm{i}u_\alpha} = \frac{1-\mathrm{i}\mathrm{e}^{\tilde{\alpha}/2}}{-\mathrm{i}+\mathrm{e}^{\tilde{\alpha}/2}} + \frac{8\mathrm{e}^{\tilde{\alpha}/2}(\mathrm{e}^{\tilde{\alpha}/2}-1)}{(-\mathrm{i}+\mathrm{e}^{\tilde{\alpha}/2})^3(\mathrm{i}+\mathrm{e}^{\tilde{\alpha}/2})} q^2 + O(q^4). \tag{4.272}$$

We obtain

$$\begin{aligned}
a_1 &= \frac{4}{\pi^2 \cosh\left(\frac{\tilde{\alpha}}{2}\right)}, \\
a_2 &= \frac{4(3\cosh(\tilde{\alpha})-1)}{\pi^2 \cosh\left(\frac{\tilde{\alpha}}{2}\right)^3}, \\
a_3 &= \frac{4(9\cosh(2\tilde{\alpha})-44\cosh(\tilde{\alpha})+43)}{3\pi^2 \cosh\left(\frac{\tilde{\alpha}}{2}\right)^5}, \\
a_4 &= \frac{19\cosh(3\tilde{\alpha})-310\cosh(2\tilde{\alpha})+1277\cosh(\tilde{\alpha})-954}{2\pi^2 \cosh\left(\frac{\tilde{\alpha}}{2}\right)^7}, \\
&\dots
\end{aligned} \tag{4.273}$$

Inserting this in (4.268), we reproduce what we found in (4.51-4.52).

More interestingly, we can consider the strong coupling expansion. We will use the $S$–dual expansions of the elliptic functions. Let us define

$$\tau_{\rm D} = -\tau^{-1}, \qquad\qquad q_{\rm D} = {\rm e}^{{\rm i}\pi\tau_{\rm D}}, \tag{4.274}$$

and consider the small $q_{\rm D}$ expansion of (4.265). We find

$$\lambda = \frac{m+n+1}{4\pi^2{\rm i}} \left(L_{\rm D}(u_\gamma) + L_{\rm D}(u_\infty) - L_{\rm D}(u_\alpha) - L_{\rm D}(u_\beta)\right), \tag{4.275}$$

where

$$\begin{aligned}
L_{\rm D}(u) = {} & 2\pi{\rm i}\tau_{\rm D} u_\infty u(u-1) + \tau_{\rm D}(u+u_\infty)\log(1-{\rm e}^{2\pi{\rm i}\tau_{\rm D}(u+u_\infty)}) \\
& - \tau_{\rm D}(u-u_\infty)\log(1-{\rm e}^{2\pi{\rm i}\tau_{\rm D}(u-u_\infty)}) \\
& - \frac{\rm i}{2\pi}\left({\rm Li}_2({\rm e}^{2\pi{\rm i}\tau_{\rm D}(u+u_\infty)}) - {\rm Li}_2({\rm e}^{2\pi{\rm i}\tau_{\rm D}(u-u_\infty)})\right) \\
& - 4\tau_{\rm D}\sum_{k=1}^{\infty}\frac{q_{\rm D}^{2k}}{k(1-q_{\rm D}^{2k})}(u_\infty\cos(2\pi k\tau_{\rm D}u_\infty)\cos(2\pi k\tau_{\rm D}u) \\
& \qquad\qquad - u\sin(2\pi k\tau_{\rm D}u_\infty)\sin(2\pi k\tau_{\rm D}u)) \\
& - 4{\rm i}\tau_{\rm D}\sum_{k=1}^{\infty}\frac{q_{\rm D}^{2k}}{k(1-q_{\rm D}^{2k})^2}\sin(2\pi k\tau_{\rm D}u_\infty)\cos(2\pi k\tau_{\rm D}u) \\
& + \frac{2}{\pi}\sum_{k=1}^{\infty}\frac{q_{\rm D}^{2k}}{k^2(1-q_{\rm D}^{2k})}\sin(2\pi k\tau_{\rm D}u_\infty)\cos(2\pi k\tau_{\rm D}u).
\end{aligned} \tag{4.276}$$

Since the absolute values of the real parts of $u_{\infty,\alpha,\beta,\gamma}$ are smaller or equal to $1/2$, the infinite sums are consistent small $q_{\rm D}$ expansions (series of $q_{\rm D}^r$ with $r>0$). The relation (4.275) should be inverted using $\tau_{\rm D} = -2\pi{\rm i}/\mathcal{F}_0''(0)$. Let us look at an example.

**The local $\mathbb{P}^2$ case.** We have $m = n = 1$, $\tilde{\alpha}, \tilde{\beta} \to -\infty$, and $\tilde{\gamma} = 0$. Also, $u_\alpha = u_\beta = u_\infty = \frac{1}{6}$ and $u_\gamma = \frac{1}{2}$ are independent of $q_{\rm D}$. We find

$$\lambda = -\frac{\tau_D^2}{36\pi} - \frac{1}{16\pi} + \frac{9 - 6\pi {\rm i}\tau_D}{8\pi^3} q_D^{2/3} + \frac{9(-3 + 4\pi {\rm i}\tau_D)}{8\pi^3} q_D^{4/3} + \frac{1 - 2\pi {\rm i}\tau_D}{8\pi^3} q_D^2 + O(q_D^{8/3}). \tag{4.277}$$

Inverting it and integrating twice, we obtain the strong 't Hooft coupling expansion of the planar free energy in the form of a trans-series:

$$\begin{aligned} \mathcal{F}_0(\lambda) = & -\frac{4}{9}\sqrt{\pi}\hat{\lambda}^{3/2} + c_1\hat{\lambda} + c_0 \\ & - \frac{3}{16\pi^4} {\rm e}^{-4\pi^{3/2}\sqrt{\hat{\lambda}}} - \frac{9}{128\pi^5}\left(5\pi + 3\pi^{-1/2}\hat{\lambda}^{-1/2}\right) {\rm e}^{-8\pi^{3/2}\sqrt{\hat{\lambda}}} \\ & - \frac{1}{384\pi^7}\left(\frac{1952}{3}\pi^3 + \frac{1215}{2}\pi^{3/2}\hat{\lambda}^{-1/2} + \frac{729}{4}\hat{\lambda}^{-1} + \frac{243}{16}\pi^{-3/2}\hat{\lambda}^{-3/2}\right) {\rm e}^{-12\pi^{3/2}\sqrt{\hat{\lambda}}} \\ & + \dots, \end{aligned} \tag{4.278}$$

where

$$\hat{\lambda} = \lambda + \frac{1}{16\pi}. \tag{4.279}$$

The constants $c_{0,1}$ have to be found by other means. We assume that $c_1 = 0$. We can also obtain the genus 0 free energy $F_0(t)$ in the large radius frame. We need to use the symplectic transformation (4.71), (4.76):

$$\begin{pmatrix} t \\ \partial_t \hat{F}_0(t) \end{pmatrix} = \begin{pmatrix} -6\pi\mathcal{F}_0'(\lambda) \\ \frac{8\pi^3}{3}\hat{\lambda} \end{pmatrix}, \tag{4.280}$$

from which we deduce the function $\lambda(t)$ (by performing the trans-series inversion), as well as

$$\partial_t^2 \hat{F}_0(t) = -\frac{4\pi^2}{9}\frac{1}{\mathcal{F}_0''(\lambda)} \tag{4.281}$$

Integrating twice, we find

$$\hat{F}_0(t) = \frac{t^3}{18} - 3{\rm e}^{-t} - \frac{45}{8}{\rm e}^{-2t} - \frac{244}{9}{\rm e}^{-3t} - \frac{12333}{64}{\rm e}^{-4t} + O({\rm e}^{-5t}), \tag{4.282}$$

which is indeed the generating series of the genus 0 Gromov–Witten invariants of the local $\mathbb{P}^2$ Calabi-Yau threefold (with the extra signs from the $B$ field).

We can also obtain interesting results for the planar connected two-point correlator $\varpi_{2,0}(X_1, X_2)$. Let us start by introducing the loop insertion operator. The loop insertion operator in matrix models is a very useful tool to obtain higher $n$–point correlators from lower ones, for example when considering hermitian matrix models [109] or $O(n)$ matrix models [104]. For this section, it is convenient to write our

integral in terms of $X_i = \mathrm{e}^{\nu_i}$:

$$Z(N) = \frac{\mathrm{i}^{N^2}}{N!} \int_{\mathbb{R}_+^N} \frac{\mathrm{d}^N X}{(2\pi)^N} \mathrm{e}^{-\hbar \sum_{i=1}^N \mathcal{V}(X_i)} \frac{\prod_{i<j} (X_i - X_j)^2}{\prod_{i,j} \left(\omega^{1/2} X_i - \omega^{-1/2} X_j\right)}. \tag{4.283}$$

The potential $\mathcal{V}(X)$ has an expansion around its minimum, and we call the expansion coefficients $v_k$:

$$\mathcal{V}(X) = \sum_{k=0}^{\infty} v_k X^k. \tag{4.284}$$

The loop-insertion operator is a differential operator, which, on quantities depending on the potential, is defined as

$$\frac{\delta}{\delta \mathcal{V}(Y)} F[\mathcal{V}] = \lim_{\epsilon \to 0} \frac{\left(F[\mathcal{V}]|_{v_k \to v_k - \epsilon Y^k}\right) - F[\mathcal{V}]}{\epsilon}. \tag{4.285}$$

We promptly find that

$$\frac{\delta}{\delta \mathcal{V}(Y)} \mathcal{V}(X) = -\frac{Y}{Y - X}\,, \qquad \frac{\delta}{\delta \mathcal{V}(Y)} \mathcal{V}'(X) = -\frac{Y}{(Y-X)^2}. \tag{4.286}$$

We also define the twisted loop-insertion operator

$$\frac{\delta}{\delta_\omega \mathcal{V}(Y)} = \frac{\delta}{\delta \mathcal{V}(\omega^{1/2} Y)} - \frac{\delta}{\delta \mathcal{V}(\omega^{-1/2} Y)}. \tag{4.287}$$

Let us apply this operator on $\log Z_N$. Using (4.283), we find straightforwardly

$$\frac{\delta}{\delta_\omega \mathcal{V}(X)} \log Z_N = \hbar \varpi_1(X), \tag{4.288}$$

and similarly,

$$\frac{\delta}{\delta_\omega \mathcal{V}(X_1)} \cdots \frac{\delta}{\delta_\omega \mathcal{V}(X_n)} \log Z_N = \hbar^n \varpi_n(X_1, \ldots, X_n). \tag{4.289}$$

The planar part of the connected two-point correlator $\varpi_2(X_1, X_2)$ is $\varpi_{2,0}(X_1, X_2)$. It is a symmetric function. We expect that, since it is the large $N$ limit of the two-point function, it can be represented in terms of a joint connected eigenvalue probability density function $\rho_c(X_1, X_2)$ as

$$\varpi_{2,0}(X_1, X_2) = \lambda^2 \int_{\mathcal{I}} \mathrm{d}X_1' \int_{\mathcal{I}} \mathrm{d}X_2'\, \rho_c(X_1', X_2') \prod_{i=1}^{2} \left( \frac{\omega^{1/2} X_i}{\omega^{1/2} X_i - X_i'} - \frac{\omega^{-1/2} X_i}{\omega^{-1/2} X_i - X_i'} \right). \tag{4.290}$$

Therefore, as a function of one of the variables with the other fixed away from the cuts, it has the same kind of branch-cuts along $\omega^{\pm 1/2} \mathcal{I}$ as the planar one-point function. It does not have other singularities. Assuming that we can commute

the loop-insertion with the 't Hooft expansion, we can use the previously derived property of the loop-insertion operator to write

$$\frac{\delta}{\delta_\omega \mathcal{V}(X_2)} \varpi_{1,0}(X_1) = \varpi_{2,0}(X_1, X_2). \tag{4.291}$$

Applying this on relation (4.171), we obtain the following condition on the planar two-point correlator $\varpi_{2,0}(X_1, X_2)$ for $X_1 \in \mathcal{I}$:

$$\begin{aligned} &\varpi_{2,0}(\omega^{-1/2}(X_1 \pm \mathrm{i}0), X_2) - \varpi_{2,0}(\omega^{1/2}(X_1 \mp \mathrm{i}0), X_2) \\ &\qquad = -\left( \frac{\omega^{1/2} X_1 X_2}{(\omega^{1/2} X_2 - X_1)^2} - \frac{\omega^{-1/2} X_1 X_2}{(\omega^{-1/2} X_2 - X_1)^2} \right). \end{aligned} \tag{4.292}$$

By symmetry in $X_1 \leftrightarrow X_2$, the same discontinuity equation is true for the second variable $X_2$. This is the same kind of equation as (4.171) with a parameter dependent meromorphic potential given by the second line. So the same techniques as for $\varpi_{1,0}(X)$ apply. The symmetry $X_1 \leftrightarrow X_2$ further constrains the solution. Let us define

$$B(X_1, X_2) = \varpi_{2,0}(X_1, X_2) + \frac{X_1 X_2}{(X_1 - X_2)^2}. \tag{4.293}$$

It satisfies for $X_1 \in \mathcal{I}$

$$B(\omega^{-1/2}(X_1 \pm \mathrm{i}0), X_2) - B(\omega^{1/2}(X_1 \mp \mathrm{i}0), X_2) = 0 \tag{4.294}$$

and similarly for $X_2$. This means that we can use again the parametrization $X(u)$. The function

$$b(u_1, u_2) = B(X(u_1), X(u_2)) \tag{4.295}$$

is an elliptic function (of periods 1 and $\tau$) in both variables $u_1$ and $u_2$, symmetric, with the only pole located at $u_1 = u_2$, which is a double pole. Expressed in terms of the $X$ variables, this double pole is of the form $\frac{X_1 X_2}{(X_1 - X_2)^2}$. Such a function is well known in the study of Riemann surfaces, and it is related to the so called *fundamental differential of the second kind*, sometimes also called the *Bergmann kernel*. All these constraints reduce the form of $B(X_1, X_2)$ to

$$B(X_1, X_2) = X_1 X_2 \partial_{X_1} \partial_{X_2} \log \vartheta_1(u(X_1) - u(X_2)) + c, \tag{4.296}$$

where $c$ is a constant. The polar behaviour is assured since

$$\begin{aligned} \log \vartheta_1(u(X_1) - u(X_2)) &= \log \left[ \text{const} \cdot (X_1 - X_2) + O(X_1 - X_2)^2 \right] \\ &= \log(X_1 - X_2) + O(X_1 - X_2)^0, \end{aligned} \tag{4.297}$$

and so

$$X_1 X_2 \partial_{X_1} \partial_{X_2} \log \vartheta_1(u(X_1) - u(X_2)) = \frac{X_1 X_2}{(X_1 - X_2)^2} + O(X_1 - X_2)^0. \tag{4.298}$$

In the $u_i$ variables, double periodicity is guaranteed using the following rewriting:

$$b(u_1, u_2) = c + \frac{X(u_1)X(u_2)}{X'(u_1)X'(u_2)} \partial_{u_1}\partial_{u_2} \log \vartheta_1(u_1 - u_2). \tag{4.299}$$

Indeed, since for $M, N \in \mathbb{Z}$ we have

$$\vartheta_1(u_1 - u_2 + M + N\tau) = \mathrm{e}^{(M+N)\pi\mathrm{i} - 2\pi\mathrm{i}N(u_1-u_2) - N^2\mathrm{i}\pi\tau}\vartheta_1(u_1 - u_2), \tag{4.300}$$

the quantity $\partial_{u_1}\partial_{u_2} \log \vartheta_1(u_1 - u_2)$ is an elliptic function for both $u_1$ and $u_2$. Moreover, we already saw that $\frac{X'(u)}{X(u)}$ is also an elliptic function so the full expression for $b(u_1, u_2)$ is elliptic in both variables. The constant $c$ is fixed to 0 by sending one of the variables $X_1$ or $X_2$ to $\infty$ and requiring the expression for $B(X_1, X_2)$ to vanish. We finally find the universal formula for the planar two-point connected correlator

$$\begin{aligned} \varpi_{2,0}(X_1, X_2) &= X_1X_2\partial_{X_1}\partial_{X_2} \log \vartheta_1(u(X_1) - u(X_2)) - \frac{X_1X_2}{(X_1 - X_2)^2} \\ &= (X_1\partial_{X_1})(X_2\partial_{X_2}) \log \frac{\vartheta_1(u(X_1) - u(X_2))}{X_1 - X_2}. \end{aligned} \tag{4.301}$$

It is universal in the same sense as $\partial_\lambda \varpi_{1,0}(X)$ is: the dependence on the potential only enters through $\tau$ and $\sqrt{ab}$ via the elliptic theta function and the parametrization $u(X)$.

Our exact expressions for $\varpi_{1,0}(X)$ and $\varpi_{2,0}(X_1, X_2)$ have been checked in the weak coupling expansion for several examples. Indeed, the weak coupling expansions can be obtained from the large $\hbar$ expansions for finite $N$, as we did for the free energies $\mathcal{F}_g$ at the beginning of section 4.3.

This concludes the study of the exact planar limit of our matrix models. It would be very interesting to push this program further, and solve the deformed $O(2)$ model at higher genus. By analogy to what has been done for other families of matrix models, the next step should be to derive the so called "loop equations". These give relations between higher genus $n$–point functions with lower genus higher $m$–point functions. Maybe results in [110] can help here. Solving these relations recursively should allow us to obtain quantities such as $\varpi_{1,1}$, and then $\varpi_{1,2}$, $\varpi_{2,1}$, $\varpi_{3,0}$, etc. In other families of matrix models, the topological recursion was shown to provide a solution for the loop equations. It would be extremely interesting to see if this works here, for the reasons stated at the beginning of this section.

# Chapter 5

# Eigenfunctions and the open topological string

The TS/ST correspondence stated in section 3.3 gives an explicit characterization of the spectral determinant $\Xi(\kappa)$ of the quantized mirror curve operator $\rho$ in terms of closed string invariants. The spectral determinant encodes all the information about the spectrum of $\rho$: its zeros are the eigenvalues, and its coefficients in the small $\kappa$ expansion are the fermionic traces (combinations of standard traces). This begs the question: what can topological strings tell us about the *eigenfunctions* of $\rho$? In other words, how to extend the TS/ST correspondence to the eigenfunctions?

Also, what do we precisely mean by eigenfunctions? In the spectral theory of a Hilbert–Schmidt operator acting on $L^2(\mathbb{R})$, the eigenfunctions $\psi_n(x)$ are square-integrable functions. In our case, these are in the image (and the domain) of the operator $\rho = \mathsf{O}^{-1}$, satisfying $(\rho\psi_n)(x) = \mathrm{e}^{-E_n}\psi_n(x)$, for a discrete set $E_n$, $n = 0, 1, 2, \ldots$ Therefore, they are also $L^2(\mathbb{R})$ functions in the domain (and the image) of the operator $\mathsf{O}$, satisfying $(\mathsf{O}\psi_n)(x) = \mathrm{e}^{E_n}\psi_n(x)$. As we saw in section 3.1, the operator $\mathsf{O}$ acts as a difference operator on the function $\psi(x)$. In the case where the mirror curve has genus one, it is a linear difference operator of order two. Formally, one can find for *any* $\kappa$ a full family of solutions to the difference equation $((\mathsf{O}+\kappa)\psi)(x) = 0$. A representative of the family can be multiplied by any function which is periodic under shifts $x \to x + \mathrm{i}\hbar$. These periodic functions are the "quasi constants". We will see that we can extend the TS/ST conjecture to obtain a full one parameter subfamily $\psi(x;\kappa)$ of these formal solutions, parametrized by the variable $\kappa$. We call these the *off-shell* eigenfunctions. These functions have the very nice property that they are entire functions of $\kappa$ at fixed $x$. However, they may not be in the image of $\rho$ for arbitrary $\kappa$, due to the lack of some analytic properties as functions of $x$ (for example insufficient decay at infinity). The true eigenfunctions are recovered

for $\kappa = -\mathrm{e}^{E_n}$. In that case, $\psi(x; -\mathrm{e}^{E_n})$ becomes a nice function which

(a) is in $L^2(\mathbb{R})$,

(b) is in the domain of $\mathsf{O}$ (= image of $\rho$).

The second condition will typically require $\psi$ to fulfill some regularity conditions: cancelation of a pole away from the real line, or stronger decay at infinity, etc. We stress that the two conditions are necessary for $\psi(x;\kappa)$ to be a true eigenfunction: we could have a $\psi(x;\kappa)$ in $L^2(\mathbb{R})$ but not an actual eigenfunction. Typically (at least for our examples), for a function $\psi(x;\kappa)$, the fulfilling of (a) and (b) requires the vanishing of the leading coefficient of the eigenfunction at large $x$. This coefficient is therefore proportional to the spectral determinant $\Xi(\kappa)$, and the off-shell eigenfunction is a kind of "perturbation" of the spectral determinant at large $x$. This gives us a hint on what should be the philosophy to extend the TS/ST correspondence to eigenfunctions: take the conjecture for the spectral determinant $\Xi(\kappa)$, and somehow "perturb" it with an extra parameter $x$. Of course this is rather naive, and we will see that the actual proposal is a bit more involved.

We will start by giving a construction of the off-shell eigenfunctions from the point of view of spectral theory. To ease the discussion, we take the symmetric local $\mathbb{P}^1 \times \mathbb{P}^1$ ($m_{\mathbb{F}_0} = 1$) as our example. We will then study its 't Hooft limit, and see how the *topological string wavefunction* emerges in this limit. Using the insight gained in this particular example, we will state the extended TS/ST conjecture for the off-shell eigenfunction $\psi(x;\kappa)$. This will involve the resummed WKB eigenfunction, and the open string amplitudes as an extra ingredient, in the form of the topological string wavefunction. We use this to fully write down off-shell eigenfunctions for the self-dual case $\hbar = 2\pi$, which we check against analytical and purely numerical results. We also point out a link between the decay of our eigenfunctions and the quantization of related integrable systems. Then, we perform some partial checks away from the self-dual case. In the end, we linger on a related but different construction of a subset of our eigenfunctions, which only uses the WKB data and the modular double structure of the related integrable system.

Eigenfunctions for a family of quantized mirror curves have been considered in [111] from the point of view of the associated gauge theory, in [20] using modular duality, and in [112] for the local $\mathbb{P}^1 \times \mathbb{P}^1$ case directly using the difference equation. These are all geometry specific results, and only give the on-shell eigenfunctions. This chapter is based on [15, 17, 19].

## 5.1 Eigenfunctions from spectral theory

Let us start by defining and investigating our off-shell eigenfunctions from the spectral theory point of view. We recall from section 3.1 the definitions for the fermionic traces and the coefficients of the spectral resolvent:

$$\begin{aligned} \Xi(\kappa) &= \sum_{N=0}^{\infty} \kappa^N Z(N) \\ D(x,t;\kappa) &= \Xi(\kappa) R(x,t;\kappa) = \sum_{N=0}^{\infty} \kappa^N B_N(x,t), \end{aligned} \tag{5.1}$$

and

$$\begin{aligned} Z(N) &= \frac{1}{N!} \int_{\mathbb{R}^N} \rho \begin{pmatrix} x_1 & x_2 & \dots & x_N \\ x_1 & x_2 & \dots & x_N \end{pmatrix} \mathrm{d}x_1 \cdots \mathrm{d}x_N, \\ B_N(x,t) &= \frac{1}{N!} \int_{\mathbb{R}^N} \rho \begin{pmatrix} x & x_1 & x_2 & \dots & x_N \\ t & x_1 & x_2 & \dots & x_N \end{pmatrix} \mathrm{d}x_1 \cdots \mathrm{d}x_N. \end{aligned} \tag{5.2}$$

where we use the notation (3.24). We assume that the integral kernel $\rho(x_1, x_2)$ has the following form (it is of course the case for our family of operators obtained in section 3.4 in variables $x_i$, which are a rescalings of $\nu_i$):

$$\rho(x_1,x_2) = \frac{\sqrt{v(x_1)}\ \overline{\sqrt{v(x_2)}}}{2\cosh\left(\frac{x_1-x_2}{2\xi} - \mathrm{i}\pi C\right)} = \frac{\sqrt{E(x_1)}\ \overline{\sqrt{E(x_2)}}}{\alpha M(x_1) + \alpha^{-1} M(x_2)}, \tag{5.3}$$

where

$$M(x) = \mathrm{e}^{x/\xi}, \qquad E(x) = v(x)M(x), \qquad \alpha = \mathrm{e}^{-\mathrm{i}\pi C}. \tag{5.4}$$

The scale $\xi$ is a positive parameter introduced for later convenience. Compared to our earlier notations, we have

$$\sqrt{v(x)} = \frac{1}{\sqrt{2\pi\xi}} \mathrm{e}^{-\frac{\hbar}{2} V(x/\xi)}. \tag{5.5}$$

We already saw in the previous chapter that this special form for the integral kernel can be used to obtain a matrix model representation of $Z(N)$. The key was the Cauchy determinant formula (4.5), which transforms determinants into products. This manipulation can also be performed for $B_N(x,t)$. We find:

$$B_N(x,t) = \rho(x,t) \left\langle\!\!\left\langle \prod_{i=1}^{N} \frac{\sinh\left(\frac{x-x_i}{2\xi}\right)}{\cosh\left(\frac{x-x_i}{2\xi} - \mathrm{i}\pi C\right)} \frac{\sinh\left(\frac{t-x_i}{2\xi}\right)}{\cosh\left(\frac{t-x_i}{2\xi} + \mathrm{i}\pi C\right)} \right\rangle\!\!\right\rangle, \tag{5.6}$$

where the unnormalized expectation value is given by

$$\langle\!\langle f(x_1,\ldots,x_N)\rangle\!\rangle = \frac{1}{N!}\int \mathrm{d}^N x\, f(x_1,\ldots,x_N)\prod_{i=1}^{N}|v(x_i)|\frac{\prod_{i<j}\left[2\sinh\left(\frac{x_i-x_j}{2\xi}\right)\right]^2}{\prod_{i,j}2\cosh\left(\frac{x_i-x_j}{2\xi}-\mathrm{i}\pi C\right)}. \tag{5.7}$$

So the $B_N(x,t)$ can be expressed in terms of expectation values in the matrix model. Let us define

$$\Psi_N(x) = \left\langle\!\!\left\langle \prod_{i=1}^{N}\frac{\sinh\left(\frac{x-x_i}{2\xi}\right)}{\cosh\left(\frac{x-x_i}{2\xi}-\mathrm{i}\pi C\right)}\right\rangle\!\!\right\rangle. \tag{5.8}$$

Looking at the limits $t\to\pm\infty$, we find

$$B_N(x,t)\approx \alpha\sqrt{v(x)M(x)}\,\overline{\sqrt{\frac{v(t)}{M(t)}}}\,\alpha^N\Psi_N(x), \qquad t\to\infty, \tag{5.9}$$

and

$$B_N(x,t)\approx \alpha^{-1}\sqrt{\frac{v(x)}{M(x)}}\,\overline{\sqrt{v(t)M(t)}}\,(-\alpha^{-1})^N\Psi_N(x), \qquad t\to-\infty. \tag{5.10}$$

In these limits, the unnormalized resolvent $D(x,t;\kappa)$ becomes

$$\begin{aligned} D(x,t;\kappa) &\approx \overline{\sqrt{\frac{v(t)}{M(t)}}}\,\alpha\,\Xi_+(x;\kappa), && t\to\infty,\\ D(x,t;\kappa) &\approx \overline{\sqrt{v(t)M(t)}}\,\alpha^{-1}\Xi_-(x;\kappa), && t\to-\infty, \end{aligned} \tag{5.11}$$

where

$$\begin{aligned} \Xi_+(x;\kappa) &= \sqrt{v(x)M(x)}\sum_{N=0}^{\infty}(\alpha\kappa)^N\Psi_N(x),\\ \Xi_-(x;\kappa) &= \sqrt{\frac{v(x)}{M(x)}}\sum_{N=0}^{\infty}(-\alpha^{-1}\kappa)^N\Psi_N(x). \end{aligned} \tag{5.12}$$

The importance of these functions comes from the Fredholm formula for the eigenfunctions (3.35) which implies that $D(x,t_0;\kappa)$ is an unnormalized eigenfunction (in the variable $x$) when $\kappa$ is an eigenvalue ($\kappa=-\mathrm{e}^{E_n}$). Here, we took the limits $t_0\to\pm\infty$ and extracted the finite parts $\Xi_\pm(x)$. Therefore, we expect them to be such unnormalized eigenfunctions when $\kappa=-\mathrm{e}^{E_n}$. Their limit behaviour for $x\to\pm\infty$ can be easily worked out by using that $\Psi_N(x)\to\alpha^N Z(N)$ (when $x\to\infty$)

and $\Psi_N(x) \to (-\alpha^{-1})^N Z(N)$ (when $x \to -\infty$):

$$\begin{aligned}
\Xi_+(x;\kappa) &\to \begin{cases} \Xi(\kappa)\sqrt{v(x)}\mathrm{e}^{|x|/2\xi}, & \text{when } x \to \infty, \\ \Xi(-\alpha^2\kappa)\sqrt{v(x)}\mathrm{e}^{-|x|/2\xi}, & \text{when } x \to -\infty, \end{cases} \\
\Xi_-(x;\kappa) &\to \begin{cases} \Xi(-\alpha^{-2}\kappa)\sqrt{v(x)}\mathrm{e}^{-|x|/2\xi}, & \text{when } x \to \infty, \\ \Xi(\kappa)\sqrt{v(x)}\mathrm{e}^{|x|/2\xi}, & \text{when } x \to -\infty. \end{cases}
\end{aligned} \tag{5.13}$$

Since $\sqrt{v(x)}$ vanishes in both limits, we find that $\Xi_\pm(x;\kappa)$ decreases, respectively, at $\mp\infty$, but not necessarily at $\pm\infty$. We recall that, when studying the Schrödinger equation for a one-dimensional confining potential $V(x)$, one can introduce functions $\psi_\pm(x)$ which satisfy

$$-\psi''_\pm(x;E) + V(x)\psi_\pm(x;E) = E\psi_\pm(x;E), \tag{5.14}$$

go to zero as $\mp\infty$, respectively, but are not necessarily square integrable, unless one tunes the value of $E$ to be a true eigenvalue (see [113, 114]). The functions $\Xi_\pm(x;\kappa)$ are precisely the analogues of these functions for our problem: as we will see in the next section, they are in the kernel of the operator $\mathsf{O} + \kappa$, they go to zero as $\pm\infty$, but they are not actual eigenfunctions of $\rho$ for generic values of $\kappa$. When $\kappa = -\mathrm{e}^{E_n}$ is a zero of the Fredholm determinant, the functions are proportional:

$$\Xi_+(x;-\mathrm{e}^{E_n}) = \text{const} \cdot \Xi_-(x;-\mathrm{e}^{E_n}), \tag{5.15}$$

and they give the true, square-integrable eigenfunctions of the spectral problem, up to an overall normalization. In this sense, $\Xi_\pm(x;\kappa)$ are also similar to the Jost functions of scattering theory in one dimension, which become square integrable and proportional to each other when one considers bound states (see for example [115]). Note that, when $\kappa = -\mathrm{e}^{E_n}$ corresponds to an eigenvalue, the leading terms of $\Xi_\pm(x;\kappa)$ vanish as $x \to \pm\infty$, since $\Xi(-\mathrm{e}^{E_n}) = 0$. But even for generic $\kappa$, the functions $\Xi_\pm(x;\kappa)$ contain a lot of spectral information about the operator $\rho$. The extension of the TS/ST correspondence to eigenfunctions is a conjectural expression for these functions at arbitrary $\kappa$.

Can we learn more about the *normalized* on-shell eigenfunctions $\psi_n(x)$? Let us use (3.34), which we recall here:

$$\psi_n(x)\psi_n^*(t) = \frac{1}{\Xi'(-\mathrm{e}^{E_n})} D(x,t;-\mathrm{e}^{E_n}). \tag{5.16}$$

From (5.13), we learn that in the large $|x|$ limit, the normalized eigenfunctions should behave as

$$\psi_n(x) \approx c_{\pm,n}\sqrt{v(x)}\mathrm{e}^{-|x|/2\xi}, \qquad x \to \pm\infty. \tag{5.17}$$

Taking the limits $t \to \pm\infty$ on both sides of (5.16), we obtain the two relations

$$\begin{aligned}\psi_n(x) &= \frac{\alpha}{\overline{c_{+,n}}\,\Xi'(-\mathrm{e}^{E_n})}\Xi_+(x,-\mathrm{e}^{E_n}) \\ &= \frac{\alpha^{-1}}{\overline{c_{-,n}}\,\Xi'(-\mathrm{e}^{E_n})}\Xi_-(x,-\mathrm{e}^{E_n}).\end{aligned} \tag{5.18}$$

Taking the limits $x \to \pm\infty$ in the above two relations, we find

$$\begin{aligned}|c_{+,n}|^2 &= \frac{\alpha}{\Xi'(-\mathrm{e}^{E_n})}\lim_{x\to+\infty}\frac{\Xi_+(x;-\mathrm{e}^{E_n})}{\sqrt{v(x)}\mathrm{e}^{-|x|/2\xi}}, \\ |c_{-,n}|^2 &= \frac{\alpha^{-1}}{\Xi'(-\mathrm{e}^{E_n})}\lim_{x\to-\infty}\frac{\Xi_-(x;-\mathrm{e}^{E_n})}{\sqrt{v(x)}\mathrm{e}^{-|x|/2\xi}}, \\ c_{+,n}\overline{c_{-,n}} &= \frac{\alpha^{-1}}{\Xi'(-\mathrm{e}^{E_n})}\lim_{x\to+\infty}\frac{\Xi_-(x;-\mathrm{e}^{E_n})}{\sqrt{v(x)}\mathrm{e}^{-|x|/2\xi}} = \alpha^{-1}\frac{\Xi(\alpha^2\mathrm{e}^{E_n})}{\Xi'(-\mathrm{e}^{E_n})},\end{aligned} \tag{5.19}$$

where in the last line we used (5.13). Overall phases remain undetermined. In the case where $\alpha = 1$ and where the eigenfunctions have a definite parity (this is the case for symmetric local $\mathbb{P}^1 \times \mathbb{P}^1$), we have that $c_{+,n} = (-1)^n c_{-,n} = c_n$, and

$$c_n^2 = (-1)^n \frac{\Xi(\mathrm{e}^{E_n})}{\Xi'(-\mathrm{e}^{E_n})}. \tag{5.20}$$

In this case, the normalized eigenfunction can be written down as

$$\psi_n(x) = \frac{1}{\sqrt{(-1)^n\Xi(\mathrm{e}^{E_n})\Xi'(-\mathrm{e}^{E_n})}}\Xi_+(x;-\mathrm{e}^{E_n}). \tag{5.21}$$

Resolvents for kernels of the form (5.3) with $\alpha = 1$ and real function $v(x)$ have been studied by Tracy and Widom in [26]. They provide a lemma which gives us another handle on the functions $\Xi_\pm(x;\kappa)$ for $\alpha = 1$. Indeed, computing them order by order in $\kappa$ would a priori imply computing the matrix model expectation values (5.8) for $\Psi_N(x)$ for $N = 1, 2, \ldots$ But the authors of [26] show that there is a more tractable recursive method to obtain these functions order by order in $\kappa$. Following [26], let us define the functions

$$\begin{aligned}\Phi_e(x) &= \frac{1}{\sqrt{E(x)}}\left[\frac{1}{1-\kappa^2\rho^2}\sqrt{E}\right](x), \\ \Phi_o(x) &= \frac{1}{\sqrt{E(x)}}\left[\frac{\kappa\rho}{1-\kappa^2\rho^2}\sqrt{E}\right](x).\end{aligned} \tag{5.22}$$

They can be written as power series in $\kappa$:

$$\begin{aligned}\Phi_e(x) &= \sum_{n=0}^{\infty}\kappa^{2n}\phi_{2n}(x), \\ \Phi_o(x) &= \sum_{n=0}^{\infty}\kappa^{2n+1}\phi_{2n+1}(x),\end{aligned} \tag{5.23}$$

with the normalization

$$\phi_0(x) = 1, \tag{5.24}$$

and the functions $\phi_j(x)$ satisfy the recursion relation

$$|\phi_j\rangle = \frac{1}{\sqrt{E}}\rho\sqrt{E}|\phi_{j-1}\rangle. \tag{5.25}$$

Let us now decompose the resolvent $\mathsf{R}$ as follows,

$$\mathsf{R} = \frac{\rho}{1+\kappa\rho} = \frac{1}{\kappa}\left(\mathsf{R}_o - \mathsf{R}_e\right), \tag{5.26}$$

where

$$\mathsf{R}_e = \frac{\kappa^2\rho^2}{1-\kappa^2\rho^2}, \qquad \mathsf{R}_o = \frac{\kappa\rho}{1-\kappa^2\rho^2}. \tag{5.27}$$

As shown in [26], the integral kernels of the operators $\mathsf{R}_{e,o}$ can be written in terms of the functions defined in (5.22):

$$\begin{aligned}
\frac{1}{\kappa}R_e(x,t) &= \frac{\sqrt{E(x)}\sqrt{E(t)}}{M(x)-M(t)}\left(\Phi_e(x)\Phi_o(t) - \Phi_o(x)\Phi_e(t)\right), \\
\frac{1}{\kappa}R_o(x,t) &= \frac{\sqrt{E(x)}\sqrt{E(t)}}{M(x)+M(t)}\left(\Phi_e(x)\Phi_e(t) - \Phi_o(x)\Phi_o(t)\right).
\end{aligned} \tag{5.28}$$

It can be shown that, if the potential $v(x)$ decays exponentially at infinity, the functions $\phi_j(x)$ go to constants at $\pm\infty$. We will denote

$$\lim_{x\to\pm\infty}\Phi_{e,o}(x) = c_{e,o}^{\pm}. \tag{5.29}$$

In addition, the functions $\phi_j(x)$ with $j \neq 0$ go to zero as $x \to \infty$, therefore we have

$$c_e^+ = 1, \qquad c_o^+ = 0. \tag{5.30}$$

We conclude from (5.28) that, as $t \to \infty$,

$$R(x,t;\kappa) \approx \sqrt{\frac{v(t)}{M(t)}}\sqrt{v(x)M(x)}\left(\Phi_e(x) - \Phi_o(x)\right). \tag{5.31}$$

By comparing this with (5.11-5.12) for $D(x,t;\kappa) = \Xi(\kappa)R(x,t;\kappa)$ and $\alpha = 1$, we find that

$$\Phi_e(x) - \Phi_o(x) = \frac{1}{\Xi(\kappa)}\sum_{N=0}^{\infty}\Psi_N(x)\kappa^N. \tag{5.32}$$

Taking the limit $x \to -\infty$ in (5.32) gives

$$c_e^- - c_o^- = \frac{\Xi(-\kappa)}{\Xi(\kappa)}. \tag{5.33}$$

By changing the sign of $\kappa$ in (5.32) we obtain

$$\Phi_e(x) + \Phi_o(x) = \frac{1}{\Xi(-\kappa)} \sum_{N=0}^{\infty} \Psi_N(x)(-\kappa)^N. \tag{5.34}$$

The results (5.32) and (5.34) lead to the following expressions for the functions $\Xi_\pm(x;\kappa)$:

$$\begin{aligned} \Xi_+(x;\kappa) &= \Xi(\kappa) \mathrm{e}^{\frac{x}{2\xi}} \sqrt{v(x)}\, (\Phi_e(x) - \Phi_o(x))\,, \\ \Xi_-(x;\kappa) &= \Xi(-\kappa) \mathrm{e}^{-\frac{x}{2\xi}} \sqrt{v(x)}\, (\Phi_e(x) + \Phi_o(x))\,. \end{aligned} \tag{5.35}$$

The recursive methods developed in [24, 78, 116] to compute the $\phi_j(x)$ make it possible to compute the functions $\Xi_\pm(x;\kappa)$ as a power series expansion in $\kappa$. General results of Fredholm theory imply that this series is convergent for any $\kappa$. In that sense, this method to calculate eigenfunctions is much better than the WKB method, which gives formal power series in $\hbar$. However, as we will see, the resummation of the WKB expansion provided by topological string theory can in some cases give us the functions $\Xi_\pm(x;\kappa)$, as exact functions of $\kappa$.

We can now use the results of [26] to verify that the functions $\Xi_\pm(x;\kappa)$ formally satisfy

$$(\mathsf{O} + \kappa)\, \Xi_\pm(x;\kappa) = 0, \tag{5.36}$$

for arbitrary $\kappa$, as mentioned above. To see this, let us write $\rho$ in operator form using (3.95) with $C = \frac{m-n+1}{2(m+n+1)} = 0$ and $F(q), v(x)$ real functions:

$$\rho = \sqrt{v(\mathsf{x})} \frac{2\pi\xi}{2\cosh(\mathsf{p}/2)} \sqrt{v(\mathsf{x})}, \tag{5.37}$$

where $\mathsf{x} = \xi b^{-2} \mathsf{q}$ so that

$$[\mathsf{x}, \mathsf{p}] = 2\pi \mathrm{i}\xi. \tag{5.38}$$

In particular,

$$2\pi\mathsf{O} = \frac{1}{\sqrt{v(\mathsf{x})}} 2\cosh(\mathsf{p}/2) \frac{1}{\sqrt{v(\mathsf{x})}}. \tag{5.39}$$

As shown in [26] the function

$$\Phi_-(x) = \Phi_e(x) - \Phi_o(x) \tag{5.40}$$

solves the difference equation

$$\Phi_-(x + \pi\mathrm{i}\xi) - \Phi_-(x - \pi\mathrm{i}\xi) = 2\pi\mathrm{i}\xi\kappa v(x)\Phi_+(x). \tag{5.41}$$

Then, the function

$$\widetilde{\Phi}_-(x) = \mathrm{e}^{\frac{x}{2\xi}} \Phi_-(x) \tag{5.42}$$

satisfies

$$\widetilde{\Phi}_-(x+\pi\mathrm{i}\xi)+\widetilde{\Phi}_-(x-\pi\mathrm{i}\xi)=-2\pi\xi\kappa v(x)\widetilde{\Phi}_-(x), \tag{5.43}$$

This is rewritten as the operator equation

$$2\cosh(\mathsf{p}/2)|\widetilde{\Phi}_-\rangle=-2\pi\kappa v(\mathsf{x})|\widetilde{\Phi}_-\rangle, \tag{5.44}$$

and

$$|\varphi\rangle=\sqrt{v(\mathsf{x})}|\widetilde{\Phi}_-\rangle \tag{5.45}$$

satisfies (5.36). But

$$\varphi(x)=\frac{1}{\Xi(\kappa)}\Xi_+(x;\kappa), \tag{5.46}$$

so $\Xi_+(x;\kappa)$ satisfies (5.36), as we wanted to show. A similar argument can be made for $\Xi_-(x;\kappa)$, by using that

$$\Phi_+(x)=\Phi_e(x)+\Phi_o(x) \tag{5.47}$$

satisfies the difference equation

$$\Phi_+(x+\pi\mathrm{i}\xi)-\Phi_+(x-\pi\mathrm{i}\xi)=-2\pi\mathrm{i}\xi\kappa v(x)\Phi_+(x). \tag{5.48}$$

Note that, even though the functions $\Xi_\pm(x;\kappa)$ are formally in the kernel of $\mathsf{O}+\kappa$ for arbitrary $\kappa$, they are not eigenfunctions of $\rho$. The reason is that they are not in the domain of $\mathsf{O}$, regarded as an unbounded operator on $L^2(\mathbb{R})$, unless $\kappa$ takes special values. In some cases, the functions $\Xi_\pm(x;\kappa)$ are not even square integrable for general $\kappa$. The fact that difference equations like (5.36) have huge kernels has led to discussions in the literature on the criteria for selecting eigenfunctions. In our framework, this problem is solved in a simple way by noting that, when $\hbar$ is real, the inverse operator $\rho$ is self-adjoint and of trace class on $L^2(\mathbb{R})$, so it leads to a well-defined and discrete spectrum.

Here we used the results of Tracy and Widom [26] to show that $\Xi_\pm(x;\kappa)$ formally satisfy the equation given by $\mathsf{O}$ when $\alpha=1$ and $\sqrt{v(x)}$ is a real function. Some of the results in [26] have been extended in [24] to the more general integral kernels considered here (where $\alpha$ is on the unit circle). One result of [24] is that the integral kernel of the $\ell^{\text{th}}$ power of $\rho$ is

$$\rho^\ell(x,y)=\alpha^{-1}\frac{\sqrt{E(x)}\overline{\sqrt{E(y)}}}{M(x)-\omega^\ell M(y)}\sum_{k=0}^{\ell-1}\omega^k\phi_k(x)\overline{\phi_{\ell-k-1}(y)}, \tag{5.49}$$

where

$$\omega=-\alpha^{-2}, \tag{5.50}$$

and where the functions $\phi_k(x)$ are given by the usual recursion

$$|\phi_k\rangle = \frac{1}{\sqrt{E}}\rho\sqrt{E}|\phi_{k-1}\rangle, \qquad \phi_0(x) = 1. \tag{5.51}$$

As for the case in the previous section, it can be seen that the limiting behaviour of $\phi_k(x)$ for $k > 0$ is given by

$$\begin{aligned} \phi_k(x) &\to 0, \qquad & x \to \infty, \\ \phi_k(x) &\to c_k, \qquad & x \to -\infty. \end{aligned} \tag{5.52}$$

Since the resolvent can be written in terms of powers of $\rho$, we have the alternative expression for $D(x,t;\kappa)$:

$$D(x,t;\kappa) = \Xi(\kappa)R(x,t,\kappa) = \Xi(\kappa)\sum_{\ell=0}^{\infty}(-\kappa)^\ell\rho^{\ell+1}(x,t). \tag{5.53}$$

Using the limiting behaviour of $\rho(x,t)$ when $t \to \pm\infty$ and comparing with (5.11), we obtain

$$\begin{aligned} \Xi_+(x;\kappa) &= \Xi(\kappa)\sqrt{E(x)}\sum_{\ell=0}^{\infty}(-\kappa)^\ell\phi_\ell(x), \\ \Xi_-(x;\kappa) &= \Xi(\kappa)\frac{\sqrt{E(x)}}{M(x)}\sum_{\ell=0}^{\infty}(-\kappa)^\ell\sum_{k=0}^{\ell}\omega^k\bar{c}_{\ell-k}\phi_k(x). \end{aligned} \tag{5.54}$$

These functions should satisfy the difference equation given by $\mathsf{O}$. This is easily checked for $\Xi_+(x;\kappa)$, since by construction we have

$$\rho\sqrt{E}|\phi_k\rangle = \sqrt{E}|\phi_{k+1}\rangle. \tag{5.55}$$

It is then immediately verified that

$$\mathsf{O}\sqrt{E}|\phi_{k+1}\rangle = \sqrt{E}|\phi_k\rangle, \qquad \mathsf{O}\sqrt{E}|\phi_0\rangle = 0, \tag{5.56}$$

which implies that $\Xi_+(x;\kappa)$ satisfies the difference equation (for any $\kappa$)

$$(\mathsf{O} + \kappa)\Xi_+(x;\kappa) = 0. \tag{5.57}$$

## 5.2 An application: eigenfunctions for local $\mathbb{P}^1 \times \mathbb{P}^1$ with $m_{\mathbb{F}_0} = 1$

As mentioned above, the functions $\phi_\ell$ can in principle be computed recursively. If the potential term $\sqrt{v(x)}$ is a tractable function, this recursion can be effectively implemented. The potential term is built out of Faddeev quantum dilogarithm

functions $\Phi_b$. When $\hbar$ is given by a rational number times $2\pi$, this potential term sometimes reduces to rationals of exponentials (these special cases for $\Phi_b$ are studied in [117]). Let us look at such an example, which is local $\mathbb{P}^1 \times \mathbb{P}^1$ with $m_{\mathbb{F}_0} = 1$ (or symmetric local $\mathbb{P}^1 \times \mathbb{P}^1$) for the self-dual case $\hbar = 2\pi$. The operator $\mathsf{O}$ in mirror curve variables reads

$$\mathsf{O} = \mathrm{e}^{\mathsf{x}} + \mathrm{e}^{-\mathsf{x}} + \mathrm{e}^{\mathsf{y}} + \mathrm{e}^{-\mathsf{y}}. \tag{5.58}$$

Using the results of section 3.4, the integral kernel $\rho(q_1, q_2)$ can be written explicitly. For this operator, we have $\tilde{\alpha} = \tilde{\gamma} = 0$, $\tilde{\beta} \to -\infty$, $(m, n) = (0, 1)$ and $C = 0$, so

$$\rho(q_1, q_2) = \frac{\sqrt{v(q_1)}\sqrt{v(q_2)}}{2\cosh\frac{q_1 - q_2}{2\xi}}, \tag{5.59}$$

where

$$\xi = \frac{b^2}{\sqrt{2}}, \qquad \hbar = \pi b^2, \tag{5.60}$$

and

$$\sqrt{v(q)} = \sqrt{\frac{1}{2^{1/2}\pi b^2}}\mathrm{e}^{\frac{\sqrt{2}}{4}q}\frac{\Phi_b\left(\frac{\sqrt{2}q}{2\pi b} + \frac{\mathrm{i}b}{4}\right)}{\Phi_b\left(\frac{\sqrt{2}q}{2\pi b} - \frac{\mathrm{i}b}{4}\right)}. \tag{5.61}$$

Here we used the variable $q$ associated to the operators $\mathsf{q}$, $\mathsf{p}$:

$$\begin{pmatrix}\mathsf{q}\\ \mathsf{p}\end{pmatrix} = \frac{1}{\sqrt{2}}\begin{pmatrix}1 & -1\\ 1 & 1\end{pmatrix}\begin{pmatrix}\mathsf{x}\\ \mathsf{y}\end{pmatrix}. \tag{5.62}$$

This is not exactly what was used in (3.93) (rescaling and exchange of the roles of $\mathsf{x}$ and $\mathsf{y}$), but it is straightforward to see from the results of section 3.4 that this linear canonical transformation also relates the operator $\mathsf{O}$ to the kernel $\rho(q_1, q_2)$. For $\hbar = 2\pi$, we have $b = \sqrt{2} = 2/b$. Using the dual difference equation (3.82), we obtain

$$\frac{\Phi_b\left(\frac{\sqrt{2}q}{2\pi b} + \frac{\mathrm{i}b}{4}\right)}{\Phi_b\left(\frac{\sqrt{2}q}{2\pi b} - \frac{\mathrm{i}b}{4}\right)} = \frac{\Phi_b\left(\frac{\sqrt{2}q}{2\pi b} + \frac{\mathrm{i}2}{b}\right)}{\Phi_b\left(\frac{\sqrt{2}q}{2\pi b} - \frac{\mathrm{i}2}{b}\right)} = \frac{1}{1 + \mathrm{e}^{q/\sqrt{2}}}, \tag{5.63}$$

so

$$\sqrt{v(q)} = \frac{2^{1/4}}{4\pi^{1/2}\cosh\left(\frac{q}{2\sqrt{2}}\right)}, \qquad \sqrt{E(q)} = \frac{2^{1/4}}{2\pi^{1/2}}\frac{1}{1 + \mathrm{e}^{q/\sqrt{2}}}, \tag{5.64}$$

and

$$\rho(q_1, q_2) = \frac{\sqrt{v(q_1)}\sqrt{v(q_2)}}{2\cosh\frac{q_1 - q_2}{2\sqrt{2}}}. \tag{5.65}$$

We can iterate the recursive definitions

$$|\phi_j\rangle = \frac{1}{\sqrt{E}}\rho\sqrt{E}|\phi_{j-1}\rangle, \qquad \phi_0(q) = 1 \tag{5.66}$$

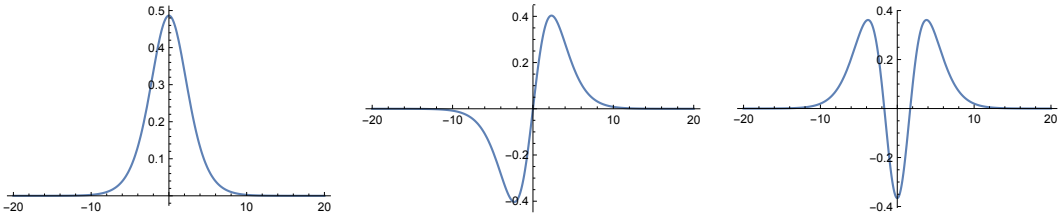


**Figure 5.1:** The first three normalized wavefunctions $\psi_n(q)$, $n = 0, 1, 2$, for local $\mathbb{P}^1 \times \mathbb{P}^1$ with $\hbar = 2\pi$ and $m_{\mathbb{F}_0} = 1$, as computed from (5.21). We use the series in $\kappa$ of $\Xi_\pm(x;\kappa)$ up to order $\kappa^{19}$. The eigenvalues are computed from the approximation of the Fredholm determinant up to order $\kappa^{24}$.

very explicitly by performing the involved integrations (the Lemma 2.1 on integrals of quasi-periodic functions in [117] is very helpful for this). We obtain

$$\begin{aligned}
\phi_1(q) &= \frac{\mathrm{e}^{q/\sqrt{2}}\left(q/\sqrt{2}-1\right)+1}{2\pi\left(\mathrm{e}^{q/\sqrt{2}}-1\right)^2}, \\
\phi_2(q) &= \frac{1}{32\pi^2\left(\mathrm{e}^{\sqrt{2}q}-1\right)^2} \\
&\quad\times\left[-2\mathrm{e}^{\sqrt{2}q}\left(\left(q^2+\pi^2\right)-2\sqrt{2}q+2\right)+\mathrm{e}^{q/\sqrt{2}}\left(4\sqrt{2}q+\pi^2+4\right)\right. \\
&\qquad\left.+\left(\pi^2-4\right)\mathrm{e}^{3q/\sqrt{2}}+4\right], \\
&\ldots
\end{aligned} \tag{5.67}$$

From these functions, we can build the $\kappa$ expansion of $\Phi_{e,o}(q;\kappa)$, which gives a convergent expansion for the functions $\Xi_\pm(q;\kappa)$. We can then set $\kappa$ to be a zero of the Fredholm determinant, of the form $\kappa = -\mathrm{e}^{E_n}$, and in this way we obtain excellent approximations for the normalized eigenfunctions $\psi_n(q)$, through (5.21). The results for $n = 0, 1, 2$ are shown in Fig. 5.1. We can see that the eigenfunctions display the nodal structure typical of confining potentials, namely, the eigenfunction of the $n^{\text{th}}$ energy level has $n$ zeros. In addition, they have definite parity, since

$$\psi_n(-q) = (-1)^n \psi_n(q). \tag{5.68}$$

This is expected from the form of the integral kernel. The above results for the eigenfunctions were checked using the direct numerical methods of section 3.2.

When $\kappa$ is not a zero of the Fredholm determinant, we obtain functions which are formally in the kernel of the operator $\mathsf{O} + \kappa$, but are not eigenfunctions of $\rho$. In the

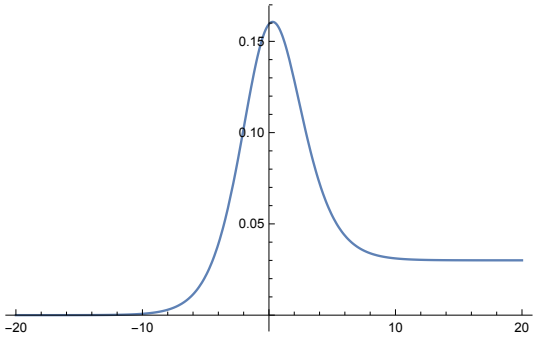


**Figure 5.2:** The function $\Xi_+(q;\kappa)$ for $\kappa = -\mathrm{e}^{E_0 - 1/7}$, for local $\mathbb{P}^1 \times \mathbb{P}^1$ with $\hbar = 2\pi$ and $m_{\mathbb{F}_0} = 1$. It decays as $q \to -\infty$ but goes to a non-zero constant when $q \to \infty$, therefore it is not square integrable.

present case, these functions are not square integrable. The function $\Xi_+(q;\kappa)$, for example, decays exponentially as $q \to -\infty$ for a generic $\kappa$, but will go to a non-zero constant as $q \to \infty$. An example of this behavior is shown in Fig. 5.2, which depicts the function $\Xi_+(q;\kappa)$ when $\kappa = -\mathrm{e}^{E_0 - 1/7}$.

These eigenfunctions are given in terms of the matrix model variable $q$ associated to the operators $\mathsf{q}, \mathsf{p}$. We would like to obtain the eigenfunctions directly in the mirror curve variable $x$ associated to $\mathsf{x}, \mathsf{y}$, which are used in (5.58), and which are related by the linear canonical transformation (5.62). Indeed, the coordinates $x, y$ of the original mirror curve are somewhat special, since they lead to topological string amplitudes with a worldsheet instanton interpretation. The rule for going from one set of coordinates to the other is particularly simple in the case of linear canonical transformations: it is just an integral transform of the eigenfunction. We will now provide a brief review of this.

Let $x, y$ canonically conjugate coordinates, and $\bar{x}$, $\bar{y}$ be the new coordinates obtained by a canonical transformation. Let $F(x, \bar{x})$ be the generating functional of the transformation, characterized by

$$y = \frac{\partial F}{\partial x}, \qquad \bar{y} = -\frac{\partial F}{\partial \bar{x}}. \tag{5.69}$$

Let us suppose that the canonical transformation is linear,

$$\begin{pmatrix} \bar{x} \\ \bar{y} \end{pmatrix} = \begin{pmatrix} A & B \\ C & D \end{pmatrix} \begin{pmatrix} x \\ y \end{pmatrix}, \qquad \begin{pmatrix} A & B \\ C & D \end{pmatrix} \in \mathrm{SL}(2,\mathbb{R}), \tag{5.70}$$

with inverse

$$\begin{pmatrix} x \\ y \end{pmatrix} = \begin{pmatrix} D & -B \\ -C & A \end{pmatrix} \begin{pmatrix} \bar{x} \\ \bar{y} \end{pmatrix}. \tag{5.71}$$

The generating functional is then given by

$$F(x,\bar{x}) = -\frac{1}{2B}\left(Ax^2 + D\bar{x}^2 - 2x\bar{x}\right). \tag{5.72}$$

The generating functional of the inverse transformation is

$$F^{-1}(\bar{x},x) = \frac{1}{2B}\left(Ax^2 + D\bar{x}^2 - 2x\bar{x}\right) = -F(x,\bar{x}). \tag{5.73}$$

Linear canonical transformations are implemented by unitary transformations acting on eigenfunctions, and one finds (see for example [118])

$$\xi(x) = \int_{\mathbb{R}} U(x,\bar{x})\bar{\xi}(\bar{x})\mathrm{d}\bar{x}, \qquad U(x,\bar{x}) = \frac{1}{\sqrt{2\pi\hbar|B|}}\mathrm{e}^{\mathrm{i}F(x,\bar{x})/\hbar}, \tag{5.74}$$

where $\xi(x)$, $\bar{\xi}(\bar{x})$ are the eigenfunctions in the coordinates $x$, $\bar{x}$, respectively.

Let us now go back to our concrete example of local $\mathbb{P}^1 \times \mathbb{P}^1$. We are interested in the canonical transformation of the eigenfunction $\Xi_+(q;\kappa)$ to the mirror curve coordinates. The coordinates are related by

$$\begin{pmatrix} q \\ p \end{pmatrix} = \frac{1}{\sqrt{2}}\begin{pmatrix} 1 & -1 \\ 1 & 1 \end{pmatrix}\begin{pmatrix} x \\ y \end{pmatrix}, \tag{5.75}$$

and the unnormalized eigenfunction in the $x$-variable is given by

$$\hat{\Xi}_+(x;\kappa) = \int_{\mathbb{R}} U(x,q)\Xi_+(q;\kappa)\mathrm{d}q, \tag{5.76}$$

where

$$U(x,q) = \frac{1}{\sqrt{2\pi\hbar}\,2^{-1/4}}\exp\left(\frac{\mathrm{i}}{2\hbar\,2^{-1/2}}\left(2^{-1/2}q^2 - 2xq + 2^{-1/2}x^2\right)\right). \tag{5.77}$$

We can write

$$\hat{\Xi}_+(x;\kappa) = \sum_{N=0}^{\infty}\psi_N(x)\kappa^N, \tag{5.78}$$

where

$$\psi_N(x) = \int_{-\infty}^{\infty} U(x,q)\sqrt{E\,(q)}\Psi_N(q)\mathrm{d}q. \tag{5.79}$$

We will now give some concrete results for this canonical transformation in the case $\hbar = 2\pi$ and $m_{\mathbb{F}_0} = 1$. These results will be crucial in order to compare with the predictions of topological string theory. Note first that the integral transform (5.74) implements a unitary transformation which acts in principle on the Hilbert space $\mathcal{H} = L^2(\mathbb{R})$. However, in (5.79) it acts on functions which are not square integrable (they decrease exponentially as $q \to -\infty$, but they go to a constant as $q \to \infty$). Fortunately, in this case, the integrals in the r.h.s. of (5.79) are well defined without

further ado. Moreover, they can be computed analytically by using the results of [117]. The reason is that the integrands in the r.h.s. of (5.79) are given as sums

$$\sum_{\ell=0}^{N} f_\ell(q) q^\ell \tag{5.80}$$

where the $f_\ell(q)$ are quasi-periodic functions. Therefore, the integration in (5.79) can be done by using Lemma 2.1 of [117], and it reduces to a residue computation. The terms $f_\ell(q)q^\ell$ with $\ell > 0$ are not quasi-periodic because of the power $q^\ell$, but they can be generated from quasi-periodic integrals by using that

$$q^\ell U(x,q) = \left[\frac{1}{\sqrt{2}}\left(2\pi \mathrm{i}\frac{\partial}{\partial x} + x\right)\right]^\ell U(x,q). \tag{5.81}$$

The result of the integration has the following structure,

$$\psi_N(x) = \mathrm{e}^{-\frac{\mathrm{i}x^2}{4\pi}} \psi_N^{(-)}(x) + \mathrm{e}^{\frac{\mathrm{i}x^2}{4\pi}} \psi_N^{(+)}(x). \tag{5.82}$$

The first term is due to residues at the $x$–dependent poles of the integrand in (5.79), while the second term is due to the $x$–independent poles. As we will see, the two contributions correspond to two different saddle points of the integral transform in the 't Hooft limit, and they will be given by two different copies of the topological string wavefunction. One finds

$$\begin{aligned}
\psi_0^{(-)}(x) &= \mathrm{e}^{\pi \mathrm{i}/4} \frac{\mathrm{e}^x\,(\mathrm{e}^x - \mathrm{i})}{\sqrt{2\pi}(\mathrm{e}^{2x}-1)}, \\
\psi_1^{(-)}(x) &= \frac{\mathrm{e}^{\pi\mathrm{i}/4}}{4\sqrt{2}\pi^{3/2}\,(\mathrm{e}^{2x}-1)^3} \mathrm{e}^x \big(\mathrm{e}^{2x}(-6\pi + 2\mathrm{i}(x-1)) + \mathrm{e}^{5x} + \mathrm{e}^{4x}(-2\mathrm{i}x - 2\pi + \mathrm{i}) \\
&\qquad + \mathrm{e}^x(2x + 4\mathrm{i}\pi + 1) + \mathrm{e}^{3x}(-2(x+1) + 4\mathrm{i}\pi) + \mathrm{i}\big), \\
&\cdots \\
\psi_0^{(+)}(x) &= -\frac{\mathrm{e}^x}{\sqrt{\pi}(\mathrm{e}^{2x}-1)}, \\
\psi_1^{(+)}(x) &= \frac{\mathrm{e}^x\left(\pi\left(6\mathrm{e}^x + 10\mathrm{e}^{3x} + \mathrm{i}\mathrm{e}^{4x} - \mathrm{i}\right) - 4\mathrm{i}\mathrm{e}^x\left(\mathrm{e}^{2x}-1\right)x\right)}{8\pi^{3/2}\,(\mathrm{e}^{2x}-1)^3}, \\
&\cdots
\end{aligned} \tag{5.83}$$

and so on. Note that each $\psi_N^{(\pm)}(x)$ is singular at $x = 0$, but $\psi_N(x)$ turns out to be an *entire* function on the full complex $x$–plane, for all $N \geq 0$. The behavior at infinity of the function $\psi(x;\kappa)$ is similar to the one of $\Xi_+(q,\kappa)$: for generic, real $\kappa$, it decreases exponentially as $x \to -\infty$, but it is an oscillatory function as $x \to \infty$. When $\kappa$ is a zero of the Fredholm determinant, $\psi(x;\kappa)$ is square integrable, and an eigenfunction of the operator $\rho$, in the $x$ representation. Let us finally note that the canonical transformation of $\Xi_-(q,\kappa)$ can be easily deduced from the one of $\Xi_+(q,\kappa)$.

## 5.3 The 't Hooft limit of the eigenfunctions

As we saw in the previous chapters, one of the main results of the TS/ST correspondence of [2] is that the conventional topological string emerges in a 't Hooft-like limit of the spectral problem, corresponding to the strongly coupled regime $\hbar \gg 1$. More precisely, in the 't Hooft expansion

$$N, \hbar \to \infty, \qquad \frac{N}{\hbar} = \lambda \tag{5.84}$$

with 't Hooft coupling $\lambda$ fixed, the spectral traces $Z(N)$ have an asymptotic expansion in terms of the topological string free energy in the conifold frame $\mathcal{F}(\lambda)$:

$$\log Z(N) \sim \sum_{g=0}^{\infty} \mathcal{F}_g(\lambda) \hbar^{2-2g}. \tag{5.85}$$

This is the proposal for genus one mirror curves, but it can be generalized to the higher genus cases [16].

In the case of eigenfunctions, the generalization of the fermionic spectral trace is the function $\Psi_N(x)$ in (5.8), which is the building block of $\Xi_{\pm}(x;\kappa)$. Since the function $\Psi_N(x)$ is defined by a matrix integral representation, we can study its 't Hooft limit by using standard tools in large $N$ matrix models, as we did in the previous chapter for $Z(N)$. Indeed, $\Psi_N(x)$ is the average value of the following determinant-like expression in the deformed $O(2)$ matrix model (4.7):

$$\Psi_N(x) = Z(N) \left\langle \det \frac{\mathrm{e}^{x/\xi} - A}{\alpha\, \mathrm{e}^{x/\xi} + \alpha^{-1} A} \right\rangle, \tag{5.86}$$

where the eigenvalues of $A$ are given by $\mathrm{e}^{q_i/\xi}$ (the rescaling by $\xi$ does not matter in normalized expectation values). It plays the same rôle that the average

$$\langle \det(x - M) \rangle \tag{5.87}$$

plays in conventional, Hermitian matrix models. It has been pointed out many times in the literature [75, 119–124] that this average defines a (D–brane) wavefunction. This strongly suggests that the 't Hooft limit of $\Psi_N(x)$ is also related to the topological string wavefunction. Let us recall how this wavefunction is constructed in the general setting of the topological recursion associated to a parametrized spectral curve $y = y(X)$. Given such a curve, one can construct an infinite sequence of meromorphic differentials [61, 63]

$$\mathcal{W}_{g,h}(X_1, \ldots, X_h) \mathrm{d}X_1 \cdots \mathrm{d}X_h, \qquad g \geq 0, \quad h \geq 1. \tag{5.88}$$

See also our discussion at the end of section 2.3. In the case $g = 0$, $h = 1$ (the "disk" amplitude) one has

$$\mathcal{W}_{0,1}(X)\mathrm{d}X = y(X)\mathrm{d}X, \tag{5.89}$$

while the case $g = 0$, $h = 2$ (the "annulus" amplitude) is essentially given by the Bergmann kernel of the curve $B(X_1, X_2)$,

$$\mathcal{W}_{0,2}(X_1, X_2)\mathrm{d}X_1\mathrm{d}X_2 = B(X_1, X_2)\mathrm{d}X_1\mathrm{d}X_2 - \frac{\mathrm{d}X_1\mathrm{d}X_2}{(X_1 - X_2)^2}. \tag{5.90}$$

(Explicit expressions for the annulus amplitude will be presented below). When the spectral curve is the mirror curve of a toric CY, the above meromorphic differentials calculate open topological string amplitudes [56, 57] associated to the toric branes introduced in [54, 55]. The *topological string wavefunction*, which we will denote by $\psi_{\mathrm{top}}(X, \mathbf{t}, g_s)$, is defined by the following asymptotic expansion around $g_s = 0$:

$$\psi_{\mathrm{top}}(X, \mathbf{t}, g_s) \sim \exp\left[\sum_{g=0}^{\infty}\sum_{h=1}^{\infty} \frac{(-\mathrm{i}g_s)^{2g-2+h}}{h!} \int^X \cdots \int^X \mathcal{W}_{g,h}(X_1, \cdots, X_h)\mathrm{d}X_1 \cdots \mathrm{d}X_h\right]. \tag{5.91}$$

The $\mathbf{t}$ are flat coordinates for the moduli of the curve. In the case of convergent, Hermitian matrix models, (5.91) gives the 't Hooft expansion of (5.87). For general spectral curves, (5.91) defines a formal asymptotic expansion.

To motivate our claim about the relationship between the 't Hooft limit of $\Psi_N(q)$ and the topological string wavefunction, let us get a closer look at the 't Hooft limit of expression (5.8) for our family of integral kernels. We start by clarifying the different coordinates we use for the eigenfunction. In the 't Hooft limit, the position coordinate of the eigenfunction should be scaled with $\hbar$. Let us call $x_m, y_m$ the natural parameters for the mirror curve $W(\mathrm{e}^{x_m}, \mathrm{e}^{y_m}) = 0$ (these were usually called $x, y$ in previous sections, as in Table 3.1 and in section 3.4). In the 't Hooft limit, the natural variables are

$$x = \frac{2\pi}{\hbar} x_m, \qquad y = \frac{2\pi}{\hbar} y_m. \tag{5.92}$$

The natural variables for the matrix models are linear canonical transforms

$$\begin{pmatrix} q_m \\ p_m \end{pmatrix} = \frac{1}{\sqrt{m+n+1}} \begin{pmatrix} -(m+1) & -n \\ 1 & -1 \end{pmatrix} \begin{pmatrix} x_m \\ y_m \end{pmatrix}, \tag{5.93}$$

and they have their rescaled version adapted for the 't Hooft limit

$$q = \frac{2\pi}{\hbar} q_m, \qquad p = \frac{2\pi}{\hbar} p_m. \tag{5.94}$$

In particular, $q_m$ is the natural variable for the functions $\Xi_\pm(q_m;\kappa)$ and their constituents $\Psi_N(q_m)$ built from the matrix model. The operators associated to these variables satisfy

$$\begin{aligned}[\mathsf{x}_m,\mathsf{y}_m]=[\mathsf{q}_m,\mathsf{p}_m]=\mathrm{i}\hbar,\\ [\mathsf{x},\mathsf{y}]=[\mathsf{q},\mathsf{p}]=\mathrm{i}\frac{4\pi^2}{\hbar}=\mathrm{i}\hbar_{\mathrm{D}}.\end{aligned} \tag{5.95}$$

In terms of variable $q$, the integral kernel $\rho(q_1,q_2)$ takes the form (5.3) with

$$\sqrt{v(q)}=\frac{1}{\sqrt{2\pi(m+n+1)^{1/2}}F^*\left(q\frac{\hbar}{2\pi}\sqrt{m+n+1}\right)} \tag{5.96}$$

and

$$\xi=\frac{1}{\sqrt{m+n+1}}. \tag{5.97}$$

Now, let us look at $\Psi_N(q_m)$. We have ($\omega=-\alpha^{-2}$)

$$\begin{aligned}\frac{\alpha^N\Psi_N(q_m)}{Z(N)}&=\left\langle\det\frac{\mathrm{e}^{q/\xi}-A}{\mathrm{e}^{q/\xi}-\omega A}\right\rangle\\ &=\left\langle\exp\sum_{k=1}^{\infty}\frac{1}{k}Q^{-k}(\omega^k-1)\,\mathrm{tr}(A^k)\right\rangle,\end{aligned} \tag{5.98}$$

where

$$Q=\mathrm{e}^{q/\xi}. \tag{5.99}$$

This can be written in terms of the connected correlators as

$$\begin{aligned}\log\frac{\alpha^N\Psi_N(q_m)}{Z(N)}&=\sum_{h=1}^{\infty}\frac{1}{h!}\left\langle\left(\sum_{k=1}^{\infty}\frac{1}{k}Q^{-k}(\omega^k-1)\mathrm{tr}(A^k)\right)^h\right\rangle^{(c)}\\ &=\sum_{h=1}^{\infty}\frac{1}{h!}\left\langle\sum_{k_1,\dots,k_h=1}^{\infty}\prod_{\ell=1}^{h}\frac{1}{k_\ell}(\omega^{k_\ell}-1)Q^{-k_\ell}\mathrm{tr}(A^{k_\ell})\right\rangle^{(c)}\\ &=\sum_{h=1}^{\infty}\frac{1}{h!}\int_\infty^Q\mathrm{d}Q_1\cdots\int_\infty^Q\mathrm{d}Q_hW_h(Q_1,...,Q_h),\end{aligned} \tag{5.100}$$

where $W_n(Q_1,\dots,Q_n)$ were introduced in eq. (4.161). By introducing the genus expansion of $W_n$ at large $\hbar$ given in (4.165), we obtain

$$\log\frac{\alpha^N\Psi_N(q_m)}{Z(N)}=\sum_{h=1}^{\infty}\sum_{g=0}^{\infty}\frac{\hbar^{2-2g-h}}{h!}\int_\infty^Q\mathrm{d}Q_1\cdots\int_\infty^Q\mathrm{d}Q_hW_{h,g}(Q_1,...,Q_h). \tag{5.101}$$

This has to be understood as a large $\hbar$ asymptotic expansion. The leading and next to leading orders are given by $W_{1,0}(Q)$ and $W_{2,0}(Q_1,Q_2)$, which can be obtained from the exact expressions for $\varpi_{1,0}(Q)$ and $\varpi_{2,0}(Q)$ of section 4.4. Expression (5.101) is

already very similar to (5.91). However, we need our function to be expressed in mirror curve variable $x$ instead of the matrix model variable $q$. This can be done by using the integral transforms (5.74) but with $\hbar_{\mathrm{D}}$ instead of $\hbar$. What we are actually interested in are the coefficients of $\Xi_{\pm}(q_m;\kappa)$, including the extra factor $\sqrt{v(q)}\mathrm{e}^{q/\xi}$ which has its own large $\hbar$ expansion. We therefore have

$$\log\left(\sqrt{v(q)}\mathrm{e}^{q/2\xi}\frac{\alpha^N\Psi_N(q_m)}{Z(N)}\right)=\sum_{n=0}^{\infty}(-\mathrm{i}\hbar_{\mathrm{D}})^{n-1}\,\mathcal{T}_n(q), \tag{5.102}$$

and the first terms are given by

$$\begin{aligned}\mathcal{T}_0(q)&=-4\pi^2\mathrm{i}\left[\int_{\infty}^{Q}W_{1,0}(Q_1)\mathrm{d}Q_1-\frac{1}{2}V_0\left(\log Q\right)\right],\\ \mathcal{T}_1(q)&=\mathrm{const}+\frac{1}{2}\log Q+\frac{1}{2}\int_{\infty}^{Q}\int_{\infty}^{Q}W_{2,0}(Q_1,Q_2)\mathrm{d}Q_1\mathrm{d}Q_2,\end{aligned} \tag{5.103}$$

where $V_0(\nu)$ is the planar potential given in (3.112). Higher $\mathcal{T}_n$ include higher order terms of the potential.

It is satisfying to realize that the $\frac{1}{2}V_0$ term is precisely what is needed in order for $\mathcal{T}_0(q)$ to be expressed as an integral on the spectral curve. To see this in detail, take the example of local $\mathbb{P}^1\times\mathbb{P}^1$ with $m_{\mathbb{F}_0}=1$ ($\tilde{\alpha}=0$). In this case $Y$ in (4.212) is

$$Y(X)=\exp\left(-2\pi^2\mathrm{i}\varpi_{1,0}(X)-\log\frac{X+1}{X-1}\right), \tag{5.104}$$

where $X,Y$ satisfy the equation (4.238), rewritten as

$$XY+\frac{1}{XY}-\frac{Y}{X}-\frac{X}{Y}=\kappa. \tag{5.105}$$

We express $P=-\mathrm{i}Y$ in terms of $Q=\mathrm{i}X$. Since we have $\omega=-1$ implying $\varpi_{1,0}(X)=\mathrm{i}W_{1,0}(\mathrm{i}X)$, we obtain

$$P(Q)=\exp\left(-2\pi^2\mathrm{i}QW_{1,0}(Q)-\log\mathrm{i}\frac{Q+\mathrm{i}}{Q-\mathrm{i}}\right), \tag{5.106}$$

where $Q,P$ satisfy

$$\left(Q+\frac{1}{Q}\right)\left(P+\frac{1}{P}\right)=\kappa. \tag{5.107}$$

Since we have that $Q=\mathrm{e}^{q/\sqrt{2}}$, and that the planar potential for this case is given by

$$V_0\left(\log Q\right)=-\frac{1}{2\pi}\log Q+\frac{1}{\pi^2\mathrm{i}}\left(\mathrm{Li}_2(\mathrm{i}Q)-\mathrm{Li}_2(-\mathrm{i}Q)\right), \tag{5.108}$$

implying

$$Q\frac{\mathrm{d}}{\mathrm{d}Q}V_0\left(\log Q\right)=-\frac{1}{\pi^2\mathrm{i}}\log\mathrm{i}\frac{Q+\mathrm{i}}{Q-\mathrm{i}}, \tag{5.109}$$

we find

$$\int_{\infty}^{Q} \frac{\log P(Q_1)}{Q_1} \mathrm{d}Q_1 = -2\pi^2 \mathrm{i} \left( \int_{\infty}^{Q} W_{1,0}(Q_1) \mathrm{d}Q_1 - \frac{1}{2} V_0 \left( \log Q \right) \right). \tag{5.110}$$

Finally, using $q, p$ with $P = \mathrm{e}^{p/\sqrt{2}}$, we obtain that $\mathcal{T}_0$ is expressed as

$$\mathcal{T}_0(q) = \int^{q} p(q') \mathrm{d}q' \tag{5.111}$$

on the spectral curve

$$\left( \mathrm{e}^{q/\sqrt{2}} + \mathrm{e}^{-q/\sqrt{2}} \right) \left( \mathrm{e}^{p/\sqrt{2}} + \mathrm{e}^{-p/\sqrt{2}} \right) = \kappa. \tag{5.112}$$

The relation between $\kappa$ and the 't Hooft coupling $\lambda$ was given through the modular parameter $q_\tau = \mathrm{e}^{\mathrm{i}\pi\tau}$ in (4.237), but, as in the case of local $\mathbb{P}^2$, it is of course also expressible as an integration on the spectral curve:

$$\begin{aligned} \lambda &= \frac{1}{2\pi \mathrm{i}} \oint_{\mathcal{I}} W_{1,0}(X) \mathrm{d}X \\ &= \frac{1}{8\pi^2} \oint_{\mathcal{A}} p(q) \mathrm{d}q, \end{aligned} \tag{5.113}$$

where $\mathcal{A}$ is the conifold $\mathcal{A}$ cycle surrounding the two branch points at $-\frac{\kappa}{4} \pm \sqrt{\kappa^2 - 16}$ in the $Q$ plane. This shrinks to a pole at the conifold point that we choose to be $\kappa = -4$, so that the matrix model regime is $\kappa \in (-\infty, -4]$. Through a straightforward residue computation for the branch

$$P(Q) = \frac{1}{2(Q + Q^{-1})} \left[ \kappa + \sqrt{\kappa^2 - 4(Q + Q^{-1})^2} \right]. \tag{5.114}$$

we find

$$\lambda = \frac{1}{8\pi^2}(-\kappa - 4) - \frac{1}{128\pi^2}(-\kappa - 4)^2 + \frac{5}{6144\pi^2}(-\kappa - 4)^3 + \dots \tag{5.115}$$

It can be easily inverted to

$$\kappa = -4 - 8\pi^2\lambda - 4\pi^4\lambda^2 - \frac{2\pi^6}{3}\lambda^3 - \frac{\pi^8}{6}\lambda^4 + \mathcal{O}(\lambda^5). \tag{5.116}$$

This agrees with the results found in section 4.4 using the parametrization in terms of the modular parameter $q_\tau = \mathrm{e}^{\mathrm{i}\pi\tau}$, which for our case reads[1]

$$\begin{aligned} \lambda &= \frac{2}{\pi^2} \sum_{k=1}^{\infty} \frac{q_\tau^{2k}}{k(1 - q_\tau^{2k})} \sin \frac{k\pi}{2} (1 - \cos \pi k), \\ \kappa &= 2 \frac{\vartheta_1(1/2)}{\vartheta_1'(0)} \left( \frac{\vartheta_1'}{\vartheta_1} \left( \frac{3}{4} \right) - \frac{\vartheta_1'}{\vartheta_1} \left( \frac{1}{4} \right) \right), \end{aligned} \tag{5.117}$$

[1] In section 4.4, $q_\tau$ was just called $q$.

where the modular parameter of the $\vartheta_1$ function is $\tau$. We can now compute (5.111) at weak $\lambda$ by performing the integral using the branch (5.114), and we obtain

$$\begin{aligned}\mathcal{T}_0(q) = -4\pi^2\mathrm{i}\Bigg(&-\frac{1}{2}V_0\left(\log Q\right) + \log\frac{Q-1}{Q+1}\lambda - \frac{Q(Q^2+1)}{(Q^2-1)^2}\pi^2\lambda^2 \\ &-\frac{Q(Q^2+1)(Q^4+22Q^2+1)}{6(Q^2-1)^4}\pi^4\lambda^3 + \mathcal{O}(\lambda^4)\Bigg).\end{aligned} \tag{5.118}$$

We can check this formula by computing the expectation value (5.86) at finite $N$ and extracting the small $\lambda$ expansion, as we did at the beginning of section 4.3 for the free energies $\mathcal{F}_g(\lambda)$. In section 4.4, we also obtained an exact expression for $W_{2,0}(Q_1, Q_2)$ in terms of $\vartheta$ functions (see (4.301) for $\varpi_{2,0}$). For our present example of local $\mathbb{P}^1 \times \mathbb{P}^1$ which is an undeformed $O(2)$ case, we can also use the exact result of [104] in terms of the endpoints of the cut $a, b^2$:

$$\begin{aligned}W^0_{++}(p,q) =& \frac{1}{4}W_{2,0}(p,q) \\ =& \frac{1}{8\sqrt{(p^2-a^2)(p^2-b^2)}\sqrt{(q^2-a^2)(q^2-b^2)}}\Bigg[a^2+b^2-2b^2\frac{\mathrm{E}\left(1-\frac{a^2}{b^2}\right)}{\mathrm{K}\left(1-\frac{a^2}{b^2}\right)} \\ &-(p^2+q^2)\left(1-\left(\frac{\sqrt{(p^2-a^2)(p^2-b^2)}-\sqrt{(q^2-a^2)(q^2-b^2)}}{p^2-q^2}\right)^2\right)\Bigg].\end{aligned} \tag{5.119}$$

Here, $p$ and $q$ are generic arguments, and $\mathrm{K}(k^2)$ and $\mathrm{E}(k^2)$ are elliptic functions of the first and second kind, respectively. In our case, the endpoints of the cut can be read from the discriminant of the curve (5.107):

$$\sigma_q(Q) = (Q^2-a^2)(Q^2-b^2) = (Q^2+1)^2 - \frac{\kappa^2 Q^2}{4}, \tag{5.120}$$

and by symmetry of the potential one has

$$a = \frac{1}{b} = \frac{1}{4}\left(\sqrt{\kappa^2-16}+\kappa\right). \tag{5.121}$$

Notice that in the present convention $a > b$ (in section 4.4 we exchanged the notations of $a$ and $b$ and had $b > a$). It turns out that this planar two-point function can be written in terms of the annulus amplitude appearing in the standard topological recursion, i.e. in terms of the Bergmann kernel, as follows:

$$\begin{aligned}2W^0_{++}(Q_1,Q_2) = \frac{1}{4}\Big(&W_0(Q_1,Q_2) + W_0(-Q_1,Q_2) \\ &+W_0(Q_1,-Q_2) + W_0(-Q_1,-Q_2)\Big),\end{aligned} \tag{5.122}$$

[2]The first minus sign of the second line is missing in [104].

where $W_0(Q_1, Q_2)$ is given by Akemann's formula [125]

$$W_0(p,q) = \frac{1}{4(p-q)^2}\left(\sqrt{\frac{(p-x_1)(p-x_4)(q-x_2)(q-x_3)}{(p-x_2)(p-x_3)(q-x_1)(q-x_4)}}+ \right. \\ \left. \sqrt{\frac{(p-x_2)(p-x_3)(q-x_1)(q-x_4)}{(p-x_1)(p-x_4)(q-x_2)(q-x_3)}}\right) \\ + \frac{(x_1-x_3)(x_2-x_4)}{4\sqrt{\prod_{i=1}^4 (p-x_i)(q-x_i)}}\frac{\mathrm{E}(k^2)}{\mathrm{K}(k^2)} - \frac{1}{2(p-q)^2}, \tag{5.123}$$

and the modulus of the elliptic integrals is given by

$$k^2 = \frac{(x_1-x_4)(x_2-x_3)}{(x_1-x_3)(x_2-x_4)}. \tag{5.124}$$

The branch points of $W_0(Q_1, Q_2)$ in (5.122) are given by

$$\{x_1, x_2, x_3, x_4\} = \{a, -a, -a^{-1}, a^{-1}\}. \tag{5.125}$$

We have all the ingredients to write down $\mathcal{T}_1(q)$. It can also be verified against a perturbative computation at small $\lambda$, as in section 4.3.

As already pointed out, we need our functions to be expressed in the mirror curve variable $x$ instead of the matrix model variable $q$, if we want them to have an enumerative interpretation. This can be done by using the integral transforms (5.74) but with $\hbar_{\mathrm{D}}$ instead of $\hbar$. Let us perform this computation for the symmetric local $\mathbb{P}^1 \times \mathbb{P}^1$. In the $x, y$ coordinates, the curve (5.107) reads

$$X + \frac{1}{X} + Y + \frac{1}{Y} = \kappa, \tag{5.126}$$

where

$$X = \mathrm{e}^x, \qquad Y = \mathrm{e}^y. \tag{5.127}$$

The curve (5.126) is identical to the local $\mathbb{P}^1 \times \mathbb{P}^1$ mirror curve

$$\mathrm{e}^x + \mathrm{e}^{-x} + \mathrm{e}^y + \mathrm{e}^{-y} + \kappa = 0, \tag{5.128}$$

except that $\kappa$ has the opposite sign. This is equivalent to changing the sign in $X$ and $Y$. We will now give evidence that, after a canonical transformation to the large radius open string coordinates, we obtain precisely the topological string wavefunction (5.91). We note that, in this parametrization, $X$ is already a flat coordinate for the open string modulus [55]. Our starting point is the asymptotic expansion (5.102). The canonical transformation is given by the transform in (5.356), with $\alpha = 1$ and $\xi = \sqrt{2}$ in our example. Since we are doing the calculation in the

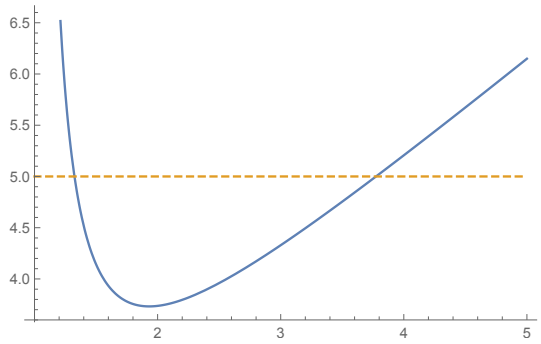


**Figure 5.3:** The function in the r.h.s. of (5.137), as a function of $\zeta$, where $Q = \mathrm{i}\zeta$. Given a real $X$, there are two values of $\zeta$ which lead to it, corresponding to two saddle points of the canonical transformation.

't Hooft limit, we have to compute the transformed eigenfunction in terms of the rescaled variables $x, q$ appearing in (5.92) and (5.94), instead of the original variables $x_m, q_m$ appearing in the original spectral curve. We then find,

$$\psi_N(x_m) = \frac{1}{\sqrt{2\pi\hbar_{\mathrm{D}}}} \int_{\mathbb{R}} \mathrm{e}^{\mathrm{i}F(x,q)/\hbar_{\mathrm{D}}} \sqrt{v(q)} \mathrm{e}^{q/2\sqrt{2}} \frac{\Psi_N(q_m)}{Z(N)} \mathrm{d}q, \tag{5.129}$$

where

$$F(x,q) = \frac{1}{2}\left(x^2 + q^2 - 2\sqrt{2}xq\right). \tag{5.130}$$

Here, we rather use the conventions for $x, y$ given by the rescaled versions of eq. (5.62), since for our present example this is equivalent. The integrand in (5.129) is given as an asymptotic expansion for $\hbar_{\mathrm{D}}$ small, and we can evaluate the integral transform in the saddle point approximation. The saddle points are defined by

$$\mathcal{T}_0'(q) + \frac{\partial F}{\partial q}(x,q) = 0. \tag{5.131}$$

The different solutions to this equation give $q$ as a function of $x$. Let us denote by $q(x)$ the resulting function for a given saddle. By expanding around this saddle, we find

$$\psi_N(x_m) \sim \exp\left[\frac{\mathrm{i}}{\hbar_{\mathrm{D}}}\mathcal{S}_0(x) + \mathcal{S}_1(x) + \mathcal{O}(\hbar_{\mathrm{D}})\right], \tag{5.132}$$

where

$$\begin{aligned} \mathcal{S}_0(x) &= \mathcal{T}_0(q(x)) + F(x, q(x)), \\ \mathcal{S}_1(x) &= \mathcal{T}_1(q(x)) - \frac{1}{2}\log\left[-\mathrm{i}(\mathcal{T}_0 + F)''(q(x))\right]. \end{aligned} \tag{5.133}$$

Here, we have denoted $F'' = \partial^2 F/\partial q^2$. The leading order term $\mathcal{T}_0(q)$ has the WKB form (5.111). This is preserved by canonical transformations: since $F(x,q)$ is the generating function of the transformation, one has

$$\mathcal{T}_0(q(x)) + F(x,q(x)) = \int^x y(x')\mathrm{d}x', \tag{5.134}$$

where $y(x)$ is determined by (5.126). Since they are two different solutions for $y(x)$, this indicates that we will have at most two saddle points. Let us see that this is indeed the case. The saddle point equation (5.131) reads

$$\frac{\partial \mathcal{T}_0}{\partial q} + q - \sqrt{2}x = 0. \tag{5.135}$$

The solution is

$$x = \frac{q}{\sqrt{2}} + \frac{p}{\sqrt{2}} = \log Q + \log P(Q), \tag{5.136}$$

or, equivalently,

$$X = QP(Q) = \frac{Q}{2(Q+Q^{-1})}\left[\kappa + \sqrt{\kappa^2 - 4(Q+Q^{-1})^2}\right]. \tag{5.137}$$

Given a real $X$, this equation has two different (imaginary) solutions $Q_{1,2}(X)$. The first solution is given by

$$Q_1(X) = \frac{\sqrt{-\sqrt{(X^2-\kappa X+1)^2 - 4X^2} - X^2 + \kappa X - 1}}{\sqrt{2}} = \mathrm{i}\left\{X - \frac{\kappa}{2} - \frac{\kappa^2}{8X} + \dots\right\}, \tag{5.138}$$

where we have expanded the result for large $X$. The second solution is

$$Q_2(X) = \frac{\sqrt{\sqrt{(X^2-\kappa X+1)^2 - 4X^2} - X^2 + \kappa X - 1}}{\sqrt{2}} = \mathrm{i}\left\{1 + \frac{\kappa}{2X} + \frac{3\kappa^2}{8X^2} + \dots\right\}. \tag{5.139}$$

Therefore, we have indeed *two* different saddle points. This is not surprising, since in the calculation of (5.82) at finite $\hbar$ we found that the eigenfunction in the $x$ variables is a sum of two pieces, coming from two different set of poles in the integral transform. The first term in the r.h.s. of (5.82) corresponds to the first saddle point (5.138), while the second term corresponds to the second saddle point (5.139). These two saddles define two different functions $y_{1,2}(x)$, through

$$y_{1,2}(x) = \frac{1}{\sqrt{2}}(-q_{1,2}(x) + p(q_{1,2}(x))). \tag{5.140}$$

They are given by

$$\begin{aligned} y_1(x) &= \log\left(\frac{-1+\kappa X - X^2 + \sqrt{(X^2-\kappa X+1)^2 - 4X^2}}{2X}\right), \\ y_2(x) &= \log\left(\frac{-1+\kappa X - X^2 - \sqrt{(X^2-\kappa X+1)^2 - 4X^2}}{2X}\right). \end{aligned} \tag{5.141}$$

These are the two different sign determinations obtained from the equation (5.126) (there is an additive ambiguity of an odd integer multiple $\pm \mathrm{i}\pi$, since we are taking the log of a negative number.) We can now verify (5.134) explicitly. The canonical transformation of the leading order term is given by

$$\mathcal{T}_0(q_{1,2}(x)) + \frac{1}{2}(x^2 + q_{1,2}^2(x) - 2\sqrt{2}x q_{1,2}(x)) \tag{5.142}$$

and it can be explicitly checked that it agrees with,

$$\int^x y_{1,2}(X')\frac{\mathrm{d}X'}{X'}, \tag{5.143}$$

up to $X$–independent terms. This is very much what is expected from the topological wavefunction expression (5.91), since the disk amplitude for $(h,g) = (1,0)$ is precisely given by the integral of $y(x)$ on the mirror curve. However, we see that we have the contribution of both branches $y_{1,2}(x)$, coming from the different saddle points.

Let us now consider the next-to-leading order of the canonical transformation. We first focus on the first saddle point, and we find

$$\mathcal{T}_1(q_1(x)) - \frac{1}{2}\log\left[-\mathrm{i}(\mathcal{T}_0 + F)''(q_1(x))\right] = \frac{1}{2}\int_\infty^X \int_\infty^X W_0(X',Y')\mathrm{d}X'\mathrm{d}Y' + \frac{1}{2}\log X, \tag{5.144}$$

where $W_0(X,Y)$ is the annulus amplitude of Akemann (5.123) associated with the curve (5.126), and

$$\mathcal{T}_0''(q) = \frac{\kappa Q(1-Q^2)}{(Q^2+1)\sqrt{\kappa^2 Q^2 - 4\left(Q^2+1\right)^2}}. \tag{5.145}$$

In $W_0(X,Y)$, the $x_i$ are the roots of the discriminant

$$(1-\kappa X + X^2)^2 - 4X^2, \tag{5.146}$$

and we have the ordering

$$\begin{aligned} \{x_1,x_2,x_3,x_4\} = \Big\{ &\frac{1}{2}\left(\kappa - \sqrt{\kappa-4}\sqrt{\kappa} - 2\right), \frac{1}{2}\left(\kappa - \sqrt{\kappa+4}\sqrt{\kappa} + 2\right), \\ &\frac{1}{2}\left(\kappa + \sqrt{\kappa+4}\sqrt{\kappa} + 2\right), \frac{1}{2}\left(\kappa + \sqrt{\kappa-4}\sqrt{\kappa} - 2\right)\Big\}. \end{aligned} \tag{5.147}$$

This ordering corresponds, in the topological string, to a choice of frame. In this case, this is the conifold frame which also appears in the 't Hooft limit (5.85) of the fermionic spectral traces. The result (5.144) is non-trivial, and it indicates that, after doing a canonical transformation to the large radius open coordinates, the first saddle point gives indeed the topological string wavefunction (5.91), with an overall factor $X^{1/2}$. Indeed, it is one of the consequences of the BKMP result that $\mathcal{W}_{2,0}(X_1, X_2)$ in (5.91) is precisely given by $W_0(X_1, X_2)$ in (5.123) [56, 57]. We conjecture that this is the case to all orders in $\hbar_{\mathrm{D}}$: in the 't Hooft limit, the part of the eigenfunction corresponding to the first saddle point is essentially the topological string wavefunction.

What happens to the contribution of the other saddle point? The situation is a bit more difficult, essentially because for the second saddle point, the inverse of the function $Q_2(X)$ in (5.139) maps $X = \infty$ to $Q = \mathrm{i}$ (instead of to $Q = \infty$, which is the natural expansion point of our functions). The leading order, up to an $X$–independent term, is given in (5.143). The difficulties arise for the next to leading term. Let us introduce some more functions related to the different curves (for more details, see Appendix A in [15]). The Abel–Jacobi map based at $Q = \infty$ relevant for the curve (5.107) and normalized in the orbifold frame is given by

$$u_q(Q) = \frac{1}{2\mathrm{K}(\kappa^2/16)} \int_\infty^Q \frac{\mathrm{d}Q'}{\sqrt{\sigma_q(Q')}}, \tag{5.148}$$

where $\sigma_q(Q')$ is given in (5.120), and the modular parameter of the curve is

$$\tau_q = \mathrm{i}\frac{\mathrm{K}(1-\kappa^2/16)}{\mathrm{K}(\kappa^2/16)}. \tag{5.149}$$

The function $W^0_{++}$ can be expressed in terms of the odd elliptic theta function as

$$W^0_{++}(p,q) = \frac{1}{4}\partial_p\partial_q \log \frac{\vartheta_1(u_q(p) - u_q(q);\tau_q)}{\vartheta_1(u_q(p) + u_q(q);\tau_q)}. \tag{5.150}$$

which can be integrated to

$$\int_\infty^Q \int_\infty^Q W^0_{++}(p,q)\mathrm{d}p\mathrm{d}q = -\frac{1}{4}\log\left[-\frac{\mathrm{K}(\kappa^2/16)\sqrt{\sigma_q(Q)}}{Q\vartheta_1'(0|\tau_q)}\vartheta_1(2u_q(Q)|\tau_q)\right]. \tag{5.151}$$

Its $Q$ dependence is totally encoded in $\sigma_q(Q)$ and the Abel–Jacobi map $u_q(Q)$. The Abel–Jacobi map based at $X = \infty$ relevant for the curve (5.126) and normalized in the large radius frame is given by

$$u(X) = \frac{\mathrm{i}\kappa}{4\mathrm{K}(16/\kappa^2)} \int_\infty^X \frac{\mathrm{d}X'}{\sqrt{\sigma(X')}}, \tag{5.152}$$

where

$$\sigma(X) = (X^2 - \kappa X + 1) - 4X^2, \tag{5.153}$$

and the modular parameter of the curve is

$$\tau_{\mathrm{lr}} = 2\mathrm{i}\frac{\mathrm{K}(1 - 16/\kappa^2)}{\mathrm{K}(16/\kappa^2)}. \tag{5.154}$$

It is related to $\tau$ used in the $\vartheta_1$ functions of (5.117) as $\tau = -1/\tau_{\mathrm{lr}}$. Finally, the Abel–Jacobi map based at $X = \infty$ for the curve (5.126) normalized for the so called orbifold frame is given by

$$u_{\mathrm{or}}(X) = \frac{1}{2\mathrm{iK}(\kappa^2/16)} \int_\infty^X \frac{\mathrm{d}X'}{\sqrt{\sigma(X')}}, \tag{5.155}$$

The modular parameter in this frame is

$$\begin{aligned} \tau_{\mathrm{or}} &= -\frac{1}{2 + \tau_{\mathrm{lr}}} \\ &= \frac{\tau_q + 1}{2}. \end{aligned} \tag{5.156}$$

Using elliptic integral identities, we have

$$u_{\mathrm{or}}(X) = -\tau_{\mathrm{or}} u(X). \tag{5.157}$$

The function $W_0(p, q)$ can be written

$$W_0(p, q) = \partial_p \partial_q \log\left(\frac{\vartheta_1(u_{\mathrm{or}}(p) - u_{\mathrm{or}}(q)|\tau_{\mathrm{or}})}{p - q}\right), \tag{5.158}$$

which leads to

$$\int_\infty^X \int_\infty^X W_0(p, q)\mathrm{d}p\mathrm{d}q = -2\log\left[\frac{2\mathrm{iK}(\kappa^2/16)(\sigma(X))^{1/4}}{\vartheta_1'(0|\tau_{\mathrm{or}})}\vartheta_1(u_{\mathrm{or}}(X)|\tau_{\mathrm{or}})\right]. \tag{5.159}$$

Its $X$ dependence is totally encoded in $\sigma(X)$ and the Abel–Jacobi map associated to it. We want to obtain

$$u_q(Q_2(X)). \tag{5.160}$$

Let us write $X_{1,2}(Q)$ for the inverse function of $Q_{1,2}(X)$. It can be checked explicitly that we have

$$\frac{X_{1,2}'(Q)^2}{\sigma(X_{1,2}(Q))} = -\frac{1}{\sigma_q(Q)}, \tag{5.161}$$

which implies

$$u_{\mathrm{or}}(X_2(Q)) = \pm(u_q(Q) - u_q(\mathrm{i})). \tag{5.162}$$

The right determination for the sign turns out to be $-$, and the second term arises because $Q_2(\infty) = \mathrm{i}$, see eq. (5.139). The remaining task is to find $u_q(\mathrm{i})$. This can be done exactly, using the high symmetry of the function $\sigma_q(Q,\kappa) = (Q^2+1)^2 - \frac{\kappa^2 Q^2}{4}$. Indeed, it satisfies the following relations (with care taken for the branch cuts):

$$\begin{aligned}
\sqrt{\sigma_q(-Q,\kappa)} &= \sqrt{\sigma_q(Q,\kappa)},\\
\sqrt{\sigma_q(1/Q,\kappa)} &= Q^{-2}\sqrt{\sigma_q(Q,\kappa)},\\
\sqrt{\sigma_q(\mathrm{i}Q,\kappa)} &= -\sqrt{\sigma_q(Q,4\sqrt{1-\kappa^2/16})}.
\end{aligned} \tag{5.163}$$

Using the obvious changes of variables for the three cases, it is easily shown that the Abel–Jacobi map $u_q(Q,\kappa)$ in (5.148) satisfies

$$\begin{aligned}
u_q(Q,\kappa) &= -u_q(-Q,\kappa) - 1,\\
u_q(Q,\kappa) &= u_q(0,\kappa) - u_q(Q^{-1},\kappa),\\
u_q(Q,\kappa) &= -\tau_q\, u_q\left(-\mathrm{i}Q, 4\sqrt{1-\kappa^2/16}\right).
\end{aligned} \tag{5.164}$$

The $-1$ in the first line comes from the fact that in deforming of the contour of integration to go from one expression to the other, we pick up a negative $A$–period. Using the three relations successively, we find for all $\kappa$:

$$\begin{aligned}
u_q(0,\kappa) &= -\frac{1}{2},\\
u_q(1,\kappa) &= \frac{1}{2}u_q(0,\kappa) = -\frac{1}{4},\\
u_q(\mathrm{i},\kappa) &= -\tau_q\, u_q(1, 4\sqrt{1-\kappa^2/16}) = \frac{\tau_q}{4}.
\end{aligned} \tag{5.165}$$

So the value we were looking for is $u_q(\mathrm{i}) = \frac{\tau_q}{4}$. Another approach to this computation is to express the Abel–Jacobi map in terms of incomplete elliptic integrals of the first kind and use its convergent expansion found in Theorem 4 of [126] (see [15]). In any case, we find

$$u_q\left(Q_2(X)\right) = -u^{\mathrm{or}}(X) + \frac{\tau_q}{4} = -u^{\mathrm{or}}(X) + \frac{\tau_{\mathrm{or}}}{2} - \frac{1}{4}, \tag{5.166}$$

whereas for the solution $Q_1(X)$, we would have found

$$u_q\left(Q_1(X)\right) = u^{\mathrm{or}}(X). \tag{5.167}$$

So the transformation of the Abel–Jacobi map to go from one solution to the other is

$$u^{\mathrm{or}}(X) \to -u^{\mathrm{or}}(X) + \frac{\tau_{\mathrm{or}}}{2} - \frac{1}{4}. \tag{5.168}$$

For the curve (5.126), and in the large radius frame, the transformation (5.166) reads (using (5.157))

$$u(X) \to -u(X) - \frac{\tau_{\rm lr}}{4} - 1, \tag{5.169}$$

where $\tau_{\rm lr}$ is the modulus appropriate to the large radius frame, and is given in (5.154). What is the interpretation of (5.169)? The shift by $-1$ is trivial in the Jacobian. One can verify that the points $u(X)$, $-u(X) - \tau/4$ correspond to the two different sheets of the Riemann surface defined by the curve (5.126).[3] To summarize this rather lengthy exposition, we find that the two saddle point contributions to the total eigenfunctions in mirror curve variable $x$ correspond to evaluating the different functions defined on the mirror curve on equivalent points on the *two different sheets* of the cover of the $X = \mathrm{e}^x$ plane. We will consider this as a guiding principle even for different geometries, and use this fact to obtain exact results for the eigenfunctions in the following sections.

What have we learned from the calculations in this section? The functions $\Psi_N(q)$ are the building blocks of the eigenfunctions. They can be computed exactly, as we showed in the last section, but they also admit a matrix integral representation which makes it possible to study their 't Hooft limit. The canonical transformation to the large radius open string coordinates can be computed in a saddle point approximation. Two different saddles contribute. The first one gives exactly the topological string wavefunction (5.91). The second saddle gives a related contribution, involving the open topological string amplitude on the second sheet of the Riemann surface.

It is possible to write down this result in a way which will be useful later on. First of all, the topological string wavefunctions are computed in the conifold frame. As shown in [47], under a change of frame, this wavefunction transforms as the topological string partition function. We can then write,

$$\psi_N(x) \sim \sum_\sigma \int \psi^{(\sigma)}_{\rm top}\left(X^{\frac{2\pi}{\hbar}}, \frac{2\pi}{\hbar}\mathbf{t} + \pi \mathrm{i}\mathbf{B}, \hbar_{\rm D}\right) \mathrm{e}^{J^{\rm WS}(\mu,\hbar) - \mu N} \mathrm{d}\mu. \tag{5.170}$$

(In this formula we have gone back to the original notation for the open string moduli, with no subscript). The topological string wavefunction on the r.h.s. is calculated in the large radius frame for both the closed and the open string moduli. The sum over $\sigma$ is over the different saddle points, which in this case correspond to the two different sheets of the Riemann surface. The shift by a $B$ field $\pi\mathrm{i}\mathbf{B}$ is zero in this example, but we anticipate that, by analogy with what happens in the closed topological string, it will be nonzero for other geometries.

[3] This is easily tested numerically. For more analytical considerations, see [15].

## 5.4 TS/ST conjecture for eigenfunctions

Armed with the insights we gathered for the symmetric local $\mathbb{P}^1 \times \mathbb{P}^1$ case, we are now ready to propose a conjectural expression for the eigenfunctions $\psi(x;\boldsymbol{\kappa})$ of the operator $\rho$ associated to mirror curves. We will directly assume the general higher genus case ($g_W > 1$), with its different eigenfunctions $|\psi^{(i)}\rangle$ ($i = 1, \ldots, g_W$), satisfying the off-shell version of eq. (3.47) associated to the different canonical operators $\mathsf{O}_i$. We suppress the label $i$ by choosing one of the $\mathsf{O}_i$ to be a preferred operator $\mathsf{O}$, with its associated eigenfunction $|\psi\rangle$ and true modulus $\kappa$. The eigenfunction $|\psi\rangle$ depends on the full set of moduli $\boldsymbol{\kappa}$, and we will write it as $\psi(x;\boldsymbol{\kappa})$ in the $x$ representation. To obtain the eigenfunctions associated to the other operators $\mathsf{O}_j$, we can simply use (3.49).

The function $\psi(x;\boldsymbol{\kappa})$ is in the kernel of the operator $\mathsf{O} + \kappa$, therefore at small $\hbar$ it can be calculated by a WKB expansion:

$$\psi(x;\boldsymbol{\kappa}) \sim \psi_{\mathrm{WKB}}(x;\boldsymbol{\kappa}) = \exp\left[\sum_{n=0}^{\infty}(-\mathrm{i}\hbar)^{n-1} S_n^{\mathrm{WKB}}(x)\right]. \tag{5.171}$$

We recall that $\mathbf{t}(\boldsymbol{\mu},\hbar)$ is the quantum mirror map of the geometry, already used in section 3.3. We recall the definition

$$X = \mathrm{e}^x. \tag{5.172}$$

To the variable $x$ we associate the following exponentiated open string modulus

$$\widehat{X} = \mathrm{e}^{x - \mathbf{r}\cdot\mathbf{t}}, \tag{5.173}$$

where $\mathbf{r}$ is a vector of rational entries which depends on the geometry. This is a kind of quantum mirror map for the open string modulus $x$. As in the closed string case, the WKB expansion in $\hbar$ in the exponent can be resummed to a function of $\hat{X}$, $\hbar$ and the closed string moduli. When expressed in terms of flat coordinates for both the open and the closed string moduli, this resummation has the structure [20, 127]

$$J_{\mathrm{open}}^{\mathrm{WKB}}(\boldsymbol{\mu},\hbar,X) = J_{\mathrm{pert}}^{\mathrm{WKB}}(\boldsymbol{\mu},\hbar,X) + \log\psi_{\mathrm{inst}}^{\mathrm{WKB}}(X,\mathbf{t}(\boldsymbol{\mu},\hbar),\hbar). \tag{5.174}$$

In this equation, $J_{\mathrm{pert}}^{\mathrm{WKB}}(\boldsymbol{\mu},\hbar,X)$ is a perturbative part which is a polynomial in $x$, and the resummed part is

$$\log\psi_{\mathrm{inst}}^{\mathrm{WKB}}(X,\mathbf{t},\hbar) = \sum_{\mathbf{d},\ell,s}\sum_{k=1}^{\infty} D^s_{\mathbf{d},\ell}\frac{\mathrm{e}^{\mathrm{i}ks\hbar}}{k(1-\mathrm{e}^{\mathrm{i}k\hbar})}(-\widehat{X})^{-k\ell}\mathrm{e}^{-k\mathbf{d}\cdot\mathbf{t}}. \tag{5.175}$$

The $D^s_{\mathbf{d},\ell}$ are integer invariants which depend on a half integer spin number $s$, a winding number $\ell$ (an integer which here is positive), and the multi-degrees $\mathbf{d}$. The

minus sign in $\widehat{X}$ in this equation is due to the fact that, in the WKB solution, the sign of $X$ is the opposite one to what is required by integrality, as one can verify in the case of local $\mathbb{P}^1 \times \mathbb{P}^1$. The WKB grand potential is obtained by adding the closed string grand potential appearing in (3.68), and the open string grand potential (5.174), i.e.

$$J^{\mathrm{WKB}}(\boldsymbol{\mu}, \hbar, X) = J^{\mathrm{WKB}}(\boldsymbol{\mu}, \hbar) + J^{\mathrm{WKB}}_{\mathrm{open}}(\boldsymbol{\mu}, \hbar, X). \tag{5.176}$$

We know from the direct calculations in the previous section that, in the 't Hooft limit, the eigenfunction $\psi(x;\kappa)$ is closely related to the topological string wavefunction (5.91), after appropriate rescaling of the variables. The standard open topological string amplitudes, in the large radius frame for both open and closed moduli, have an integrality structure which has been fully determined in [44, 45]. The total open free energy of the standard topological string can be written as (see eq. (2.18)):

$$\begin{aligned} F_{\mathrm{open}}(V, \mathbf{t}, g_s) = & \sum_{\mathbf{d}} \sum_{g=0}^{\infty} \sum_{h=1}^{\infty} \sum_{\boldsymbol{\ell}} \sum_{w=1}^{\infty} \frac{\mathrm{i}^h}{h!} n_{g,\mathbf{d},\boldsymbol{\ell}} \frac{1}{w} \left(2 \sin \frac{w g_s}{2}\right)^{2g-2} \\ & \times \prod_{i=1}^{h} \left(2 \sin \frac{w \ell_i g_s}{2}\right) \frac{1}{\ell_1 \cdots \ell_h} \mathrm{Tr}\, V^{w\ell_1} \cdots \mathrm{Tr}\, V^{w\ell_h} \mathrm{e}^{-w \mathbf{d} \cdot \mathbf{t}}. \end{aligned} \tag{5.177}$$

In this expression, $n_{g,\mathbf{d},\boldsymbol{\ell}}$ are integer invariants which generalize the Gopakumar–Vafa invariants of closed topological strings. They depend on the genus, the multi-degree $\mathbf{d}$ and the winding numbers $\boldsymbol{\ell} = (\ell_1, \cdots, \ell_h)$. The open topological string wavefunction (5.91) is a particular case of (5.177) when we set

$$\mathrm{Tr} V^n = X^{-n}, \qquad n \in \mathbb{Z}. \tag{5.178}$$

We then find the following integrality structure for the standard topological string wavefunction

$$\begin{aligned} \log \psi_{\mathrm{top}}(X, \mathbf{t}, g_s) = & \sum_{\mathbf{d}} \sum_{g=0}^{\infty} \sum_{h=1}^{\infty} \sum_{\boldsymbol{\ell}} \sum_{w=1}^{\infty} \frac{\mathrm{i}^h}{h!} n_{g,\mathbf{d},\boldsymbol{\ell}} \frac{1}{w} \left(2 \sin \frac{w g_s}{2}\right)^{2g-2} \\ & \times \prod_{i=1}^{h} \left(2 \sin \frac{w \ell_i g_s}{2}\right) \frac{1}{\ell_1 \cdots \ell_h} X^{-w(\ell_1 + \cdots + \ell_h)} \mathrm{e}^{-w \mathbf{d} \cdot \mathbf{t}}, \end{aligned} \tag{5.179}$$

which can be considered as an alternative, $g_s$–resummed counterpart of (5.91). We now introduce the worldsheet contribution for the grand potential,

$$J^{\mathrm{WS}}(\boldsymbol{\mu}, \hbar, X) = J^{\mathrm{WS}}(\boldsymbol{\mu}, \hbar) + J^{\mathrm{WS}}_{\mathrm{open}}(\boldsymbol{\mu}, \hbar, X). \tag{5.180}$$

The first term in the r.h.s. is the worldsheet grand potential appearing in (3.70), while

$$J^{\mathrm{WS}}_{\mathrm{open}}(\boldsymbol{\mu},\hbar,X)=\log\psi_{\mathrm{top}}\left(\widehat{X}^{2\pi/\hbar},\frac{2\pi}{\hbar}\mathbf{t}(\boldsymbol{\mu},\hbar)+\pi\mathrm{i}\mathbf{B},\hbar_{\mathrm{D}}\right). \tag{5.181}$$

The total, $X$–dependent grand potential is

$$J(\boldsymbol{\mu},\hbar,X)=J^{\mathrm{WKB}}(\boldsymbol{\mu},\hbar,X)+J^{\mathrm{WS}}(\boldsymbol{\mu},\hbar,X). \tag{5.182}$$

The first term in the r.h.s. of this equation is a resummation of the WKB expansion, while the second term is a non-perturbative correction in $\hbar$ to the perturbative WKB result. This is a generalization of expression (3.65) with additional $X$–dependent terms.

Note that both terms in the sum of $J(\boldsymbol{\mu},\hbar,X)$ have poles when $\hbar/2\pi$ is a rational number. However, as in the closed string case, they should cancel when we add both functions, in a sort of open version of the HMO mechanism.[4] Let us verify this. First, we note that the poles in the topological string (or "WS") contribution are only due to the term with $g=0$, $h=1$, and occur when $\hbar$ is of the form

$$\hbar=2\pi\frac{w}{k}. \tag{5.183}$$

For each multi-degree $\mathbf{d}$ and winding number $\ell$, we find a simple pole with residue

$$-\mathrm{i}n_{0,\mathbf{d},\ell}\frac{(-1)^{k\ell+w\mathbf{B}\cdot\mathbf{d}}}{k^2}\mathrm{e}^{-k\mathbf{d}\cdot\mathbf{t}}\hat{X}^{-k\ell}. \tag{5.184}$$

Let us now look at the resummed WKB part. For the same value of $\hbar$, we find a simple pole with residue

$$\mathrm{i}\left(\sum_s D^s_{\mathbf{d},\ell}\right)\frac{(-1)^{k\ell+2ws}}{k^2}\mathrm{e}^{-k\mathbf{d}\cdot\mathbf{t}}\hat{X}^{-k\ell}. \tag{5.185}$$

Expression (5.184) is the contribution at multi-degree $\mathbf{d}$ and winding $\ell$ to the disk amplitude, which is known to be equal (up to the sign in $X$ noted in (5.174)) to the leading part of the WKB function $S_0(x)$ [54, 55]. This implies in particular that

$$\sum_s D^s_{\mathbf{d},\ell}=n_{0,\mathbf{d},\ell}. \tag{5.186}$$

We now see that poles cancel, provided that

$$(-1)^{\mathbf{B}\cdot\mathbf{d}}=(-1)^{2s} \tag{5.187}$$

[4] The $\hbar$ dependence of $\mathbf{t}$ through the quantum mirror map should be imposed *after* cancelling the poles.

for all $\mathbf{d}$ and $s$ such that $D^s_{\mathbf{d},\ell} \neq 0$. This condition on the $B$ field has also been found in [20], in the framework of a different proposal for the eigenfunctions. The $B$ field has to be chosen in such a way that poles cancel in the closed string sector, and it is natural to conjecture that the same choice will satisfy (5.187). This is the case in local $\mathbb{P}^1 \times \mathbb{P}^1$, where $B = 0$ [2] and the spins $s$ of the non-vanishing invariants are all integers [20].

We now conjecture that the eigenfunction $\psi(x;\kappa)$ is obtained from the total grand potential by

$$\psi(x;\boldsymbol{\kappa}) = \sum_{\sigma} \psi_\sigma(x;\boldsymbol{\kappa}), \tag{5.188}$$

where

$$\psi_\sigma(x;\boldsymbol{\kappa}) = \sum_{\mathbf{n}\in\mathbb{Z}^{g_W}} \exp\left[J_\sigma(\boldsymbol{\mu} + 2\pi \mathrm{i}\mathbf{n}, \hbar, X)\right]. \tag{5.189}$$

Here, $\sigma$ labels the saddle points which contribute in the topological string sector, as in (5.170). From the discussion of the previous section, we expect each contribution to correspond to a sheet of the Riemann surface defining the mirror curve. After summing over the different sheets, we expect to find an entire function on the complex plane, as pointed out in [119] in the context of non-critical strings, and as we will see later in examples. In the example of local $\mathbb{P}^1 \times \mathbb{P}^1$ analyzed in detail in the previous section, the disk contribution of the different saddle points is the same up to an overall sign, and by changing the corresponding sign in the WKB contribution, pole cancellation is again achieved. This mechanism is likely to be present in other examples as well.

In writing the open string grand potential, we have made an implicit choice of a preferred sheet. It is the choice of sheet that we implicitly made when building the WKB eigenfunction (5.171), and the corresponding consistent choice when building the topological wavefunction. When the mirror curve is hyperelliptic (as in all the following examples), we only have two different sheets that we label by $\sigma = \pm$ (this label reflects a choice of sign determinations in various functions). In that case, we will take $-$ to be the preferred sheet, so that $J_-(\boldsymbol{\mu}, \hbar, X)$ is constructed as (5.182) using the formulas above, and $J_+(\boldsymbol{\mu}, \hbar, X)$ is its analytic continuation to the second sheet in $X$. By construction, we have that

$$\lim_{X\to\infty} J_-(\boldsymbol{\mu}, \hbar, X) = J^{\mathrm{WKB}}_{\mathrm{pert}}(\boldsymbol{\mu}, \hbar, X) + J(\boldsymbol{\mu}, \hbar), \tag{5.190}$$

where $J(\boldsymbol{\mu}, \hbar)$ is the modified grand potential of the closed sector (3.65). We can see (5.189) as an $x$–dependent generalization of the conjecture (3.73) for the Fredholm determinant

$$\Xi(\boldsymbol{\kappa}) = \sum_{\mathbf{n}\in\mathbb{Z}^{g_W}} \mathrm{e}^{J(\boldsymbol{\mu}+2\pi\mathrm{i}\mathbf{n},\hbar)}. \tag{5.191}$$

In particular, since $J^{\rm WKB}_{\rm pert}(\boldsymbol{\mu},\hbar,X)$ depends on $\mu_i$ through $\kappa_i = {\rm e}^{\mu_i}$, we have at large $X = {\rm e}^x$

$$\psi_-(x;\boldsymbol{\kappa}) \sim {\rm e}^{J^{\rm WKB}_{\rm pert}(\boldsymbol{\mu},\hbar,X)}\Xi(\boldsymbol{\kappa}). \tag{5.192}$$

We learn that setting the eigenfunction on-shell ($\kappa = -{\rm e}^{E_n}$) implies the vanishing of the leading coefficient of $\psi_-(x;\boldsymbol{\kappa})$ at large $x$.

What our conjecture fundamentally says, is that the contribution of the standard open topological string gives a non-perturbative correction to the resummed WKB eigenfunction. In the construction for $\psi(x;\boldsymbol{\kappa})$, the sums over $\mathbf{n} \in \mathbb{Z}^{g_W}$ and over $\sigma$ can be regarded as sums over the different sheets for the closed and the open string moduli, respectively.

Let us verify that the conjecture (5.188-5.189) incorporates the results of the previous section, for which we had only one modulus $\kappa$. From the expansion (5.78) for $\psi_-(x;\kappa)$, we have

$$\psi_N(x) = \oint_0 \frac{{\rm d}\kappa}{2\pi{\rm i}} \kappa^{-N-1}\psi_-(x;\kappa). \tag{5.193}$$

As in the derivation in the beginning of section 4.2, the contour integral on the r.h.s. can be combined with the sum over $n$ in (5.189) into an Airy type of integral

$$\psi_N(x) = \sum_\sigma \int_{\mathcal{C}} {\rm e}^{J_\sigma(\mu,\hbar,X)-\mu N} \frac{{\rm d}\mu}{2\pi{\rm i}}. \tag{5.194}$$

In the 't Hooft limit, the only contribution to $J_\sigma(\mu,\hbar,X)$ comes from the topological open string wavefunction in (5.181), and one recovers the asymptotic result (5.170).

We should mention that the implementation of the sum over the different sheets turns out to be quite subtle for general values of $\hbar$. In the hyperelliptic case, the eigenfunction for the $\sigma = -$ sheet involves standard BPS invariants, as obtained from the WKB expansion and the topological vertex. The eigenfunction with $\sigma = +$ is obtained by transforming $\psi_-(x;\boldsymbol{\kappa})$ to the second sheet of the Riemann surface. As we will see in the next section, this can be done in detail in the self-dual case where $\hbar = 2\pi$. However, for general values of $\hbar$ the transformation is more difficult to implement.

## 5.5 Checking the conjecture for the self-dual case

One nice consequence of the TS/ST correspondence is that the theory becomes particularly simple when

$$\hbar = 2\pi. \tag{5.195}$$

This is the self-dual value for the Planck constant, for which we have $\hbar = \hbar_{\rm D}$. For this value, the expressions for the spectral determinant and for the eigenfunctions become

exact at one-loop in the topological string expansion and in the WKB expansion. By this, we mean that many contributions vanish in the infinite sums giving the different components of $J(\boldsymbol{\mu}, \hbar, X)$. Moreover, those that survive are associated with genus $g = 0$ and $g = 1$ quantities, and can be resummed into exact functions. We will now write down explicit and general expressions for the eigenfunctions in the self-dual case and for almost arbitrary toric geometry. For simplicity, we will assume in the following that there are no mass parameters in the model, so the matrix $C$ appearing in (3.61) reduces to an invertible matrix (the inclusion of mass parameters is straightforward but it requires some additional ingredients and notation).

Let us introduce the following shorthand notation for the quantum mirror map

$$\mathbf{t}_\hbar = \mathbf{t}(\boldsymbol{\mu}, \hbar). \tag{5.196}$$

In the self-dual case $\hbar = 2\pi$, the only contribution from the topological string wavefunction (5.179) involves the disk amplitude $g = 0$, $h = 1$, and the annulus amplitude $g = 0$, $h = 2$. Let us introduce the functions

$$\begin{aligned} \widetilde{D}(X) &= \sum_{\mathbf{d},\ell} n_{0,\mathbf{d},\ell} \sum_{w=1}^{\infty} \frac{1}{w^2} \mathrm{e}^{-w\mathbf{d}\cdot\mathbf{t}} (-\widehat{X})^{-w\ell}, \\ \widetilde{A}(X) &= \sum_{\mathbf{d},\ell_1,\ell_2} n_{0,\mathbf{d},\ell_1,\ell_2} \sum_{w=1}^{\infty} \frac{1}{w} \mathrm{e}^{-w\mathbf{d}\cdot\mathbf{t}} (-\widehat{X})^{-w(\ell_1+\ell_2)}. \end{aligned} \tag{5.197}$$

Here, we use the "classical" Kähler parameters $\mathbf{t} \equiv \mathbf{t}_0$. Up to a change of sign in the exponentiated open string moduli, these functions are, respectively, the disk amplitude and the annulus amplitude $A(X_1, X_2)$ for $X_1 = X_2 = -\widehat{X}$. In order to proceed, we define two constant vectors $\mathbf{c_1}$ and $\mathbf{c_2}$ by the equality,

$$\mathbf{t}_{2\pi} + \mathrm{i}\pi\mathbf{B} = \mathbf{t}(\boldsymbol{\mu} + \mathrm{i}\pi\mathbf{c_1}, 0) + 2\pi\mathrm{i}\mathbf{c_2}, \tag{5.198}$$

where $\mathbf{B}$ is the $B$ field of the geometry. Using these two vectors, we can define the following transformations in the closed and open moduli,

$$\boldsymbol{\mu} \to \boldsymbol{\mu} + \mathrm{i}\pi\mathbf{c_1}, \qquad x \to x + \mathrm{i}\pi\mathbf{r}\cdot(\mathbf{B} - 2\mathbf{c_2}). \tag{5.199}$$

We can use these transformations to obtain new functions $D(X)$, $A(X)$ from the standard disk and annulus amplitudes (5.197):

$$D(X) = \widetilde{D}(X)\Big|_{\substack{\boldsymbol{\mu} \to \boldsymbol{\mu} + \mathrm{i}\pi\mathbf{c_1} \\ x \to x + \mathrm{i}\pi\mathbf{r}\cdot(\mathbf{B} - 2\mathbf{c_2})}}, \qquad A(X) = \widetilde{A}(X)\Big|_{\substack{\boldsymbol{\mu} \to \boldsymbol{\mu} + \mathrm{i}\pi\mathbf{c_1} \\ x \to x + \mathrm{i}\pi\mathbf{r}\cdot(\mathbf{B} - 2\mathbf{c_2})}}. \tag{5.200}$$

These functions depend on $\mathbf{t}_{2\pi}$ after using (5.198). The remaining ingredient is the following part of the next-to-leading term in the WKB expansion,

$$\widetilde{D}_1(X) = \sum_{\mathbf{d},\ell,s} \sum_{k=1}^{\infty} \frac{D^s_{\mathbf{d},\ell}(\frac{1}{2} - s)}{k} \mathrm{e}^{-k\mathbf{d}\cdot\mathbf{t}} (-\widehat{X})^{-k\ell}. \tag{5.201}$$

This is essentially the one-loop correction to the WKB eigenfunction. After transforming the closed and open moduli as in (5.199), we obtain the function $D_1(X)$. Let us consider $J(x,\boldsymbol{\mu},\hbar)$ for $\hbar \to 2\pi$. As we mentioned, the different ingredients composing $J(x,\boldsymbol{\mu},\hbar)$ have poles, but these cancel among each other. An explicit calculation of the finite part, using all the above ingredients, leads to the following expression

$$\begin{aligned} J(x,\boldsymbol{\mu},2\pi) = J^{\mathrm{WKB}}_{\mathrm{pert}}(x,2\pi) + \frac{\mathrm{i}}{2\pi}\left(x\frac{\partial D(X)}{\partial x} + \mathbf{t}_{2\pi}\cdot\frac{\partial D(X)}{\partial \mathbf{t}_{2\pi}} - D(X)\right) \\ - \frac{1}{2}A(X) + D_1(X) + J(\boldsymbol{\mu},2\pi). \end{aligned} \tag{5.202}$$

All the quantities appearing here can be computed explicitly in terms of geometric ingredients on the mirror curve. First of all, since the theory at the self-dual point $\hbar = 2\pi$ involves the shift of the moduli given in (5.199), we implement this transformation directly in the equation for the mirror curve. We will denote by $y(x)$ the solution corresponding to the transformed equation. At large $x$, this solution has the form $y(x) = p(x) + \tilde{y}(x)$, where $p(x)$ is a polynomial in $x$ and $\tilde{y}(x) = \mathcal{O}(\mathrm{e}^{-x})$. Let us now define the following set of differentials,

$$\omega_i = -\partial_{\kappa_i}\tilde{y}(x)\mathrm{d}x, \qquad i = 1,\cdots,g_\Sigma, \tag{5.203}$$

and the associated matrix of $A$–periods,

$$\alpha_{ij} = \oint_{\mathcal{A}_j}\omega_i. \tag{5.204}$$

By using the normalized differentials

$$\mathrm{d}\mathbf{u} = \alpha^{-1}\boldsymbol{\omega}, \tag{5.205}$$

we define the Abel–Jacobi map as

$$\mathbf{u}(X) = \int_\infty^x \mathrm{d}\mathbf{u}, \tag{5.206}$$

with the basepoint at $\infty$. A fundamental result in the open local B–model is that the disk invariants can be read from the equation of the mirror curve [54, 55]. This leads to

$$D(X) = \int_\infty^x \tilde{y}(x')\mathrm{d}x', \qquad \partial_{\mathbf{t}}D(X) = -2\pi\mathrm{i}(C^{-1})^{\mathrm{T}}\mathbf{u}(X), \tag{5.207}$$

where $C_{ij}$ is the matrix appearing in (3.61) (we have no mass parameters so no $\alpha_{ik}$). For the second line, we made use of the fact that the Kähler moduli $\mathbf{t}$ are related to the $A$–periods $\boldsymbol{\Pi}_A$ of the curve $\tilde{y}(x)$ through the matrix $C$ as $\mathbf{t}_{2\pi} = (-2\pi\mathrm{i})^{-1}C\boldsymbol{\Pi}_A$,

so that we have the relation $\alpha_{ij} = 2\pi \mathrm{i} \partial_{\kappa_i} t_{2\pi,k} C^{-1}_{jk}$. Using the above information, we can write

$$J(x, \boldsymbol{\mu}, 2\pi) = J(\boldsymbol{\mu}, 2\pi) + J^{\mathrm{WKB}}_{\mathrm{pert}}(x, 2\pi) + \frac{\mathrm{i}}{2\pi}\Sigma(x, \boldsymbol{\mu}) - \frac{1}{2}A(X) + D_1(x), \tag{5.208}$$

where

$$\Sigma(x, \boldsymbol{\mu}) = x\tilde{y}(x) - \int_\infty^x \tilde{y}(x')\mathrm{d}x' - 2\pi\mathrm{i}\mathbf{t}_{2\pi} \cdot (C^{-1})^{\mathrm{T}}\mathbf{u}(X). \tag{5.209}$$

In order to obtain the eigenfunction, we have to sum over all the shifts of $\boldsymbol{\mu}$ by $2\pi\mathrm{i}\mathbf{n}$. Since $\kappa_i = \mathrm{e}^{\mu_i}$ and $\mathbf{t}_{2\pi} = C\boldsymbol{\mu} + \boldsymbol{F}(\boldsymbol{\kappa})$, only terms with explicit factors of $\mathbf{t}_{2\pi}$ inherit the shift:

$$\mathbf{t}_{2\pi} \to \mathbf{t}_{2\pi} + 2\pi\mathrm{i}C\mathbf{n}. \tag{5.210}$$

To proceed, we have to be more explicit about the structure of the closed string contribution to the grand potential. Let us denote by $\widehat{F}_g$, $\widehat{F}^{\mathrm{NS}}_n$ the standard and NS free energies in which $\mathbf{t}_\hbar$ has been shifted by the $B$ field in the worldsheet instanton part. The resulting free energies have the following structure

$$\begin{aligned}
\widehat{F}_0 &= \frac{1}{6}\sum_{i,j,k=1}^{n_\Sigma} a_{ijk} t^i_{2\pi} t^j_{2\pi} t^k_{2\pi} + \widehat{F}^{\mathrm{inst}}_0, \\
\widehat{F}_1 &= \sum_{i=1}^{n_\Sigma} b_i t^i_{2\pi} + \widehat{F}^{\mathrm{inst}}_1, \\
\widehat{F}^{\mathrm{NS}}_1 &= \sum_{i=1}^{n_\Sigma} b^{\mathrm{NS}}_i t^i_{2\pi} + \widehat{F}^{\mathrm{NS,inst}}_1,
\end{aligned} \tag{5.211}$$

where the instanton contributions, labelled by "inst", are invariant under the shift (5.210). Also, the quantity $a_{ijk}$ is totally symmetric in its labels. The $\hbar \to 2\pi$ limit for the functions involving the closed sector have been worked out in [2, 16]. In our notations, the result is

$$\begin{aligned}
J(x, \boldsymbol{\mu} + 2\pi\mathrm{i}\mathbf{n}, 2\pi) = J(x, \boldsymbol{\mu}, 2\pi) &+ 2\mathrm{i}\pi\left(v_k + u_k(X)\right) n_k + \mathrm{i}\pi\tau_{ij} n_i n_j \\
&- \frac{\mathrm{i}\pi}{3} a_{ijk} C_{im} C_{jn} C_{kp} n_m n_n n_p,
\end{aligned} \tag{5.212}$$

where repeated indices are now summed over, and

$$\begin{aligned}
\mathbf{v} &= C^{\mathrm{T}}\left[\frac{1}{4\pi^2}\left((\partial^2_{\mathbf{t}_{2\pi}}\widehat{F}_0)\mathbf{t}_{2\pi} - \partial_{\mathbf{t}_{2\pi}}\widehat{F}_0)\right) + \mathbf{b} + \mathbf{b}^{\mathrm{NS}}\right], \\
\tau &= \frac{\mathrm{i}}{2\pi} C^{\mathrm{T}} (\partial^2_{\mathbf{t}_{2\pi}}\widehat{F}_0) C.
\end{aligned} \tag{5.213}$$

In all the examples that have been considered, the cubic term in $n$ in (5.212) could always be absorbed into constant linear and quadratic terms, thus introducing shifts

in $\mathbf{v}$ and $\tau$. We will call these shifted quantities $\hat{\mathbf{v}}$ and $\hat{\tau}$. To write down the final answer for the eigenfunction, we have to use the Riemann theta function with characteristics $\mathbf{a}$, $\mathbf{b}$:

$$\vartheta\begin{bmatrix}\mathbf{a}\\ \mathbf{b}\end{bmatrix}(\mathbf{u};\tau) = \sum_{\mathbf{n}\in\mathbb{Z}^{gW}} \mathrm{e}^{\mathrm{i}\pi(\mathbf{n}+\mathbf{b})^{\mathrm{T}}\tau\,(\mathbf{n}+\mathbf{b})+2\mathrm{i}\pi(\mathbf{u}+\mathbf{a})\cdot(\mathbf{n}+\mathbf{b})}. \tag{5.214}$$

It is an odd function when $4\mathbf{a}\cdot\mathbf{b}$ is odd. For definiteness, we call $\vartheta_{\mathrm{odd}}$ the theta function with $\mathbf{a}=\mathbf{b}=(0,\dots,0,1/2)^{\mathrm{T}}$. Its genus one version is proportional to the function $\vartheta_1(u)$ we defined in eq. (4.177):

$$\vartheta\begin{bmatrix}1/2\\ 1/2\end{bmatrix}(u;\tau) = -\vartheta_1(u;\tau). \tag{5.215}$$

The Riemann theta function with $\mathbf{a}=\mathbf{b}=0$ will be denoted simply by $\vartheta(\mathbf{u};\tau)$. The normalized $B$–periods of the (transformed) mirror curve can be written as

$$\oint_{\mathcal{B}_j} \mathrm{d}\mathbf{u} = \tau + S, \tag{5.216}$$

where $S$ is a matrix of constants. According to the theory of the B–model presented in [56, 57], the annulus amplitude $A(X)$ can be written in terms of the Bergman kernel of the mirror curve and one finds,

$$A(X) = \log\left(\frac{\vartheta_{\mathrm{odd}}(\mathbf{u}(X);\tau+S)^2}{\mathcal{C}\nabla_{\mathbf{u}}\vartheta_{\mathrm{odd}}(0;\tau+S)\cdot\mathbf{u}'(X)}\right), \tag{5.217}$$

where

$$\mathcal{C} = \lim_{X\to\infty} X^2\nabla_{\mathbf{u}}\vartheta_{\mathrm{odd}}(0;\tau+S)\cdot\mathbf{u}'(X), \tag{5.218}$$

is a $\kappa$ dependent constant, and $\mathbf{u}'(X)$ is the derivative of the Abel–Jacobi map with respect to $X$ (not $x$). This is the generalization of (5.159) for higher genus geometries. Our final expression for $\psi(x;\boldsymbol{\kappa})$ is then,

$$\begin{aligned}\psi(x;\boldsymbol{\kappa}) = \mathrm{e}^{J(\boldsymbol{\mu},2\pi)}&\sqrt{\mathcal{C}\nabla_{\mathbf{u}}\vartheta_{\mathrm{odd}}(0;\tau+S)\cdot\mathbf{u}'(X)}\\ &\times\frac{\vartheta(\mathbf{u}(X)+\hat{\mathbf{v}};\hat{\tau})}{\vartheta_{\mathrm{odd}}(\mathbf{u}(X);\tau+S)}\mathrm{e}^{J^{\mathrm{WKB}}_{\mathrm{pert}}(x,2\pi)+\frac{\mathrm{i}}{2\pi}\Sigma(x,\boldsymbol{\mu})+D_1(x)}.\end{aligned} \tag{5.219}$$

This wavefunction is very similar to a classical Baker–Akhiezer function on the mirror curve [128] (see for example [129, 130]), although there are also some important differences (for example, the term $D_1(x)$ is not part of the standard Baker–Akhiezer function).

So far we have not been explicit about the multi-covering structure of the mirror curve. When the mirror curve is hyperelliptic, so that the Riemann surface is a

two–sheeted covering of the complex plane, the wavefunction (5.219) corresponds to the contribution of the first sheet $\psi_-(x;\boldsymbol{\kappa})$, and it involves the standard open BPS invariants. The second contribution $\psi_+(x;\boldsymbol{\kappa})$ is obtained by considering the analytic continuation of (5.219) to the second sheet. Since we have been able to write down everything in terms of exact functions, this analytic continuation is now feasible. This involves a detailed analysis of the covering structure, but in the self-dual case its calculation is in principle straightforward. One intriguing aspect of this transformation is that the contribution of the second sheet seems to involve a different realization of the open string BPS invariants. We will see an illustration of this in the example of local $\mathbb{P}^2$. Let us look at some examples.

**Symmetric local** $\mathbb{P}^1 \times \mathbb{P}^1$. This is local $\mathbb{P}^1 \times \mathbb{P}^1$ with $m_{\mathbb{F}_0} = 1$. We have suppressed the mass parameter, and we have only one true modulus $\kappa$. The $B$ field is trivial. The operator eigenvalue equation is

$$(\mathsf{O}_{\mathbb{P}^1\times\mathbb{P}^1} + \kappa)|\psi\rangle = 0, \qquad \mathsf{O}_{\mathbb{P}^1\times\mathbb{P}^1} = \mathrm{e}^{\mathsf{x}} + \mathrm{e}^{-\mathsf{x}} + \mathrm{e}^{\mathsf{y}} + \mathrm{e}^{-\mathsf{y}}, \tag{5.220}$$

which, in the $x$ representation, translates into the difference equation (for $\hbar = 2\pi$):

$$(\mathrm{e}^{x} + \mathrm{e}^{-x})\psi(x) + \psi(x - \mathrm{i}\hbar) + \psi(x + \mathrm{i}\hbar) = -\kappa\psi(x). \tag{5.221}$$

The mirror curve is

$$\mathrm{e}^{x} + \mathrm{e}^{-x} + \mathrm{e}^{y} + \mathrm{e}^{-y} + \kappa = 0, \tag{5.222}$$

but we need to find the associated curve which incorporates the effect of the quantum mirror map evaluated at $\hbar = 2\pi$. By studying the resummation of the WKB eigenfunction, we find that $\mathbf{r} = 2$ in this geometry. The quantum mirror map $t(\mu, \hbar)$ has been computed in several references, see [2, 6, 74]. We find

$$\begin{aligned} t(\mu,\kappa) = 2\mu - 4\mathrm{e}^{-2\mu} - 2\left(7 + \mathrm{e}^{\mathrm{i}\hbar} + \mathrm{e}^{-\mathrm{i}\hbar}\right)\mathrm{e}^{-4\mu} \\ - 4\left(58 + 18(\mathrm{e}^{\mathrm{i}\hbar} + \mathrm{e}^{-\mathrm{i}\hbar}) + 3(\mathrm{e}^{2\mathrm{i}\hbar} + \mathrm{e}^{-2\mathrm{i}\hbar})\right)\mathrm{e}^{-6\mu} + \dots \end{aligned} \tag{5.223}$$

We conclude that $C = 2$, and that, since this is invariant under $\hbar = 0 \to \hbar = 2\pi$,

$$t_0 = t_{2\pi} \equiv t. \tag{5.224}$$

We can choose $c_1 = c_2 = 0$ in (5.199). So the curve for $\hbar = 2\pi$ is the same as (5.222). Solving for $y(x)$, we find

$$y(x) = -x \pm \mathrm{i}\pi + \tilde{y}(x), \tag{5.225}$$

with

$$\tilde{y}(x) = \log\left(X^2 + \kappa X + 1 - \sqrt{\sigma(X)}\right), \tag{5.226}$$

and

$$\sigma(X) = (X^2 + \kappa X + 1)^2 - 4X^2, \tag{5.227}$$

where as usual $X = \mathrm{e}^x$. We therefore obtain

$$\omega = -\partial_\kappa \tilde{y}(x)\mathrm{d}x = \frac{\mathrm{d}X}{\sqrt{\sigma(X)}}. \tag{5.228}$$

In the large radius regime $\kappa > 4$, the four solutions of $\sigma(X) = 0$, which are the four branch points of the Riemann surface $a_i$, satisfy

$$a_1 < a_2 < -1 < a_3 < a_4 < 0. \tag{5.229}$$

We take the $\mathcal{A}$ cycle to encircle positively $a_3$ and $a_4$, and the $\mathcal{B}$ cycle to be its dual, encircling $a_2$ and $a_3$ (it intersects only once with the $\mathcal{A}$ cycle because of the sheet structure). Using this choice of basis of cycles, corresponding to the large radius frame, we obtain

$$\oint_{\mathcal{A}} \omega = \frac{4\mathrm{i}}{\kappa}\mathrm{K}(16/\kappa^2), \qquad \oint_{\mathcal{B}} \omega = -\frac{8}{\kappa}\mathrm{K}(1 - 16/\kappa^2), \tag{5.230}$$

and so,

$$\alpha = \frac{4\mathrm{i}}{\kappa}\mathrm{K}(16/\kappa^2), \qquad u(X) = \alpha^{-1}\int_\infty^X \omega, \qquad \tau_{\mathrm{lr}} = \int_{\mathcal{B}} \mathrm{d}u = 2\mathrm{i}\frac{\mathrm{K}(1 - 16/\kappa^2)}{\mathrm{K}(16/\kappa^2)}. \tag{5.231}$$

These correspond to what we had in section 5.3. Comparing to $\partial_t^2 \widehat{F}_0$ using the well known result

$$\widehat{F}_0 = \frac{1}{6}t^3 - 4\mathrm{e}^{-t} - \frac{9}{2}\mathrm{e}^{-2t} - \frac{328}{27}\mathrm{e}^{-3t} - \frac{777}{16}\mathrm{e}^{-4} + \dots, \tag{5.232}$$

we find $S = 0$, so

$$\tau = \tau_{\mathrm{lr}} \tag{5.233}$$

We also have $b = -b^{\mathrm{NS}} = \frac{1}{12}$, from which we find

$$v = \frac{1}{4\pi\mathrm{i}}\tau t - \frac{1}{2\pi^2}\partial_t \widehat{F}_0. \tag{5.234}$$

In terms of $\kappa$, the functions $t$ and $\partial_t \widehat{F}_0$ are basically the $\kappa$ integrals of the periods (5.230) and can be written in terms of hypergeometric and Meijer $G$ functions,

$$\begin{aligned} t &= 2\log(\kappa) - \frac{4}{\kappa^2}\,{}_4F_3\left(1, 1, \frac{3}{2}, \frac{3}{2}; 2, 2, 2; \frac{16}{\kappa^2}\right) \\ &= 2\log(\kappa) - \frac{4}{\kappa^2} - \frac{18}{\kappa^4} - \frac{400}{3\kappa^6} - \frac{1225}{\kappa^8} + \mathcal{O}(\kappa^{-10}), \end{aligned} \tag{5.235}$$

and

$$\begin{aligned}\partial_t \widehat{F}_0 &= \frac{1}{\pi} G^{3,2}_{3,3}\left( \begin{array}{c} \frac{1}{2},\frac{1}{2},1 \\ 0,0,0 \end{array} \middle| \frac{16}{\kappa^2} \right) - \frac{2\pi^2}{3}, \\ &= -2\log(\kappa)^2 + 2\log(\kappa)t + \frac{4}{\kappa^2} + \frac{33}{\kappa^4} + \frac{2560}{9\kappa^6} + \frac{33635}{12\kappa^8} + +\mathcal{O}(\kappa^{-10})\end{aligned} \tag{5.236}$$

with

$$\begin{aligned}\oint_{\mathcal{A}} \omega &= \alpha = \mathrm{i}\pi\partial_\kappa t, \\ \oint_{\mathcal{B}} \omega &= -2\partial_\kappa \partial_t \widehat{F}_0.\end{aligned} \tag{5.237}$$

It can be checked that

$$\begin{aligned}\oint_{\mathcal{A}} \tilde{y}(x)\mathrm{d}x &= -\mathrm{i}\pi(t - 2\pi\mathrm{i}), \\ \oint_{\mathcal{B}} \tilde{y}(x)\mathrm{d}x &= 2\partial_t \widehat{F}_0 - \frac{2\pi^2}{3}.\end{aligned} \tag{5.238}$$

To find the shifted quantities $\hat{\tau}$ ad $\hat{v}$, we notice that the cubic term in (5.212), when exponentiated, satisfies for all integer $n$:

$$\mathrm{e}^{-\frac{8\pi\mathrm{i}}{3}n^3} = \mathrm{e}^{-\frac{2\pi\mathrm{i}}{3}n}. \tag{5.239}$$

So we have

$$\hat{v} = v - \frac{1}{3}, \qquad \hat{\tau} = \tau. \tag{5.240}$$

The quantity $\mathcal{C}$ is easily obtained

$$\mathcal{C} = -\alpha^{-1}\vartheta'_{\mathrm{odd}}(0;\tau + S), \tag{5.241}$$

so

$$\sqrt{\mathcal{C}\nabla_{\mathbf{u}}\vartheta'_{\mathrm{odd}}(0;\tau+S)\cdot\mathbf{u}'(X)} = \vartheta'_{\mathrm{odd}}(0;\tau+S)\alpha^{-1}\sigma(X)^{-1/4}. \tag{5.242}$$

To obtain the unnormalized version of the eigenfunction $\psi_-(x;\tau)$, the only thing we need is the quantities coming from the WKB part, $J^{\mathrm{WKB}}_{\mathrm{pert}}(x,2\pi)$ and $D_1(x)$. Only the leading and subleading parts of the WKB eigenfunction contribute to $J^{\mathrm{WKB}}_{\mathrm{pert}}(x,2\pi)$. From a straightforward computation, we find

$$\begin{aligned}J^{\mathrm{WKB}}_{\mathrm{pert}}(x,2\pi) &= -\frac{\mathrm{i}x^2}{4\pi}, \\ D_1(x) &= \frac{1}{4}\log\left(\frac{X^4}{\sigma(X)}\right).\end{aligned} \tag{5.243}$$

Putting everything together, we find

$$\psi_-(x;\kappa) = \mathrm{e}^{J(\mu,2\pi)}\frac{\kappa\vartheta'_1(0;\tau)}{4\mathrm{i}\mathrm{K}(16/\kappa^2)}\frac{1}{\sqrt{\sigma(X)}}\frac{\vartheta\left(u(X)+v-\frac{1}{3};\tau\right)}{\vartheta_1\left(u(X);\tau\right)}\mathrm{e}^{-\frac{\mathrm{i}}{4\pi}x^2+x+\frac{\mathrm{i}}{2\pi}\Sigma(x,\mu)}, \tag{5.244}$$

with

$$\begin{aligned}\Sigma(x,\mu) &= x\tilde{y}(x) - \int_{\infty}^{x} \tilde{y}(x')\mathrm{d}x' - \mathrm{i}\pi t\, u(X) \\ &= \int_{\infty}^{x} x'\partial_x\tilde{y}(x')\mathrm{d}x' - \mathrm{i}\pi t\, u(X)\end{aligned} \tag{5.245}$$

(the second line can be used for numerical evaluations). It is very easy to check that this satisfies the difference equation (5.221) for any $\kappa$. Indeed, for this purpose, the only important part of the expression is $\mathrm{e}^{-\frac{\mathrm{i}}{4\pi}x^2+x-\frac{\mathrm{i}}{2\pi}x\tilde{y}(x)}$. Everything else is a "quasi constant" since it only depends on $x$ through $X=\mathrm{e}^x$ and so is invariant under the shifts $x \to x \pm 2\pi\mathrm{i}$.[5] The presence of the remaining part is nevertheless crucial because it provides good analytic properties to the overall expression. For example, this expression has the monodromy invariance typical of Baker–Akhiezer functions, which means the overall combination $\psi_-(x;\kappa)$ does not depend on the path of integration used implicitly in the different functions to reach the point $x$. Indeed, going $m$ times around the $\mathcal{A}$ cycle and $n$ times around the $\mathcal{B}$ cycle, we have (using (5.238))

$$\begin{aligned} u(X) &\to u(X) + m + n\tau, \\ \frac{\mathrm{i}}{2\pi}\Sigma(x,\mu) &\to \frac{\mathrm{i}}{2\pi}\Sigma(x,\mu) + \mathrm{i}\pi(m+n) + 2\pi\mathrm{i}n\left(v-\frac{1}{3}\right). \end{aligned} \tag{5.246}$$

Using standard properties of the theta functions, we find

$$\frac{\vartheta\left(u(X)+v-\frac{1}{3};\tau\right)}{\vartheta_1\left(u(X);\tau\right)} \to \frac{\vartheta\left(u(X)+v-\frac{1}{3};\tau\right)}{\vartheta_1\left(u(X);\tau\right)}\mathrm{e}^{-\mathrm{i}\pi(m+n)-2\pi\mathrm{i}n\left(v-\frac{1}{3}\right)}. \tag{5.247}$$

So $\psi_-(x;\kappa)$ is monodromy invariant for any values of $\kappa$.

Now that we have the exact function $\psi_-(x;\kappa)$, we can find $\psi_+(x;\kappa)$ by performing the analytical continuation of all the involved functions to the second sheet of the Riemann surface. For functions which are not integrated, this is quite trivial, it is just changing the sign in front of $\sqrt{\sigma(X)}$. In particular, we have

$$\begin{aligned} \sqrt{\sigma(X)} &\to -\sqrt{\sigma(X)}, \\ \mathrm{d}u(X) &\to -\mathrm{d}u(X), \\ \tilde{y}(x) &\to -\tilde{y}(x) + 2x. \end{aligned} \tag{5.248}$$

For functions which are integrated over the Riemann surface, such as $u(X)$, we should be careful *not* to move the integration base point. Therefore, if $f(x)$ is

[5] This is also true for $\tilde{y}(x)$ in spite of the notation, as can be checked for example by looking at the large $X$ expansion of expression (5.226). The part depending polynomially on $x$ was factored out in (5.225).

a function on the Riemann surface with $f_-(X)$ its branch on the first sheet and $f_+(X)$ its branch on the second sheet, we have

$$\int_\infty^X f_-(X')\mathrm{d}X' \to \int_\infty^{a_1} f_-(X')\mathrm{d}X' + \int_{a_1}^X f_+(X')\mathrm{d}X', \tag{5.249}$$

where we choose to go through the branch cut close to the branch point $a_4$. We therefore find

$$\begin{aligned} u(X) &\to -u(X) + 2u(a_1), \\ \int_\infty^x \tilde{y}(x')\mathrm{d}x' &\to -\int_\infty^x \tilde{y}(x')\mathrm{d}x' + 2\int_\infty^{\log a_1} \tilde{y}(x')\mathrm{d}x' + x^2 - (\log a_1)^2 \\ &= -\int_\infty^x \tilde{y}(x')\mathrm{d}x' + x^2 + c(\kappa). \end{aligned} \tag{5.250}$$

The value $u(a_1)$ can be obtained by different means (for example, expand the integral around the conifold point $\kappa = 4$ and recognise the series as a multiple of the $B$–period), and we find

$$u(a_1) = -\frac{1}{8}\tau. \tag{5.251}$$

so

$$u(X) \to -u(X) - \frac{1}{4}\tau. \tag{5.252}$$

Differentiating the second line of (5.250) with respect to $\kappa$ and comparing to the first line, we find

$$c'(\kappa) = \frac{1}{2}\partial_\kappa \partial_t \widehat{F}_0 \qquad \Longrightarrow \qquad c(\kappa) = -\frac{1}{2}\partial_t \widehat{F}_0 - \frac{4\pi^2}{3}, \tag{5.253}$$

where the constant can be found by numerically evaluating the integrals. Using all these transformation rules, we find that the function $\Sigma(x,\mu)$ transforms as

$$\Sigma(x,\mu) \to -\Sigma(x,\mu) + x^2 - \pi^2\left(v - \frac{1}{3}\right) + \pi^2. \tag{5.254}$$

We see that the changing of sheets exactly involves the quantity $v - \frac{1}{3}$ which was otherwise introduced in the construction through the conjecture. We now have everything to perform the analytic continuation of $\psi_-(x,\kappa)$ to the second sheet by performing all the above substitutions, and find $\psi_+(x,\kappa)$:

$$\begin{aligned} \psi_+(x;\kappa) = \mathrm{e}^{J(\mu,2\pi)} &\frac{\kappa\vartheta_1'(0;\tau)}{4\mathrm{i}\mathrm{K}(16/\kappa^2)}(-\mathrm{i})\,\mathrm{e}^{-\frac{\mathrm{i}\pi}{2}(v-1/3)} \\ &\times \frac{1}{\sqrt{\sigma(X)}}\frac{\vartheta\left(-u(X) - \frac{\tau}{4} + v - \frac{1}{3};\tau\right)}{\vartheta_1\left(-u(X) - \frac{\tau}{4};\tau\right)}\mathrm{e}^{\frac{\mathrm{i}}{4\pi}x^2 + x - \frac{\mathrm{i}}{2\pi}\Sigma(x,\mu)}. \end{aligned} \tag{5.255}$$

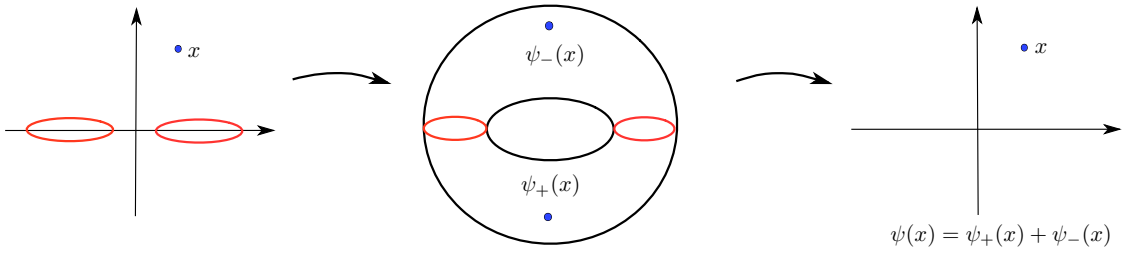


**Figure 5.4:** The eigenfunctions $\psi_\pm(x;\kappa)$ obtained with the topological string data are defined on the cut $x$ plane, and in particular they have singularities at the branchpoints. After adding the contribution of the two Riemann sheets, we obtain an entire function defined on the $x$ plane with no cuts.

Monodromy invariance of $\psi_+(x;\kappa)$ follows from that of $\psi_-(x;\kappa)$, and it also satisfies the differential equation (5.221). The sum

$$\psi_-(x,\kappa)+\psi_+(x,\kappa) \tag{5.256}$$

is the unnormalized eigenfunction corresponding to $\Xi_-(x;\kappa)$ for $\hbar = 2\pi$. This function seems to have singularities, coming for example from the $\sqrt{\sigma(X)}$ in the denominator. These are similar to the WKB turning point singularities (in fact, $1/\sqrt{\sigma(X)}$ is precisely what we would get for the WKB eigenfunction). However, the symmetric sum $\psi_-(x,\kappa)+\psi_+(x,\kappa)$ smooths out these square-root singularities. Indeed, since we are summing over the different sheets of a global function on the Riemann surface, the singularities cancel and we are left with an entire function in the $x$ plane, as sketched in Fig. 5.4.

We can now investigate our expression for the eigenfunction, and do some checks. First let us perform a numerical check against the on-shell eigenfunctions. Since $\kappa_n = -\mathrm{e}^{E_n}$, the on shell regime is $\kappa < -4$, which necessitates to analytically continue our functions to negative $\kappa$, which we do in the vicinity of $\infty$. The functions where we must be careful are those involving $\log\kappa$. Let us consistently use the branch of the log such that $\log\kappa = \log(-\kappa) + \mathrm{i}\pi$. We find that we have

$$\begin{aligned}
\tau(\kappa) &= \tau(-\kappa) - 4,\\
t(\kappa) &= t(-\kappa) + 2\pi\mathrm{i},\\
\partial_t\widehat{F}_0(\kappa) &= \partial_t\widehat{F}_0(-\kappa) + 2\pi\mathrm{i}t(-\kappa) - 2\pi^2,\\
v(\kappa) &= v(-\kappa) - 1 + \frac{1}{2}\tau(\tilde{\kappa}).
\end{aligned} \tag{5.257}$$

First of all, we see that when $x \to \infty$, the part $\psi_-(x;\kappa)$ behaves as

$$\psi_-(x;\kappa) \approx \text{const} \cdot \mathrm{e}^{-\frac{\mathrm{i}}{4\pi}x^2}\theta\left(v-\frac{1}{3};\tau\right). \tag{5.258}$$

Requiring this leading behaviour to vanish is the on-shell condition

$$\theta\left(v(\kappa)-\frac{1}{3};\tau(\kappa)\right)=0, \tag{5.259}$$

corresponding to the quantization condition

$$v(-\kappa)-\frac{1}{3}=n+\frac{1}{2}. \tag{5.260}$$

This corresponds to the result of [7], and gives the *exact* eigenvalues $\kappa_n=-\mathrm{e}^{E_n}$ of the spectral problem. The first ones are

$$\begin{aligned} E_0 &= 2.8818154299... \\ E_1 &= 4.2545915285... \\ E_2 &= 5.2881953071... \end{aligned} \tag{5.261}$$

For the $n$th level, we have the relation $v-\frac{1}{3}=n+\frac{3}{2}+\frac{\tau}{2}$. Using the relation

$$\vartheta\left(u+\frac{1}{2}+\frac{\tau}{2};\tau\right)=\mathrm{i}\mathrm{e}^{-\frac{\mathrm{i}\pi}{4}\tau-\mathrm{i}\pi u}\vartheta_1(u;\tau), \tag{5.262}$$

we find that in the expression for the on-shell eigenfunctions the theta functions collapse, and we are left with

$$\psi(x;\kappa_n)\propto\frac{\mathrm{e}^x}{\sqrt{\sigma(\mathrm{e}^x)}}\left(\mathrm{e}^{-\frac{\mathrm{i}}{4\pi}x^2+\frac{\mathrm{i}}{2\pi}\tilde{\Sigma}(x)}-\mathrm{e}^{-\frac{\mathrm{i}\pi}{2}\left(n+\frac{1}{2}\right)}\mathrm{e}^{\frac{\mathrm{i}}{4\pi}x^2-\frac{\mathrm{i}}{2\pi}\widetilde{\Sigma}(x)}\right), \tag{5.263}$$

where

$$\begin{aligned} \widetilde{\Sigma}(x) &= \Sigma(x,\mu_n)-2\pi^2u(X) \\ &= x\tilde{y}(x)-\int_\infty^x\tilde{y}(x')\mathrm{d}x'-\mathrm{i}\pi t(-\kappa_n)\,u(X). \end{aligned} \tag{5.264}$$

Expression (5.263) can be checked to be equivalent to the results of [112] for $\hbar=2\pi$, which were directly derived by studying the difference equation. In Fig. 5.5, we can see the comparison between expression (5.263) and purely numerical eigenfunctions obtained from the numerical diagonalization of the local $\mathbb{P}^1\times\mathbb{P}^1$ operator as explained in section 3.2. We can also study the off-shell eigenfunctions given by the sum of (5.244) and (5.255) for arbitrary value of $\kappa$. An example can be seen in Fig. 5.6 for $\kappa=-65$, which is not an eigenvalue of the system.

Another important check can be performed by looking at the small $\kappa$ expansion of expressions (5.244) and (5.255). We recall that the small $\kappa$ expansion of the exact

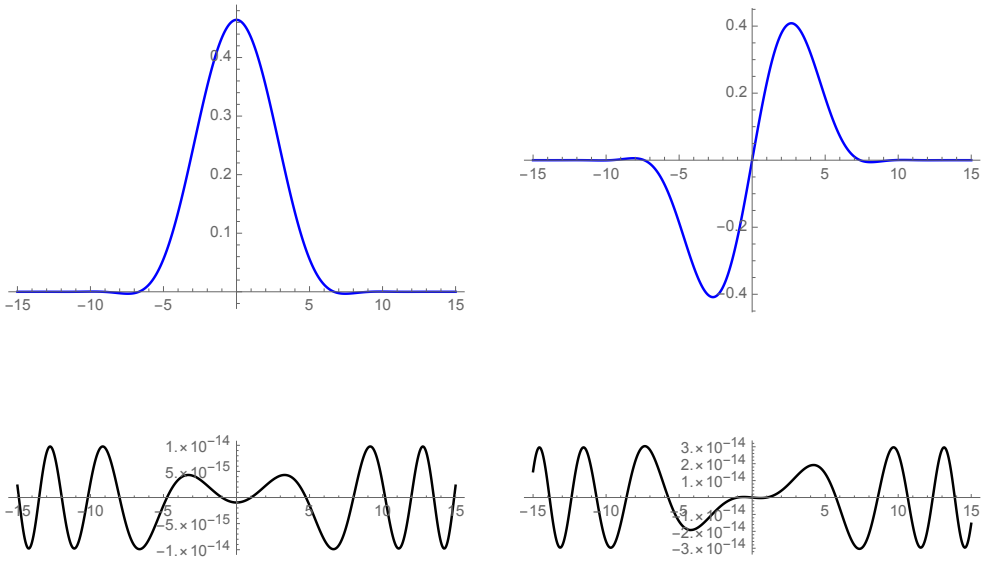


**Figure 5.5:** On-shell eigenfunctions (5.263) for $n = 0, 1$ (in blue) and difference with numerical eigenfunctions computed as in section 3.2 (in black) using a $200 \times 200$ matrix. The normalization of (5.263) is chosen such that the numerical and conjectural expressions match at $x = 1$. In this case, the on-shell functions turn out to be real. The numerical eigenfunctions have a precision which is estimated to be around $10^{-14}$ for a matrix of this size. This is precisely the difference with the conjectural exact eigenfunctions (5.263).

result (directly computed from spectral theory) was obtained in section 5.2, using the Tracy–Widom lemma. To proceed, the first thing to do is to obtain expressions for the different periods which are suited for expansions around $\kappa = 0$, also known as the orbifold point.[6] We can use results in [7, 80]. In particular, we have

$$\begin{aligned} \alpha &= \frac{4\mathrm{i}}{\kappa}\mathrm{K}(16/\kappa^2) = \mathrm{K}(1-\kappa^2/16) + \mathrm{i}\mathrm{K}(\kappa^2/16) \\ &= -\log\left(\frac{\kappa}{16\mathrm{i}}\right) - \frac{1+\log\left(\frac{\kappa}{16\mathrm{i}}\right)}{64}\kappa^2 - \frac{3(7+6\log\left(\frac{\kappa}{16\mathrm{i}}\right))}{32768}\kappa^4 + \mathcal{O}(\kappa^6), \end{aligned} \tag{5.265}$$

[6] The name comes from the fact that at this point in the moduli space, the underlying toric Calabi–Yau threefold degenerates to a geometry with an orbifold singularity.

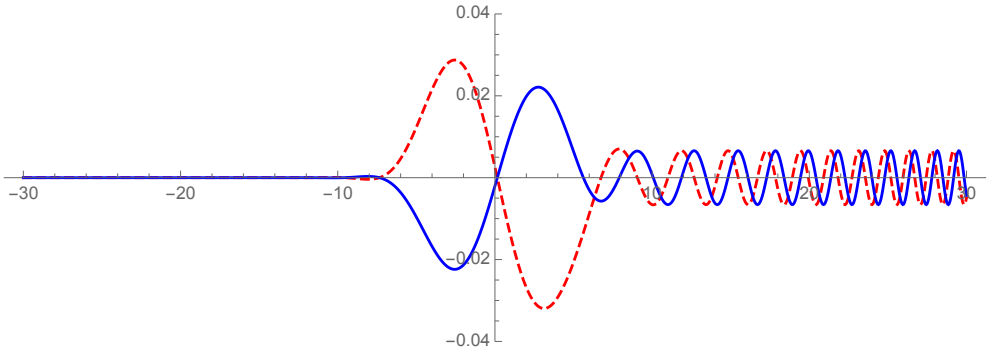


**Figure 5.6:** Off-shell eigenfunction $\psi_-(x;\kappa)+\psi_+(x;\kappa)$ for $\kappa = -65$, without the overall factor $\mathrm{e}^{J(\mu,2\pi)}$. In blue is the real part and in red dashed the imaginary part. Our value of $\kappa$ is close to the first excited state $n=1$ shown in the previous figure, with $\kappa = -\mathrm{e}^{E_1} \approx -70.428$. This off-shell eigenfunction does not decay for $x \to \infty$.

and

$$\begin{aligned} t(\kappa) &= \frac{\kappa}{2}\,{}_3F_2\left(\frac{1}{2},\frac{1}{2},\frac{1}{2};1,\frac{3}{2};\frac{\kappa^2}{16}\right) - \frac{\mathrm{i}\kappa}{4\pi^2}G^{2,3}_{3,3}\left(\begin{array}{c}\frac{1}{2},\frac{1}{2},\frac{1}{2}\\ 0,0,-\frac{1}{2}\end{array}\middle|\,\frac{\kappa^2}{16}\right) + \mathrm{i}\pi \\ &= \mathrm{i}\pi - \frac{\mathrm{i}(1-\log\left(\frac{\kappa}{16\mathrm{i}}\right))}{\pi}\kappa - \frac{\mathrm{i}(2+3\log\left(\frac{\kappa}{16\mathrm{i}}\right))}{576\pi}\kappa^3 + \mathcal{O}(\kappa^5). \end{aligned} \tag{5.266}$$

We also have

$$\begin{aligned} \partial_t \widehat{F}_0 &= \frac{\kappa}{4\pi}G^{2,3}_{3,3}\left(\begin{array}{c}\frac{1}{2},\frac{1}{2},\frac{1}{2}\\ 0,0,-\frac{1}{2}\end{array}\middle|\,\frac{\kappa^2}{16}\right) - \frac{2\pi^2}{3} \\ &= -\frac{2\pi^2}{3} + \left(1-\log\left(\frac{\kappa}{16}\right)\right)\kappa - \frac{\left(2+3\log\left(\frac{\kappa}{16}\right)\right)}{576}\kappa^3 + O(\kappa^5). \end{aligned} \tag{5.267}$$

We will also use the following modular parameter, adapted for the orbifold expansion:

$$\begin{aligned} \tau_{\mathrm{or}} &= -\frac{1}{\tau+2} \\ &= -\frac{1}{2} + \frac{\mathrm{i}\mathrm{K}(1-\kappa^2/16)}{2\mathrm{K}(\kappa^2/16)} \\ &= -\frac{\mathrm{i}}{\pi}\log\left(\frac{\kappa}{16\mathrm{i}}\right) - \frac{\mathrm{i}\kappa^2}{64\pi} - \frac{13\mathrm{i}\kappa^4}{32768\pi} + \mathcal{O}(\kappa^6). \end{aligned} \tag{5.268}$$

In order to use $\tau_{\mathrm{or}}$ as the modular parameter in the theta functions, we need to use

the Jacobi $S$–transformation formulas

$$\begin{aligned}\vartheta\left(u;-\frac{1}{\tau}\right) &= (-\mathrm{i}\tau)^{1/2}\mathrm{e}^{\mathrm{i}\pi\tau u^2}\vartheta\left(\tau u;\tau\right),\\ \vartheta_1\left(u;-\frac{1}{\tau}\right) &= -\mathrm{i}(-\mathrm{i}\tau)^{1/2}\mathrm{e}^{\mathrm{i}\pi\tau u^2}\vartheta_1\left(\tau u;\tau\right).\end{aligned} \tag{5.269}$$

We will also make use of the results of [7] (the case of local $\mathbb{P}^1\times\mathbb{P}^1$ for $\hbar=2\pi$ is the ABJ(M) case with $k=2$, $M=1$ of that reference):

$$\begin{aligned}\Xi(\kappa) &= \mathrm{e}^{J(\mu,2\pi)}\theta\left(v-\frac{1}{3};\tau\right)\\ &= 1+\frac{1}{4\pi}\kappa+\frac{(\pi^2-8)\kappa^2}{128\pi^2}+\frac{(5\pi^2-48)\kappa^3}{4608\pi^3}+\frac{(81\pi^4-848\pi^2+480)\kappa^4}{294912\pi^4}+O(\kappa^5).\end{aligned} \tag{5.270}$$

Let us define

$$\begin{aligned}u_{\mathrm{or}}(X) &= -\tau_{\mathrm{or}}u(X),\\ \Sigma_{\mathrm{or}}(x,\mu) &= x\tilde{y}(x)-\int_\infty^x\tilde{y}(x')\mathrm{d}x'-\mathrm{i}\pi u_{\mathrm{or}}(X)\left(\frac{\mathrm{i}}{\pi}t-\frac{1}{\pi^2}\partial_t\widehat{F}_0-\frac{2}{3}\right).\end{aligned} \tag{5.271}$$

The last parenthesis can actually be rewritten in terms of the orbifold frame $A$–period. Using the appropriate transformations on the theta functions (which is $ST^2$ in our case), we can write down $\psi_\pm$ in the following way:

$$\psi_-(x;\kappa)=\Xi(\kappa)\frac{\tau_{\mathrm{or}}}{\alpha}\frac{\vartheta_1'(0;\tau_{\mathrm{or}})\vartheta\left(-u_{\mathrm{or}}(X)+\tau_{\mathrm{or}}(v-\frac{1}{3});\tau_{\mathrm{or}}\right)}{\vartheta_1\left(-u_{\mathrm{or}}(X);\tau_{\mathrm{or}}\right)\vartheta\left(\tau_{\mathrm{or}}(v-\frac{1}{3});\tau_{\mathrm{or}}\right)}\frac{1}{\sqrt{X}}\mathrm{e}^{-\frac{\mathrm{i}}{4\pi}x^2+x+\frac{\mathrm{i}}{2\pi}\Sigma_{\mathrm{or}}(x,\mu)}, \tag{5.272}$$

and

$$\begin{aligned}\psi_+(x;\kappa)=\Xi(\kappa)\frac{\tau_{\mathrm{or}}}{\alpha}(-\mathrm{i})\mathrm{e}^{\mathrm{i}\pi\tau_{\mathrm{or}}(v-\frac{1}{3})}&\frac{\vartheta_1'(0;\tau_{\mathrm{or}})\vartheta\left(u_{\mathrm{or}}(X)+\frac{1}{2}\tau_{\mathrm{or}}+\frac{1}{4}+\tau_{\mathrm{or}}(v-\frac{1}{3});\tau_{\mathrm{or}}\right)}{\vartheta_1\left(u_{\mathrm{or}}(X)+\frac{1}{2}\tau_{\mathrm{or}}+\frac{1}{4};\tau_{\mathrm{or}}\right)\vartheta\left(\tau_{\mathrm{or}}(v-\frac{1}{3});\tau_{\mathrm{or}}\right)}\\ &\times\frac{1}{\sqrt{X}}\mathrm{e}^{\frac{\mathrm{i}}{4\pi}x^2+x-\frac{\mathrm{i}}{2\pi}\Sigma_{\mathrm{or}}(x,\mu)}.\end{aligned} \tag{5.273}$$

These expressions can be expanded in small $\kappa$ using the small $q$ expansions of the theta functions. It is very satisfying to see that in this expansion, we retrieve the expressions $\psi_N^\pm(x)$ obtained from spectral theory in eq. (5.83), namely

$$\begin{aligned}\psi_-(x;\kappa)+\psi_+(x;\kappa) &= \mathrm{e}^{\frac{3\pi\mathrm{i}}{4}}\sqrt{2\pi}\hat{\Xi}_+(x;\kappa)\\ &= \mathrm{e}^{\frac{3\pi\mathrm{i}}{4}}\sqrt{2\pi}\sum_{N\geq 0}\kappa^N\left(\mathrm{e}^{-\frac{\mathrm{i}}{4\pi}x^2}\psi_N^-(x)+\mathrm{e}^{\frac{\mathrm{i}}{4\pi}x^2}\psi_N^+(x)\right),\end{aligned} \tag{5.274}$$

order by order in small $\kappa$. This analytic check concludes our example of symmetric local $\mathbb{P}^1\times\mathbb{P}^1$. Let us now give evidence that the conjecture also works for other

geometries.

**Local $\mathbb{P}^2$.** Here we study the case of local $\mathbb{P}^2$ for $\hbar = 2\pi$. It is also a genus one case, and there is no mass parameter. The spectral problem is

$$(\mathsf{O}_{\mathbb{P}^2} + \kappa)\,|\psi\rangle = 0, \qquad \mathsf{O}_{\mathbb{P}^2} = \mathrm{e}^{\mathsf{x}} + \mathrm{e}^{\mathsf{y}} + \mathrm{e}^{-\mathsf{x}-\mathsf{y}}, \tag{5.275}$$

which corresponds to the difference equation

$$\mathrm{e}^{x}\psi(x) + \psi(x - \mathrm{i}\hbar) + \mathrm{e}^{-\mathrm{i}\hbar/2}\mathrm{e}^{-x}\psi(x + \mathrm{i}\hbar) = -\kappa\psi(x). \tag{5.276}$$

The mirror curve for local $\mathbb{P}^2$ is

$$\mathrm{e}^{x} + \mathrm{e}^{y} + \mathrm{e}^{-x-y} + \kappa = 0, \tag{5.277}$$

but we need to find the modified curve for $\hbar = 2\pi$ that takes into account the $B$ field and the quantum mirror map. The $B$ field is $B = 1$ in this geometry [2]. The quantum mirror map of local $\mathbb{P}^2$ can be found in [2, 74]:

$$\begin{aligned} t(\mu,\kappa) = {} & 3\mu + 3\left(\mathrm{e}^{\mathrm{i}\hbar/2} + \mathrm{e}^{-\mathrm{i}\hbar/2}\right)\mathrm{e}^{-3\mu} - 3\left(6 + \frac{7}{2}\left(\mathrm{e}^{\mathrm{i}\hbar} + \mathrm{e}^{-\mathrm{i}\hbar}\right) + 2\left(\mathrm{e}^{2\mathrm{i}\hbar} + \mathrm{e}^{-2\mathrm{i}\hbar}\right)\right)\mathrm{e}^{-6\mu} \\ & + 3\left[48\left(\mathrm{e}^{\mathrm{i}\hbar/2} + \mathrm{e}^{-\mathrm{i}\hbar/2}\right) + \frac{88}{3}\left(\mathrm{e}^{3\mathrm{i}\hbar/2} + \mathrm{e}^{-3\mathrm{i}\hbar/2}\right) + 12\left(\mathrm{e}^{5\mathrm{i}\hbar/2} + \mathrm{e}^{-5\mathrm{i}\hbar/2}\right)\right. \\ & \left. +3\left(\mathrm{e}^{7\mathrm{i}\hbar/2} + \mathrm{e}^{-7\mathrm{i}\hbar/2}\right) + \left(\mathrm{e}^{9\mathrm{i}\hbar/2} + \mathrm{e}^{-9\mathrm{i}\hbar/2}\right)\right]\mathrm{e}^{-9\mu} + \ldots, \end{aligned} \tag{5.278}$$

and we find $C = 3$, $c_1 = 1$, $c_2 = -1$. In addition, by looking at the WKB resummation, we find $r = 1/3$. The transformation (5.199) therefore becomes

$$\kappa \to -\kappa, \qquad x \to x + \mathrm{i}\pi. \tag{5.279}$$

We can now write down the ingredients appearing in (5.209). We will be a bit less detailed than in the previous example. The functions $y(x)$ and $\tilde{y}(x)$ are given by

$$\begin{aligned} y(X) &= -2x + \mathrm{i}\pi + \tilde{y}(X), \\ \tilde{y}(X) &= \log\left(\frac{-X^2 - \kappa X + \sqrt{\sigma(X)}}{2X^{-1}}\right), \end{aligned} \tag{5.280}$$

where

$$\sigma(X) = X(4 + X(X + \kappa)^2). \tag{5.281}$$

The Abel–Jacobi map is

$$u(X) = \mathcal{K}\frac{\partial}{\partial\kappa}\int_{\infty}^{X}\frac{\mathrm{d}X'}{X'}\tilde{y}(X'), \tag{5.282}$$

where

$$\begin{aligned}\mathcal{K} &= -\frac{3}{2\pi\mathrm{i}}\left(\frac{\partial t_{2\pi}(\kappa)}{\partial\kappa}\right)^{-1},\\ t_{2\pi} &= 3\log(\kappa) - \frac{6}{\kappa^3}\,{}_4F_3\left(1,1,\frac{4}{3},\frac{5}{3};2,2,2;\frac{27}{\kappa^3}\right),\\ \partial_{t_{2\pi}}\widehat{F}_0 &= \frac{1}{2\pi\sqrt{3}}G^{3,2}_{3,3}\left(\begin{array}{c}\frac{1}{3},\frac{2}{3},1\\ 0,0,0\end{array}\middle|\frac{27}{\kappa^3}\right) - \frac{5\pi^2}{18}.\end{aligned} \tag{5.283}$$

The perturbative WKB piece is given by

$$J^{\mathrm{WKB}}_{\mathrm{pert}}(x,2\pi) = -\frac{\mathrm{i}x^2}{2\pi}. \tag{5.284}$$

For the annulus amplitude, one finds

$$A(X) = -\log\left(\frac{\vartheta_1(u(X);\tau)^2}{\mathcal{K}^2\vartheta_1'(0;\tau)^2}\sqrt{\sigma(X)}\right), \tag{5.285}$$

where the elliptic modulus is given by

$$\tau = \frac{9\mathrm{i}}{2\pi}\partial^2_{t_{2\pi}}\widehat{F}_0 = \mathrm{i}\sqrt{3}\,\frac{{}_2F_1\left(\frac{1}{3},\frac{2}{3};1;1-\frac{27}{\kappa^3}\right)}{{}_2F_1\left(\frac{1}{3},\frac{2}{3};1;\frac{27}{\kappa^3}\right)}. \tag{5.286}$$

Finally, the function $D_1(X)$ is given by

$$D_1(X) = \frac{1}{4}\log\left(\frac{X^4}{\sigma(X)}\right). \tag{5.287}$$

This can be easily found by a standard WKB expansion. Using all these data, (as well as $b=\frac{1}{12}$, $b^{\mathrm{NS}}=-\frac{1}{24}$ and $a=\frac{1}{3}$) one finds

$$\psi_-(x;\kappa) = \mathrm{e}^{J(\mu,2\pi)}\mathcal{K}\vartheta_1'(0;\tau)\,\mathrm{e}^{-\frac{\mathrm{i}x^2}{2\pi}+x}\frac{\mathrm{e}^{\frac{\mathrm{i}}{2\pi}\Sigma(x)}}{\sqrt{\sigma(X)}}\frac{\vartheta(u(X)+\xi-\frac{3}{8};\tau)}{\vartheta_1(u(X);\tau)}, \tag{5.288}$$

where

$$\begin{aligned}\Sigma(x) &= x\tilde{y}(X) - \int_\infty^X \frac{\mathrm{d}X'}{X'}\tilde{y}(X') - \frac{2\pi\mathrm{i}}{3}\,t_{2\pi}u(X),\\ \xi &= \frac{3}{4\pi^2}(t_{2\pi}\partial^2_{t_{2\pi}}\widehat{F}_0 - \partial_{t_{2\pi}}\widehat{F}_0).\end{aligned} \tag{5.289}$$

The closed string grand potential $J(\mu,2\pi)$ has been calculated in [2]. The condition that $\psi_-(x;\kappa)$ decays at large $x$ is satisfied if the ratio of theta functions goes to a constant in the large $x$ limit. This gives the on-shell condition

$$\vartheta\left(\xi-\frac{3}{8};\tau\right) = 0, \tag{5.290}$$

which is precisely the quantization condition found in [2]. This condition determines a discrete set of values for $\kappa_n = -\mathrm{e}^{E_n}$, giving the spectrum of the operator $\mathsf{O}$ in (5.275) when $\hbar = 2\pi$.

To find the second part $\psi_+(x;\kappa)$ of the eigenfunction, we need to analytically continue $\psi_-(x;\kappa)$ to the second sheet of the Riemann surface. The transformation to the second sheet is similar to what was done for local $\mathbb{P}^1 \times \mathbb{P}^1$. Since we want to eventually use these results to write down the on-shell eigenfunctions, we will directly assume that $\kappa = -|\kappa| + \mathrm{i}0$, with $|\kappa| > 3$. The transformation of the Abel–Jacobi map turns out to be given by

$$u(X) \to -\frac{\tau}{3} - 1 - u(X). \tag{5.291}$$

By integrating this relation and fixing the integration constant carefully, one finds

$$\int_\infty^X \frac{\mathrm{d}X'}{X'}\tilde{y}(X') \to -\int_\infty^X \frac{\mathrm{d}X'}{X'}\tilde{y}(X') - \partial_t \widehat{F}_0 + \frac{2\pi\mathrm{i}}{3}t + \frac{3}{2}x^2 - \pi\mathrm{i}x + \frac{3\pi^2}{2}. \tag{5.292}$$

In addition, the function $\tilde{y}(x)$ changes as

$$\tilde{y}(x) \to 3x - \mathrm{i}\pi - \tilde{y}(x). \tag{5.293}$$

We can now write the eigenfunction associated to the second sheet,

$$\psi_+(x;\kappa) = \mathrm{e}^{\frac{\pi\mathrm{i}}{4}}\mathrm{e}^{J(\mu,2\pi)-\frac{2\pi\mathrm{i}}{3}\xi}\mathcal{K}\vartheta_1'(0;\tau)\,\mathrm{e}^{\frac{\mathrm{i}x^2}{4\pi}+x}\frac{\mathrm{e}^{-\frac{\mathrm{i}}{2\pi}\Sigma(x)}}{\sqrt{\sigma(X)}}\frac{\vartheta(u(X)+\xi-\frac{3}{8}+\frac{\tau}{3};\tau)}{\vartheta_1(u(X)+\frac{\tau}{3};\tau)}. \tag{5.294}$$

The total eigenfunction is the sum of (5.288) and (5.294), and it has no singularities at the turning points. In fact, it is an entire function in the complex plane.

As for the previous example, the expression for the eigenfunction simplifies considerably when one evaluates it "on-shell," i.e. for $\kappa = -\mathrm{e}^{E_n}$, $n = 0, 1, 2, \ldots$ This is due to the fact that, when $\xi$ satisfies the quantization condition (5.290), the quotients of theta functions in (5.288) and (5.294) simplify to elementary functions of $u$ and $\tau$. After some massaging, one finds a relatively simple formula for the eigenfunctions. To write this formula, let $X_0$ be the zero of $\sigma(X)$ given by

$$X_0 = \mathrm{e}^{x_0} = -\frac{2\kappa}{3} - \frac{\mathrm{e}^{-\frac{2\mathrm{i}\pi}{3}}\kappa^2}{3\nu(\kappa)^{1/3}} + \frac{\mathrm{e}^{\frac{2\mathrm{i}\pi}{3}}}{3}\nu(\kappa)^{1/3}, \tag{5.295}$$

with

$$\nu(\kappa) = 54 - \kappa^3 - 6\sqrt{3}\sqrt{27-\kappa^3}. \tag{5.296}$$

Let us also introduce the real Kähler parameter for $\kappa < 0$,

$$\tilde{t} = 3\log(-\kappa) - \frac{6}{\kappa^3}\,{}_4F_3\left(1,1,\frac{4}{3},\frac{5}{3};2,2,2;\frac{27}{\kappa^3}\right). \tag{5.297}$$

Finally, we introduce the functions

$$\varphi_n^{\pm}(x) = \exp\left[\pm\frac{\mathrm{i}}{2\pi}\int_{X_0}^X \mathrm{d}X'\left(-\frac{\log(X')(3X'+\kappa)}{2\sqrt{\sigma(X')}} - \frac{\tilde{t}}{\partial_\kappa \tilde{t}}\frac{1}{\sqrt{\sigma(X')}}\right)\right]. \tag{5.298}$$

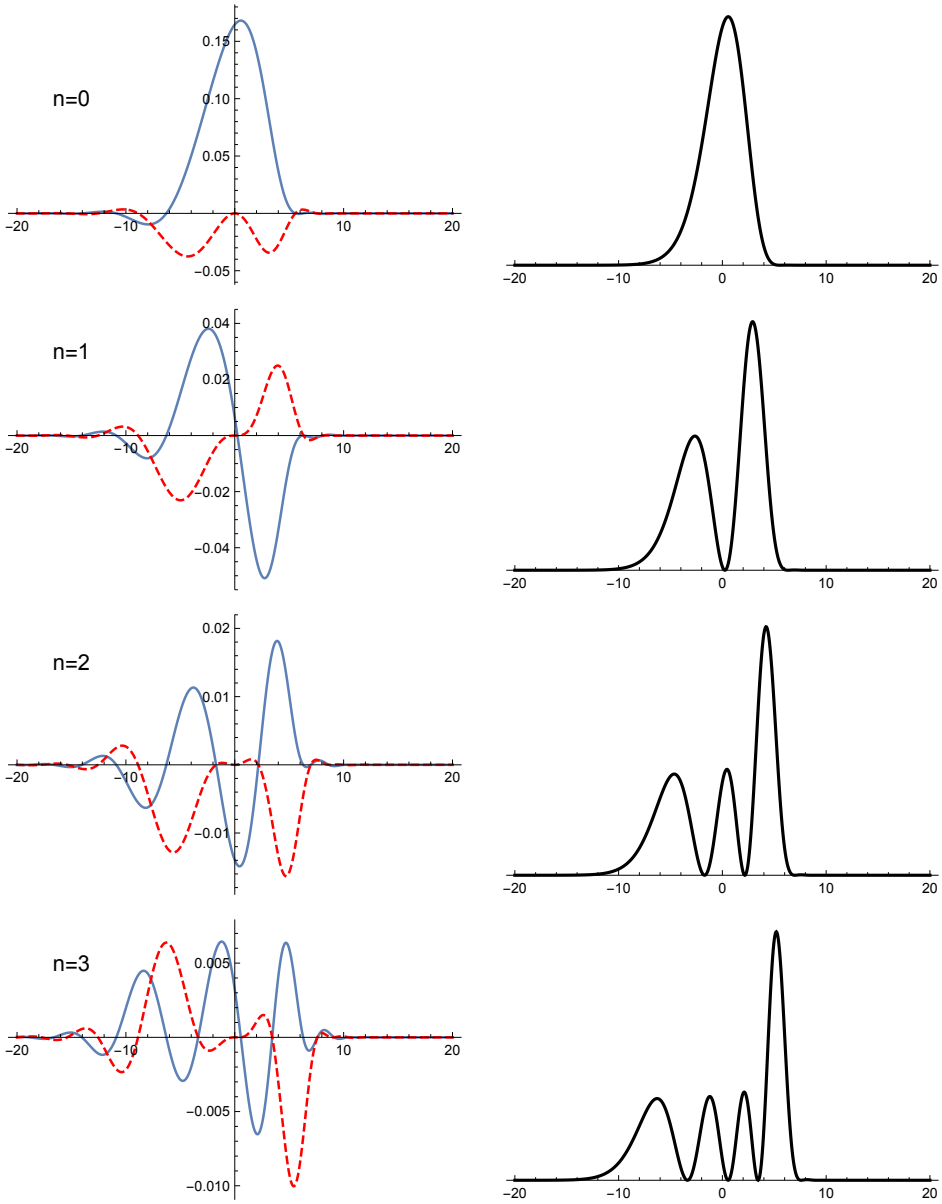


**Figure 5.7:** Evaluation of the eigenfunctions of local $\mathbb{P}^2$ and $\hbar = 2\pi$, by using the expression (5.299), for the ground state wavefunction and the first three excited states. On the left, the blue line is the real part and the red dashed line is the imaginary part. On the right we represent the square of the absolute value, showing $n+1$ peaks for the $n^{\text{th}}$ level.

It is understood that one should set $\kappa = \kappa_n$ in these equations. Then, the eigenfunctions are given by

$$\psi_n(x;\kappa_n) = \mathrm{i}\frac{\mathrm{e}^{-\frac{\mathrm{i}x^2}{8\pi}+x}}{\sqrt{\sigma(X)}}\left(\varphi_n^+(x)-\varphi_n^-(x)\right), \tag{5.299}$$

up to an overall normalization constant. This expression is very useful for explicit calculations. In Fig. 5.7 we show the resulting eigenfunctions for the very first energy levels, together with their squared absolute value. We have verified that these eigenfunctions agree with a direct calculation by using the numerical diagonalization technique of section 3.2.

As we mentioned before, the contribution from the second sheet seems to involve a different realization of the open string invariants. This is seen more clearly in the annulus amplitude of the geometry. In the first sheet, this is given by (5.285), which has the large $X$ expansion

$$\begin{aligned} A(X)_- = &\frac{Q+4Q^2+35Q^3+400Q^4+O(Q^5)}{(-\widehat{X})^2}+\frac{2Q+6Q^2+48Q^3+522Q^4+O(Q^5)}{(-\widehat{X})^3} \\ &+\frac{3Q+\frac{23}{2}Q^2+70Q^3+690Q^4+O(Q^5)}{(-\widehat{X})^4}+\mathcal{O}(\widehat{X}^{-5}), \end{aligned} \tag{5.300}$$

where $Q = \mathrm{e}^{-t_{2\pi}}$. However, after the transformation to the second sheet, implemented by (5.291), one finds the expansion

$$\begin{aligned} A(X)_+ = &-\log(-\kappa X^2)+\left(5Q+\frac{51}{2}Q^2+\frac{806}{3}Q^3+\frac{13235}{4}Q^4+O(Q^5)\right) \\ &+\frac{-2+10Q^2+128Q^3+1716Q^4+O(Q^5)}{-\widehat{X}} \\ &+\frac{1+3Q+4Q^2-7Q^3-325Q^4+O(Q^5)}{(-\widehat{X})^2} \\ &+\frac{-\frac{2}{3}-6Q-12Q^2-48Q^3-216Q^4+O(Q^5)}{(-\widehat{X})^3}+\mathcal{O}(\widehat{X}^{-4}), \end{aligned} \tag{5.301}$$

where $\hat{X} = XQ^{1/3}$. Interestingly, one can also extract integer invariants from this expression by using the multicovering formula in (5.197), and they seem to correspond to a different open BPS sector. It would be important to have a deeper understanding of this new sector, associated to the second sheet of the Riemann surface. This would provide eventually a framework to obtain the precise contribution of the second sheet in the general case.

**Resolution of $\mathbb{C}^3/\mathbb{Z}_5$.** The resolved $\mathbb{C}^3/\mathbb{Z}_5$ orbifold geometry, which has $g_W = 2$, was studied in detail in [16] from the point of view of the TS/ST correspondence.

We take this geometry as our preferred testing ground for investigating the conjecture at higher genus. This higher genus example will also allow us to comment on some aspects of quantum integrable systems, as we will see in the next chapter. Let us first recall some results from [16]. As we saw in section 3.1 eq. (3.42), there are two canonical forms for the mirror curve of this CY. The first one is

$$W_1(\mathrm{e}^{x'},\mathrm{e}^{y'}) = \mathrm{e}^{x'} + \mathrm{e}^{y'} + \mathrm{e}^{-2x'-2y'} + \kappa_2 \mathrm{e}^{-x'-y'} + \kappa_1 = 0, \tag{5.302}$$

We will call this the *symmetric parametrization*, because $x'$ and $y'$ appear symmetrically. The associated spectral problem is

$$(\mathsf{O}_1 + \kappa_1)\,\psi(x') = 0, \qquad \mathsf{O}_1 = \mathrm{e}^{\mathsf{x}'} + \mathrm{e}^{\mathsf{y}'} + \mathrm{e}^{-2\mathsf{x}'-2\mathsf{y}'} + \kappa_2 \mathrm{e}^{-\mathsf{x}'-\mathsf{y}'}. \tag{5.303}$$

In the second canonical form, the mirror curve is

$$W_2(\mathrm{e}^{x},\mathrm{e}^{y}) = \mathrm{e}^{x} + \mathrm{e}^{y} + \mathrm{e}^{-3x-y} + \kappa_1 \mathrm{e}^{-x} + \kappa_2 = 0. \tag{5.304}$$

We will call this the *hyperelliptic parametrization*, because it leads to a hyperelliptic curve in the exponentiated variables. The corresponding spectral problem is

$$(\mathsf{O}_2 + \kappa_2)\,\psi(x) = 0, \qquad \mathsf{O}_2 = \mathrm{e}^{\mathsf{x}} + \mathrm{e}^{\mathsf{y}} + \mathrm{e}^{-3\mathsf{x}-\mathsf{y}} + \kappa_1 \mathrm{e}^{-\mathsf{x}}. \tag{5.305}$$

The coordinates $x', y'$ and $x, y$ appearing in (5.302) and (5.304) are related by the following linear canonical transformation

$$\begin{pmatrix} x \\ y \end{pmatrix} = \begin{pmatrix} -1 & -1 \\ 2 & 1 \end{pmatrix} \begin{pmatrix} x' \\ y' \end{pmatrix}. \tag{5.306}$$

We will focus on the hyperelliptic parametrization, since it leads to a two-sheet covering of the complex plane where we can use the simple prescriptions of the previous section. We can always obtain the eigenfunctions in the symmetric parametrization by using (3.49).

In order to write down these eigenfunctions, we recall some basic ingredients from the special geometry of the resolved $\mathbb{C}^3/\mathbb{Z}_5$ orbifold. The toric and the web diagram of the geometry are shown in Fig. 5.8. This geometry has no mass parameters, and the Batyrev coordinates in moduli space are given by

$$z_1 = \frac{\kappa_2}{\kappa_1^3}, \qquad z_2 = \frac{\kappa_1}{\kappa_2^2}. \tag{5.307}$$

The corresponding Kähler parameters will be denoted by $t_1, t_2$ (explicit formulae for the classical and quantum mirror maps of this geometry can be found in [16]). The $C$ matrix is

$$C = \begin{pmatrix} 3 & -1 \\ -1 & 2 \end{pmatrix}. \tag{5.308}$$

The B field is given by $\mathbf{B} = (1, 0)$. We have to determine the vectors $\mathbf{r}$, $\mathbf{c_1}$ and $\mathbf{c_2}$ appearing in (5.173) and (5.198). One finds that $\mathbf{c_1} = (0, 1)$, $\mathbf{c_2} = (1, -1)$ and $\mathbf{r} = (\frac{1}{5}, \frac{3}{5})$, so (5.199) reads

$$\kappa_1 \to \kappa_1, \quad \kappa_2 \to -\kappa_2, \quad x \to x + \mathrm{i}\pi. \tag{5.309}$$

Correspondingly, the function $\tilde{y}(x)$ is given by

$$\tilde{y}(X) = \log\left(\frac{X^3 + \kappa_1 X + \kappa_2 X^2 + \sqrt{\sigma(X)}}{2X^3}\right), \tag{5.310}$$

where

$$\sigma(X) = 4X + (X^3 + \kappa_1 X + \kappa_2 X^2)^2. \tag{5.311}$$

The integral of $\tilde{y}(x)$ calculates (up to the transformation (5.309)) the generating functional of disk invariants $\widetilde{D}(X)$ in (5.197), corresponding to a toric D–brane in the external leg $III$ shown in Fig. 5.8. The Abel–Jacobi map is

$$u_i(X) = -\frac{1}{2\pi\mathrm{i}} C_{il} \left(\frac{\partial t_{2\pi}}{\partial \kappa}\right)^{-1}_{lj} \int_\infty^X \partial_{\kappa_j} \tilde{y}(X') \frac{\mathrm{d}X'}{X'}, \qquad i = 1, 2. \tag{5.312}$$

The perturbative WKB piece is

$$J^{\mathrm{WKB}}_{\mathrm{pert}}(x, 2\pi) = \frac{\mathrm{i}x^2}{4\pi}. \tag{5.313}$$

Expressions for $t_{2\pi,i}(\kappa_1, \kappa_2)$ and $\partial_{t_{2\pi,i}} \widehat{F}_0(\kappa_1, \kappa_2)$, which are periods of $\tilde{y}(x)$, can be worked out from [16]. Their large $\kappa$ expansion is

$$\begin{aligned} t_{2\pi,1} &= 3\log(\kappa_1) - \log(\kappa_2) - 6\frac{\kappa_2}{\kappa_1^3} + \frac{\kappa_1}{\kappa_2^2} - 45\frac{\kappa_2^2}{\kappa_1^4} + \frac{3}{2}\frac{\kappa_1^2}{\kappa_2^6} + \dots, \\ t_{2\pi,2} &= 2\log(\kappa_2) - \log(\kappa_1) + 2\frac{\kappa_2}{\kappa_1^3} - 2\frac{\kappa_1}{\kappa_2^2} + 15\frac{\kappa_2^2}{\kappa_1^6} - 3\frac{\kappa_1^2}{\kappa_2^4} + \dots, \end{aligned} \tag{5.314}$$

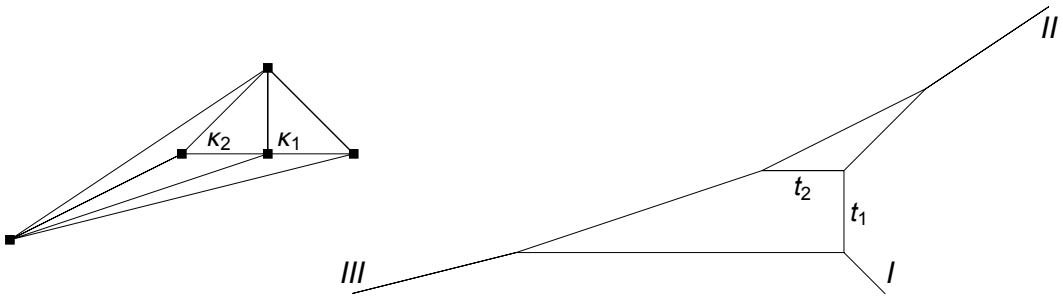


**Figure 5.8:** Toric diagram and dual web for $\mathbb{C}^3/\mathbb{Z}_5$.

and

$$\begin{aligned}\partial_{t_{2\pi,1}}\widehat{F}_0 &= \left(\frac{3}{2}\log(\kappa_1)^2 - \log(\kappa_1)\log(\kappa_2) + \log(\kappa_2)^2\right) + \frac{\kappa_1}{\kappa_2^2}(\log(\kappa_1) - 2\log(\kappa_2)) \\ &\quad + \frac{\kappa_2}{\kappa_1^3}(3 - 6\log(\kappa_1) + 2\log(\kappa_2)) - \frac{3\kappa_2^2}{4\kappa_1^6}(-47 + 60\log(\kappa_1) - 20\log(\kappa_2)) \\ &\quad + \frac{\kappa_1^2}{2\kappa_2^4}(2 + 3\log(\kappa_1) - 6\log(\kappa_2)) + \dots, \\ \partial_{t_{2\pi,2}}\widehat{F}_0 &= \frac{5}{2}\log(\kappa_2)^2 + \frac{\kappa_1}{\kappa_2^2}(2 - 5\log(\kappa_2)) + \frac{\kappa_1^2}{2\kappa_2^4}(14 - 15\log(\kappa_2)) + \dots.\end{aligned} \tag{5.315}$$

but we will usually evaluate them by performing numerical integrations over the corresponding cycles. The annulus amplitude is given by

$$A(X) = \log\left(\frac{\mathrm{e}^{-\frac{\mathrm{i}\pi}{4}}\vartheta_{\mathrm{odd}}(\mathbf{u}(X);\tau)^2\sqrt{\sigma(X)}}{\mathcal{C}'(0)\mathcal{C}(X)}\right), \tag{5.316}$$

where the $\tau$ matrix is

$$\tau_{ij} = -\frac{1}{2\pi\mathrm{i}}C_{im}C_{jn}\frac{\partial^2\widehat{F}_0}{\partial t_{2\pi,m}\partial t_{2\pi,n}}, \tag{5.317}$$

and the function $\mathcal{C}(X)$ reads

$$\mathcal{C}(X) = \frac{1}{2\pi\mathrm{i}}[\nabla_{\mathbf{u}}\vartheta_{\mathrm{odd}}(\mathbf{0})]^{\mathrm{T}}C\left(\frac{\partial t_{2\pi}}{\partial\kappa}\right)^{-1}\begin{pmatrix}1\\X\end{pmatrix}. \tag{5.318}$$

Finally, the function $D_1(X)$ is given by

$$D_1(X) = \frac{1}{4}\log\left(\frac{X^6}{\sigma(X)}\right). \tag{5.319}$$

These ingredients determine the open string grand potential. The eigenfunction (5.219) is in this case given by

$$\psi_-(x;\boldsymbol{\kappa}) = \mathrm{e}^{J(\boldsymbol{\mu},2\pi)}\sqrt{\mathcal{C}'(0)}\sqrt{\frac{\mathcal{C}(X)}{\sigma(X)}}\frac{\vartheta\begin{bmatrix}\mathbf{0}\\\mathbf{0}\end{bmatrix}(\mathbf{u}(X)+\mathbf{v}+\mathbf{s};\tau)}{\vartheta_{\mathrm{odd}}(\mathbf{u}(X);\tau)}\,\mathrm{e}^{\frac{\mathrm{i}}{4\pi}x^2+\frac{3}{2}x+\frac{\mathrm{i}}{2\pi}\Sigma(x)}, \tag{5.320}$$

and it corresponds to the first sheet of the Riemann surface. In the expression (5.320), $\mathbf{v}$ is given by

$$v_k = C_{ik}\left[\frac{1}{4\pi^2}\left(\frac{\partial^2\widehat{F}_0}{\partial t_{2\pi,i}\partial t_{2\pi,i}}t_j - \frac{\partial\widehat{F}_0}{\partial t_{2\pi,i}}\right) + b_i + b_i^{\mathrm{NS}}\right], \tag{5.321}$$

where the vectors $\mathbf{b}$, $\mathbf{b}^{\mathrm{NS}}$ are, for this geometry [16],

$$\mathbf{b} = \begin{pmatrix} 2/15 \\ 3/20 \end{pmatrix}, \qquad \mathbf{b}^{\mathrm{NS}} = \begin{pmatrix} -1/12 \\ -1/8 \end{pmatrix}, \tag{5.322}$$

and the constant shift $\mathbf{s}$ is given by

$$\mathbf{s} = \begin{pmatrix} 1/2 \\ 2/3 \end{pmatrix}. \tag{5.323}$$

The quantization condition is obtained by requiring the function (5.320) to decay at infinity. At large $X = \mathrm{e}^x$ we have that

$$\mathcal{C}(X) \approx X, \qquad \sigma(X) \approx X^6, \qquad u(X) \approx X^{-1}, \qquad \vartheta_{\mathrm{odd}}(\mathbf{u}(X);\tau) \approx X^{-1}. \tag{5.324}$$

Therefore, in order for $\psi_-(x,\boldsymbol{\kappa})$ to vanish at infinity, we need to choose $\kappa_1$ and $\kappa_2$ in such a way that

$$\vartheta \begin{bmatrix} \mathbf{0} \\ \mathbf{0} \end{bmatrix} (\mathbf{v} + \mathbf{s}; \tau) = 0. \tag{5.325}$$

For fixed $\kappa_1$, this gives a quantization condition for $-\kappa_2 = \mathrm{e}^{E_2}$. Conversely, for fixed $\kappa_2$, this gives a quantization condition for $-\kappa_1 = \mathrm{e}^{E_1}$. The quantization condition (5.325) turns out to be equivalent to the vanishing of the spectral determinant $\Xi(\kappa_1, \kappa_2; 2\pi)$, and it agrees with the quantization condition for this spectral problem found in [16].

We should now consider the part of the eigenfunction associated to the second sheet. The transformation rules require a detailed analysis of the Riemann surface defined by (5.310). One finds that the Abel–Jacobi map changes as

$$\mathbf{u}(X) \to (\tau C^{-1} + 3)\mathbf{e}_2 - \mathbf{u}(X), \qquad \mathbf{e}_2 = \begin{pmatrix} 0 \\ 1 \end{pmatrix}, \tag{5.326}$$

while the integral of $\tilde{y}(x)$ changes as

$$\begin{aligned} \int_\infty^X \tilde{y}(X') \frac{\mathrm{d}X'}{X'} \to &- \frac{19\pi^2}{6} + \partial_{t_{2\pi,2}} \widehat{F}_0 - 2\mathrm{i}\pi \left( \frac{3}{5} t_{2\pi,1} + \frac{9}{5} t_{2\pi,2} \right) - \frac{5x^2}{2} + \mathrm{i}\pi x \\ &- \int_\infty^X \tilde{y}(X') \frac{\mathrm{d}X'}{X'}. \end{aligned} \tag{5.327}$$

This is valid when $\kappa_2 < 0$. When $\kappa_2$ is interpreted as minus the eigenvalue of $\mathsf{O}_2$, we have indeed $\kappa_2 < 0$ if for example $\kappa_1 > 0$. After implementing these transformations

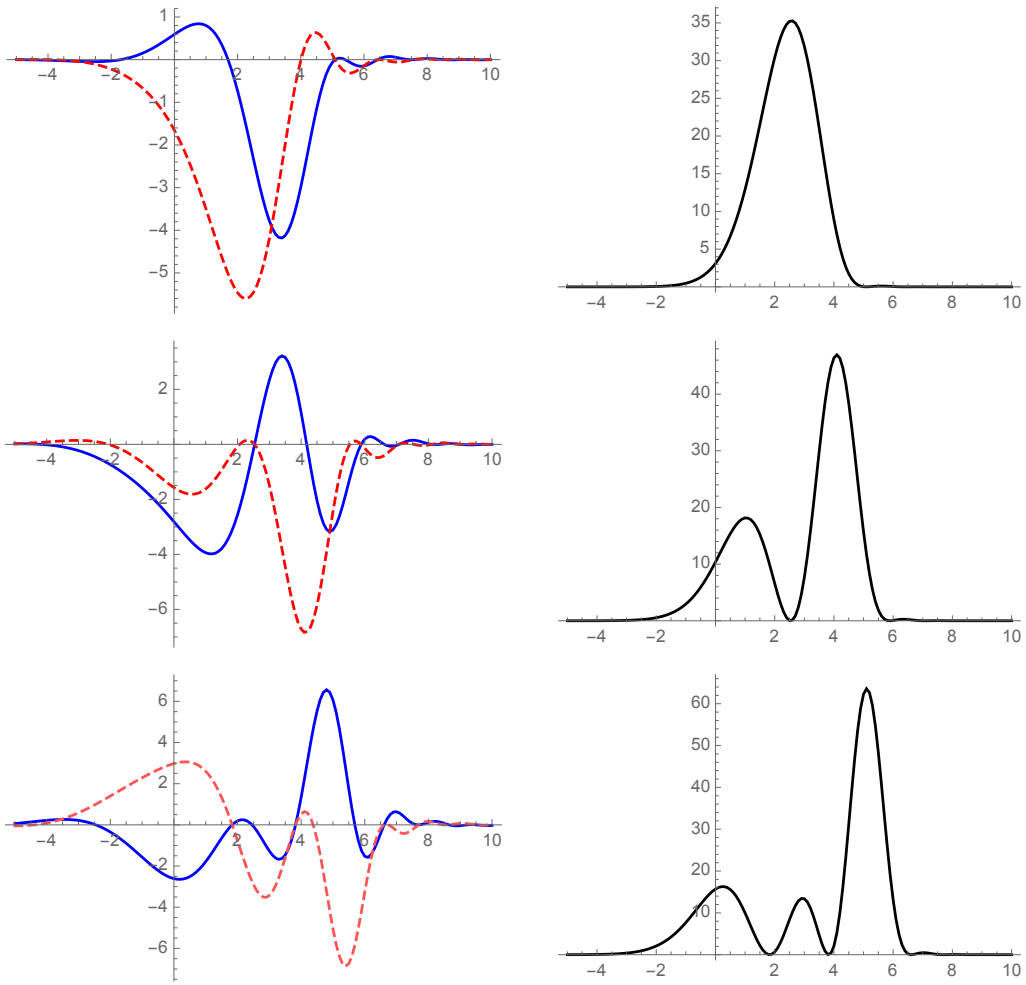

**Figure 5.9:** Exact eigenfunctions for the ground state and two first excited states, as obtained numerically from (5.329) without the overall constants. Here we set $\kappa_1 = \mathrm{e}^4$. On the left, the blue line shows the real part, while the red dashed line shows the imaginary part. The plots on the right show the squared absolute value.

in $\psi_-(x;\boldsymbol{\kappa})$, we find

$$\begin{aligned}\psi_+(x;\boldsymbol{\kappa}) = \mathrm{e}^{J(\boldsymbol{\mu})}\sqrt{\mathcal{C}'(0)}\mathrm{e}^{\frac{23}{15}\pi\mathrm{i}+2\pi\mathrm{i}\mathbf{e}_2^t C^{-1}\mathbf{v}}\sqrt{\frac{\mathcal{C}(X)}{\sigma(X)}} \\ \times \frac{\vartheta\begin{bmatrix}\mathbf{0}\\ \mathbf{0}\end{bmatrix}(\tau C^{-1}\mathbf{e}_2+\mathbf{v}+\mathbf{s}-\mathbf{u}(X);\tau)}{\vartheta_{\mathrm{odd}}(\tau C^{-1}\mathbf{e}_2-\mathbf{u}(X);\tau)}\,\mathrm{e}^{-\frac{\mathrm{i}}{\pi}x^2+\frac{3}{2}x-\frac{\mathrm{i}}{2\pi}\Sigma(x)}.\end{aligned} \tag{5.328}$$

The full eigenfunction is then the sum of (5.320) and (5.328),

$$\psi(x;\boldsymbol{\kappa}) = \psi_-(x;\boldsymbol{\kappa}) + \psi_+(x;\boldsymbol{\kappa}). \tag{5.329}$$

The resulting eigenfunction is entire on the complex plane of the $x$ variable, and it belongs to $L^2(\mathbb{R})$ when the quantization condition (5.325) is imposed. In Fig. 5.9 we show the exact eigenfunctions for the ground state and the first two excited states (we have removed the overall $x$–independent constant $\mathrm{e}^{J(\boldsymbol{\mu},2\pi)}\sqrt{\mathcal{C}'(0)}$). Note that in this case $\kappa_1$ plays the role of a parameter and we have set $\kappa_1 = \mathrm{e}^4$. We have tested these results against a direct numerical calculation of the eigenfunctions, and we have found full agreement. This is a highly non-trivial test of the conjecture in the higher genus case, where the solution involves full-fledged Riemann theta functions at genus two. Also, in contrast to the genus one cases studied above, when setting the values $\kappa_1, \kappa_2$ such that the on-shell condition (5.325) is satisfied (i.e. the eigenfunction is on-shell), the genus two theta functions do not in general collapse to simpler functions.

Once the eigenfunctions have been found in the hyperelliptic parametrization (5.304), one can use the general transformation rule (3.49) to obtain the eigenfunctions in the symmetric parametrization (5.302), i.e. for the spectral problem (5.303). In this case, the operator appearing in (3.48) is $\mathsf{P}_{12} = \mathrm{e}^{-\times}$. One also has to take into account the linear canonical transformation (5.306) relating the two variables. By implementing this transformation as a unitary operator [118], we find that the eigenfunction in (5.303) is related to the eigenfunction in (5.305) by

$$\psi\left(x'\right) = \int \mathrm{e}^{\frac{\mathrm{i}}{2\hbar}(x^2-2xx'-x'^2)-\frac{x}{2}}\psi(x)\,\mathrm{d}x, \tag{5.330}$$

up to an overall normalization constant (since our eigenfunctions are not normalized anyway, we do not keep track of these constants). When we plug in the integrand of the r.h.s. the eigenfunction (5.329) for parameter $\kappa_1$ and eigenvalue $-\kappa_2$, we obtain the eigenfunction of (5.303) with parameter $\kappa_2$ and eigenvalue $-\kappa_1$. This eigenfunction can be succesfully compared to the result of a numerical diagonalization of the operator $\mathsf{O}_1$.

## 5.6 A comment on integrability

In this section, let us make a brief detour into the world of quantum integrable systems. An integrable system in quantum mechanics can be defined as a set of $N$ commuting hamiltonian operators $\mathsf{H}_i$, and the eigenstates of the integrable system are the eigenfunctions simultaneously diagonalizing all the Hamiltonians. It has

been known for some time that many integrable systems can be solved using supersymmetric gauge theories in 4 or 5 dimensions [30]. Some of these gauge theories can be "engineered" from topological strings on toric Calabi–Yau threefolds, thus offering an effective link between topological strings and quantum integrable systems. Such a prominent example is the link between the resolution of $A_{N-1}$ singularity (topological string side) and the relativistic Toda lattice of $N$ particles, which was investigated from this point of view in [72] (the $N = 2$ case corresponds to the local $\mathbb{P}^1 \times \mathbb{P}^1$ geometry). Actually, all the toric Calabi–Yau geometries can be associated to an integrable system, through the Goncharov–Kenyon construction [131]. These are the cluster integrable systems. Their $N - 1$ quantization conditions[7] were obtained in [18] using the topological string partition function in the NS limit. These quantization conditions are built by extending the construction of [31] which can be considered as another (though related) aspect of the TS/ST correspondence. The genus $g_W$ of the mirror curve is equal to $N - 1$.

However, the TS/ST correspondence at higher genus of [16], as considered here (with its extension to the eigenfunctions), only give *one* quantization condition for the quantum mirror curve, with a codimension one space of solutions in the space of the $g_W$ "true" moduli $\kappa_i$. Therefore it gives too many solutions from the point of view of the integrable system. On the integrable system side, the quantum mirror curve turns out to correspond to the so called *quantum Baxter equation*, relevant in the solution of the integrable system in the separation of variables method (see for example [132, 133] for the case of the periodic Toda lattice). The quantum Baxter equation can usually be obtained by quantizing the spectral curve of the integrable system, whose moduli $\kappa_i$ (appearing as parameters in the curve) are related to the Hamiltonians. The philosophy of the separation of variables method is that one should look for appropriate solutions of the quantum Baxter equation, or in our language, appropriate eigenfunctions of the quantum mirror curve. By appropriate, it is meant that it should be entire and sufficiently fast decaying so that it can be used to build up the proper eigenfunctions of the integrable system through the separation of variables method. The precise condition is to be derived from the integrable system through a more detailed analysis, as done in [134–136] for the Toda lattice. So the picture we gather is the following. The eigenfunctions constructed by our conjecture are in $L^2(\mathbb{R})$ (and in the domain of $\mathsf{O}$) when a single quantization condition is satisfied: these are our on-shell eigenfunctions. It can be interpreted as the quantization of a preferred modulus $\kappa_i$ if we fix the other $\kappa_j$, $j \neq i$ to arbitrary values. However, when the other $\kappa_j$ take some specific values,

[7] One of the commuting Hamiltonians is the conserved total momentum of the system, which has continuous spectrum.

our eigenfunction should have an enhanced decay. In that case, it should become a valid solution of the quantum Baxter equation from the point of view of the integral system, and should give a solution for that associated cluster integrable system. The full set of moduli $\kappa_i$, $i = 1, ..., g_W$ which is fixed by this requirement should give the eigenvalues of the quantum Hamiltonians of the integrable system, and it should correspond to the solutions obtained from the $g_W$ quantization conditions mentioned in the previous paragraph.

Armed with the explicit results obtained in the previous section for the resolved $\mathbb{C}^3/\mathbb{Z}_5$ at $\hbar = 2\pi$, we can address how the underlying cluster integrable system manifests itself in the decaying behaviour of the eigenfunctions. First of all, we note that the eigenfunction (5.329), after imposing the on-shell condition (5.325), has the following behavior as $|x| \to \infty$:

$$\psi(x;\boldsymbol{\kappa}) \sim \begin{cases} \mathrm{e}^{-x}\left(\mathrm{e}^{\frac{\mathrm{i}}{4\pi}x^2}\mathcal{O}(1) + \mathrm{e}^{-\frac{\mathrm{i}}{\pi}x^2}\mathcal{O}(1)\right), & x \to \infty, \\ \mathrm{e}^{x}\left(\mathrm{e}^{-\frac{3\mathrm{i}}{8\pi}x^2}\mathcal{O}(1) + \mathrm{e}^{-\frac{3\mathrm{i}}{8\pi}x^2}\mathcal{O}(1)\right), & x \to -\infty. \end{cases} \tag{5.331}$$

In addition, we find that $\psi(x;\boldsymbol{\kappa})$ decays at infinity in the strip $-\frac{4\pi}{3} < \mathrm{Im}(x) < \frac{\pi}{2}$ around the real axis. The decay as $x \to \infty$ is guaranteed by the quantization condition, which can be written as

$$\vartheta \begin{bmatrix} \mathbf{0} \\ \mathbf{0} \end{bmatrix} (\mathbf{u}(\infty) + \mathbf{v} + \mathbf{s}; \tau) = 0, \tag{5.332}$$

to emphasize that this leads to an improved behavior when $X = \infty$. Due to Riemann's vanishing theorem, the genus two theta function vanishes at two points on the Riemann surface. The quantization condition (5.332) imposes that one of these points is $X = \infty$. In order to improve the decay properties of the eigenfunction at infinity, we can impose the other vanishing point to be $X = 0$, i.e. $x = -\infty$. This leads to the additional condition

$$\vartheta \begin{bmatrix} \mathbf{0} \\ \mathbf{0} \end{bmatrix} (\mathbf{u}(0) + \mathbf{v} + \mathbf{s}; \tau) = 0. \tag{5.333}$$

When this additional condition is imposed, the decay properties of the eigenfunction are enhanced to

$$\psi(x;\boldsymbol{\kappa}) \sim \begin{cases} \mathrm{e}^{-x}\left(\mathrm{e}^{\frac{\mathrm{i}}{4\pi}x^2}\mathcal{O}(1) + \mathrm{e}^{-\frac{\mathrm{i}}{\pi}x^2}\mathcal{O}(1)\right), & x \to \infty \\ \mathrm{e}^{\frac{3}{2}x}\left(\mathrm{e}^{-\frac{3\mathrm{i}}{8\pi}x^2}\mathcal{O}(1) + \mathrm{e}^{-\frac{3\mathrm{i}}{8\pi}x^2}\mathcal{O}(1)\right), & x \to -\infty \end{cases}. \tag{5.334}$$

In addition, one finds that $\psi(x)$ decays in the strip $-2\pi < \mathrm{Im}(x) < \frac{\pi}{2}$, which is larger than the strip obtained before. The on-shell condition (5.333) is equivalent to the

vanishing of the generalized Fredholm determinant (3.51) associated to the $\mathbb{C}^3/\mathbb{Z}_5$ operators $\Xi(\kappa_1, \kappa_2) = 0$. It can be verified that the condition (5.333) is equivalent to the vanishing of the rotated spectral determinant considered in [18], i.e. to the condition

$$\Xi\left(\mathrm{e}^{\frac{6\pi\mathrm{i}}{5}}\kappa_1, \mathrm{e}^{-\frac{2\pi\mathrm{i}}{5}}\kappa_2\right) = 0. \tag{5.335}$$

This can be checked directly if we use the following result for the value of the Abel–Jacobi map at the origin:

$$\mathbf{u}(0) = -\tau C^{-1}\mathbf{e}_1 + \mathbf{e}_1 - \mathbf{e}_2, \tag{5.336}$$

where $\mathbf{e}_i$ are unit vectors with 1 in the $i^{\text{th}}$ entry. Together, the two conditions (5.325), (5.333) are equivalent to the two quantization conditions proposed in [18] to determine the spectrum of the cluster integrable system associated to $\mathbb{C}^3/\mathbb{Z}_5$. This check involves the so called vector of Riemann constants $\mathbf{K}$, which is a set of constants associated to the Riemann surface in the following way. Suppose $X_i$ are the $g_W$ vanishing points of the Riemann theta function on the Riemann surface:

$$\vartheta\begin{bmatrix}\mathbf{0}\\ \mathbf{0}\end{bmatrix}(\mathbf{u}(X_i) - \mathbf{c}; \tau) = 0, \qquad\qquad i = 1, \ldots, g_w. \tag{5.337}$$

Then they satisfy

$$\sum_{i=1}^{g_W} \mathbf{u}(X_i) = \mathbf{c} - \mathbf{K}. \tag{5.338}$$

In our case, the Riemann constant can be evaluated as

$$\mathbf{K} = \begin{pmatrix} -\frac{3}{2} + \frac{2}{5}\tau_{11} - \frac{3}{10}\tau_{12} \\ \frac{1}{2} + \frac{2}{5}\tau_{12} - \frac{7}{10}\tau_{22} \end{pmatrix}, \tag{5.339}$$

and our two conditions (5.332) and (5.333) are then equivalent to

$$\mathbf{u}(0) = \mathbf{v} + \mathbf{s} - \mathbf{K}, \tag{5.340}$$

where we used $\mathbf{u}(\infty) = 0$. Now that we have explicit quantization conditions, we can go "fully on-shell"[8] and plug this value for $\mathbf{v}+\mathbf{s}$ in the expressions of the eigenfunction $\psi_-(x;\boldsymbol{\kappa}) + \psi_+(x;\boldsymbol{\kappa})$. The outcome is that, this time, the theta functions collapse to simpler functions.

Let us go back to the discussion of the decay of the eigenfunction. There is a simple WKB argument which relates the quantization conditions of the cluster integrable system to the decay behaviour of the eigenfunctions of the Baxter operator

[8] on-shell from the point of view of the integrable system

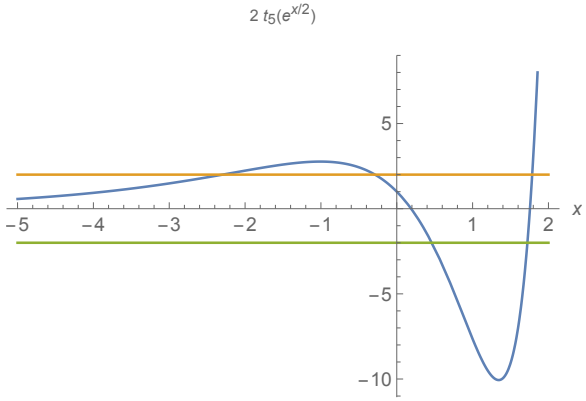


**Figure 5.10:** The function $2t_5\left(\mathrm{e}^{\mathsf{x}/2}\right)$ as a function of $x$ and $\kappa_1 = -\kappa_2 = 7$, showing the two "intervals of instability" where $|t_5(\mathrm{e}^{x/2})| \geq 1$.

(this is based on a similar argument in [133] for the Toda lattice). We first note that, as pointed out in [18], under the symplectic linear transformation,

$$\mathsf{y} \to \mathsf{p} = \mathsf{y} + \frac{3}{2}\mathsf{x}, \qquad \mathsf{x} \to \mathsf{x}, \tag{5.341}$$

the operator associated to the hyperelliptic parametrization (5.304) becomes

$$\mathsf{O}_2 + \kappa_2 = \mathrm{e}^{-\frac{3\mathsf{x}}{4}}\,\mathsf{B}\,\mathrm{e}^{-\frac{3\mathsf{x}}{4}}, \tag{5.342}$$

where the Baxter operator $\mathsf{B}$ is given by

$$\mathsf{B} = \mathrm{e}^{\mathsf{p}} + \mathrm{e}^{-\mathsf{p}} + 2t_5(\mathrm{e}^{\mathsf{x}/2}) \tag{5.343}$$

and

$$2t_5(z) = z^5 + \kappa_2 z^3 + \kappa_1 z. \tag{5.344}$$

A function $Q(x)$ annihilated by the Baxter operator satisfies,

$$Q(x + \mathrm{i}\hbar) + Q(x - \mathrm{i}\hbar) + 2t_5(\mathrm{e}^{\mathsf{x}/2})Q(x) = 0, \tag{5.345}$$

and the eigenfunctions of the operator $\mathsf{O}_2$ are related to $Q(x)$ by

$$\psi(x;\boldsymbol{\kappa}) = \mathrm{e}^{\frac{3}{4}x}Q(x). \tag{5.346}$$

The WKB solution for $Q(x)$ is exactly of the form found in [133],

$$Q(x) \approx \frac{1}{\sqrt{\sinh S_0'(x)}}\mathrm{e}^{-\frac{\mathrm{i}}{\hbar}\int^x S_0'(u)\mathrm{d}u - \frac{\pi}{\hbar}x}, \tag{5.347}$$

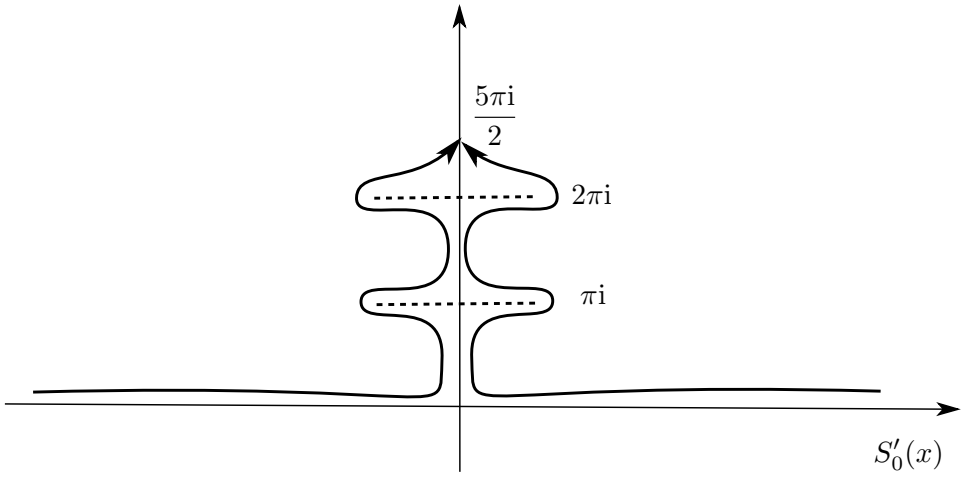


**Figure 5.11:** The map $S_0'(x)$ as we go from $x \to \infty$ to $x \to -\infty$ above the real axis (line on the right) and below the real axis (line on the left).

where the function $S_0(x)$ is determined by

$$\cosh S_0'(x) = t_5(\mathrm{e}^{x/2}). \tag{5.348}$$

Let us study the behaviour of this WKB solution as $x \to \infty$. Since

$$2\cosh S_0'(x) \approx \mathrm{e}^{5x/2}, \tag{5.349}$$

we have

$$Q(x) \approx \mathrm{e}^{-\frac{\pi}{\hbar}x - \frac{5}{4}x}, \qquad x \to \infty \tag{5.350}$$

(we did not write the oscillatory behaviour coming from $S_0(x)$). As $x \to -\infty$, we have $t_5(\mathrm{e}^{x/2}) \to 0$, and we cross two "intervals of instability," as shown in Fig. 5.10. Between these intervals, $|t_5(\mathrm{e}^{x/2})| \leq 1$ and $S_0'(x)$ must be imaginary. We can choose $S_0'(x)$ as shown in Fig. 5.11, so that

$$S_0'(x) \approx \frac{5\pi\mathrm{i}}{2}, \qquad x \to -\infty, \tag{5.351}$$

provided it satisfies the quantization conditions

$$\oint_{C_k} S_0'(u) = 2\pi\hbar n_k, \qquad k = 1, 2, \tag{5.352}$$

where $n_1$, $n_2$ are integers. If this is the case, $Q(x)$ behaves as

$$Q(x) \approx \mathrm{e}^{\frac{3\pi}{2\hbar}x}, \qquad x \to -\infty. \tag{5.353}$$

This decay analysis was performed in the WKB ansatz in the small $\hbar$ limit, but it is valid also at finite $\hbar$. Indeed, it is easy to verify from (5.350), (5.353) and (5.346) that the function $\psi(x;\boldsymbol{\kappa})$ for $\hbar = 2\pi$ will have precisely the asymptotic behavior given in (5.334). The quantization conditions (5.352) give the leading WKB approximation to the exact quantization conditions proposed in [18].

Our main conclusion is that, at least in this example, the quantization conditions of the cluster integrable system are conditions for an enhanced decay at infinity of the eigenfunctions of the Baxter equation. This gives a physical interpretation to the observation made in [18], where it was noted that the spectrum of the cluster integrable system is recovered when the additional condition (5.335) is imposed. It would be interesting to see whether the "rotated" spectral determinants introduced in [85], by generalizing the observation in [18], can be also related to the behavior of the eigenfunctions at infinity.

Of course, in order to have a complete picture of the relationship between the two spectral problems, one should find an explicit relationship between the eigenfunctions of the quantum mirror curve and the eigenfunctions of the cluster integrable system itself, as it was done in [136] for the Toda lattice. The enhanced decay properties that we have found should arise as necessary conditions for the square integrability of the eigenfunctions of the cluster integrable system.

## 5.7 Partial checks away from the self-dual case

So far, our tests of the extended TS/ST conjecture for the eigenfunctions have been done in the self-dual case. There is a good reason for this: when $\hbar = 2\pi$, one can write the functions $\psi_{\mp}(x;\boldsymbol{\kappa})$ in closed form, and in particular one can implement the transformation to the second sheet in complete detail, as we did in the previous examples. However, our conjecture can also be used to obtain information about the exact eigenfunction for general values of $\hbar$.

In order to do this, it is useful to review some relevant aspects of the closed string case. For general $\hbar$, the total grand potential $J(\boldsymbol{\mu},\hbar)$ in (3.65) can be computed as power series in $\mathrm{e}^{-\mathsf{t}}$, by using the information on the BPS invariants of the toric CY threefold $X$. From this, one can in principle compute the corresponding expansion of the spectral determinant. This was done in some genus one geometries in section 3.2 of [2]. It is however easier to calculate the spectral determinant by considering the so-called fermionic spectral traces $Z(\boldsymbol{N};\hbar)$ of the operators, as done in section 4.2 for the genus one case. We recall that these are defined by the coefficients in the

expansion of the spectral determinant around the origin,

$$\Xi(\boldsymbol{\kappa};\hbar) = \sum_{N_1\geq 0} \cdots \sum_{N_{g_W}\geq 0} Z(\boldsymbol{N};\hbar)\kappa_1^{N_1}\cdots\kappa_{g_W}^{N_{g_W}}. \tag{5.354}$$

This expansion can be inverted to

$$Z(\boldsymbol{N};\hbar) = \frac{1}{(2\pi\mathrm{i})^{g_W}} \int_{-\mathrm{i}\infty}^{\mathrm{i}\infty} \mathrm{d}\mu_1 \cdots \int_{-\mathrm{i}\infty}^{\mathrm{i}\infty} \mathrm{d}\mu_{g_W}\, \exp\left\{ J(\boldsymbol{\mu},\hbar) - \sum_{i=1}^{g_W} N_i\mu_i \right\}. \tag{5.355}$$

The contour integrations along the imaginary axes can be deformed to contours where the integral is convergent. For example, in the genus one case, the integration contour is the one defining the Airy function, as in section 4.2. It turns out that the large radius expansion of $J(\boldsymbol{\mu},\hbar)$ leads to a convergent series expansion for the spectral traces, which can be evaluated numerically to high precision. This provides very non-trivial tests of the TS/ST conjecture, as for example in [2, 16, 82, 83].

What is the analogue of this procedure in the open string case? The eigenfunctions are conjecturally obtained through (5.188) and (5.189). The open string analogue of the fermionic spectral traces is simply obtained by expanding each of the eigenfunctions in (5.189):

$$\psi_\sigma(x;\boldsymbol{\kappa}) = \sum_{N_1\geq 0} \cdots \sum_{N_{g_W}\geq 0} \psi_{\boldsymbol{N},\sigma}(x)\kappa_1^{N_1}\cdots\kappa_{g_W}^{N_{g_W}}. \tag{5.356}$$

The analogue of the integral formula (5.355) is

$$\psi_{\boldsymbol{N},\sigma}(x) = \int_{-\mathrm{i}\infty}^{\mathrm{i}\infty} \frac{\mathrm{d}\mu_1}{2\pi\mathrm{i}} \cdots \int_{-\mathrm{i}\infty}^{\mathrm{i}\infty} \frac{\mathrm{d}\mu_{g_W}}{2\pi\mathrm{i}}\, \exp\left\{ J_\sigma(x,\boldsymbol{\mu},\hbar) - \sum_{i=1}^{g_W} N_i\mu_i \right\}. \tag{5.357}$$

Note that the expansion in (5.356) requires that $\kappa$ takes arbitrary values. As we mentioned above, we refer to these as "off-shell" eigenfunctions. In section 5.1 we showed how to obtain these eigenfunctions by factorizing in an appropriate way the resolvent of the corresponding trace class operator. We performed this explicitly for symmetric local $\mathbb{P}^1\times\mathbb{P}^1$ for $\hbar = 2\pi$ in section 5.2, but it can be generalized for any $\hbar$ of the form $2\pi\times$rational. In this way, one can compute the functions $\psi_{\boldsymbol{N},\sigma}(x)$ directly in spectral theory, and for separate $\sigma$. On the other hand, the function $J_-(x,\boldsymbol{\mu},\hbar)$ can be computed as a power series expansion at large radius and large open modulus $X\to\infty$, for any finite $\hbar$. By using this expansion, and integrating, one finds an expansion of $\psi_{\boldsymbol{N},-}(x)$ at fixed $N$ and large $X$, where each coefficient can be computed numerically to high precision. This result can be then compared with the results for the off-shell eigenfunctions.

In the case of $\psi_{\boldsymbol{N},+}(x)$, the calculation is more involved, since the transformation required to go to the second sheet cannot be implemented order by order in $1/X$.

Indeed, the large $X$ expansions have different structures in different sheets, as we saw for example for the annulus amplitude in local $\mathbb{P}^2$. For this reason, we will restrict ourselves to tests of $\psi_{\boldsymbol{N},-}(x)$.

Let us go back to our favourite example, symmetric local $\mathbb{P}^1 \times \mathbb{P}^1$ (with mass set to 1), and recall a few facts already stated. The mirror curve is given by

$$\mathrm{e}^{x} + \mathrm{e}^{-x} + \mathrm{e}^{y} + \mathrm{e}^{-y} + \kappa = 0. \tag{5.358}$$

The mass parameter is set to one, so that effectively we have a single Kähler parameter $t$. We will denote

$$Q = \mathrm{e}^{-t}. \tag{5.359}$$

The spectral problem to be solved is,

$$(\mathsf{O} + \kappa)\psi(x) = 0, \qquad \mathsf{O} = \mathrm{e}^{\mathsf{x}} + \mathrm{e}^{-\mathsf{x}} + \mathrm{e}^{\mathsf{y}} + \mathrm{e}^{-\mathsf{y}}. \tag{5.360}$$

One finds that

$$\widehat{X} = Q^{1/2} X, \tag{5.361}$$

and the $B$ field is in this case zero. In order to calculate $J_-(x, \mu, \hbar)$ for this geometry, we first determine the WKB piece. There are two possible methods for this. The simplest one is to solve the difference equation (5.360) in a WKB expansion, order by order in $\hbar$, i.e. to calculate the functions $S_n^{\mathrm{WKB}}(x)$ appearing in (5.171). Then, one has to resum them in the form prescribed by (5.174). Another strategy consists in solving the difference equation exactly in $\hbar$, but order by order in $1/X$, akin to what was done originally in this example in [74]. This method will be described in more details in the next section. Either way we obtain:

$$\begin{aligned} J^{\mathrm{WKB}}_{\mathrm{open}}(x, \mu, \hbar) &= J^{\mathrm{WKB}}_{\mathrm{pert}}(x, \hbar) \\ &+ \left( -\frac{q}{q-1} - \frac{2qQ_\hbar}{q-1} + \frac{\left(q^2+q+1\right) Q_\hbar^2}{1-q} \right. \\ &\qquad \left. - \frac{2\left(q^4+q^3+q^2+q+1\right) Q_\hbar^3}{(q-1)q} + \mathcal{O}\left(Q_\hbar^4\right) \right) \frac{1}{\widehat{X}} \\ &+ \left( \frac{q^2}{2\left(q^2-1\right)} + \frac{q^2 Q_\hbar}{q-1} + \frac{q\left(q^2+3q+1\right) Q_\hbar^2}{q^2-1} \right. \\ &\qquad \left. + \frac{2\left(q^3+q^2+q+1\right) Q_\hbar^3}{q-1} + \mathcal{O}\left(Q_\hbar^4\right) \right) \frac{1}{\widehat{X}^2} \\ &+ \mathcal{O}\left(\widehat{X}^{-3}\right), \end{aligned} \tag{5.362}$$

where

$$q = \mathrm{e}^{\mathrm{i}\hbar}, \qquad Q_\hbar = \mathrm{e}^{-t_\hbar}, \tag{5.363}$$

and

$$J^{\rm WKB}_{\rm pert}(x,\hbar) = -\frac{\mathrm{i}}{2\hbar}x^2 + \frac{1}{2}\left(\frac{2\pi}{\hbar} - 1\right)x. \tag{5.364}$$

The calculation of $J^{\rm WS}_{\rm open}(x,\mu,\hbar)$ is even simpler, since we can use the topological vertex [48] to resum the expansion in $\hbar_{\rm D}$. We find,

$$\begin{aligned}\log\,\psi_{\rm top}\left(X,t,\hbar_{\rm D}\right) = &\left(\frac{\sqrt{q_{\rm D}}}{q_{\rm D}-1} + \frac{2\sqrt{q_{\rm D}}Q}{q_{\rm D}-1} + \frac{3\sqrt{q_{\rm D}}Q^2}{q_{\rm D}-1} + \frac{10\sqrt{q_{\rm D}}Q^3}{q_{\rm D}-1} + \mathcal{O}\left(Q^4\right)\right)\frac{1}{X}\\ &+\left(\frac{q_{\rm D}}{2\left(q_{\rm D}^2-1\right)} + \frac{q_{\rm D}Q}{q_{\rm D}-1} + \frac{q_{\rm D}(2q_{\rm D}+3)Q^2}{q_{\rm D}^2-1} + \frac{8q_{\rm D}Q^3}{q_{\rm D}-1} + \mathcal{O}\left(Q^4\right)\right)\frac{1}{X^2}\\ &+\mathcal{O}(X^{-3}),\end{aligned} \tag{5.365}$$

where

$$q_{\rm D} = \mathrm{e}^{\mathrm{i}\hbar_{\rm D}} = \mathrm{e}^{\frac{4\pi^2\mathrm{i}}{\hbar}}. \tag{5.366}$$

These expansions can be used to calculate the open grand potential for arbitrary values of $\hbar$. The expression (5.357) becomes, in this genus one example,

$$\psi_{-,N}(x) = \int_{\mathcal{C}}\frac{\mathrm{d}\mu}{2\pi\mathrm{i}}\,\mathrm{e}^{J(\mu,X,\hbar)-N\mu}, \tag{5.367}$$

where $\mathcal{C}$ is the integration contour for the Airy function. The closed string grand potential has the structure,

$$J(\mu,\hbar) = \frac{C(\hbar)}{3}\mu^3 + B(\hbar)\mu + A(\hbar) + \mathcal{O}\left(\mathrm{e}^{-\mu}\right), \tag{5.368}$$

where $A(\hbar)$, $B(\hbar)$, $C(\hbar)$ are constants related to $A, a, b, b^{\rm NS}$ and $C$ used in section 3.3. We can then write the integrand in the l.h.s. of (5.367) as a double expansion at large $\mu$ and $X$,

$$\mathrm{e}^{J(\mu,X,\hbar)-N\mu} = \mathrm{e}^{\frac{C(\hbar)}{3}\mu^3-(-B(\hbar)+N)\mu+A(\hbar)+J^{\rm WKB}_{\rm pert}(x,\hbar)}\sum_{\alpha,\beta}\frac{x^\beta}{X^\alpha}\sum_{n,\ell}c^{(\alpha,\beta)}_{\ell,n}(\hbar)\mathrm{e}^{-n\mu}\mu^\ell. \tag{5.369}$$

We obtain,

$$\psi_{-,N}(x) = \mathrm{e}^{J^{\rm WKB}_{\rm pert}(x,\hbar)}\sum_{\alpha,\beta}f_{\alpha,\beta}(N,\hbar)\frac{x^\beta}{X^\alpha}, \tag{5.370}$$

where the numerical coefficients $f_{\alpha,\beta}(N,\hbar)$ are given by a (convergent) sum of Airy functions,

$$f_{\alpha,\beta}(N,\hbar) = \mathrm{e}^{A(\hbar)}C^{-1/3}(\hbar)\sum_{n,\ell}c^{(\alpha,\beta)}_{\ell,n}(\hbar)\left(-\frac{\partial}{\partial N}\right)^\ell \mathrm{Ai}\left(\frac{N-B(\hbar)+n}{C^{1/3}(\hbar)}\right). \tag{5.371}$$

This is the prediction of our conjecture for the values of the eigenfunction $\psi_{-,N}(x)$, in terms of open and closed BPS invariants of the geometry (which are encoded in the coefficients $c_{\ell,n}^{(\alpha,\beta)}(\hbar)$).

To illustrate these predictions even more concretely, let us consider the value $\hbar = 4\pi$, which is particularly useful for a comparison with the results of spectral theory. One finds the following double expansion of the open string grand potential, at large $\mu$ and large $X$:

$$\begin{aligned} J(x,\mu,4\pi) = J(\mu,4\pi) - \frac{\mathrm{i}}{8\pi}x^2 - \frac{x}{4} \\ - \left\{ \frac{\mathrm{i}}{2}\mathrm{e}^{\mu/2} + \mathrm{i}\mathrm{e}^{-\mu/2} + \mathrm{i}\mathrm{e}^{-3\mu/2} + 6\mathrm{i}\mathrm{e}^{-5\mu/2} + \mathcal{O}\left(\mathrm{e}^{-7\mu/2}\right) \right\} \frac{1}{\sqrt{X}} \\ + \left\{ \left( -\frac{\mathrm{i}x}{4\pi} + \frac{\mathrm{i}\mu}{4\pi} - \frac{\mathrm{i}}{4\pi} - \frac{1}{2} \right) \mathrm{e}^{\mu} + \frac{1}{2} + \left( -\frac{\mathrm{i}\mu}{\pi} - \frac{\mathrm{i}}{2\pi} + 1 \right) \mathrm{e}^{-\mu} + 4\mathrm{e}^{-2\mu} \right. \\ \left. + \left( -\frac{5\mathrm{i}\mu}{\pi} - \frac{\mathrm{i}}{4\pi} + 12 \right) \mathrm{e}^{-3\mu} + \mathcal{O}\left(\mathrm{e}^{-4\mu}\right) \right\} \frac{1}{X} + \mathcal{O}\left(X^{-3/2}\right). \end{aligned} \tag{5.372}$$

The closed string grand potential is

$$J(\mu,4\pi) = \frac{\mu^3}{6\pi^2} - \frac{\mu}{4} + A(4\pi) - \mathrm{e}^{-\mu} + \left( -\frac{2\mu^2}{\pi^2} - \frac{\mu}{\pi^2} - \frac{1}{2\pi^2} \right) \mathrm{e}^{-2\mu} - \frac{16}{3}\mathrm{e}^{-3\mu} + \mathcal{O}\left(\mathrm{e}^{-4\mu}\right). \tag{5.373}$$

In spectral theory, the function $\psi_{-,N}(x)$ for $\hbar = 4\pi$ can be computed exactly as it was done in section 5.2 in the self-dual case. The only difference is the form of the integral kernel $\rho(q_1, q_2)$. Since the value of $\hbar$ is a rational number times $2\pi$, the Faddeev quantum dilogarithm functions collapse to rational functions of the exponentiated variable, and we find

$$\rho(q_1,q_2) = \frac{\sqrt{v(q_1)}\sqrt{v(q_2)}}{2\cosh\frac{q_1-q_2}{2\xi}}, \tag{5.374}$$

with

$$\sqrt{v(q)} = \frac{1}{2^{5/4}\pi^{1/2}\left(\cosh\left(\frac{q}{2\sqrt{2}}\right) + \sqrt{2}\right)}, \qquad \xi = 2\sqrt{2}. \tag{5.375}$$

After performing the integral transformation to go to mirror curve variable $x$, one finds, for $N = 0$, the following expression:

$$\begin{aligned} \psi_{-,0}(x) &= \mathrm{e}^{-\frac{\mathrm{i}x^2}{8\pi} - \frac{x}{4}} \frac{\mathrm{e}^{\frac{5\mathrm{i}\pi}{16}}\mathrm{e}^{x}\left(-\mathrm{i}\sqrt{2}\mathrm{e}^{x/2} + \mathrm{e}^{x} - \mathrm{i}\right)}{2\sqrt{\pi}\left(\mathrm{e}^{2x} - 1\right)} \\ &= \mathrm{e}^{J^{\mathrm{WKB}}_{\mathrm{pert}}(x,\hbar)} \frac{\mathrm{e}^{\frac{5\mathrm{i}\pi}{16}}}{2\sqrt{\pi}} \left(1 - \mathrm{i}\sqrt{2}X^{-1/2} - \mathrm{i}X^{-1} + X^{-2} + \ldots\right). \end{aligned} \tag{5.376}$$

For $N = 1$ and $N = 2$, the exact expressions are somewhat long, but their expansion reads,

$$\begin{aligned}\psi_{-,1}(x) &= \mathrm{e}^{J^{\mathrm{WKB}}_{\mathrm{pert}}(x,\hbar)}\frac{\mathrm{e}^{\frac{5\mathrm{i}\pi}{16}}}{2\sqrt{\pi}}\left(\frac{4-\pi}{16\pi}-\frac{\mathrm{i}}{8\sqrt{2}}\sqrt{2}X^{-1/2}\right.\\ &\qquad\left.+\frac{\mathrm{i}(-4x+(1+10\mathrm{i})\pi+4)}{16\pi}X^{-1}+\dots\right),\\ \psi_{-,2}(x) &= \mathrm{e}^{J^{\mathrm{WKB}}_{\mathrm{pert}}(x,\hbar)}\frac{\mathrm{e}^{\frac{5\mathrm{i}\pi}{16}}}{2\sqrt{\pi}}\left(\frac{5\pi^2-8\pi-24}{512\pi^2}-\frac{\mathrm{i}(\pi^2-8)}{256\sqrt{2}\pi^2}X^{-1/2}\right.\\ &\qquad\left.+\frac{8\mathrm{i}(\pi-4)x+\pi^2(20+3\mathrm{i})-\pi(80+8\mathrm{i})+24\mathrm{i}}{512\pi^2}X^{-1}+\dots\right).\end{aligned} \tag{5.377}$$

The coefficients of the monomials $x^\beta X^{-\alpha}$ inside the parentheses are reproduced by our Airy formula (5.371) (up to the overall normalization factor $\mathrm{e}^{\frac{5\mathrm{i}\pi}{16}}/2\sqrt{\pi}$). Expanding the grand potential in (5.372) up to order $\mathrm{e}^{-3\mu}$ (as it is given in the explicit expression) yields around 16–18 significant digits. If we increase the number of terms and use an expansion up to order $\mathrm{e}^{-6\mu}$, the precision is increased to 30–32 significant digits. This provides a strong check of our conjecture at $\hbar = 4\pi$.

The same procedure can be performed for other values of $\hbar$, for example $\hbar = 2\pi/3$. For that value, we have

$$\sqrt{v(q)} = \frac{3^{1/2}}{2^{3/4}\pi^{1/2}}\frac{\sinh\left(\frac{q}{\sqrt{2}}\right)}{\sinh\left(\frac{3q}{2\sqrt{2}}\right)}, \qquad \xi = \frac{\sqrt{2}}{3}. \tag{5.378}$$

and the exact $\psi_{-,N}(x)$ can also be expressed using elementary functions. The grand potential for $\hbar = 2\pi/3$ is

$$\begin{aligned}J\left(x,\mu,\frac{2\pi}{3}\right) &= J\left(\mu,\frac{2\pi}{3}\right)-\frac{3\mathrm{i}x^2}{4\pi}+x\\ &+\left(-\frac{3-\mathrm{i}\sqrt{3}}{6}\mathrm{e}^{\mu}\right)\frac{1}{X}+\left(\frac{(3+\mathrm{i}\sqrt{3})\mathrm{e}^{2\mu}}{12}-1\right)\frac{1}{X^2}+\left(-\frac{\pi+\mathrm{i}(1+3x-3\mu)}{6\pi}\mathrm{e}^{3\mu}\right.\\ &\left.+\frac{(9\pi+\mathrm{i}\sqrt{3})\pi+18\mathrm{i}(x-\mu)}{6\pi}\mathrm{e}^{\mu}+\mathcal{O}(\mathrm{e}^{-\mu})\right)\frac{1}{X^3}+\mathcal{O}(X^{-4}),\end{aligned} \tag{5.379}$$

with $J\left(\mu,\frac{2\pi}{3}\right)$ given by

$$J\left(\mu,\frac{2\pi}{3}\right) = \frac{\mu^3}{\pi^2}+\frac{4\mu}{9}+A\left(\frac{2\pi}{3}\right)+\frac{-4\pi^2-54\mu^2+3\sqrt{3}\pi(2\mu+1)}{9\pi^2}\mathrm{e}^{-2\mu}+\mathcal{O}(\mathrm{e}^{-4\mu}). \tag{5.380}$$

Again, by using (5.371), we find perfect agreement with the exact eigenfunction computed from spectral theory.

## 5.8 Fully on-shell eigenfunctions from resummed WKB

As we saw in section 5.6, from the point of view of integrable systems, for quantized values of all the true moduli $\kappa_i$, the eigenfunctions have increased decaying behaviour. We call these the "fully on-shell" eigenfunctions (i.e. on-shell from the point of view of the integrable system). Also, as we mentioned in our higher genus example, it is only when fully on-shell that the exact expression for the eigenfunction is free of theta functions. Indeed, they collapse to simpler functions when all the quantization conditions are imposed. We recall from our general discussion of the self-dual case $\hbar = 2\pi$ that one of the theta function comes from the topological string wavefunction (it is essentially the annulus amplitude). The fact that it gets suppressed when fully on-shell may point to the fact that in this special circumstance, the eigenfunction may be constructed without the data from the topological string wavefunction; all the data required would then be the resummed WKB wavefunction. This supposition is supported by the fact that, for quantities only involving closed string data, this is quite true: the conjectured expression for the spectral determinant $\Xi(\boldsymbol{\kappa})$ involves both the standard topological string free energy and the resummed WKB periods (in the form of the NS free energy), whereas the quantization conditions of [18, 31] only involves the resummed WKB periods. Of course, the WKB answer to the spectral problem, even if resummed, is not well defined since there are poles at $\hbar/2\pi \in \mathbb{Q}$ which should be cancelled by something. That is, it should still be completed by something non-perturbative in $\hbar$. The answer to this problem for the quantization conditions of [18, 31] is the following: take the WKB period given by $\partial_{\mathbf{t}} F_{\mathrm{NS}}(\mathbf{t}, \hbar)$, and add its dual given by the substitution

$$\hbar \to \hbar_{\mathrm{D}} = \frac{4\pi^2}{\hbar}, \qquad \mathbf{t} \to \frac{2\pi}{\hbar}\mathbf{t}. \tag{5.381}$$

Therefore, the full expression is made invariant under this duality as pointed out in [137]. This is very natural from the point of view of the integrable system. Indeed, because they are constructed using exponentiated operators $\mathrm{e}^{\mathsf{x}}, \mathrm{e}^{\mathsf{y}}$, the cluster integrable systems associated to our spectral problems enjoy a very nice property called the *modular double structure*, first described in [21]. The main point is that, even if the operators $\mathrm{e}^{\mathsf{x}}, \mathrm{e}^{\mathsf{y}}$ do not commute ($\mathrm{e}^{\mathsf{x}}\mathrm{e}^{\mathsf{y}} = \mathrm{e}^{\mathrm{i}\hbar}\mathrm{e}^{\mathsf{y}}\mathrm{e}^{\mathsf{x}}$), we still have

$$\mathrm{e}^{\mathsf{x}}\mathrm{e}^{\frac{2\pi}{\hbar}\mathsf{y}} = \mathrm{e}^{\mathrm{i}\hbar\frac{2\pi}{\hbar}}\mathrm{e}^{\frac{2\pi}{\hbar}\mathsf{y}}\mathrm{e}^{\mathsf{x}} = \mathrm{e}^{\frac{2\pi}{\hbar}\mathsf{y}}\mathrm{e}^{\mathsf{x}}, \tag{5.382}$$

and similarly with $\mathsf{x}$ and $\mathsf{y}$ exchanged. So the algebra of operators built from the set $\{\mathrm{e}^{\mathsf{x}}, \mathrm{e}^{\mathsf{y}}\}$ commutes (at least formally) with the algebra of operators built from $\{\mathrm{e}^{\frac{2\pi}{\hbar}\mathsf{x}}, \mathrm{e}^{\frac{2\pi}{\hbar}\mathsf{y}}\}$. The invariance of the quantization conditions under the transformation (5.381) should somehow be a consequence of the modular double structure of the

integrable system. Also, this duality structure of the spectrum could be used in [138] to obtain exact expressions for the quantum mirror map at rational $\hbar/2\pi$.

The point of view taken in [20] is that something similar should be true for the eigenfunctions, which should be constructed by dualizing the WKB wavefunction. In this section, we build on the insight of [20], and show how fully on-shell eigenfunctions (and the corresponding quantization conditions) can be constructed only by using the resummed WKB data and the modular double structure. Explicit results can be obtained when $\hbar/2\pi \in \mathbb{Q}$. The techniques of [138] are also used and extended in the process.

For a given toric CY threefold, our spectral problem is given by quantizing its mirror curve defined by the vanishing of

$$W(\mathrm{e}^x, \mathrm{e}^y) = \sum_{k=1}^{m+3} \xi_k \mathrm{e}^{\mu_k x + \nu_k y} + \kappa. \tag{5.383}$$

Here, we singled out one of the "true" moduli and called it $\kappa$, whereas the other moduli (including mass parameters) are among the $\xi_k$. The corresponding operator

$$\mathsf{O} = \sum_{k=1}^{m+3} \xi_k \mathrm{e}^{\mu_k \mathsf{x} + \nu_k \mathsf{y}} \tag{5.384}$$

is then a difference operator acting on functions. When the parameters $\xi_k$ take values in the appropriate range, the inverse of $\mathsf{O}$ is a positive definite trace class operator, and admits a discrete set of eigenvalues $(-\kappa_n)^{-1}$ and eigenfunctions $\psi_n(x)$. As we saw previously, we can have off-shell eigenfunctions for any values of $\kappa$, i.e. functions in the kernel of the quantized mirror curve. These functions satisfy the difference equation

$$\sum_{n=1}^{m+3} \xi_k \, \mathrm{e}^{-\mu_k \nu_k \frac{\mathrm{i}\hbar}{2}} \, \mathrm{e}^{\mu_n x} \psi(x - \nu_n \mathrm{i}\hbar) + \kappa \psi(x) = 0, \tag{5.385}$$

but only for the specific values $\kappa = \kappa_n$ do we find on-shell eigenfunctions. When the eigenfunctions are "fully on-shell", all the true moduli are quantized. We define the dual of the operator $\mathsf{O}$:

$$\widetilde{\mathsf{O}} = \sum_{n=1}^{m+3} \tilde{\xi}_n \mathrm{e}^{\mu_n \frac{2\pi}{\hbar} \mathsf{x} + \nu_n \frac{2\pi}{\hbar} \mathsf{y}}. \tag{5.386}$$

It commutes with $\mathsf{O}$, and so it can be diagonalized simultaneously by the set of on-shell eigenfunctions of the operator $\mathsf{O}$. The eigenvalue of $\widetilde{\mathsf{O}}$ will be denoted $-\tilde{\kappa}$. The operator $\widetilde{\mathsf{O}}$ has essentially the same form as $\mathsf{O}$, but a priori the different moduli and parameters could take arbitrary values. In the following, we will see some examples of relations between $\kappa$ and $\tilde{\kappa}$ (and $\xi_n$ and $\tilde{\xi}_n$), and how they arise concretely. The

difference equation given by the dual operator is

$$\sum_{n=1}^{m+3} \tilde{\xi}_n \, \mathrm{e}^{-\mu_n \nu_n \frac{\mathrm{i}\hbar}{2} \frac{4\pi^2}{\hbar^2}} \, \mathrm{e}^{\mu_n \frac{2\pi x}{\hbar}} \psi(x - 2\pi \mathrm{i} \nu_n) + \tilde{\kappa} \psi(x) = 0. \tag{5.387}$$

By rescaling the eigenfunction $\tilde{\psi}(x) = \psi\left(\frac{\hbar}{2\pi} x\right)$, and renaming

$$\hbar_{\mathrm{D}} = \frac{4\pi^2}{\hbar}, \qquad x_{\mathrm{D}} = \frac{2\pi x}{\hbar}, \tag{5.388}$$

this gives

$$\sum_{n=1}^{m+3} \tilde{\xi}_n \, \mathrm{e}^{-\mu_n \nu_n \frac{\mathrm{i}\hbar_{\mathrm{D}}}{2}} \, \mathrm{e}^{\mu_n x_{\mathrm{D}}} \tilde{\psi}(x_{\mathrm{D}} - \nu_n \mathrm{i}\hbar_{\mathrm{D}}) + \tilde{\kappa} \tilde{\psi}(x_{\mathrm{D}}) = 0, \tag{5.389}$$

which is exactly of the same form as the initial difference equation (5.385), but using the dual variables. We call this the dual difference equation. If we consider only the difference equation given by $\mathsf{O}$, we remark that any $\mathrm{i}\hbar$–periodic function can be multiplied to a solution in order to get another solution. These are the "quasi constants" already mentioned. By requiring that a solution is simultaneously a solution for the dual difference equation given by $\widetilde{\mathsf{O}}$, we may expect to obtain a unique eigenfunction for each level, since this constraint may be enough to fix the multiplicative ambiguity. We will see in the examples that this is the case. Since the dual difference equation has the same form as the original difference equation, the small $\hbar$ expansion and the small $\hbar_{\mathrm{D}}$ of the eigenfunction should be closely related. We will use this argument when constructing the eigenfunction from the resummed WKB wavefunction.

Let us study the difference equation (5.385) at small $\hbar$ (or equivalently (5.389) at small $\hbar_{\mathrm{D}}$). The well known WKB ansatz is:

$$\psi_{\mathrm{WKB}}(x) = \exp\left( -\frac{1}{\mathrm{i}\hbar} \sum_{n=0}^{\infty} S_n(x) (-\mathrm{i}\hbar)^n \right). \tag{5.390}$$

Using this ansatz, we can write for any $d \in \mathbb{C}$,

$$\frac{\psi_{\mathrm{WKB}}(x + d\,\mathrm{i}\hbar)}{\psi_{\mathrm{WKB}}(x)} = \exp\left[ -\frac{1}{\mathrm{i}\hbar} \sum_{n=1}^{\infty} (-\mathrm{i}\hbar)^n \left( \sum_{k=0}^{n-1} \frac{(-d)^{n-k}}{(n-k)!} S_k^{(n-k)}(x) \right) \right]. \tag{5.391}$$

Inserting this into the difference equation and expanding everything at small $\hbar$, we can recursively solve for $S_n'(x)$ order by order in $-\mathrm{i}\hbar$. Then, we can integrate to obtain $S_n(x)$. Let us define $y(x)$ to be the solution of $W(x, y) = 0$. We find for the first orders

$$\begin{aligned} S_0(x) &= \int^x y(x) \mathrm{d}x, \\ S_1(x) &= \frac{1}{2} \log \frac{\partial y(x)}{\partial \kappa}. \end{aligned} \tag{5.392}$$

The natural domain of $y(x)$ is not the $\mathbb{C}$ plane, but the spectral curve itself, which is a multi-sheeted cover of the plane. We will consider hyperelliptic cases only, implying that we have only two sheets.[9] We need to take either branch of the function $y(x)$, which we also call $y(x)$ by abuse of notation. The two choices of the branch of $y(x)$ correspond to the WKB expansions of two independent solutions of the difference equation. Let us define

$$X = \mathrm{e}^{x}. \tag{5.393}$$

At large $X$, we have

$$\begin{aligned} S_0(x) &= s_0(x) + S_0^{\mathrm{inst}}(X) = s_0(x) + \int_{\infty}^{X} \tilde{y}(X')\frac{\mathrm{d}X'}{X'}, \\ S_1(x) &= s_1(x) + S_1^{\mathrm{inst}}(X), \end{aligned} \tag{5.394}$$

where $s_0(x)$ is an order 2 polynomial, $s_1(x)$ is an order 1 polynomial, and $\tilde{y}(X)$ is equal to $y(x)$ minus the polynomial part in $x$ which appears in the large $X$ expansion. Both $s_0$ and $s_1$ are independent of $\kappa$. It can be verified that the higher $S_n(x)$ are only functions of $X$: by this we mean that there is no polynomial in $x$ in the large $X$ expansion. We use this remark and build the truncated WKB function

$$\Psi_{\mathrm{WKB}}(X) = \psi_{\mathrm{WKB}}(x)\mathrm{e}^{-(-\mathrm{i}\hbar)^{-1}s_0(x)-s_1(x)}, \tag{5.395}$$

which only depends on $x$ through $X$. The part which is factored out is what we called the perturbative WKB contribution $J^{\mathrm{WKB}}_{\mathrm{pert}}(\boldsymbol{\mu}, \hbar, X)$ in previous sections.

By adapting the manipulations done in [74], we can resum the small $\hbar$ WKB expansion order by order in another expansion parameter, here $X^{-1}$. Let us define

$$q = \mathrm{e}^{\mathrm{i}\hbar}. \tag{5.396}$$

Shifts of $\mathrm{i}\hbar$ in $x$ in the function $\psi_{\mathrm{WKB}}(x)$ correspond to multiplying $X$ by $q$ in the truncated function $\Psi_{\mathrm{WKB}}(X)$. The difference equation can be rewritten in terms of $\Psi_{\mathrm{WKB}}(X)$ only, by using the explicit forms of $s_0(x), s_1(x)$. In our hyperelliptic cases, it can be put in the form

$$\Psi_{\mathrm{WKB}}(q^{-1}X) - a(X)\Psi_{\mathrm{WKB}}(X) + b(X)\Psi_{\mathrm{WKB}}(qX) = 0, \tag{5.397}$$

where $a(X)$ and $b(X)$ are rational functions of $X$, which also may depend on the moduli and parameters, as well as on $q^{1/2}$. It is useful to change variables and use

$$\tilde{X} = \frac{X}{\kappa}, \tag{5.398}$$

[9] Strictly speaking, it is $\mathrm{e}^{y(x)}$ which is defined on a two-sheeted cover.

and

$$\widetilde{\Psi}_{\rm WKB}(\tilde{X}) = \Psi_{\rm WKB}(X). \tag{5.399}$$

Using this, we find that (for the appropriate parametrization) the difference equation takes the rather general form

$$(1+\tilde{X}^{-1})\widetilde{\Psi}_{\rm WKB}(\tilde{X}) - \widetilde{\Psi}_{\rm WKB}(q^{-1}\tilde{X}) + \frac{1}{\kappa^r}P[\widetilde{\Psi}_{\rm WKB}] = 0, \tag{5.400}$$

where $r$ is a strictly positive integer, and $P$ is the remaining part coming from the difference equation. This form suggests that we can solve this $q$–equation in a large $\kappa$ expansion. The ansatz we use is

$$\widetilde{\Psi}_{\rm WKB}(\tilde{X}) = \widetilde{\Psi}^{(0)}(\tilde{X}) \mathrm{e}^{\sum_{k=1}^{\infty}\phi_k(\tilde{X})\kappa^{-k}}. \tag{5.401}$$

The leading part $\Psi^{(0)}(\tilde{X})$ is universal, and is essentially a quantum dilogarithm:

$$\widetilde{\Psi}^{(0)}(\tilde{X}) = \prod_{N=0}^{\infty}(1+X^{-1}q^{-N-1}) = \exp\left(\sum_{k=1}^{\infty}\frac{1}{k(1-q^k)}(-\tilde{X})^k\right). \tag{5.402}$$

To perform the recursion at large $\kappa$, we divide everything by $\Psi_{\rm WKB}(\tilde{X})$ and use that

$$\begin{aligned}\frac{\widetilde{\Psi}_{\rm WKB}(q^{-1}\tilde{X})}{\widetilde{\Psi}_{\rm WKB}(\tilde{X})} &= (\tilde{X}^{-1}+1)\mathrm{e}^{\sum_{k=1}^{\infty}g_k(\tilde{X})\kappa^{-k}},\\ \frac{\widetilde{\Psi}_{\rm WKB}(q\tilde{X})}{\widetilde{\Psi}_{\rm WKB}(\tilde{X})} &= \frac{1}{q^{-1}\tilde{X}^{-1}+1}\mathrm{e}^{-\sum_{k=1}^{\infty}g_k(q\tilde{X})\kappa^{-k}}.\end{aligned} \tag{5.403}$$

At each order in large $\kappa$, we get a linear equation determining $g_k(\tilde{X})$ recursively. The recursion can be solved for $g_k(\tilde{X})$, which are rational functions of $\tilde{X}$. The functions $\phi_k(\tilde{X})$ are given by

$$g_k(\tilde{X}) = \phi_k(q^{-1}\tilde{X}) - \phi_k(\tilde{X}), \tag{5.404}$$

which can be formally solved in the following way:

$$\phi_k(\tilde{X}) = -\sum_{n=0}^{\infty}g_k(q^{-n}\tilde{X}). \tag{5.405}$$

This is especially useful if we work with a large $\tilde{X}$ expansion of $g_k(\tilde{X})$, since

$$\sum_{n=0}^{\infty}(q^{-n}\tilde{X})^{-k} = \frac{\tilde{X}^{-k}}{1-q^k}, \tag{5.406}$$

Also, we find that the larger $k$ is, the larger is the leading power of $\frac{1}{\tilde{X}}$ in the large $\tilde{X}$ expansion of $g_k(\tilde{X})$. In the end, after going back to the original variable $X$, we

find the following structure:

$$\begin{aligned}\log V(X) &\equiv \log \frac{\Psi_{\rm WKB}(q^{-1}\tilde{X})}{\Psi_{\rm WKB}(\tilde{X})} \\ &= \sum_{k=1} f_k(\kappa, \boldsymbol{\xi}, q) X^{-k},\end{aligned} \tag{5.407}$$

and so, formally,

$$\log \Psi_{\rm WKB}(X) = \sum_{k=1} \frac{f_k(\kappa, \boldsymbol{\xi}, q)}{q^k - 1} X^{-k}. \tag{5.408}$$

In the above, we have collected the $\{\xi_i\}_{i\geq 1}$ into the vector $\boldsymbol{\xi}$. The $f_k(\kappa, \boldsymbol{\xi}, q)$ are polynomials in the variables $\kappa$ and $\xi_i$. If we expand this expression at small $\hbar$, we retrieve the large $X$ expansion of all the WKB corrections. So this expression is effectively a resummation of the small $\hbar$ WKB expansion. Of course, replacing $\hbar$ and $x$ by their duals, and $\kappa, \xi_i$ by $\tilde{\kappa}, \tilde{\xi}_i$, we obtain the dual WKB resummation for the dual difference equation.

To illustrate this procedure, we give here as examples the resummed WKB wavefunctions for some cases which are associated with mirror curves of toric Calabi-Yau threefolds. For local $\mathbb{P}^1 \times \mathbb{P}^1$, we have one true modulus which is $\kappa$, and one extra parameter $\xi_1$ which is a mass parameter. We rename it $m$. The mirror curve and the WKB wavefunction are

$$\begin{aligned}&W(\mathrm{e}^x, \mathrm{e}^y) = \mathrm{e}^x + m\mathrm{e}^{-x} + \mathrm{e}^y + \mathrm{e}^{-y} + \kappa, \\ &\log \Psi_{\rm WKB}(X) = \frac{\kappa}{(q-1)X} + \frac{-2mq + \kappa^2 q + 2}{(2q - 2q^3) X^2} + \frac{\kappa\left(q\left(-3mq + \kappa^2 q + 3\right) + 3\right)}{3q^2\left(q^3 - 1\right) X^3} \\ &\qquad - \frac{2(mq-1)\left(q^2(mq-1) - 2\right) + 4\kappa^2 q\left(-mq^3 + q^2 + q + 1\right) + \kappa^4 q^4}{4q^4\left(q^4 - 1\right) X^4} + \dots\end{aligned} \tag{5.409}$$

For the resolved $\mathbb{C}^3/\mathbb{Z}_5$, we have two true moduli, $\kappa$ and an extra one which is $\xi_1$. We rename this second one $\kappa_1$. The mirror curve and the WKB eigenfunction are

$$\begin{aligned}&W(x, y) = \mathrm{e}^x + \mathrm{e}^y + \mathrm{e}^{-3x-y} + \kappa_1 \mathrm{e}^{-x} + \kappa, \\ &\log \Psi_{\rm WKB}(X) = \frac{\kappa}{(q-1)X} + \frac{\kappa^2 - 2\kappa_1}{(2 - 2q^2) X^2} + \frac{\kappa^3 - 3\kappa\kappa_1}{3\left(q^3 - 1\right) X^3} \\ &\qquad + \frac{\kappa^4 - 4\kappa^2\kappa_1 + 2\kappa_1^2}{(4 - 4q^4) X^4} + \frac{-\kappa^5 + 5\kappa^3\kappa_1 - 5\kappa\kappa_1^2 + \frac{5}{q^{5/2}}}{(5 - 5q^5) X^5} \\ &\qquad - \frac{-\left(\kappa^2 - 2\kappa_1\right)\left(\kappa^4 - 4\kappa^2\kappa_1 + \kappa 1^2\right) + \frac{6\kappa}{q^{5/2}} + \frac{6\kappa}{q^{7/2}}}{(6 - 6q^6) X^6} + \dots\end{aligned} \tag{5.410}$$

In each of these cases, the polynomial part of the large $X$ WKB expansion is given

by[10]

$$\frac{1}{-\mathrm{i}\hbar}s_0(x)+s_1(x)=\frac{\mathrm{i}}{2\hbar}x^2-\frac{1}{2}\left(\frac{2\pi}{\hbar}+1\right)x. \tag{5.411}$$

We mention in passing that by inserting in $\log\Psi_{\mathrm{WKB}}(X)$ the quantum mirror maps for the moduli, as well as substituting $X$ for $\widehat{X}$ in (5.173), we obtain $\log\psi_{\mathrm{inst}}^{\mathrm{WKB}}$ in eq. (5.175).

Let us now focus on the case where $\hbar$ is of the form $\frac{\hbar}{2\pi}\in\mathbb{Q}$ which we will call the *rational case*. We define the coprime numbers $P,Q$ such that

$$\hbar=2\pi\frac{P}{Q}. \tag{5.412}$$

Then, the quantity $q=\mathrm{e}^{\mathrm{i}\hbar}$ is a root of unity:

$$q^Q=1. \tag{5.413}$$

The formal solution (5.408) is ill-defined since it has poles when $k$ is a multiple of $Q$. We introduce a regulating parameter $\epsilon$ and consider the small $\epsilon$ expansion by setting

$$\hbar=2\pi\frac{P}{Q}+\epsilon. \tag{5.414}$$

We expand (5.408) in small $\epsilon$ by using

$$\frac{1}{q^{\ell Q}-1}=-\frac{\mathrm{i}}{\epsilon\ell Q}-\frac{1}{2}+\mathcal{O}(\epsilon), \tag{5.415}$$

and find

$$\log\Psi_{\mathrm{WKB}}(X)=-\frac{\mathrm{i}}{\epsilon}\sum_{\ell=1}^{\infty}\frac{f_{\ell Q}(\kappa,\boldsymbol{\xi},q)}{\ell Q}X^{-\ell Q}+\mathcal{O}(1). \tag{5.416}$$

As it is, the naive resummation of the WKB expansion given by $\log\Psi_{\mathrm{WKB}}$ is singular at rational $\hbar/2\pi$. This is of course something we already established in section 5.4. We conclude that it has to be corrected by something which

1) is non pertubative at small $\hbar$ so that it is invisible in the small $\hbar$ WKB expansion,

2) cancels the poles in the rational case.

Also, we have not taken into account the modular duality structure outlined in the previous section. Indeed, our point of view was to start with the small $\hbar$ WKB resummation of the eigenfunction. However, we could have equally well started from the dual equation (5.389) also satisfied by the on-shell eigenfunction, and consider

[10] This depends on the choice of branch for $y(x)$. Here we choose the one which reproduces (5.411).

its small $\hbar_{\rm D}$ WKB expansion. By doing the same recursive procedure, we would end up with a very similar expression for the truncated dual-WKB eigenfunction

$$\log \Psi^{\rm D}_{\rm WKB}(X) = \sum_{k=1} \frac{f_k(\tilde\kappa, \tilde{\boldsymbol\xi}, q_{\rm D})}{{q_{\rm D}}^k - 1} X_{\rm D}^{-k}, \tag{5.417}$$

where $X_{\rm D} = {\rm e}^{x_{\rm D}} = {\rm e}^{\frac{2\pi}{\hbar}x}$, $\hbar_{\rm D} = 4\pi^2/\hbar$ and $q_{\rm D} = {\rm e}^{{\rm i}\hbar_{\rm D}} = {\rm e}^{\frac{2\pi Q}{P}}$. The $f_k$ are precisely the same polynomials as in (5.408), since the dual equation is of the same form as the initial equation. So we would expect an eigenfunction which is symmetric under the exchanges $\hbar \leftrightarrow \frac{4\pi^2}{\hbar}$ and $(\kappa, \boldsymbol\xi) \leftrightarrow (\tilde\kappa, \tilde{\boldsymbol\xi})$. In line with what is suggested in [20], let us add its dual to the resummed WKB, which is a non-perturbative contribution at small $\hbar$:

$$\begin{aligned}\log \Psi(X) &= \log \Psi_{\rm WKB}(X) + \log \Psi^{\rm D}_{\rm WKB}(X) \\ &= \sum_{k=1} \frac{f_k(\kappa, \boldsymbol\xi, q)}{q^k - 1} X^{-k} + \sum_{k=1} \frac{f_k(\tilde\kappa, \tilde{\boldsymbol\xi}, q_{\rm D})}{{q_{\rm D}}^k - 1} X_{\rm D}^{-k}.\end{aligned} \tag{5.418}$$

The dual part also has poles when $k = \ell P$ for integer $\ell$. Using (5.414) and expanding at small $\epsilon$, we obtain

$$\log \Psi^{\rm D}_{\rm WKB}(X) = \frac{\rm i}{\epsilon}\frac{P}{Q} \sum_{\ell=1}^{\infty} \frac{f_{\ell P}(\tilde\kappa, \tilde{\boldsymbol\xi}, q_{\rm D})}{\ell Q} X^{-\ell Q} + O(1). \tag{5.419}$$

In the full expression (5.418), this pole cancels with the corresponding pole in (5.416) if the following condition is fulfilled:

$$P\, f_{\ell P}(\tilde\kappa, \tilde{\boldsymbol\xi}, q_{\rm D}) = Q\, f_{\ell Q}(\kappa, \boldsymbol\xi, q), \tag{5.420}$$

for all positive integers $\ell$. This defines relations

$$\tilde\kappa(\kappa, \boldsymbol\xi; \hbar), \qquad \text{and} \qquad \tilde{\boldsymbol\xi}(\kappa, \boldsymbol\xi; \hbar). \tag{5.421}$$

Since the $f_k$ are polynomials in $\kappa$ and $\xi_k$, these relations are algebraic *at fixed rational* $\hbar$. Actually, this system of equation seems madly overdetermined. Nevertheless, we find that there actually are solutions as a consequence of the form of the $f_k$. Some examples can be found below. The on-shell values of $\kappa$ depend on $\hbar$, so we should write $\kappa(\hbar)$ and $\tilde\kappa(\kappa(\hbar), \boldsymbol\xi; \hbar), \tilde{\boldsymbol\xi}(\kappa(\hbar), \boldsymbol\xi; \hbar)$. Once these relations are fixed, our claim is that (5.418) is the full non-pertrubatively complete truncated WKB eigenfunction in the large $X$ expansion. Let us remark quickly that, in contrast with [20], we did not make use of the quantum mirror map, since in this section we do not really bother with the enumerative interpretation of the WKB wavefunction. In [20], and also in the setup of the TS/ST correspondence, the quantum mirror map fixes the

relations between the moduli/parameters $\kappa$ and $\xi_i$ and their duals $\tilde{\kappa}$ and $\tilde{\xi}_i$. Here, we impose these relations in the rational case using pole cancellation. This is less general but more straightforward from the point of view of the difference equation.

Now that we cancelled the poles, we need to find the finite term in the small $\epsilon$ expansion. This can be done quite straightforwardly. As we will see, it only involves under different guises the function $\log V(X)$ defined in (5.407), as well as its $\hbar$ derivative. To write done the answer, let us define for $k = 1, \dots, Q$

$$\begin{aligned} \varphi_k(X) &= \sum_{\ell=0}^{\infty} f_{\ell Q+k}(\kappa, \boldsymbol{\xi}, q) X^{-\ell Q-k} = \frac{1}{Q} \sum_{m=0}^{Q-1} \log V(q^m X) q^{mk}, \\ \partial_\hbar \varphi_Q(X) &= \frac{1}{Q} \sum_{m=0}^{Q-1} \frac{\partial_\hbar V}{V}\bigg|_{X \to q^m X}, \end{aligned} \tag{5.422}$$

and their duals for $k = 1, \dots, P$,

$$\begin{aligned} \tilde{\varphi}_k(X_{\mathrm{D}}) &= \sum_{\ell=0}^{\infty} f_{\ell P+k}(\tilde{\kappa}, \tilde{\boldsymbol{\xi}}, q_{\mathrm{D}}) X_{\mathrm{D}}^{-\ell P-k} = \frac{1}{P} \sum_{m=0}^{P-1} \log V_{\mathrm{D}}(q_{\mathrm{D}}^m X_{\mathrm{D}}) q_{\mathrm{D}}^{mk}, \\ \partial_{\hbar_{\mathrm{D}}} \tilde{\varphi}_P(X) &= \frac{1}{P} \sum_{m=0}^{P-1} \frac{\partial_\hbar V}{V}\bigg|_{X_{\mathrm{D}} \to {q_{\mathrm{D}}}^m X_{\mathrm{D}}}. \end{aligned} \tag{5.423}$$

In the above, the dual $V_{\mathrm{D}}$ of $V$ is

$$\log V_{\mathrm{D}}(X_{\mathrm{D}}) \equiv \sum_{k=1} f_k(\tilde{\kappa}, \tilde{\boldsymbol{\xi}}, q_{\mathrm{D}}) X_{\mathrm{D}}^{-k}, \tag{5.424}$$

which is basically $\log V(X)$ where we replaced all the variables by their duals. There is a relation between $\psi_Q$ and $\tilde{\psi}_P$ as a consequence of (5.420):

$$\tilde{\varphi}_P(X_{\mathrm{D}}) = \frac{Q}{P} \varphi_Q(X). \tag{5.425}$$

Using these functions, it can be shown by direct computation that the finite term in (5.418) after pole cancellation is

$$\begin{aligned} \log \Psi(X) = \frac{\mathrm{i}Q}{2\pi P} \Bigg( &- \int_\infty^X \varphi_Q(X') \frac{\mathrm{d}X'}{X'} + \lambda \int_\infty^X \partial_\kappa \varphi_Q(X') \frac{\mathrm{d}X'}{X'} \\ &+ \boldsymbol{\lambda}_\xi \cdot \int_\infty^X \partial_{\boldsymbol{\xi}} \varphi_Q(X') \frac{\mathrm{d}X'}{X'} + x \varphi_Q(X) \Bigg) \\ &- \frac{1}{2} \left(1 + \frac{Q}{P}\right) \varphi_Q(X) + \int_\infty^X \mathrm{i} \partial_\hbar \varphi_Q(X') \frac{\mathrm{d}X'}{X'} + \int_\infty^{X_{\mathrm{D}}} \mathrm{i} \partial_{\hbar_{\mathrm{D}}} \tilde{\varphi}_P(X'_{\mathrm{D}}) \frac{\mathrm{d}X'_{\mathrm{D}}}{X'_{\mathrm{D}}} \\ &+ \sum_{k=1}^{Q-1} \frac{\varphi_k(X)}{q^k - 1} + \sum_{k=1}^{P-1} \frac{\tilde{\varphi}_k(X_{\mathrm{D}})}{{q_{\mathrm{D}}}^k - 1}. \end{aligned} \tag{5.426}$$

In the above computation, it was very important to vary the $\tilde{\kappa}$ and $\tilde{\xi}_i$ with respect to $\hbar$. In the answer, we have collected in $\lambda$ and $\boldsymbol{\lambda}_\xi$ all the terms in front of the corresponding integrals, involving terms such as $\partial_\hbar \tilde{\kappa}$. These terms cannot be determined directly by our method, and we will use monodromy invariance of the eigenfunction to fix them. Let us also notice that on the r.h.s. in the first parenthesis, the first and last term can be put together using integration by parts, to give $\int x \mathrm{d}\varphi_Q(x)$. So, this first line corresponds to the integral of what is called the "deformed symplectic potential" for the special case studied in [112][11], with deformation parameters $\lambda$ and $\boldsymbol{\lambda}_\xi$. Once we know how to build $\log V$ and $\log V_{\mathrm{D}}$ and their $\hbar$ derivative, everything is exactly determined. We will give an algorithm to construct them now.

We recall the definition of $V(X)$:

$$V(X) = \frac{\Psi_{\mathrm{WKB}}(q^{-1}X)}{\Psi_{\mathrm{WKB}}(X)}. \tag{5.427}$$

The difference equation (5.397), can be rewritten for $V(X)$ as

$$V(X)V(qX) - a(X)V(qX) + b(X) = 0, \tag{5.428}$$

where we remind that $a(X)$ and $b(X)$ are rational functions of $X$. The key feature of the rational case is that this equation can be solved algebraically (using $q^Q = 1$). To proceed, we shorten the notation using

$$v_k = V(q^k X). \tag{5.429}$$

The label $k$ of $v_k$ is thus defined modulo $Q$. The previous equation can be shifted, which gives the closed system of $Q$ quadratic equations for the $Q$ variables $v_k$, where $k = 0, 1, \ldots, Q-1$:

$$v_k v_{k+1} - a(q^k X)v_{k+1} + b(q^k X) = 0, \qquad k = 0, 1, \ldots, Q-1. \tag{5.430}$$

To efficiently solve this system, we proceed by recursion. We define $a^{(k)}(X)$ and $b^{(k)}(X)$ through the following relations

$$\begin{aligned} &a^{(1)}(X) = a(X), \\ &b^{(1)}(X) = b(X), \\ &v_0 v_1 \cdots v_k - a^{(k)}(X)v_k + b^{(k)}(X) = 0. \end{aligned} \tag{5.431}$$

The next term is obtained by multiplying the last line by $v_{k+1}$, and using (5.430):

$$\begin{aligned} 0 &= v_0 v_1 \cdots v_k v_{k+1} - a^{(k)}(X)v_k v_{k+1} + b^{(k)}(X)v_{k+1} \\ &= v_0 v_1 \cdots v_{k+1} - [a(q^k X)a^{(k)} - b^{(k)}(X)]v_{k+1} + b(q^k X)a^{(k)}(X). \end{aligned} \tag{5.432}$$

[11] It was already anticipated through a private communication by R. Kashaev, one of the authors of [112], that an algorithm of the kind we present here can generalize their result.

From this we read out the relation

$$\begin{pmatrix} a^{(k+1)}(X) \\ b^{(k+1)}(X) \end{pmatrix} = \begin{pmatrix} a(q^k X) & -1 \\ b(q^k X) & 0 \end{pmatrix} \begin{pmatrix} a^{(k)}(X) \\ b^{(k)}(X) \end{pmatrix}. \tag{5.433}$$

This recursion can be easily solved, and we find, for example for $k = Q$,

$$\begin{pmatrix} a^{(Q)}(X) \\ b^{(Q)}(X) \end{pmatrix} = \mathcal{M}(X) \begin{pmatrix} 1 \\ 0 \end{pmatrix} = \begin{pmatrix} \mathcal{M}_{11}(X) \\ \mathcal{M}_{21}(X) \end{pmatrix}, \tag{5.434}$$

where the matrix

$$\mathcal{M}(X) = \prod_{k=1}^{Q} \begin{pmatrix} a(q^{-k}X) & -1 \\ b(q^{-k}X) & 0 \end{pmatrix} \tag{5.435}$$

is defined such that the product is ordered from left to right as $k$ increases. Using that

$$\mathcal{M}(qX) = \begin{pmatrix} a(X) & -1 \\ b(X) & 0 \end{pmatrix} \mathcal{M}(X) \begin{pmatrix} a(X) & -1 \\ b(X) & 0 \end{pmatrix}^{-1}, \tag{5.436}$$

we get

$$\begin{pmatrix} a^{(Q)}(qX) \\ b^{(Q)}(qX) \end{pmatrix} = \begin{pmatrix} \mathcal{M}_{22}(X) - a(X)\mathcal{M}_{12}(X) \\ b(X)\mathcal{M}_{12}(X) \end{pmatrix}. \tag{5.437}$$

Let us define

$$\Pi v = v_0 v_1 \cdots v_{Q-1}, \tag{5.438}$$

which is invariant under $q$–shifts. We obtain from (5.431) for $k = Q$

$$\begin{cases} v_0(\Pi v - a^{(Q)}(X)) + b^{(Q)}(X) = 0, \\ v_1(\Pi v - a^{(Q)}(qX)) + b^{(Q)}(qX) = 0. \end{cases} \tag{5.439}$$

The second line is just the $q$–shift of the first. Using the expressions of $a^{(Q)}$ and $b^{(Q)}$ in terms of the entries of $\mathcal{M}$ and then (5.430) to remove $v_1$, we can rewrite this system as

$$\begin{pmatrix} \mathcal{M}_{11}(X) - \Pi v & \mathcal{M}_{21}(X) \\ \mathcal{M}_{12}(X) & \mathcal{M}_{22}(X) - \Pi v \end{pmatrix} \begin{pmatrix} -v_0 \\ 1 \end{pmatrix} = \begin{pmatrix} 0 \\ 0 \end{pmatrix}, \tag{5.440}$$

which has solutions only if

$$0 = \det(\mathcal{M}^{\mathrm{T}} - \Pi v\, \mathbf{1}) = \det(\mathcal{M} - \Pi v\, \mathbf{1}). \tag{5.441}$$

We conclude that $\Pi v$ is an eigenvalue of the matrix $\mathcal{M}$(X):

$$\Pi v = v_0 v_1 \cdots v_{Q-1} = \frac{\mathrm{tr}\mathcal{M}(X) \pm \sqrt{\Delta(X)}}{2}, \tag{5.442}$$

where

$$\Delta(X) = (\mathrm{tr}\mathcal{M}(X))^2 - 4\ \det\mathcal{M}(X). \tag{5.443}$$

Both $\det\mathcal{M}(X)$ and $\mathrm{tr}\mathcal{M}(X)$ are invariant under $q$–shifts (see (5.436)) and so depend on $X$ through $X^Q$. The function $v_0$ can be found for example using the second line of (5.440):

$$v_0 = \frac{\Pi v - \mathcal{M}_{22}(X)}{-\mathcal{M}_{12}(X)} = \frac{\mathcal{M}_{11}(X) - \mathcal{M}_{22}(X) \pm \sqrt{\Delta(X)}}{-2\mathcal{M}_{12}(X)}. \tag{5.444}$$

The other $v_k$ can be obtained by $q$–shifting $v_0$. We thus provided the solution of the $q$–equation (5.428) for all the rational cases: the solution is encoded in the matrix $\mathcal{M}(X)$, which can be obtained by (5.435), the product of $Q$ matrices which are $q$–shifted. Finally, we find the following results for $\log V(X)$ and $\varphi_Q(X)$:

$$\begin{aligned} \log V(X) &= \log\left(\frac{\mathcal{M}_{11}(X) - \mathcal{M}_{22}(X) \pm \sqrt{\Delta(X)}}{-2\mathcal{M}_{12}(X)}\right), \\ \varphi_Q(X) &= \frac{1}{Q}\log\left(\frac{\mathrm{tr}\mathcal{M}(X) \pm \sqrt{\Delta(X)}}{2}\right). \end{aligned} \tag{5.445}$$

The dual quantities $\log V_{\mathrm{D}}(X_{\mathrm{D}})$ and $\tilde{\varphi}_P(X_{\mathrm{D}})$ can be obtained by exchanging $Q$ and $P$ and replacing variables by their duals $X_{\mathrm{D}}$, $\tilde{\kappa}$ and $\tilde{\boldsymbol{\xi}}$. This means redefining $a(X)$ and $b(X)$ since they depend on $\kappa$, $\boldsymbol{\xi}$ and perhaps $q$. For convenience, we write the results here:

$$\begin{aligned} \widetilde{\mathcal{M}}(X_{\mathrm{D}}) &= \prod_{k=1}^{P} \begin{pmatrix} a_{\mathrm{D}}(q^{-k}X_{\mathrm{D}}) & -1 \\ b_{\mathrm{D}}(q^{-k}X_{\mathrm{D}}) & 0 \end{pmatrix}, \\ \Delta_{\mathrm{D}}(X_{\mathrm{D}}) &= (\mathrm{tr}\widetilde{\mathcal{M}}(X_{\mathrm{D}}))^2 - 4\det\widetilde{\mathcal{M}}(X_{\mathrm{D}}), \\ \log V_{\mathrm{D}}(X_{\mathrm{D}}) &= \log\left(\frac{\widetilde{\mathcal{M}}_{11}(X_{\mathrm{D}}) - \widetilde{\mathcal{M}}_{22}(X_{\mathrm{D}}) \pm \sqrt{\Delta_{\mathrm{D}}(X_{\mathrm{D}})}}{-2\widetilde{\mathcal{M}}_{12}(X_{\mathrm{D}})}\right), \\ \tilde{\varphi}_P(X_{\mathrm{D}}) &= \frac{1}{P}\log\left(\frac{\mathrm{tr}\widetilde{\mathcal{M}}(X_{\mathrm{D}}) \pm \sqrt{\Delta_D(X_{\mathrm{D}})}}{2}\right). \end{aligned} \tag{5.446}$$

All these functions are determined up to the sign in front of the square root. This freedom of choice corresponds to the branch choice of $y(x)$ in the WKB method, but here at finite $\hbar$. As we will see, in the final result for the eigenfunctions, both choices appear in a symmetric way.

By now, the only ingredients appearing in (5.426) which have not been explicitly constructed are $\partial_\hbar\varphi_Q(X)$ and its dual. They cannot be obtained by simply taking $\hbar$ derivatives of $\varphi_Q$ and $\tilde{\varphi}_P$ because we do not know their explicit $\hbar$ dependence as exact functions. We know only their $\hbar$ dependence as a large $X$ expansion, or an $\hbar$ dependent algorithm to build them in the rational case. To find an expression for $\partial_\hbar\varphi_Q(X)$ in the rational case, we basically perform a first order WKB expansion

but around $\hbar = 2\pi P/Q$ instead of $\hbar = 0$. In order to do this, let us take a total $\hbar$–derivative of equation (5.428), which is valid for any $\hbar$:

$$\begin{aligned} 0 = {} & \partial_\hbar V(X)V(qX) + V(X)\partial_\hbar V(qX) + \mathrm{i}V(X)\partial_x V(qX) \\ & - \partial_\hbar a(X)V(qX) - a(X)\partial_\hbar V(qX) - \mathrm{i}a(X)\partial_x V(qX) + \partial_\hbar b(X). \end{aligned} \tag{5.447}$$

This is the $q$–equation obeyed by the first derivative of $V$. It can be solved in the rational case. Using the notation

$$\delta(X) \equiv \frac{\partial_\hbar V}{V}(X), \tag{5.448}$$

this can be rewritten as

$$\begin{aligned} 0 = {} & \delta(qX) + \delta(X)\left(1 - \frac{a(X)}{V(X)}\right)^{-1} \\ & + \left(\mathrm{i}\partial_x \log V(qX) - \left(1 - \frac{a(X)}{V(X)}\right)^{-1} \frac{\partial_\hbar a(X)}{V(X)} + \frac{\partial_\hbar b(X)}{b(X)}\right). \end{aligned} \tag{5.449}$$

Similarly, as before, let us introduce the notations

$$\delta_k = \delta(q^k X), \tag{5.450}$$

and

$$\begin{aligned} \alpha(X) &= -\left(1 - \frac{a(X)}{v_0}\right)^{-1}, \\ \beta(X) &= -\left(\mathrm{i}\partial_x \log v_1 - \left(1 - \frac{a(X)}{v_0}\right)^{-1} \frac{\partial_\hbar a(X)}{v_0} + \frac{\partial_\hbar b(X)}{b(X)}\right). \end{aligned} \tag{5.451}$$

Up to simplification, both $\alpha(X)$ and $\beta(X)$ are of the form

$$(\text{rational of } X) \pm (\text{rational of } X) \times \sqrt{\Delta(X)}. \tag{5.452}$$

Every further manipulations will leave this structure invariant, so the final result will also be of this form. Equation (5.449) can be written as

$$0 = \delta_1 - \alpha(X)\delta_0 - \beta(X), \tag{5.453}$$

which can be treated similarly as eq. (5.430). It is formally even simpler since it is a polynomial of order 1 in the $\delta_k$ instead of order 2 (although its actual expression is uglier since $\alpha$ and $\beta$ are more complicated functions). By recursion,

$$\begin{aligned} &\alpha^{(1)}(X) = \alpha(X), \\ &\beta^{(1)}(X) = \beta(X), \\ &\delta_k - \alpha^{(k)}(X)\delta_0 - \beta^{(k)}(X) = 0. \end{aligned} \tag{5.454}$$

After shift,

$$\begin{aligned} 0 &= \delta_{k+1} - \alpha^{(k)}(qX)\delta_1 - \beta^{(qk)}(X), \\ &= \delta_{k+1} - \alpha^{(k)}(qX)\alpha(X)\delta_0 - (\beta^{(k)}(qX) + \alpha^{(k)}\beta(X)), \end{aligned} \tag{5.455}$$

from which we read out

$$\begin{pmatrix} \alpha^{(k+1)}(X) \\ \beta^{(k+1)}(X) \end{pmatrix} = \begin{pmatrix} \alpha(X) & 0 \\ \beta(X) & 1 \end{pmatrix} \begin{pmatrix} \alpha^{(k)}(qX) \\ \beta^{(k)}(qX) \end{pmatrix}. \tag{5.456}$$

From this, we get

$$\begin{pmatrix} \alpha^{(Q)}(X) \\ \beta^{(Q)}(X) \end{pmatrix} = \mathcal{A}(X) \begin{pmatrix} 1 \\ 0 \end{pmatrix}, \tag{5.457}$$

where

$$\mathcal{A}(X) = \prod_{k=0}^{Q-1} \begin{pmatrix} \alpha(q^k X) & 0 \\ \beta(q^k X) & 1 \end{pmatrix}. \tag{5.458}$$

Since we have $\delta_Q = \delta_0$, we end up with

$$0 = \delta_0 - \alpha^{(Q)}(X)\delta_0 - \beta^{(Q)}(X), \tag{5.459}$$

which is solved by

$$\delta_0 \equiv \frac{\partial_\hbar V}{V}(X) = \frac{\beta^{(Q)}(X)}{1 - \alpha^{(Q)}(X)}. \tag{5.460}$$

From the recursion (or its solution given by the matrix $\mathcal{A}$), it is easily seen that

$$\alpha^{(k)}(X) = \prod_{\ell=0}^{k-1} \alpha(q^\ell X), \tag{5.461}$$

which means that for $k = Q$, it is invariant under $q$–shifts. Also,

$$\beta^{(Q)}(X) = \sum_{k=0}^{Q-1} \beta(q^k X)\alpha^{(Q-1-k)}(q^{k+1}X), \tag{5.462}$$

where we used the convention $\alpha^{(0)}(X) = 1$. Finally, according to the second line of (5.422),

$$\partial_\hbar \varphi_Q(X) = \frac{1}{Q} \sum_{k=0}^{Q-1} \frac{\beta^{(Q)}(q^k X)}{1 - \alpha^{(Q)}(q^k X)} = \frac{1}{Q} \frac{\sum_{k=0}^{Q-1} \beta^{(Q)}(q^k X)}{1 - \alpha^{(Q)}(X)}, \tag{5.463}$$

where we used invariance of $\alpha^{(Q)}(qX)$ under $q$–shifts. We can change the order of summation, to obtain the following form, which is more useful in actual computations:

$$\partial_\hbar \varphi_Q(X) = \frac{1}{Q(1 - \alpha^{(Q)}(X))} \sum_{N=0}^{Q-1} \beta(q^N X) \left( \sum_{k=0}^{Q-1} \alpha^{(k)}(q^{N+1}X) \right). \tag{5.464}$$

The dual quantity $\partial_{\hbar_{\mathrm{D}}}\tilde{\varphi}_P(X_{\mathrm{D}})$ is of course built in the same way, where we exchange $Q$ and $P$ and use the dual quantities everywhere. In principle, we now have all the ingredients to write down (5.426) exactly. Let us remark that all these ingredients are functions which are multivalued (the sign ambiguity in front of the square-root). So we must consistently choose a branch of these functions. As we will see in the final result, both choices will contribute.

We recall that we need some conditions on the functions $f_k$ for pole cancellation, which translate to relations between $\kappa, \boldsymbol{\xi}$ and $\tilde{\kappa}, \tilde{\boldsymbol{\xi}}$. Here, we make this relation more explicit for the rational case, using the exact result for $\log V(X)$, $\psi_Q(X)$, and their duals obtained in eq. (5.445) and (5.446). As we have already seen, condition (5.420) can be rewritten as the functional relation

$$Q\varphi_Q(X,\kappa,\boldsymbol{\xi}) = P\tilde{\varphi}_P(X_{\mathrm{D}},\tilde{\kappa},\tilde{\boldsymbol{\xi}}), \tag{5.465}$$

valid for all $X$. Using results from the previous subsection, this is equivalent to

$$\mathrm{tr}\mathcal{M}(X) \pm \sqrt{\Delta(X)} = \mathrm{tr}\mathcal{M}_{\mathrm{D}}(X_{\mathrm{D}}) \pm \sqrt{\Delta_{\mathrm{D}}(X_{\mathrm{D}})}. \tag{5.466}$$

A necessary condition for this to hold is the equality of the traces for all $X$

$$\mathrm{tr}\mathcal{M}(X) = \mathrm{tr}\mathcal{M}_{\mathrm{D}}(X_{\mathrm{D}}). \tag{5.467}$$

This is a relation between two rational functions of $X^Q$ (we remind that $X_{\mathrm{D}} = X^{Q/P}$). Often, they are Laurent polynomials of $X^Q$ which are of the same order, and equating each order gives algebraic relations between $\kappa, \boldsymbol{\xi}$ and the duals $\tilde{\kappa}, \tilde{\boldsymbol{\xi}}$. More generally, these relations can always be extracted even if we have rational functions instead of Laurent polynomials. These relations are essentially the same as the ones presented in [138, 139] for local $\mathbb{P}^1 \times \mathbb{P}^1$ and local $\mathcal{B}_3$. Here, we put their procedure in a more general context. If this does not give enough conditions as in the case of full $\mathcal{B}_3$, one can use in addition the condition of equating the determinant too, or just the condition given by

$$\Delta(X) = \Delta_{\mathrm{D}}(X_{\mathrm{D}}). \tag{5.468}$$

So in the end, even that case can be dealt with using $2 \times 2$ matrices instead of the larger ones given in [139]. In any case, the relations between $\tilde{\kappa}, \tilde{\boldsymbol{\xi}}$ and $\kappa, \boldsymbol{\xi}$ are fully determined by (5.466). Let us give some examples. For local $\mathbb{P}^1 \times \mathbb{P}^1$ we have $\kappa$, and a mass parameter $m \equiv \xi_1$. We find

$$a(X) = 1 + \frac{\kappa}{X} + \frac{m}{X^2}, \qquad b(X) = \frac{q^{-1}}{X^2}. \tag{5.469}$$

The relations in some rational cases are

$$\begin{aligned}
&P=1,\,Q=1, && \tilde\kappa=\kappa,\\
& && \tilde m=m,\\
&P=1,\,Q=2, && \tilde\kappa=-\kappa^2+2(m+1),\\
& && \tilde m=m^2,\\
&P=1,\,Q=3, && \tilde\kappa=\kappa^3-3(m+1)\kappa,\\
& && \tilde m=m^3,\\
&P=2,\,Q=3, && -\tilde\kappa^2+2(\tilde m+1)=\kappa^3-3(m+1)\kappa,\\
& && \tilde m^2=m^3,\\
&P=1,\,Q=4, && \tilde\kappa=-\kappa^4+4(m+1)\kappa^2-2(m^2+1),\\
& && \tilde m=m^4,\\
&P=3,\,Q=4, && \tilde\kappa^3-3(\tilde m+1)\tilde\kappa=-\kappa^4+4(m+1)\kappa^2-2(m^2+1),\\
& && \tilde m^3=m^4.
\end{aligned} \tag{5.470}$$

For the resolved $\mathbb{C}^3/\mathbb{Z}_5$, we have $\kappa$ and another true modulus $\kappa_1\equiv\xi_1$. We find

$$a(X)=1+\frac{\kappa}{X}+\frac{\kappa_1}{X^2},\qquad b(X)=\frac{q^{-5/2}}{X^5}. \tag{5.471}$$

The relations in some rational cases are

$$\begin{aligned}
&P=1,\,Q=1, && \tilde\kappa=\kappa,\\
& && \tilde\kappa_1=\kappa_1,\\
&P=1,\,Q=2, && \tilde\kappa=-\kappa^2+2\kappa_1,\\
& && \tilde\kappa_1=\kappa_1^2,\\
&P=1,\,Q=3, && \tilde\kappa=\kappa^3-3\kappa\kappa_1,\\
& && \tilde\kappa_1=\kappa_1^3+3\kappa,\\
&P=2,\,Q=3, && -\tilde\kappa^2+2\tilde\kappa_1=\kappa^3-3\kappa\kappa_1,\\
& && \tilde\kappa_1^2=\kappa_1^3-3\kappa,\\
&P=1,\,Q=4, && \tilde\kappa=-\kappa^4+4\kappa^2\kappa_1-2\kappa_1^2,\\
& && \tilde\kappa_1=\kappa_1^4+4\sqrt{2}\kappa\kappa_1,\\
&P=3,\,Q=4, && \tilde\kappa^3-3\tilde\kappa\tilde\kappa_1=-\kappa^4+4\kappa^2\kappa_1-2\kappa_1^2,\\
& && \tilde\kappa_1^3-3\tilde\kappa=\kappa_1^4-4\sqrt{2}\kappa\kappa_1.
\end{aligned} \tag{5.472}$$

We see that here, in contrast with local $\mathbb{P}^1\times\mathbb{P}^1$, the extra parameter $\kappa_1$ does not have a trivial transformation rule. This is certainly because it is a "true" modulus, whereas $m$ in local $\mathbb{P}^1\times\mathbb{P}^1$ is a simple mass parameter.

To obtain the full eigenfunction from expression (5.426), we need to do two more steps. First, add the polynomial part in $x$, which was truncated in (5.395). Second, since we are in the hyperelliptic case, we should linearly combine it with the second part of the eigenfunction which corresponds to the second solution of WKB. This consists in taking the second branch of the function $y(x)$ when performing the small $\hbar$ WKB. It is not hard to convince oneself that in expression (5.426) this corresponds to evaluate all the ingredients of (5.426) on their second branch. For the integral expressions, the base point should not be changed (it remains at $\infty$ on the first sheet), but the path of integration should extend to the point $\bar{X}$ on the second sheet, which is the image of $X$ under the obvious involution that exchanges the two sheets of the cover. This is exactly the prescription which was used in the previous sections to build eigenfunctions from open topological string data.[12] Let us denote $\Psi(X)$ the exponential of expression (5.418). In the rational case, it is the exponential of expression (5.426). We propose that the exact eigenfunction is given by

$$\psi(X) = \mathrm{e}^{(-\mathrm{i}\hbar)^{-1}s_0(x)+s_1(x)} \left(\Psi(X) + \Psi(\bar{X})\right). \tag{5.473}$$

In the rational case, this is a completely explicit expression. The point $\bar{X}$ can be reached through different inequivalent paths when evaluating integrated expressions. Requiring single valuedness of the resulting eigenfunction, we should impose that the difference between two inequivalent integrations give $2\pi\mathrm{i} \times$ integer. In this way, the final eigenfunction will not depend on the path chosen to reach $\bar{X}$. This leads to the well known argument of monodromy invariance, which we will use to find the spectrum. Let us now proceed to the testing of this construction in some examples. We will use numerical integration to evaluate the various integrals composing the exact expressions. The eigenfunctions and eigenvalues thus obtained will be compared to purely numerical results which can be obtained using the method of section 3.2.

**Local $\mathbb{P}^1 \times \mathbb{P}^1$.** This is a genus one example, so the "fully on-shell" eigenfunctions should correspond to the on-shell eigenfunctions. In an appropriate parametrization, the mirror curve of local $\mathbb{P}^1 \times \mathbb{P}^1$ is given by the zero locus of

$$W(\mathrm{e}^x, \mathrm{e}^y) = \mathrm{e}^x + m\mathrm{e}^{-x} + \mathrm{e}^y + \mathrm{e}^{-y} + \kappa, \tag{5.474}$$

which leads to the difference equation

$$(\mathrm{e}^x + m\mathrm{e}^{-x})\psi(x) + \psi(x - \mathrm{i}\hbar) + \psi(x + \mathrm{i}\hbar) = -\kappa\psi(x). \tag{5.475}$$

[12] Although, the reasoning behind this prescription is a priori different: the sum of the two related functions comes from the contribution of two distinct saddles, as we saw in section 5.3.

If we look at this system as the quantization of some classical one dimensional system, the classically allowed region in the real phase space $(x, y)$ is non-empty for $\kappa < -2 - 2\sqrt{m}$. We will assume this regime for $\kappa$. We now build the exact eigenfunctions and quantization conditions for the spectrum using the technology developed in the previous sections.

Let us work out the self-dual case $\hbar = 2\pi$. This is the simplest possible case with $P = Q = 1$. We obtain

$$\begin{aligned}\log \Psi(X) = \frac{\mathrm{i}}{2\pi} \Bigg( & \int_\infty^X \log(X') \left( -\frac{1}{X'} + \frac{X'^2 - m}{X' \sqrt{\sigma(X')}} \right) \mathrm{d}X' \\ & + \lambda \int_\infty^X \frac{\mathrm{d}X'}{\sqrt{\sigma(X')}} + \lambda_m \int_\infty^X \frac{\mathrm{d}X'}{X' \sqrt{\sigma(X')}} \Bigg) \\ & + \frac{1}{2} \log \left( \frac{X^4}{\sigma(X)} \right),\end{aligned} \tag{5.476}$$

where

$$\sigma(X) = -4X^2 + (m + X(X + \kappa))^2 = \prod_{n=1}^4 (X - A_n). \tag{5.477}$$

In the regime of $\kappa$ we are interested in, all the branch points $A_n$ are positive real. We order them increasingly. We define the cycle $\mathcal{A}$ encircling $A_3$ and $A_4$ counterclockwise, the cycle $\tilde{\mathcal{A}}$ encircling $A_1$ and $A_2$ counterclockwise, and the cycle $\mathcal{B}$ encircling $A_2$ and $A_3$. Indeed, since we have two undetermined constants $\lambda$ and $\lambda_m$, we need three monodromy conditions for the quantization condition (two to fix the constants and one to fix the eigenvalue). Fortunately, the cycles $\mathcal{A}$ and $\tilde{\mathcal{A}}$ are inequivalent since the integral in front of $\lambda_m$ picks up a residue at the pole $X = 0$ when we deform the cycle $\mathcal{A}$ to $\tilde{\mathcal{A}}$. It is then better to consider the set $\mathcal{A}$, $\mathcal{A} + \tilde{\mathcal{A}}$ and $\mathcal{B}$ as the set of independent cycles. Let us define

$$\begin{aligned}\Pi_{A,A+\tilde{A},B} &= \oint_{\mathcal{A},\mathcal{A}+\tilde{\mathcal{A}},\mathcal{B}} \log(X) \left( -\frac{1}{X} + \frac{X^2 - m}{X \sqrt{\sigma(X)}} \right) \mathrm{d}X, \\ \Pi^{(\lambda)}_{A,A+\tilde{A},B} &= \oint_{\mathcal{A},\mathcal{A}+\tilde{\mathcal{A}},\mathcal{B}} \frac{\mathrm{d}X}{\sqrt{\sigma(X)}}, \\ \Pi^{(\lambda_m)}_{A,A+\tilde{A},B} &= \oint_{\mathcal{A},\mathcal{A}+\tilde{\mathcal{A}},\mathcal{B}} \frac{\mathrm{d}X}{X\sqrt{\sigma(X)}}.\end{aligned} \tag{5.478}$$

Monodromy invariance is expressed as

$$\begin{aligned}\log \Psi_{\mathrm{WKB}}|_{\mathcal{A}} &= \frac{\mathrm{i}}{2\pi} \left( \Pi_A + \lambda \Pi^{(\lambda)}_A + \lambda_m \Pi^{(\lambda_m)}_A \right) = 2\pi \mathrm{i} M, \\ \log \Psi_{\mathrm{WKB}}|_{\mathcal{A}+\tilde{\mathcal{A}}} &= \frac{\mathrm{i}}{2\pi} \left( \Pi_{A+\tilde{A}} + \lambda \Pi^{(\lambda)}_{A+\tilde{A}} + \lambda_m \Pi^{(\lambda_m)}_{A+\tilde{A}} \right) = 2\pi \mathrm{i} \tilde{M}, \\ \log \Psi_{\mathrm{WKB}}|_{\mathcal{B}} &= \frac{\mathrm{i}}{2\pi} \left( \Pi_B + \lambda \Pi^{(\lambda)}_B + \lambda_m \Pi^{(\lambda_m)}_B \right) = 2\pi \mathrm{i} N,\end{aligned} \tag{5.479}$$

where $M, \tilde{M}, N$ are integers. It turns out that the $A$ and $\tilde{A}$ periods are purely imaginary whereas $\lambda$ and $\lambda_m$ should be real, so this fixes $M{=}\tilde{M}{=}0$. It is actually easy to compute the periods for $\mathcal{A}+\tilde{\mathcal{A}}$. By deforming the contour and taking the residue at $X=0$, we find

$$\Pi^{(\lambda)}_{A+\tilde{A}} = 0, \qquad \Pi^{(\lambda_m)}_{A+\tilde{A}} = \frac{2\pi \mathrm{i}}{m}. \tag{5.480}$$

Also, using that $\sigma(m/X) = m^2\sigma(X)/X^4$, we find after a change of variables

$$\Pi_{A+\tilde{A}} = -2\pi \mathrm{i} \log m. \tag{5.481}$$

Then, the quantization condition for the cycle $\mathcal{A}+\tilde{\mathcal{A}}$ yields

$$\lambda_m = m \log m. \tag{5.482}$$

It turns out that the combination of $B$ periods in the third line of (5.479) is positive for our regime of $\kappa$. So the remaining two monodromy conditions give the following quantization condition:

$$\frac{\mathrm{i}}{2\pi}\left(\Pi_B - \left(\frac{\Pi_A + m\log(m)\Pi_A^{(\lambda_m)}}{\Pi_A^{(\lambda)}}\right)\Pi_B^{(\lambda)} + m\log(m)\Pi_B^{(\lambda_m)}\right) = 2\pi\mathrm{i}(n+1). \tag{5.483}$$

In the case $m=1$ we retrieve the results of [112]. By numerical computation of the periods and Newton's method for numerically solving the quantization condition, we can get the eigenvalues $\kappa_n$, $n=0,1,2,....$ Here, we list some results, which have been checked using numerical diagonalization. For $m=1$,

$$\begin{aligned} E_0 &= \log(-\kappa_0) = 2.881815429926296 78247..., \\ E_1 &= \log(-\kappa_1) = 4.254591528581993 78358..., \\ E_2 &= \log(-\kappa_2) = 5.288195307144185 47625..., \\ &\dots \end{aligned} \tag{5.484}$$

For $m=1/3$,

$$\begin{aligned} E_0 &= \log(-\kappa_0) = 2.621640980255130 43508..., \\ E_1 &= \log(-\kappa_1) = 3.988895973124651 76636..., \\ E_2 &= \log(-\kappa_2) = 5.020683177844453 69322..., \\ &\dots \end{aligned} \tag{5.485}$$

The eigenfunctions match the numerical results from hamiltonian truncation. For the case $m=1$, up to an overall phase, the eigenfunction is equivalent to the exact result of [112] and also to our on-shell results (5.263).

Let us now take $\hbar = 2\pi/3$, which is a more involved case. We have $P = 1$ and $Q = 3$. Also, $\tilde{\kappa} = \kappa^3 - 3(m+1)\kappa$, $\tilde{m} = m^3$ and $X_{\rm D} = X^3$. Let us define

$$\begin{aligned}\sigma(X) &= -4X^6 + (X^6 + X^3(\kappa^3 - 3(m+1)\kappa) + m^3)^2 \\ &\equiv \prod_{n=1}^{4}(X - A_n)(X - \mathrm{e}^{\frac{2\pi\mathrm{i}}{3}}A_n)(X - \mathrm{e}^{\frac{4\pi\mathrm{i}}{3}}A_n),\end{aligned} \tag{5.486}$$

and

$$\begin{aligned}p_1(X) &= X^8\kappa + X^7(2-2m) + X^6 m\kappa + X^5(\kappa^4 - (5+3m)\kappa^2 + 4 - 4m) \\ &\quad + X^4(-2m\kappa^3 + 6m^2\kappa + 14m\kappa) + X^3(m\kappa^4 - (5+3m)m\kappa^2 + 4m - 4m^2) \\ &\quad + X^2 m^3\kappa + X m^3(2-2m) + m^4\kappa, \\ p_2(X) &= X^4 - X^3\kappa + X^2(\kappa^2 - m - 1) - X\kappa m + m^2.\end{aligned} \tag{5.487}$$

Using (5.426) and the methods given in the previous sections to compute the different ingredients, we obtain after some simplifications:

$$\begin{aligned}\log\Psi(X) = \frac{3\mathrm{i}}{2\pi}\Bigg(&\int_\infty^X \log(X')\left(-\frac{1}{X'} + \frac{X'^6 - m^3}{X'\sqrt{\sigma(X')}}\right)\mathrm{d}X' \\ &+\lambda\int_\infty^X \frac{(\kappa^2 - m - 1)X'^2\mathrm{d}X'}{\sqrt{\sigma(X')}} + \lambda_m\int_\infty^X \frac{(m^2 - X'^3\kappa)\mathrm{d}X'}{X'\sqrt{\sigma(X')}}\Bigg) \\ &+\int_\infty^X \frac{\mathrm{i}}{2\sqrt{3}}\frac{p_1(X)}{p_2(X)\sqrt{\sigma(X)}}\mathrm{d}X' + \frac{1}{2}\log\left(\frac{X^8 p_2(X)}{\sigma(X)}\right).\end{aligned} \tag{5.488}$$

In a suitable regime, we have real positive $A_n$ which we order increasingly. As before, we define the cycle $\mathcal{A}$ encircling $A_3$ and $A_4$ counterclockwise, the cycle $\tilde{\mathcal{A}}$ encircling $A_1$ and $A_2$ counterclockwise, and the cycle $\mathcal{B}$ encircling $A_2$ and $A_3$. Here, we have an additional contribution to monodromy given by the first term of the last line. We define

$$\begin{aligned}\Pi_{A,\tilde{A},B} &= \oint_{\mathcal{A},\tilde{\mathcal{A}},\mathcal{B}}\left[\log(X)\left(-\frac{1}{X} + \frac{X^6 - m^3}{X\sqrt{\sigma(X)}}\right) + \frac{\pi}{3\sqrt{3}}\frac{p_1(X)}{p_2(X)\sqrt{\sigma(X)}}\right]\mathrm{d}X, \\ \Pi^{(\lambda)}_{A,\tilde{A},B} &= \oint_{\mathcal{A},\tilde{\mathcal{A}},\mathcal{B}}\frac{(\kappa^2 - m - 1)X^2\mathrm{d}X}{\sqrt{\sigma(X)}}, \\ \Pi^{(\lambda_m)}_{A,\tilde{A},B} &= \oint_{\mathcal{A},\tilde{\mathcal{A}},\mathcal{B}}\frac{(m^2 - X^3\kappa)\mathrm{d}X}{X\sqrt{\sigma(X)}}.\end{aligned} \tag{5.489}$$

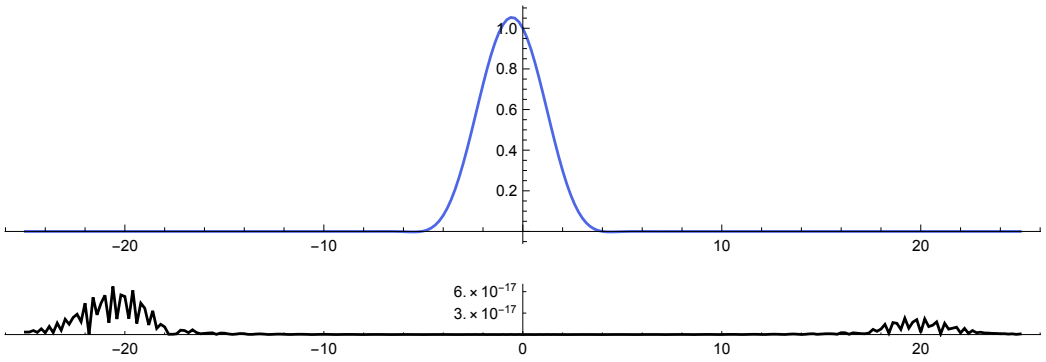


**Figure 5.12:** Local $\mathbb{P}^1 \times \mathbb{P}^1$ at $\hbar = 2\pi/3$ and $m = 1/3$: exact ground state eigenfunction (which is purely real) and the absolute difference with numerics coming from numerical diagonalization of a $200 \times 200$ matrix (rescaled to match the exact eigenfunctions at $x = 0$). For this size of the matrix, the maximal difference is of the order $10^{-17}$.

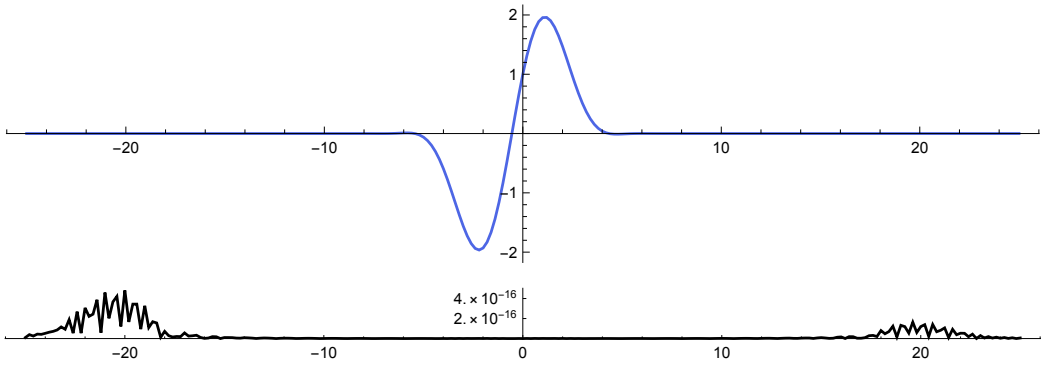


**Figure 5.13:** Local $\mathbb{P}^1 \times \mathbb{P}^1$ at $\hbar = 2\pi/3$ and $m = 1/3$: same plot as in Fig. 5.12, for the first excited state. The maximal difference is of the order $10^{-16}$.

Monodromy invariance is expressed as

$$\begin{aligned}
\log \Psi_{\mathrm{WKB}}|_{\mathcal{A}} &= \frac{3\mathrm{i}}{2\pi}\left(\Pi_A + \lambda \Pi_A^{(\lambda)} + \lambda_m \Pi_A^{(\lambda_m)}\right) = 2\pi \mathrm{i} M, \\
\log \Psi_{\mathrm{WKB}}|_{\tilde{\mathcal{A}}} &= \frac{3\mathrm{i}}{2\pi}\left(\Pi_{\tilde{A}} + \lambda \Pi_{\tilde{A}}^{(\lambda)} + \lambda_m \Pi_{\tilde{A}}^{(\lambda_m)}\right) = 2\pi \mathrm{i} \tilde{M}, \\
\log \Psi_{\mathrm{WKB}}|_{\mathcal{B}} &= \frac{3\mathrm{i}}{2\pi}\left(\Pi_B + \lambda \Pi_B^{(\lambda)} + \lambda_m \Pi_B^{(\lambda_m)}\right) = 2\pi \mathrm{i} N.
\end{aligned} \tag{5.490}$$

Again, the $A$ and $\tilde{A}$ periods are purely imaginary, so $M = \tilde{M} = 0$ and the first two equations determine $\lambda, \lambda_m$. The last line gives the quantization condition, which again can be written as

$$\frac{3\mathrm{i}}{2\pi}\left(\Pi_B - \left(\frac{\Pi_A + m\log(m)\Pi_A^{(\lambda_m)}}{\Pi_A^{(\lambda)}}\right)\Pi_B^{(\lambda)} + m\log(m)\Pi_B^{(\lambda_m)}\right) = 2\pi\mathrm{i}(n+1), \quad (5.491)$$

for $n = 0, 1, 2, \ldots$ Numerical implementation of the integration and then solving the quantization condition yields the spectrum. Here are some examples, which have been checked in the usual way. For $m = 1$,

$$\begin{aligned} E_0 &= \log(-\kappa_0) = 1.90354643917859092548..., \\ E_1 &= \log(-\kappa_1) = 2.61019754103359928676..., \\ E_2 &= \log(-\kappa_2) = 3.17373350397478965748..., \\ &\ldots \end{aligned} \quad (5.492)$$

For $m = 1/3$,

$$\begin{aligned} E_0 &= \log(-\kappa_0) = 1.653431255487499979601..., \\ E_1 &= \log(-\kappa_1) = 2.351194617546936444270..., \\ E_2 &= \log(-\kappa_2) = 2.911361623248592459660..., \\ &\ldots \end{aligned} \quad (5.493)$$

Let us mention that the quantization expression (5.491) is really an exact resummation of the conjectural quantization condition of [18, 31]. We can also test the eigenfunction given by formula (5.473). The symmetric sum in (5.473) as well as monodromy invariance ensure that the final eigenfunction is free of branch points, and single valued and analytic on the $X$ plane (at least in a strip of the $X$ plane containing the positive real line). Examples of exact eigenfunctions can be seen in Fig. 5.12 and Fig. 5.13. The difference between the exact results and the purely numerical results decrease as we increase the size of the numerical truncated hamiltonian. In Fig. 5.14, we show the importance of monodromy invariance in our construction: we compare an eigenfunction which is on-shell against the evaluation of our expression for the eigenfunction for a generic value of $\kappa$. When $\kappa$ is generic, monodromy invariance is not ensured, and our expression develops a singularity. Then, it is not a good eigenfunction for the difference equation. The true off-shell eigenfunction should be built as in section 5.4, using the full TS/ST conjecture extended to eigenfunctions. This involves an extra ingredient, the topological wavefunction, which would presumably contribute with something rendering the eigenfunction monodromy invariant and singularity free for *any* $\kappa$ (in the self-dual case, this was given by theta functions).

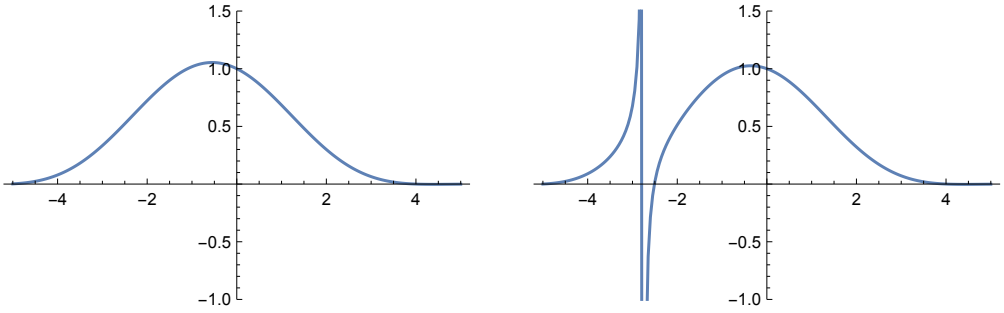


**Figure 5.14:** Local $\mathbb{P}^1 \times \mathbb{P}^1$ at $\hbar = 2\pi/3$ and $m = 1/3$: On the left, the eigenfunction computed using $\kappa = \kappa_0 \approx -5.22487$ (on-shell value), on the right, the same function computed for a generic value $\kappa = -5.5$ (off-shell value). Our expression for the eigenfunction is singular when off-shell.

Let us now look at the resolved $\mathbb{C}^3/\mathbb{Z}_5$ geometry, which is the simplest genus two example. This is interesting, since we have a second true modulus $\kappa_1$. In an appropriate parametrization, its mirror curve is given by

$$W(\mathrm{e}^x, \mathrm{e}^y) = \mathrm{e}^x + \mathrm{e}^y + \mathrm{e}^{-3x-y} + \kappa_1 \mathrm{e}^{-x} + \kappa, \tag{5.494}$$

which leads to the difference equation

$$(\mathrm{e}^x + \kappa_1 \mathrm{e}^{-x})\psi(x) + \psi(x - \mathrm{i}\hbar) + \mathrm{e}^{-\frac{3\mathrm{i}\hbar}{2}} \mathrm{e}^{-3x} \psi(x + \mathrm{i}\hbar) = -\kappa\psi(x). \tag{5.495}$$

Doing the analysis as in the previous examples in order to find a good regime of $\kappa$ in terms of $\kappa_1$ is more involved. We will restrict ourselves to the regime where $\kappa$ is negative with large absolute value and $\kappa_1$ is positive, since it was found to be the good regime from the point of view of the underlying cluster integrable system [18].

Let us look at the case $\hbar = \pi$. We have $P = 1$ and $Q = 2$, so the relations between the parameters are $\tilde{\kappa} = -\kappa^2 + 2\kappa_1$ and $\tilde{\kappa}_1 = \kappa_1^2$. We obtain

$$\begin{aligned} \log \Psi(X) = \frac{\mathrm{i}}{\pi} \Bigg( & \int_\infty^X \log X' \left( -\frac{5}{2X'} + \frac{X'(5X'^4 + 3X'^2(-\kappa^2 + 2\kappa_1) + \kappa_1^2}{2\sqrt{\sigma(X')}} \right) \mathrm{d}X' \\ & + \lambda \int_\infty^X \frac{-2\kappa X'^3 \mathrm{d}X'}{\sqrt{\sigma(X')}} + \lambda_1 \int_\infty^X \frac{2X'(X'^2 + \kappa_1)\mathrm{d}X'}{\sqrt{\sigma(X')}} \Bigg) \\ & + \int_\infty^X \frac{\mathrm{i}}{2} \frac{5X'^2 - 3X'\kappa + \kappa_1}{(X'^2 - X'\kappa + \kappa_1)\sqrt{\sigma(X')}} \mathrm{d}X' + \frac{1}{2} \log \left( \frac{X^{10}(X^2 - X\kappa + \kappa_1)}{\sigma(X)} \right), \end{aligned} \tag{5.496}$$

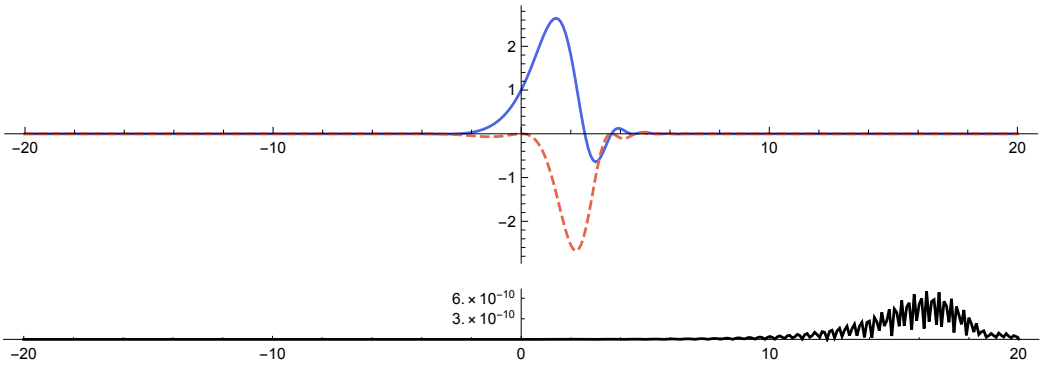


**Figure 5.15:** Local $\mathbb{C}^3/\mathbb{Z}_5$ at $\hbar = \pi$: exact $(0,0)$ eigenfunction (real part in blue and imaginary part in red dashed) and the absolute difference with numerics coming from numerical diagonalization of a $250 \times 250$ matrix (rescaled to match the exact eigenfunctions at $x = 0$). For this size of the matrix, the maximal difference is of the order $10^{-9}$.

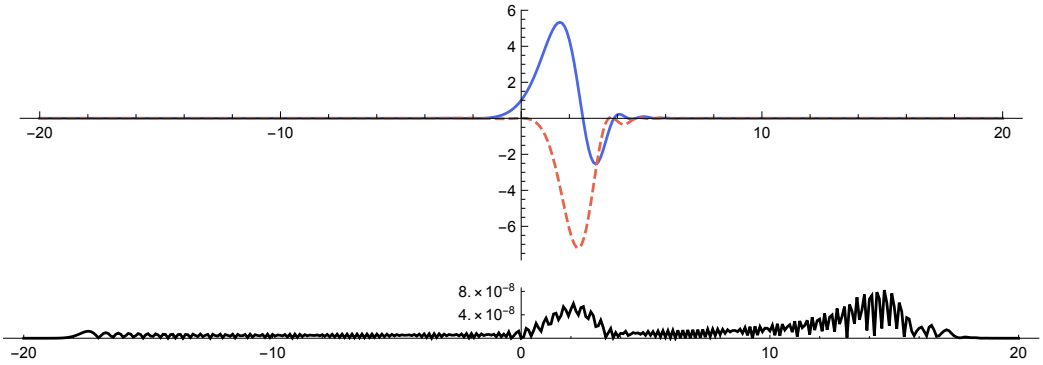


**Figure 5.16:** Local $\mathbb{C}^3/\mathbb{Z}_5$ at $\hbar = \pi$: same plot as in Fig. 5.15 for the exact $(0,1)$ eigenfunction. The maximal difference is of the order $10^{-8}$.

with

$$\begin{aligned}\sigma(X) &= -4X^2 + X^4(X^4 + (-\kappa^2 + 2\kappa_1)X^2 + \kappa_1^2)^2 \\ &\equiv X^2 \prod_{n=1}^{5}(X - A_n)(X + A_n).\end{aligned} \tag{5.497}$$

In our case, the branch points $A_n$ are positive real and we order them increasingly. We define the $\mathcal{A}_1$ cycle to be the one that encircles $A_4$ and $A_5$ counterclockwise,

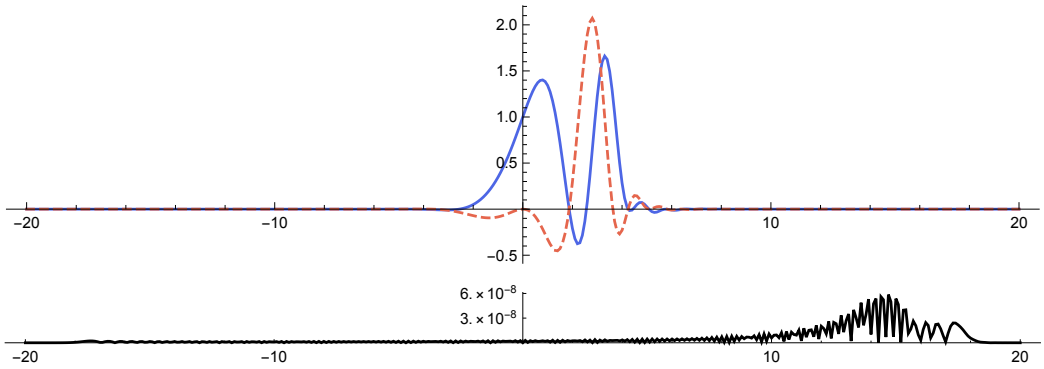


**Figure 5.17:** Local $\mathbb{C}^3/\mathbb{Z}_5$ at $\hbar = \pi$: same plot as in Fig. 5.15 for the exact $(1,0)$ eigenfunction. The maximal difference is of the order $10^{-8}$.

the $\mathcal{A}_2$ cycle encircling $A_2$ and $A_3$ counterclockwise. We also define the $\mathcal{B}_1$ cycle encircling $A_1$ and $A_4$, and the $\mathcal{B}_2$ cycle encircling $A_1$ and $A_3$. For a cycle $\mathcal{C} \in \{\mathcal{A}_1, \mathcal{A}_2, \mathcal{B}_1, \mathcal{B}_2\}$, we define

$$\begin{aligned}
\Pi_{\mathcal{C}} &= \oint_{\mathcal{C}} \left[ \log X \left( -\frac{5}{2X} + \frac{X(5X^4 + 3X^2(-\kappa^2 + 2\kappa_1) + \kappa_1^2}{2\sqrt{\sigma(X)}} \right) \right. \\
&\qquad \left. + \frac{\pi}{2} \frac{5X^2 - 3X\kappa + \kappa_1}{(X^2 - X\kappa + \kappa_1)\sqrt{\sigma(X)}} \right] \mathrm{d}X, \\
\Pi_{\mathcal{C}}^{(\lambda)} &= \oint_{\mathcal{C}} \frac{-2\kappa X^3 \mathrm{d}X}{\sqrt{\sigma(X)}}, \\
\Pi_{\mathcal{C}}^{(\lambda_1)} &= \oint_{\mathcal{C}} \frac{2X(X^2 + \kappa_1)\mathrm{d}X}{\sqrt{\sigma(X)}}.
\end{aligned} \tag{5.498}$$

Then, by monodromy invariance along all the periods, we have to solve

$$\begin{aligned}
\frac{\mathrm{i}}{\pi} \left( \Pi_{\mathcal{A}_i} + \lambda \Pi_{\mathcal{A}_i}^{(\lambda)} + \lambda_1 \Pi_{\mathcal{A}_i}^{(\lambda_1)} \right) &= 2\pi \mathrm{i} M_i, \qquad i = 1, 2, \\
\frac{\mathrm{i}}{\pi} \left( \Pi_{\mathcal{B}_i} + \lambda \Pi_{\mathcal{B}_i}^{(\lambda)} + \lambda_1 \Pi_{\mathcal{B}_i}^{(\lambda_1)} \right) &= 2\pi \mathrm{i} N_i, \qquad i = 1, 2.
\end{aligned} \tag{5.499}$$

From reality considerations, we find that $M_1 = M_2 = 0$, so

$$\begin{pmatrix} \lambda \\ \lambda_1 \end{pmatrix} = - \begin{pmatrix} \Pi_{\mathcal{A}_1}^{(\lambda)} & \Pi_{\mathcal{A}_1}^{(\lambda_1)} \\ \Pi_{\mathcal{A}_2}^{(\lambda)} & \Pi_{\mathcal{A}_2}^{(\lambda_1)} \end{pmatrix}^{-1} \begin{pmatrix} \Pi_{\mathcal{A}_1} \\ \Pi_{\mathcal{A}_2} \end{pmatrix}. \tag{5.500}$$

Then, the two equations in the second line of (5.499) give the quantization conditions

for $\kappa$ and $\kappa_1$. Let us define $N_1 = n_1 + n_2 + 2$, and $N_2 = n_2 + 1$. We find

$$\begin{aligned}
&(n_1, n_2) = (0, 0), && (\kappa, \kappa_1)_{0,0} = (\ -12.108260493297777783...,\ 14.559207122129454382...),\\
&(n_1, n_2) = (1, 0), && (\kappa, \kappa_1)_{1,0} = (\ -25.786257255292478834...,\ 19.332115669949562433...),\\
&(n_1, n_2) = (0, 1), && (\kappa, \kappa_1)_{0,1} = (\ -17.514284419555278234...,\ 40.988214882454531661...),\\
&\quad \dots
\end{aligned} \tag{5.501}$$

and so on. The case $(n_1, n_2) = (1, 0)$ has been computed in [18] through other means, and our result matches that result. Some eigenfunctions and the comparison with numerical results can be seen in Fig. 5.15, 5.16 and 5.17. We find good agreement for both eigenvalues and eigenfunctions. For our eigenfunction to make sense in our construction, we need to have monodromy invariance around all the periods. As we saw above, this fixes specific values for both $\kappa$ and $\kappa_1$. The discrete set of pairs $(\kappa, \kappa_1)$ that we find here are actually exactly those which correspond to the spectrum of the underlying cluster integrable system, in our case composed of two mutually commuting hamiltonians which are both quantized [18].

# Chapter 6

# Quantum curves as quantum distributions

In the last three chapters, we defined and analysed spectral problems arising from the quantization of mirror curves $W(\mathrm{e}^x, \mathrm{e}^y) = 0$, and studied their relationship with enumerative data of the underlying geometry (as computed by topological strings). It would be tempting to say that the spectral problem defines a *quantum mirror curve*, i.e. that it quantizes the geometry given by the mirror curve. But what could possibly be meant by this? Intuitively, we would expect a quantum object which would, in a certain semiclassical limit, display some sort of quantum fluctuations around the classical curve; and reduce to it in the strict classical limit

This is typically what happens in elementary quantum mechanics. Let us take a Hamiltonian for a one dimensional mechanical system. It is a function $H(x, p)$ on phase space, and the curve in phase space defining the classical motion of energy $E$ is given be the submanifold

$$H(x, p) = E \tag{6.1}$$

This can be regarded as the classical geometry of the system. What would be a good notion of the quantum version of this curve? The typical answer is to appropriately quantize the Hamiltonian, and thus write the operator version of (6.1) which is the time independent Schrödinger equation on a Hilbert space,

$$\mathsf{H}|\psi\rangle = E|\psi\rangle. \tag{6.2}$$

The drawback of formulating the quantum problem in terms of operators is that the classical limit, and in particular the curve $H(x, p) = E$, is not easy to recover. This is due to the conceptual mismatch between operators on a Hilbert space and functions on phase space. However, there is another route to quantization that could

be taken instead: the phase space formulation of quantum theories (overviews can be found in [140, 141]). The characteristic feature of this formulation of quantum mechanics is that the quantum objects are distributions on phase space, rather than operators and vectors in an abstract Hilbert space. Therefore, classical objects are retrieved straightforwardly in the small $\hbar$ limit. In particular, the classical curve (6.1) is retrieved as a limiting support of a quantum distribution.

Using phase space formulation and Wigner distributions to describe quantum geometry has been proved a rather fruitful approach for various problems related to quantum gravity, as for example in [142–144] to study the Hartle–Hawking wavefunction of the universe [145]. Closer to this work, in non-critical string theory, the so called FZZT brane wavefunction has been studied in [146, 147] using the Wigner distribution, this description giving a notion of "quantum Riemann surface" arising from associated double-scaled matrix models [119, 148]. The FZZT brane can also be modelled as a system of fermions [75]. In a slightly different context, in type IIB superstring theory, some classical backgrounds can be modelled using two dimensional curves, interpreted as the Fermi surfaces for a dual system of non-interacting fermions [149, 150]. The quantum distributions associated to these Fermi droplets have been used in [151] to understand the emergence of classical geometry from the quantum system (see [152–154] for further developments along these lines). We see that, somehow, fermions tend to enter the game of probing quantum geometry using dual quantum systems.

In the case of mirror curves of CY threefolds and their associated spectral problems, we saw in the previous chapters that the geometric description (in terms of topological string data) rather arises in the 't Hooft limit, so for $\hbar \to \infty$ instead of 0. The matrix models for $Z(N, \hbar)$ associated to our mirror curves are easily interpreted as partition functions for a gas of non-interacting fermions at finite temperature with a non-standard one particle density matrix, which is precisely given by the operator $\rho$. Through the TS/ST conjecture [2], this provides a Fermi gas description of topological strings on toric CY threefolds.

As in [151], we will study a well known statistical observable, the reduced one-particle density matrix of the Fermi gas. We will give evidence that in the "classical" limit, its Wigner transform gives a distribution with support on the classical mirror curve, plus quantum fluctuations. Arguably, it can then be taken as a precise definition for the quantum geometry of the mirror curve. Interestingly, the involved "classical" limit is not the standard semiclassical limit of the Fermi gas ($\hbar \to 0$), but rather a strong quantum coupling limit ($\hbar \to \infty$), more precisely the 't Hooft limit. In other words, what we have is a quantum system with a dual geometric description emerging in the limit of strong quantum coupling and large number of

degrees of freedom. It turns out that for the Fermi gas description of our quantized mirror curves, the 't Hooft limit corresponds to the classical and zero temperature limit in some dual variables. This is related to the modular duality structure of our operators, which we pointed out in the previous section.

We will first introduce the Fermi gas description related to our spectral problem, in particular the reduced one particle density matrix. The Wigner distribution of highly excited states for one dimensional systems has a universal leading quantum fluctuation pattern first found by Berry [155]. For the reduced density matrix the corresponding universal pattern was found by Balazs–Zipfel [23]. We will propose a slightly improved version of this result, that we will derive for the prototypical example of the one dimensional quantum harmonic oscillator. Then, we will turn our attention to quantum mirror curves. We will first give evidence that the 't Hooft limit encodes the classical geometry given by the mirror curve, which can be obtained purely from spectral data. The classical mirror curve emerges as the boundary of the support of the Wigner transformed reduced density matrix. We will then argue through numerical examples that the leading behaviour of the quantum oscillations follow the improved Balazs-Zipfel approximation. We also show how this result can be obtained from a direct computation for the local $\mathbb{P}^1 \times \mathbb{P}^1$ geometry.

This chapter is based on [22].

## 6.1 Classical and quantum geometry in Fermi gases

Let us start by reviewing the thermodynamics of non-interacting Fermi gases. We consider a system of $N$ non-interacting fermions, with total Hamiltonian

$$\mathsf{H}_N = \sum_{i=1}^{N} \mathsf{H}(i), \tag{6.3}$$

where $\mathsf{H}(i)$ is the one particle Hamiltonian for the $i^{\text{th}}$ particle. We assume that $\mathsf{H}$ has a discrete, infinite spectrum. This is the case for example in the presence of a confining potential. We denote $\{|\varphi_n\rangle\}_{n=0,1,2\ldots}$ the orthonormal basis of eigenfunctions for the one-particle Hilbert space, satisfying

$$\mathsf{H}|\varphi_n\rangle = E_n|\varphi_n\rangle, \tag{6.4}$$

where $E_n$ is the eigenvalue for the $n^{\text{th}}$ state. We will write $\varphi_n(x)$ for the state $|\varphi_n\rangle$ in the position representation $\varphi_n(x) = \langle x|\varphi_n\rangle$. The multi-particle states are Slater determinants given by

$$|\Psi_{\mathbf{k}}\rangle = \frac{1}{\sqrt{N!}} \sum_{\sigma\in S_N} (-1)^{\epsilon(\sigma)} \bigotimes_{i=1}^{N} |\varphi_{k_{\sigma(i)}}\rangle, \tag{6.5}$$

where $S_N$ is the permutation group of $N$ elements and $(-1)^{\epsilon(\sigma)}$ is the parity of the permutation $\sigma \in S_N$. The vector $\mathbf{k} = (k_1, \dots, k_N)$ is a set of strictly increasing non-negative integers labelling the level of the $i^{\text{th}}$ (indistinguishable) fermionic particle for $i = 1, \dots N$. In coordinate representation where we project on the state $|x_1\rangle \otimes \cdots \otimes |x_N\rangle$, this can be written as

$$\Psi_{\mathbf{k}}(x_1, \dots, x_N) = \frac{1}{\sqrt{N!}} \det_{i,j=1,\dots,N} \varphi_{k_j}(x_i). \tag{6.6}$$

The ground state is given by the state where the $N$ first energy levels are occupied, and will be denoted by the label 0:

$$|\Psi_0\rangle = \frac{1}{\sqrt{N!}} \sum_{\sigma \in S_N} (-1)^{\epsilon(\sigma)} |\varphi_{\sigma(1)}\rangle \otimes \cdots \otimes |\varphi_{\sigma(N)}\rangle. \tag{6.7}$$

The unnormalized canonical density matrix of the Fermi gas of $N$ particles at inverse temperature $\beta$ is

$$\begin{aligned} \rho_N &= \mathrm{e}^{-\beta \mathsf{H}_N} \\ &= \sum_{\substack{\mathbf{k} \in \mathbb{Z}^N_{\geq 0}, \\ k_1 < \dots < k_N}} |\Psi_{\mathbf{k}}\rangle\langle\Psi_{\mathbf{k}}| \mathrm{e}^{-\beta \sum_{i=1}^N E_{k_i}}. \end{aligned} \tag{6.8}$$

This is written in position representation as

$$\begin{aligned} &\rho_N(x_1, \dots, x_N, x'_1, \dots, x'_N) \\ &\qquad = \frac{1}{N!} \sum_{\substack{\mathbf{k} \in \mathbb{Z}^N_{\geq 0}, \\ k_1 < \dots < k_N}} \mathrm{e}^{-\beta \sum_{j=1}^N E_{k_j}} \left( \det_{i,j=1,\dots,N} \varphi^*_{k_j}(x'_i) \right) \left( \det_{i,j=1,\dots,N} \varphi_{k_j}(x_i) \right), \end{aligned} \tag{6.9}$$

where $\varphi^*_k(x)$ is the complex conjugate of $\varphi_k(x)$. Using an infinite version of the Cauchy–Binet formula, this can be simplified to

$$\rho_N(x_1, \dots, x_N, x'_1, \dots, x'_N) = \frac{1}{N!} \det_{i,j=1,\dots,N} \rho(x_i, x'_j), \tag{6.10}$$

where $\rho(x_i, x'_j)$ is the unnormalized single particle density matrix

$$\rho = \mathrm{e}^{-\beta \mathsf{H}} \tag{6.11}$$

in the position representation. This simplification occurs because the fermions are non-interacting. The canonical partition function of the Fermi gas is the trace of its $N$ particle density matrix:

$$\begin{aligned} Z(N) &= \operatorname{tr}(\rho_N) \\ &= \sum_{\substack{\mathbf{k} \in \mathbb{Z}^N_{\geq 0}, \\ k_1 < \dots < k_N}} \mathrm{e}^{-\beta \sum_{i=1}^N E_{k_i}}. \end{aligned} \tag{6.12}$$

In position representation, this becomes

$$Z(N) = \frac{1}{N!}\int_{\mathbb{R}^N} \mathrm{d}x_1 \cdots \mathrm{d}x_N \det_{i,j=1,\ldots,N} \rho(x_i, x_j), \tag{6.13}$$

which is precisely the expression of the coefficients $Z(N)$ of the Fredholm determinant of the operator $\rho$. Therefore, the fermionic trace defined in eq. (3.23) is precisely the canonical partition function of a gas of $N$ non-interacting fermions at $\beta = 1$ with the unnormalized single particle density function $\rho$ given by the inverse of the quantized mirror curve $\rho = \mathsf{O}^{-1}$. This was precisely the point of view taken in [4] in the different but related context of ABJ(M) and other quiver Chern–Simons–matter matrix models. Also, the Fermi gas interpretation of the TS/ST correspondence was already prominent in [2]. The grand canonical partition function of the Fermi gas at chemical potential $\mu = \log \kappa$ is given by

$$\Xi(\kappa) = 1 + \sum_{N=1}^{\infty} \kappa^N Z(N). \tag{6.14}$$

This is precisely the expression for the Fredholm determinant itself, see eq. (3.20-3.22). Another interesting quantity related to many-body systems is the *reduced one-particle density matrix*. It is essentially given by integrating out $N-1$ particles in the $N$ particle density matrix (6.10). Its unnormalized version is

$$\begin{aligned} \rho_1^{(N)}(x, x') &= N \int_{\mathbb{R}^{N-1}} \mathrm{d}^{N-1}t \; \rho_N(x, t_1, \ldots, t_{N-1}, x', t_1, \ldots, t_{N-1}) \\ &= \frac{1}{(N-1)!}\int_{\mathbb{R}^{N-1}} \mathrm{d}^{N-1}t \; \rho \begin{pmatrix} x & t_1 & \ldots & t_{N-1} \\ x' & t_1 & \ldots & t_{N-1} \end{pmatrix}, \end{aligned} \tag{6.15}$$

where we used the notation defined in eq. (3.24). Comparing with (3.33), we find that

$$\rho_1^{(N)}(x, x') = B_{N-1}(x, x'). \tag{6.16}$$

Its normalized version is given by

$$C_N(x, x') = \frac{1}{NZ(N)} \rho_1^{(N)}(x, x'). \tag{6.17}$$

It will be our basic observable in the following. Using "second quantization" notation often used in many-body physics, this can also be defined as

$$C_N(x, y) = \frac{1}{N} \mathrm{Tr}\left(\hat{\rho}_N \, \hat{\psi}^\dagger(y)\hat{\psi}(x)\right), \tag{6.18}$$

where $\hat{\rho}_N$ is the normalized canonical density matrix, and $\hat{\psi}^\dagger(x), \hat{\psi}(x)$ are standard creation/annihilation operators for fermions in the position state $|x\rangle$ (see e.g. [156]). The reduced one-particle density matrix is normalized:

$$\int_{\mathbb{R}} C_N(x, x)\mathrm{d}x = 1, \tag{6.19}$$

and the probabilistic interpretation of $C_N(x,x)$ is clear from its definition: it is the probability density of finding a fermion at position $x$ in the presence of $N-1$ other fermions, at inverse temperature $\beta$. In the zero temperature limit ($\beta \to \infty$), the non-interacting Fermi gas is in the state (6.7), and we find

$$C_N(x,x') = \frac{1}{N}\sum_{i=0}^{N-1} \varphi_i^*(x')\varphi_i(x). \tag{6.20}$$

A useful formula valid for the non-interacting case is Landsberg's recursion formula (see e.g. [157]), which implies

$$\rho_1^{(N)}(x,x') = \sum_{\ell=1}^{N} (-1)^{\ell-1}\rho^\ell(x,x')Z(N-\ell). \tag{6.21}$$

It is not too hard to derive. Using the following decomposition of the determinant,

$$\begin{aligned}
\rho\begin{pmatrix} x & t_1 & \dots & t_{N-1} \\ x' & t_1 & \dots & t_{N-1}\end{pmatrix} &= \rho(x,x') \sum_{\sigma\in S_{N-1}} (-1)^\sigma \prod_{i=1}^{N-1} \rho(t_i, t_{\sigma(i)}) \\
&+ \sum_{k_1=1}^{N-1} \rho(x,t_{k_1})\rho(t_{k_1},x') \sum_{\sigma\in S_{N-2}} (-1)(-1)^\sigma \prod_{i=1}^{N-2} \rho(\tilde{t}_i, \tilde{t}_{\sigma(i)}) \\
&+ \sum_{k_1\neq k_2} \rho(x,t_{k_1})\rho(t_{k_1},t_{k_2})\rho(t_{k_2},x') \sum_{\sigma\in S_{N-3}} (-1)^2(-1)^\sigma \prod_{i=1}^{N-3} \rho(\tilde{t}_i, \tilde{t}_{\sigma(i)}) \\
&+ \dots \\
&+ \sum_{k_1\neq k_2\neq \dots \neq k_{N-1}} \rho(x,t_{k_1})\rho(t_{k_1},t_{k_2})\cdots\rho(t_{k_{N-1}},x')(-1)^{N-1}
\end{aligned} \tag{6.22}$$

(where the $\tilde{t}_i$ in each line are those $t_i$ not appearing in the product of $\rho$ before the sums over $\sigma$) and integrating it over $t_1,\dots,t_{N-1}$, we find

$$(N-1)!\rho_1^{(N)}(x,x') = \sum_{\ell=1}^{N} \frac{(N-1)!}{(N-\ell)!}\rho^\ell(x,x')(-1)^{\ell-1}(N-\ell)!Z(N-\ell), \tag{6.23}$$

which is equivalent to (6.21). Using this relation as well as

$$\rho(x,x') = \sum_{n=0}^{\infty} \mathrm{e}^{-\beta E_n}\varphi_n^*(x')\varphi_n(x), \tag{6.24}$$

we obtain a useful representation for the reduced density matrix,

$$C_N(x,x') = \sum_{n=0}^{\infty} c_n^{(N)}\varphi_n^*(x')\varphi_n(x), \tag{6.25}$$

where the coefficients $c_n^{(N)}$ are given by

$$c_n^{(N)} = \frac{1}{NZ(N)} \sum_{\ell=1}^{N} (-1)^{\ell-1} \mathrm{e}^{-\ell\beta E_n} Z(N-\ell). \tag{6.26}$$

They are totally determined by the spectrum of $\rho$. Note that (6.19) implies

$$\sum_{n=0}^{\infty} c_n^{(N)} = 1. \tag{6.27}$$

We can also write these coefficients in terms of the occupation numbers $n_\ell \in \{0, 1\}$ of the energy levels (see e.g. [158]),

$$c_k^{(N)} = \frac{1}{N} \frac{\sum_{\{n_\ell\}} n_k \mathrm{e}^{-\beta \sum_\ell n_\ell E_\ell}}{\sum_{\{n_\ell\}} \mathrm{e}^{-\beta \sum_\ell n_\ell E_\ell}}. \tag{6.28}$$

The sums are over all the states labelled by occupation numbers $\{n_\ell\}$ such that $\sum_{\ell=0}^{\infty} n_\ell = N$. From this expression it is obvious that, in the limit of zero temperature, the $c_k^{(N)}$ have the following behavior

$$c_k^{(N)} \to \begin{cases} 1/N & \text{if } 0 \le k \le N-1, \\ 0 & \text{if } k \ge N. \end{cases} \tag{6.29}$$

Therefore, (6.25) is the generalization of (6.20) to the finite temperature case. We can also construct the grand canonical version of the reduced one-particle density matrix at chemical potential $\mu = \log \kappa$:

$$\rho_1^{\mathrm{GC}}(x, x'; \kappa) = \sum_{N=1}^{\infty} \rho_1^{(N)}(x, x') \kappa^N. \tag{6.30}$$

Using relation (6.21), and changing the order of summation, we find

$$\rho_1^{\mathrm{GC}}(x, x'; \kappa) = \kappa \Xi(\kappa) \langle x | \mathsf{R} | x' \rangle, \tag{6.31}$$

where

$$\mathsf{R} = \frac{1}{\mathrm{e}^{\beta \mathsf{H}} + \kappa} = \frac{\rho}{1 + \kappa\rho}. \tag{6.32}$$

This is precisely the resolvent operator of eq. (3.26). Therefore, its integral kernel is

$$R(x, x'; \kappa) = \langle x | \mathsf{R} | x' \rangle = \frac{1}{\kappa \Xi(\kappa)} \rho_1^{\mathrm{GC}}(x, x'; \kappa, \beta). \tag{6.33}$$

This confirms relation (6.16) through the expansion of $D(x, x'; \kappa) = \Xi(\kappa) R(x, x'; \kappa)$ given in (3.32).

We wish to define an appropriate notion of quantum geometry associated to the classical curve given by the single particle Hamiltonian $H(x,p) = E$. Concretely, we wish to have a quasi-probability distribution on phase space which becomes "localized" on the classical curve in the classical limit. A good candidate is the Wigner distribution of the reduced one-particle density matrix $C_N(x,x')$. But before studying this object, let us recall that the Wigner transform of an eigenstate $\varphi_n(x)$ of the quantum Hamiltonian $\mathsf{H}$ is given by

$$f_n(x,p) = \frac{1}{2\pi\hbar}\int_{\mathbb{R}} \varphi_n^*\left(x+\frac{y}{2}\right)\varphi_n\left(x-\frac{y}{2}\right)\mathrm{e}^{\frac{\mathrm{i}}{\hbar}py}\mathrm{d}y. \tag{6.34}$$

To understand the semiclassical limit of the Wigner distribution, we have to look at highly excited states $n \gg 1$, as expected from WKB analysis. In the leading WKB approximation, the energy levels are given by the Bohr–Sommerfeld approximation

$$I(E) = \hbar\left(n+\frac{1}{2}\right), \qquad n = 0,1,\dots \tag{6.35}$$

In this equation, $I(E)$ is the classical action variable, which is obtained as follows. Let $\mathcal{R}$ be the region in phase space inside the curve (6.1), and let $\mathcal{C}$ be a path along the boundary of $\mathcal{R}$. Then,

$$I(E) = \frac{1}{2\pi}\oint_{\mathcal{C}} p(x)\mathrm{d}x, \tag{6.36}$$

and it is proportional to the volume of the region $\mathcal{R}$. Let us now consider the double-scaling limit

$$n\to\infty, \qquad \hbar\to 0, \qquad n\hbar = \xi \qquad \text{fixed}. \tag{6.37}$$

In this limit, the Bohr–Sommerfeld approximation becomes exact and defines implicitly a function $E(\xi)$ through

$$I(E) = \xi. \tag{6.38}$$

It turns out that the Wigner function becomes in this limit a delta function distribution concentrated on the classical curve (6.1) [155, 159]

$$f_n(x,p) \to \frac{1}{2\pi}\delta(H(x,p) - E(\xi)). \tag{6.39}$$

This limit only holds in the sense of distributions, against integration of appropriate functions (see [160] for a detailed analysis of this limit in the case of the harmonic oscillator). In fact, the Wigner function approaches a delta function in a highly non-trivial way: it decays very fast outside the classical curve, it has a peak approximately at the classical curve, and it oscillates very rapidly around zero inside the curve. At small but nonzero $\hbar$, this non-trivial structure is captured by a universal

-

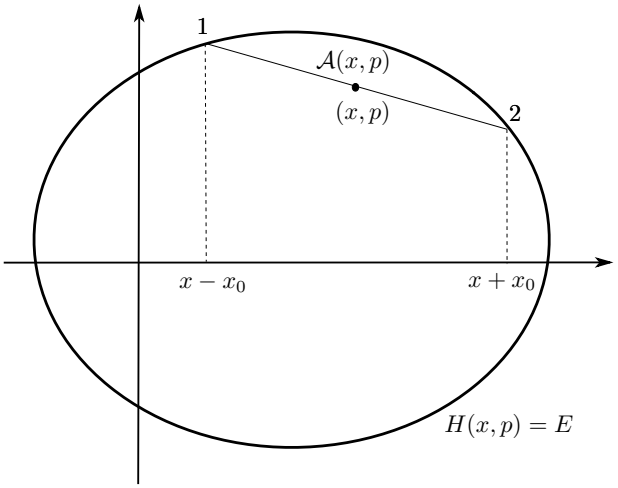


**Figure 6.1:** Berry's chord construction. The point $(x,p)$ is the midpoint of a segment (or chord) whose endpoints lie on the classical curve $H(x,p)=E$. The area of the region between the chord and the curve is denoted by $\mathcal{A}(x,p)$ and we refer to it as the area of the chord.

limiting form which was derived by Berry in [155]. To state the result of [155], let us assume that the region $\mathcal{R}$ in phase space enclosed by the curve (6.1) is simply connected and convex. The equation for the curve defines locally a function $p(x)$. Given an arbitrary point $(x,p)$ in phase space, we obtain a value of $E$ through (6.1) , therefore a value of $I$ through (6.36). This defines the function $I(x,p)=I(H(x,p))$. Suppose now that we fix $E$. For an arbitrary point $(x,p)$ inside the region $\mathcal{R}$, we define $x_0$ to be a solution of

$$p(x+x_0)+p(x-x_0)=2p. \tag{6.40}$$

If $x_0$ is a solution, $-x_0$ is a solution, too. We obtain in this way two points

$$\begin{aligned}(1)&=(x-x_0,p(x-x_0)),\\(2)&=(x+x_0,p(x+x_0)),\end{aligned} \tag{6.41}$$

which lie on the curve, see Fig. 6.1. They are both at equal distance of the point $(x,p)$. The segment joining these two points is usually called the chord through the point $(x,p)$. The area of the region between the chord and the curve will be called the *chord area*, and we will denote it by $\mathcal{A}(x,p)$. We also define

$$\Delta_{1,2}(x,p)=\partial_x I(1)\partial_p I(2)-\partial_x I(2)\partial_p I(1), \tag{6.42}$$

where (1) and (2) label the two points (6.41). Berry's formula for the uniform, semiclassical approximation to the Wigner function is given by

$$f_n(x,p) \approx \frac{\sqrt{2}}{\pi\hbar^{2/3}} \frac{(\frac{3}{2}\mathcal{A}(x,p))^{1/6}}{\sqrt{\Delta_{1,2}(x,p)}} \,\mathrm{Ai}\left[-\left(\frac{3\mathcal{A}(x,p)}{2\hbar}\right)^{2/3}\right], \tag{6.43}$$

where $\mathrm{Ai}(z)$ denotes the Airy function. The quantum number $n$ enters the r.h.s. through the energy $E_n$, which should satisfy the Bohr–Sommerfeld quantization condition (6.35). In principle, (6.43) is valid for points $(x,p)$ inside $\mathcal{R}$, where the geometric chord construction makes sense. However, one can analytically continue the function $\mathcal{A}(x,p)$ to points outside $\mathcal{R}$, where it becomes a complex number with phase $3\pi/2$, in such a way that the argument of the Airy function is positive. When $(x,p)$ is near the classical curve(6.1), one can further approximate (6.43) by the so-called "transitional approximation," given by

$$f_n(x,p) \approx \frac{1}{\pi}\left(\frac{1}{\hbar^2 B(x,p)}\right)^{1/3} \mathrm{Ai}\left[2\frac{I(x,p)-I(E_n))}{\hbar^{2/3}B^{1/3}(x,p)}\right]. \tag{6.44}$$

Here,

$$B(x,p) = I_p^2 I_{xx} + I_x^2 I_{pp} - 2I_p I_x I_{px}. \tag{6.45}$$

The formula (6.44) gives a universal scaling form for the Wigner function near the classical curve. From (6.44), (6.39) follows.

The double-scaling limit (6.37) is mathematically well-defined, but it would be nice to implement it physically. This is when the Fermi gas picture comes into play. Indeed, one way to achieve this is to consider a system of $N$ non-interacting fermions at low temperature, with one-particle Hamiltonian $\mathsf{H}(\mathsf{x},\mathsf{p})$. The Fermi exclusion principle guarantees that, in the thermodynamic limit in which $N$ is large, the edge of the Fermi sea will be in a highly excited state. The appropriate quantum distribution describing the Fermi gas is the Wigner transform of the reduced one-particle density matrix (6.18):

$$\mathcal{W}_N(x,p) = \frac{1}{2\pi\hbar}\int_{\mathbb{R}} C_N\left(x-\frac{y}{2}, x+\frac{y}{2}\right) \mathrm{e}^{\mathrm{i}py/\hbar}\mathrm{d}y. \tag{6.46}$$

At zero temperature, this distribution can be evaluated directly from (6.20) as a sum of Wigner functions,

$$\mathcal{W}_N(x,p) = \frac{1}{N}\sum_{n=0}^{N-1} f_n(x,p). \tag{6.47}$$

Let us now consider the following double-scaling limit

$$N\to\infty, \quad \hbar\to 0, \qquad N\hbar = \xi_F \qquad \text{fixed.} \tag{6.48}$$

This combines the thermodynamic limit $N \to \infty$ with the semiclassical limit of Quantum Mechanics $\hbar \to 0$. Using again the Bohr–Sommerfeld quantization condition, the limit (6.48) defines a Fermi energy $E_F$ as a function of $\xi_F$,

$$I(E_F) = \xi_F. \tag{6.49}$$

In this limit, the distribution at zero temperature (6.47) becomes a constant in the region inside the classical curve $H(x,p) = E_F$, and zero outside, i.e.

$$\mathcal{W}_N(x,p) \approx \frac{1}{2\pi I(E_F)} \Theta(E_F - H(x,p)), \tag{6.50}$$

where $\Theta$ is the Heaviside step function. This result goes back to the Thomas–Fermi approximation for fermionic systems. A recent derivation can be found in [161] (we note however that in [161] the Fermi energy is fixed using the normalization of the distribution, while in our case we use the Bohr–Sommerfeld quantization condition). The limiting behavior (6.50) shows that, in a non-interacting Fermi gas at zero temperature, there is a natural definition of "quantum geometry" based on the Wigner distribution associated with the reduced one-particle density matrix. The classical curve in phase space emerges in the double-scaling limit (6.48) as the boundary of the support of the distribution. Note that, at low but finite temperature, the Heaviside behavior in (6.50) is smoothed out by thermal fluctuations [161]. The strict classical limit of the geometry is only achieved at zero temperature.

As in the case of the Wigner function associated to a highly excited state, the limit (6.50) occurs in a non-trivial way: outside the classical curve, the distribution decays rapidly, while inside the curve we have oscillations around its average value $(2\pi I(E_F))^{-1}$. It is natural to look for analogues of (6.43) and (6.44) for the quantum distribution (6.47). The first result along this direction was obtained by Balazs and Zipfel in 1973 in [23]. The Balazs–Zipfel scaling form is valid near the classical curve, and it is given by an integrated Airy function,

$$\mathcal{W}_N(x,p) \approx \frac{1}{2\pi I(E_F)} \mathcal{I}(t_{\mathrm{BZ}}), \tag{6.51}$$

where

$$\begin{aligned} \mathcal{I}(z) &= \int_z^\infty \mathrm{Ai}(t)\mathrm{d}t \\ &= \frac{3^{1/3} z}{\Gamma\left(-\frac{1}{3}\right)} {}_1F_2\left(\frac{1}{3}; \frac{2}{3}, \frac{4}{3}; \frac{z^3}{9}\right) + \frac{3^{1/6} z^2 \Gamma\left(\frac{2}{3}\right)}{4\pi} {}_1F_2\left(\frac{2}{3}; \frac{4}{3}, \frac{5}{3}; \frac{z^3}{9}\right) + \frac{1}{3}, \end{aligned} \tag{6.52}$$

and the argument $t_{\mathrm{BZ}}$ is

$$t_{\mathrm{BZ}} = \left(\frac{2}{\hbar}\right)^{2/3} \frac{I(x,p) - I(E_F)}{I(E_F)^{1/3}}. \tag{6.53}$$

However, we have found in some examples that this result can be upgraded to a uniform approximation involving Berry's chord construction. The *improved Balazs–Zipfel approximation* to the Wigner distribution is given by,

$$\mathcal{W}_N(x,p) \approx \frac{1}{2\pi I(E_F)} \mathcal{I}\left(-\left(\frac{3\mathcal{A}(x,p)}{2\hbar}\right)^{2/3}\right), \tag{6.54}$$

where $\mathcal{A}(x,p)$ is the area of the chord associated to the classical curve $H(x,p) = E_F$. In the improved version, the scaling function remains the same, but the argument $t_{\mathrm{BZ}}$ changes. In the next section, we derive this improved result in the case of the harmonic oscillator. It is easy to check that, as $\hbar \to 0$, (6.54) gives back (6.50). One can derive from (6.54) a "transitional approximation" near the classical curve, as in (6.44), which reads,

$$\mathcal{W}_N(x,p) \approx \frac{1}{2\pi I(E_F)} \mathcal{I}\left(2\frac{I(x,p) - I(E_F))}{\hbar^{2/3} B^{1/3}(x,p)}\right). \tag{6.55}$$

In the case of the harmonic oscillator, this transitional approximation agrees with the original result of Balasz and Zipfel, but in general they are different. In the examples we have considered, (6.54) gives a better match than (6.55), which in turn is better than (6.51).

## 6.2 A simple example: the harmonic oscillator

Before turning to the case of quantum mirror curves, let us illustrate some of the notions introduced in the previous section and derive the improved Balazs–Zipfel approximation at zero temperature for the harmonic oscillator. Its classical Hamiltonian in appropriate units is

$$H(x,p) = \frac{p^2}{2} + \frac{x^2}{2}, \tag{6.56}$$

and the eigenfunctions of the quantum Hamiltonian are given by

$$\varphi_n(x) = \frac{1}{\sqrt{2\pi h_n}} \mathrm{e}^{-\frac{1}{2\hbar}x^2} p_n(x), \qquad n = 0, 1, 2, \cdots, \tag{6.57}$$

where

$$p_n(x) = \left(\frac{\hbar}{4}\right)^{n/2} H_n\left(x/\sqrt{\hbar}\right), \qquad h_n = \frac{1}{\sqrt{2\pi}} n! \left(\frac{\hbar}{2}\right)^{n+1/2}, \tag{6.58}$$

and $H_n(x)$ is the $n^{\text{th}}$ Hermite polynomial. The normalized reduced one-particle density matrix $C_N(x,x')$ in the zero temperature limit can be obtained using the

Christoffel–Darboux formula for the Hermite polynomials:

$$C_N(x,x') = \frac{1}{N}\sum_{n=0}^{N-1}\varphi_n(x)\varphi_n(x') = \sqrt{\frac{\hbar}{2N}}\frac{\varphi_N(x)\varphi_{N-1}(x') - \varphi_N(x')\varphi_{N-1}(x)}{x-x'}. \tag{6.59}$$

Let us derive the improved Balazs-Zipfel approximation (6.54) for this case. The Wigner transform of the reduced one-particle density matrix at zero temperature is

$$\mathcal{W}_N(x,p) = \frac{1}{2\pi\sqrt{2N\hbar}} \times \int_{\mathbb{R}} \mathrm{d}y\, \frac{\varphi_N\left(x+\frac{y}{2}\right)\varphi_{N-1}\left(x-\frac{y}{2}\right) - \varphi_N\left(x-\frac{y}{2}\right)\varphi_{N-1}\left(x+\frac{y}{2}\right)}{y} \mathrm{e}^{\frac{\mathrm{i}py}{\hbar}}. \tag{6.60}$$

This is an exact expression which can be evaluated exactly or numerically. But let us look at its expansion in the double-scaling limit (6.48). In the first step, we replace $\psi_n(x)$ by its WKB approximation, which is given, in the classically allowed region, by

$$\varphi_n^{\mathrm{WKB}}(x) = \frac{1}{\sqrt{2\pi p(x,E_n)}}\left(\mathrm{e}^{\frac{\mathrm{i}}{\hbar}S_n(x)+\frac{\mathrm{i}\pi}{4}} + \mathrm{e}^{-\frac{\mathrm{i}}{\hbar}S_n(x)-\frac{\mathrm{i}\pi}{4}}\right), \tag{6.61}$$

where we have denoted

$$p(x,E_n) = \sqrt{2E_n - x^2},$$
$$S_n(x) = \int_{\sqrt{2E_n}}^{x} p(x',E_n)\mathrm{d}x' = \frac{x}{2}\sqrt{2E_n-x^2} + \mathrm{i}E_n \log\left(\frac{x+\mathrm{i}\sqrt{2E_n-x^2}}{\sqrt{2E_n}}\right). \tag{6.62}$$

The energy $E_n$ is given by the Bohr–Sommerfeld condition (6.35), which is exact in the case of the harmonic oscillator:

$$E_n = \hbar\left(n+\frac{1}{2}\right). \tag{6.63}$$

The integral (6.60) is well defined since the apparent pole at $y=0$ is suppressed by a zero of the numerator. However, let us avoid the point $y=0$ by going above it in the integration path. If we introduce the function

$$w_{M,N}(x,p) = \int_{\mathbb{R}+\mathrm{i}0}\mathrm{d}y \frac{\varphi_M^{\mathrm{WKB}}\left(x+\frac{y}{2}\right)\varphi_N^{\mathrm{WKB}}\left(x-\frac{y}{2}\right)}{y}\mathrm{e}^{\frac{\mathrm{i}py}{\hbar}}, \tag{6.64}$$

we find that

$$\mathcal{W}_N(x,p) \approx \frac{1}{2\pi\sqrt{2N\hbar}}\left(w_{N,N-1}(x,p) + \text{c.c.}\right), \tag{6.65}$$

where "c.c." is the complex conjugate. Furthermore, we are interested in the limit (6.48). In this limit

$$\begin{aligned} S_N(x) &= \mathcal{S}_0(x) + \hbar\mathcal{S}_1(x) + \mathcal{O}(\hbar^2), \\ S_{N-1}(x) &= \mathcal{S}_0(x) - \hbar\mathcal{S}_1(x) + \mathcal{O}(\hbar^2), \end{aligned} \tag{6.66}$$

where

$$\begin{aligned}\mathcal{S}_0(x) &= \frac{1}{2}x\sqrt{2\xi_F - x^2} + \mathrm{i}\xi_F \log\left(\frac{x + \mathrm{i}\sqrt{2\xi_F - x^2}}{\sqrt{2\xi_F}}\right),\\ \mathcal{S}_1(x) &= \frac{\mathrm{i}}{2}\log\left(\frac{x + \mathrm{i}\sqrt{2\xi_F - x^2}}{\sqrt{2\xi_F}}\right),\end{aligned} \tag{6.67}$$

and

$$p(x, E_N) = \sqrt{2\xi_F - x^2} + \mathcal{O}(\hbar), \qquad p(x, E_{N-1})(x) = \sqrt{2\xi_F - x^2} + \mathcal{O}(\hbar). \tag{6.68}$$

In the calculation of (6.64) there are in principle four different terms. It can be seen that, in the saddle point approximation, only one term contributes to the final result, and which one of the four terms contributes depends on the location of the point $(x, p)$. However, once the contribution from a single term is formulated geometrically, in terms of area of chords, the result is universal. Moreover, although we are doing the calculation in the classically allowed region, the result is valid everywhere, provided the area of the chord is analytically continued (see [162] for a detailed discussion of these issues in the context of Berry's original derivation of (6.43)). In our case, it is enough to consider the term

$$w_{N,N-1}(x, p) \approx \frac{1}{2\pi}\int_{\mathbb{R}+\mathrm{i}0} \mathrm{d}z \frac{f(x - z)f(x + z)}{z} \mathrm{e}^{\frac{\mathrm{i}}{\hbar}\Sigma(z)}, \tag{6.69}$$

where we have rescaled $z \to 2z$. In this expression, we have

$$\begin{aligned}\Sigma(z) &= \mathcal{S}_0(x - z) - \mathcal{S}_0(x + z) + 2pz,\\ f(x) &= \frac{1}{(2\xi_F)^{1/4}} \frac{\sqrt{x + \mathrm{i}\sqrt{2\xi_F - x^2}}}{(2\xi_F - x^2)^{1/4}}.\end{aligned} \tag{6.70}$$

To perform the integral (6.69), we will use, as in [155], the uniform saddle point approximation of [163]. We introduce a new integration variable $u$ (a uniformization variable) which satisfies

$$\Sigma(z) = \frac{u^3}{3} - \zeta u, \tag{6.71}$$

with a yet undetermined parameter $\zeta$. This gives the implicit relation $z(u)$. Since $\Sigma(z)$ is odd, the point $u = 0$ satisfies $z = 0$. The value of $\zeta$ can be obtained from the saddle points $\pm z^*$ satisfying

$$0 = \Sigma'(\pm z_*) = -\mathcal{S}_0{}'(x + z_*) - \mathcal{S}_0{}'(x - z_*) + 2p. \tag{6.72}$$

This is, with a slightly different notation, the condition (6.40), which defines a chord passing through the point $(x, p)$ inside a circle of squared radius $2\xi$. After taking a derivative in (6.71) and evaluating the result at the saddle points, one finds

$$u(\pm z_*) = \pm\zeta^{1/2}, \tag{6.73}$$

and

$$\zeta = \left(-\frac{3}{2}\Sigma(z_*)\right)^{2/3} = \left(\frac{3}{2}\mathcal{A}(x,p)\right)^{2/3}, \tag{6.74}$$

where $\mathcal{A}(x,p)$ is the area of the Berry chord passing through the point $(x,p)$. For the harmonic oscillator, it is given by:

$$\mathcal{A}(x,p) = 2\xi_F \left\{ \arccos\left(\sqrt{\frac{H(x,p)}{\xi_F}}\right) - \sqrt{\frac{H(x,p)}{\xi_F}}\sqrt{1-\frac{H(x,p)}{\xi_F}} \right\}, \tag{6.75}$$

where $H(x,p)$ is the classical Hamiltonian (6.56). We now expand the remaining piece in the integrand of (6.69) as

$$\frac{f(x-z(u))f(x+z(u))}{z(u)}\frac{\mathrm{d}z(u)}{\mathrm{d}u} = \frac{a_{-1}}{u} + \sum_{m\geq 0} a_m u(u^2-\zeta)^m, \tag{6.76}$$

where

$$a_{-1} = f(x)^2 = \frac{1}{\sqrt{2\xi_F}}\left(\frac{x}{\sqrt{2\xi_F - x^2}} + \mathrm{i}\right). \tag{6.77}$$

If we keep just the first term in the expansion (6.76), we are left with the integral

$$\frac{1}{2\pi}\int_{\mathbb{R}+\mathrm{i}0} \frac{\mathrm{d}u}{u}\, \mathrm{e}^{\frac{\mathrm{i}}{\hbar}(u^3/3-\zeta u)} = -\mathrm{i}\mathcal{I}(-\hbar^{-2/3}\zeta), \tag{6.78}$$

where $\mathcal{I}$ is the integral of the Airy function introduced in (6.52). We conclude that

$$w_{N,N-1}(x,p) \approx -\mathrm{i}f(x)^2\,\mathcal{I}\left(-\left(\frac{3\mathcal{A}(x,p)}{2\hbar}\right)^{2/3}\right), \tag{6.79}$$

and

$$\mathcal{W}_N(x,p) \approx \frac{1}{2\pi\xi_F}\,\mathcal{I}\left(-\left(\frac{3\mathcal{A}(x,p)}{2\hbar}\right)^{2/3}\right), \tag{6.80}$$

which is the improved Balazs–Zipfel approximation. A comparison between the exact function $\mathcal{W}_N(x,p)$ evaluated directly from (6.60) and the improved Balazs–Zipfel approximation is shown in Fig. 6.2. The agreement is very good. It is easy to verify that the improved Balazs–Zipfel approximation is closer to the exact result than the conventional Balazs–Zipfel approximation (6.55) (in particular, it reproduces much better the pattern of fluctuations).

It is possible to check that the neglected terms in (6.76) give an explicitly calculable series of corrections in powers of $\hbar^{2/3}$, involving Airy functions and their derivatives. Let us work out the first correction, coming from the term with $a_0$ in (6.76). Evaluating (6.76) at $z = z_*$, we find the relation

$$\frac{a_{-1}}{\zeta^{1/2}} + a_0\zeta^{1/2} = \frac{f(x-z_*)f(x+z_*)}{z_*}\left(\frac{\mathrm{d}u(z_*)}{\mathrm{d}\xi}\right)^{-1}. \tag{6.81}$$

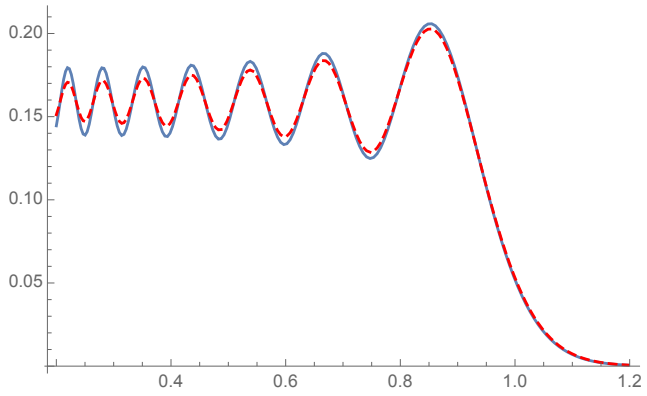


**Figure 6.2:** The improved Balazs–Zipfel approximation to the quantum distribution of non-interacting fermions at zero temperature in a harmonic potential, (6.80) (dashed red line), compared to the exact function $\mathcal{W}_N$ (6.60) (full blue line), as a function of $H(x,p)$, for $N=30$, $\hbar=1/30$, and $\xi_F=1$.

Using the expansions

$$\begin{aligned} u(z) &= \zeta^{1/2} + \frac{\mathrm{d}u(z_*)}{\mathrm{d}z}(z-z_*) + O(z-z_*)^2, \\ \Sigma(z) &= \frac{u(z)^3}{3} - \zeta u(z) = \Sigma(z_*) + \frac{1}{2}\Sigma''(z_*)(z-z_*)^2 + O(z-z_*)^3, \end{aligned} \tag{6.82}$$

we obtain from (6.71)

$$\frac{\mathrm{d}u(z_*)}{\mathrm{d}z} = \frac{\sqrt{\frac{1}{2}\Sigma''(z_*)}}{(-\frac{3}{2}\Sigma(z_*))^{1/6}}. \tag{6.83}$$

Therefore, we find

$$a_0 = \frac{f(x-z_*)f(x+z_*)}{\left(\frac{3}{2}\mathcal{A}(x,p)\right)^{1/6} z_* \sqrt{\frac{1}{2}\Sigma''(z_*)}} - \frac{f(x)^2}{\left(\frac{3}{2}\mathcal{A}(x,p)\right)^{2/3}}. \tag{6.84}$$

It will be convenient to introduce the function $p(x)=\sqrt{2\xi_F - x^2}$, and the labels (1) and (2) corresponding to the points

$$\begin{aligned} x(1) &= x + z_*, \qquad & p(1) &= p(x+z_*), \\ x(2) &= x - z_*, \qquad & p(2) &= p(x-z_*). \end{aligned} \tag{6.85}$$

Then we find

$$\Sigma''(z_*) = \frac{x(1)}{p(1)} - \frac{x(2)}{p(2)}. \tag{6.86}$$

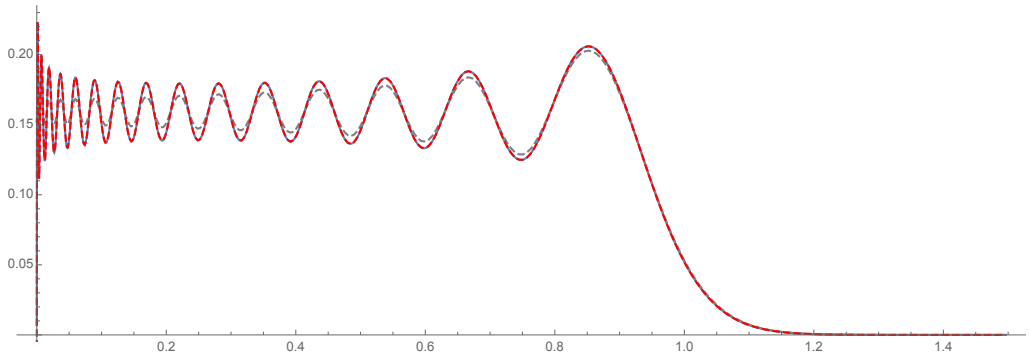


**Figure 6.3:** Comparing (6.91) (dashed red line) and the previous approximation (6.80) (dashed gray line) to the exact function $\mathcal{W}_N$ as function of $H(x,p)$ (blue line) for $N = 30$, $\hbar = 1/30$, $\xi_F = 1$. Oscillations are correctly reproduced by the new expression, which is indistinguishable from the exact function at this scale.

Let us also define the angle $\phi$ of the point $(x,p)$ in phase space:

$$\phi = \arg(x + \mathrm{i}p), \tag{6.87}$$

so that

$$z_* = \sqrt{2\xi_F}\sqrt{1 - \frac{H(x,p)}{\xi_F}}\,\sin\phi, \tag{6.88}$$

and

$$\frac{f(x - z_*)f(x + z_*)}{\sqrt{\frac{1}{2}\Sigma''(z_*)}} = \frac{\sqrt{2}\mathrm{e}^{\mathrm{i}\phi}}{\sqrt{x(1)p(2) - x(2)p(1)}}. \tag{6.89}$$

In the end, using

$$\frac{1}{2\pi}\int_{\mathbb{R}+\mathrm{i}0} \mathrm{d}u\, u\, \mathrm{e}^{\frac{\mathrm{i}}{\hbar}(u^3/3 - \zeta u)} = -\mathrm{i}\hbar^{2/3}\mathrm{Ai}'(-\hbar^{-2/3}\zeta), \tag{6.90}$$

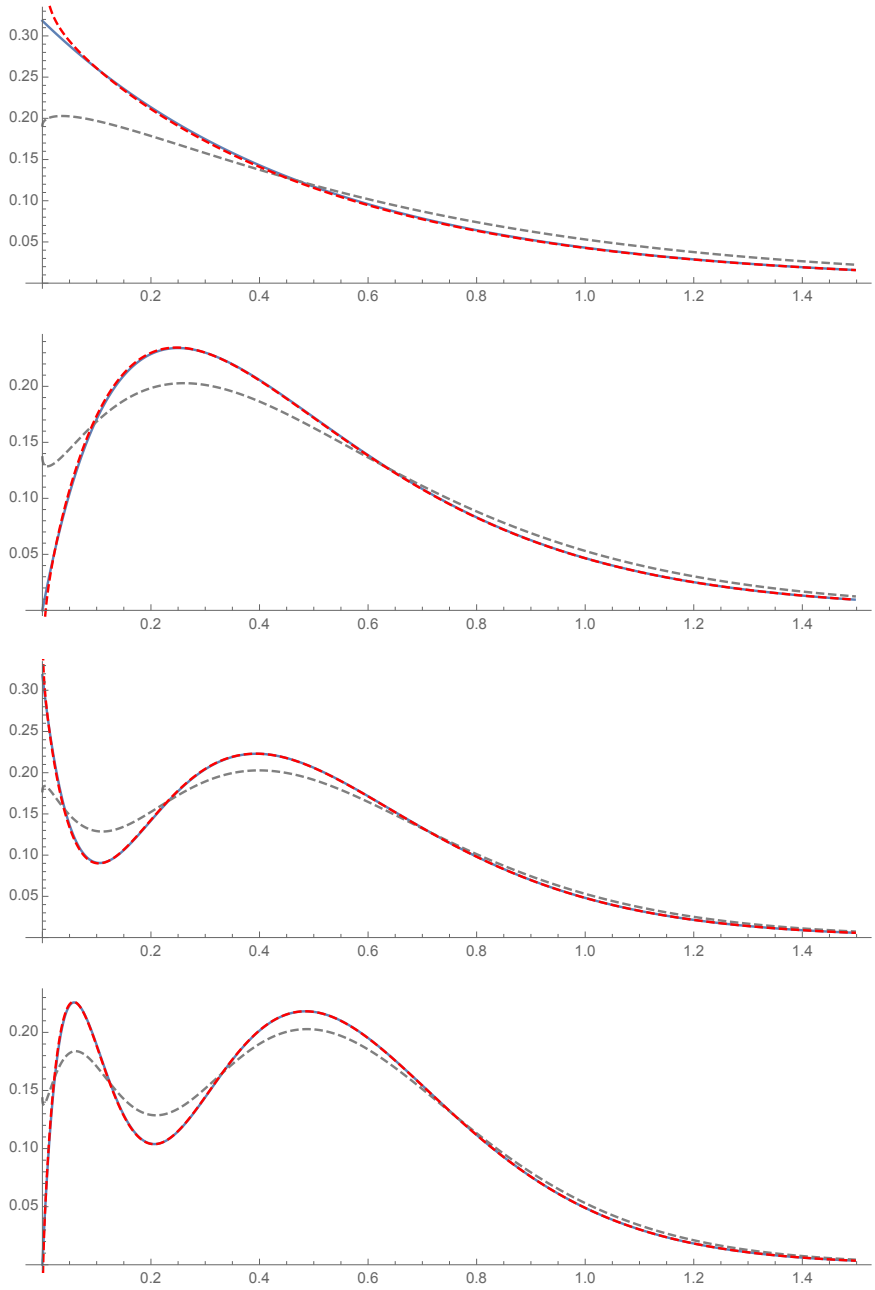


**Figure 6.4:** Similar plots for $\xi_F = 1$ with $N = 1, 2, 3, 4$. Except for $N = 1$, the approximation (6.91) is indistinguishable from the exact function. On the other hand, for these low values of $N$, approximation (6.91) in dashed gray is not as good.

and putting everything together, we find

$$\begin{aligned}\mathcal{W}_N(x,p) \approx \frac{1}{2\pi\xi_F}\Bigg\{&\mathcal{I}\left(-\left(\frac{3}{2\hbar}\right)^{2/3}\mathcal{A}(x,p)^{2/3}\right)\\ &+\hbar^{2/3}\Bigg[\frac{2\sqrt{\xi_F}}{\left(\frac{3}{2}\right)^{1/6}\mathcal{A}(x,p)^{1/6}\sqrt{2\xi_F}\sqrt{1-\frac{H(x,p)}{\xi_F}}\sqrt{x(1)p(2)-x(2)p(1)}}\\ &\qquad\qquad -\frac{1}{(\frac{3}{2})^{2/3}\mathcal{A}(x,p)^{2/3}}\Bigg]\\ &\times\mathrm{Ai}'\left(-\left(\frac{3}{2\hbar}\right)^{2/3}\mathcal{A}(x,p)^{2/3}\right)\Bigg\}.\end{aligned} \tag{6.91}$$

On the r.h.s, the first line is the improved Balazs–Zipfel approximation (6.80), and the next lines are the first small $\hbar$ correction of this approximation. The expression $x(1)p(2)-x(2)p(1)$ is a particular case of (6.42) appearing in Berry's formula, since $I(x,p)=H(x,p)$ for the harmonic oscillator. The approximation (6.91) with its first subleading correction reproduces the exact expression with high precision, as can be seen in Fig. 6.3 and Fig. 6.4.

## 6.3 The quantum geometry for mirror curves

We now turn our attention to quantum mirror curves, where $\rho$ is the inverse operator (3.14) associated to the mirror curve

$$\mathcal{O}(\mathrm{e}^x,\mathrm{e}^y)-\kappa=0. \tag{6.92}$$

We limit the discussion to genus one mirror curves. We have deliberately changed the sign of $\kappa$ for the purpose of the discussion of this section. Quantizing this operator involves replacing $x$ with the position operator $\mathsf{x}$, and $y$ by the conjugate momentum quantum operator. Therefore, in this section we will change the notation and call the conjugate coordinate $p$, and the corresponding operator $\mathsf{p}$. We recall that $\rho$ is a positive definite trace class, self-adjoint operator on $L^2(\mathbb{R})$ for appropriate values of the mass parameters. Therefore, it is natural to regard $\rho$ as a canonical density matrix for a quantum Hamiltonian, i.e.

$$\rho=\mathrm{e}^{-\mathsf{H}}. \tag{6.93}$$

The inverse temperature $\beta$ is set to one, although, as we will see in a moment, there is a natural notion of low temperature limit.

Through the TS/ST correspondence, the spectral determinant $\Xi(\kappa)$ of $\rho$ can be obtained from topological string data [2] as explained in section 3.3. Its vanishing locus gives the spectrum. A conjectural quantization condition has also been proposed in [31] which equivalently gives the spectrum, using the topological string free energy in the NS limit. According to [31], the exact quantization condition for genus one geometries can be written as

$$\frac{rC\tilde{t}^2}{2}+B(\hbar)+\hbar\left(f_{\rm NS}\left(\tilde{t},\hbar\right)+f_{\rm NS}\left(\frac{2\pi\tilde{t}}{\hbar},\frac{4\pi^2}{\hbar}\right)\right)=2\pi\hbar\left(n+\frac{1}{2}\right),\qquad n=0,1,2,... \tag{6.94}$$

In this equation,

$$B(\hbar)=B\left(1+\frac{\hbar^2}{4\pi^2}\right), \tag{6.95}$$

$C$, $r$, and $B$ are constant coefficients depending on the geometry under consideration, and $\tilde{t}$ is the Kähler parameter associated to the "true" modulus, and is related to the energy through the quantum mirror map (3.64). We express it in terms of the energy $E$ related to $\mathsf{H}$, so that $\kappa=\mathrm{e}^E=-\mathrm{e}^{\mu}$, or $\mu=E+\mathrm{i}\pi$. Since we assume that we have a genus one mirror curve $g_W=1$, the quantum mirror maps in (3.64) can be given in terms of a single function $\tilde{t}=\tilde{t}(E,\hbar)$, as

$$\begin{aligned} t_i(\hbar)&=C_i\mu-\alpha_{ik}\log m_k+O(\mathrm{e}^{-\mu}).\\ &=C_i(E+\mathrm{i}\pi)-\alpha_{ik}\log m_k+O(\mathrm{e}^{-\mu})\\ &=c_i\tilde{t}(E,\hbar)-\alpha_{ik}\log m_k+\mathrm{i}\pi c_i r, \end{aligned} \tag{6.96}$$

where $c_i=C_i/r$. The equation (6.94) determines the energy levels $E_n$, $n=0,1,2,...$ of the Hamiltonian $\mathsf{H}$ defined by (6.93). When $\hbar\to 0$, the quantum mirror map becomes the classical mirror map $\tilde{t}=\tilde{t}(E)$ relating the Kähler parameter to the modulus $\kappa$. We also note that, for large $E$ and fixed $\hbar$, the quantum mirror map behaves as

$$\tilde{t}(E,\hbar)=rE+\mathcal{O}(\mathrm{e}^{-rE}). \tag{6.97}$$

Finally, the function $f_{\rm NS}(t,\hbar)$ can be expressed in terms of the Nekrasov–Shatashvili (NS) limit $F_{\rm NS}(t,\hbar)$ of the refined topological string free energy, given in (2.39), as,

$$f_{\rm NS}(\tilde{t},\hbar)=\sum_{i=1}^{n_W}C_i\frac{\partial F_{\rm NS}^{\rm inst}}{\partial t_i}=r\frac{\partial F_{\rm NS}^{\rm inst}}{\partial\tilde{t}}, \tag{6.98}$$

where the superscript indicates that we only keep the instanton part of the NS free energy, given in (2.38). We note that

$$F_{\rm NS}=\frac{1}{\hbar}F_0(\tilde{t})+\mathcal{O}(\hbar), \tag{6.99}$$

where $F_0(\tilde{t})$ is the genus zero free energy of the toric CY in the large radius frame,

$$F_0(\tilde{t}) = \frac{C}{6}\tilde{t}^3 + F_0^{\rm inst}(\tilde{t}). \tag{6.100}$$

It is instructive to verify how the conventional Bohr–Sommerfeld quantization condition emerges from the exact quantization condition (6.94). In the standard WKB limit (6.37), the spectrum is of the form

$$E_n \approx E(\tilde{t}), \tag{6.101}$$

where the function $E(\tilde{t})$ is determined by the condition

$$r\left(\frac{\partial F_0}{\partial \tilde{t}}\right)_{\tilde{t}=\tilde{t}(E)} + B = 2\pi\tilde{t}. \tag{6.102}$$

This is indeed of the form (6.38), and we learn in addition that

$$I(E) = \frac{1}{2\pi}\left\{r\left(\frac{\partial F_0}{\partial \tilde{t}}\right)_{\tilde{t}=\tilde{t}(E)} + B\right\}. \tag{6.103}$$

However, we learned in section 4.2 that the limit in which one makes contact with the conventional (or standard) topological string is not the standard WKB limit of the gas (6.48), but rather the non-conventional limit

$$N, \hbar \to \infty, \qquad \frac{N}{\hbar} = \lambda \quad \text{fixed}, \tag{6.104}$$

In this limit, which we will usually call the 't Hooft limit, the conjecture of [2] implies the canonical partition function of the Fermi gas, $Z(N,\hbar)$, has the asymptotic expansion

$$\log Z(N,\hbar) \sim \sum_{g\geq 0} \hbar^{2-2g}\mathcal{F}_g(\lambda). \tag{6.105}$$

In this expansion $\mathcal{F}_g(\lambda)$ is the genus $g$ topological string free energy of the toric CY in the so-called conifold frame, and $\lambda$ is a flat coordinate (in particular, it vanishes at the conifold point). Therefore, the all-genus topological string emerges in the limit (6.104) of the Fermi gas, which provides a non-perturbative definition of the topological string partition function. This limit corresponds to the $g_s \to 0$ limit of the topological string. In the quantum Fermi gas, we can regard it as a "dual" semiclassical limit, in which the dual Planck constant

$$\hbar_{\rm D} = \frac{4\pi^2}{\hbar} \tag{6.106}$$

goes to zero. We will now show that (6.104) is effectively a low temperature limit for the non-interacting Fermi gas. To see this, let us study the spectrum of $\mathsf{O}$ when

$$\hbar_{\rm D} \to 0, \qquad n \to \infty, \qquad \hbar_{\rm D} n = \xi_{\rm D} \quad \text{fixed}. \tag{6.107}$$

The key fact to understand this regime is that, as emphasized in [137], the exact quantization condition (6.94) is invariant under the S–duality transformation

$$\tilde{t} \to \frac{2\pi\tilde{t}}{\hbar}, \qquad \log m_k \to \frac{2\pi \log m_k}{\hbar}, \qquad \hbar \to \hbar_{\mathrm{D}}. \tag{6.108}$$

This sort of invariance is expected from the modular duality of Weyl operators [21]. After multiplication by $4\pi^2/\hbar^2$, the quantization condition (6.94) can be written as

$$\frac{Cr}{2}\left(\frac{2\pi\tilde{t}}{\hbar}\right)^2 + B(\hbar_{\mathrm{D}}) + \hbar_{\mathrm{D}}\left(f_{\mathrm{NS}}\left(\tilde{t},\hbar\right) + f_{\mathrm{NS}}\left(\frac{2\pi\tilde{t}}{\hbar},\hbar_{\mathrm{D}}\right)\right) = 2\pi\hbar_{\mathrm{D}}\left(n+\frac{1}{2}\right), \tag{6.109}$$

for $n = 0, 1, 2, \ldots$ From this form of the quantization condition, it is clear that, when $\hbar \to \infty$, $\tilde{t}$ (and $E$) should scale like $\hbar$ (this scaling was already noted in [9]). Let us then assume that, in the limit (6.107), the energy levels behave like

$$E_n \approx \hbar \mathcal{E}(\xi_{\mathrm{D}}), \tag{6.110}$$

and let us determine the function $\mathcal{E}(\xi_{\mathrm{D}})$. Since $\tilde{t}, E \approx \hbar$ are large, we can drop exponentially small corrections in these quantities, like those appearing e.g. in the quantum mirror map $\tilde{t}(E,\hbar)$. We also have

$$\hbar_{\mathrm{D}} f_{\mathrm{NS}}\left(\frac{2\pi\tilde{t}}{\hbar}, \frac{4\pi^2}{\hbar}\right) = r\frac{\partial F_0^{\mathrm{inst}}}{\partial\tilde{t}}\bigg|_{\tilde{t}\to\frac{2\pi\tilde{t}}{\hbar}} + \mathcal{O}(\hbar_D). \tag{6.111}$$

The equation determining $\mathcal{E}$ as a function of $\xi_{\mathrm{D}}$ is then

$$r\left(\frac{\partial F_0}{\partial\tilde{t}}\right)_{\tilde{t}=2\pi r\mathcal{E}} + B = 2\pi\xi_{\mathrm{D}}. \tag{6.112}$$

It is important to point out that, in spite of the formal invariance of the exact quantization condition under the transformation (6.108), the spectrum itself is *not* invariant. In fact, the spectrum scales like $\mathcal{O}(\hbar^0)$ in the standard semiclassical limit $\hbar \to 0$, while it scales like $\mathcal{O}(\hbar)$ in the dual limit $\hbar \to \infty$. However, the comparison between (6.112) and (6.103) suggests introducing a "dual" energy $E_{\mathrm{D}}$ through the equation

$$2\pi r\mathcal{E} = \tilde{t}(E_{\mathrm{D}}), \tag{6.113}$$

in such a way that the quantization condition (6.112) reads now

$$I(E_{\mathrm{D}}) = \xi_{\mathrm{D}} \tag{6.114}$$

and it has the same form as (6.38). This dual energy will be important in order to describe the emergent classical geometry in the limit (6.104). One consequence of (6.110) is that the limit (6.107) is effectively a *zero temperature limit*, since in

(6.110) the $\hbar$ factor acts like an effective inverse temperature $\beta = (k_B T)^{-1}$ for small $T$. In other words, in any thermal computation involving the Hamiltonian $\mathsf{H}$ in (6.93), we can regard the limit (6.107) as a limit in which we take simultaneously a zero temperature limit and a WKB limit with effective energy levels given by $\mathcal{E}(\xi_D)$.

As a further check of this picture, we can compute the partition function $Z(N, \hbar)$ in the limit (6.104) at leading order in $N^2$ (a similar calculation was performed in [92]). Since we have a system of $N$ fermions at zero temperature, its canonical partition function is approximately given by

$$Z(N, \hbar) \approx \mathrm{e}^{-\mathcal{G}}, \tag{6.115}$$

where

$$\mathcal{G} = \sum_{n=0}^{N-1} E_n \tag{6.116}$$

is the energy of the ground state of the Fermi gas with $N$ particles. The energy levels $E_n$ in the limit (6.104) are given by (6.110), with

$$\xi_{\mathrm{D}} = 4\pi^2 \zeta \lambda, \qquad \zeta = \frac{n}{N}. \tag{6.117}$$

At large $N$, $\zeta$ can be regarded as a continuous parameter that varies between 0 and 1, and

$$\sum_{n=0}^{N-1} \to N \int_0^1 \mathrm{d}\zeta. \tag{6.118}$$

If we write

$$\mathcal{G} \approx -\hbar^2 \mathcal{F}_0(\lambda), \tag{6.119}$$

we find

$$-\mathcal{F}_0(\lambda) \approx \frac{1}{\hbar^2} \sum_{n=0}^{N-1} E_n \approx \frac{N}{2\pi r \hbar} \int_0^1 \tilde{t}\,(\lambda\zeta)\,\mathrm{d}\zeta = \frac{1}{2\pi r} \int_0^\lambda \tilde{t}(u)\mathrm{d}u, \tag{6.120}$$

where we changed variables to $u = \lambda\zeta$, and we wrote $\tilde{t}$ as the function of $\lambda$ defined implicitly by (6.112), i.e. by

$$r \frac{\partial F_0}{\partial \tilde{t}} + B = 8\pi^3 \lambda. \tag{6.121}$$

By taking a derivative of (6.120) w.r.t. $\lambda$, we conclude that

$$\frac{\partial \mathcal{F}_0}{\partial \lambda} = -\frac{\tilde{t}(\lambda)}{2\pi r}. \tag{6.122}$$

The equations (6.121), (6.122) are precisely the equations defining $\lambda$ as a conifold flat coordinate, and $\mathcal{F}_0(\lambda)$ as the prepotential in the conifold frame. This agrees

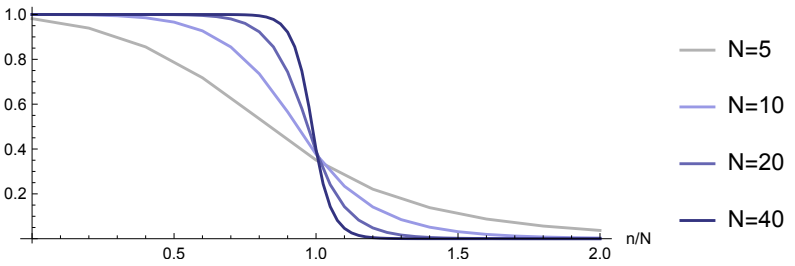


**Figure 6.5:** The numerical values of $Nc_k^{(N)}$ as function of $k$, for different values of $N$. Here $\hbar$ is chosen so that $\lambda = N/\hbar = 1$. As $N$ becomes large, the coefficients display the step behavior (6.29) typical of a Fermi gas at zero temperature.

with section 4.2 up to slight notational differences. As a further verification of the low-temperature nature of the limit (6.104), let us look at a concrete geometry. As usual, our main example in this section will be the toric CY known as local $\mathbb{P}^1 \times \mathbb{P}^1$. We will focus on the symmetric case, where the mass parameter is set to 1. In this case, the function $\mathcal{O}(\mathrm{e}^x, \mathrm{e}^p)$ is given by

$$\mathcal{O}(\mathrm{e}^x, \mathrm{e}^p) = \mathrm{e}^p + \mathrm{e}^{-p} + \mathrm{e}^x + \mathrm{e}^{-x}. \tag{6.123}$$

The corresponding quantum operator is

$$\mathsf{O} = \mathrm{e}^{\mathsf{p}} + \mathrm{e}^{-\mathsf{p}} + \mathrm{e}^{\mathsf{x}} + \mathrm{e}^{-\mathsf{x}}. \tag{6.124}$$

The energy levels of the corresponding Hamiltonian $\mathsf{H}$ are given by the (conjectural) exact quantization condition (6.94) with $r = 2$, $C = 1$, and $B = -2\pi^2/3$. Using the spectrum of $\mathsf{H}$ and the explicit expression (6.28), it is possible to calculate numerically the coefficients $c_k^{(N)}(\hbar)$ (with $\beta = 1$) appearing in (6.25). We can then study their behavior in the limit (6.104). The results for $N/\hbar = 1$ and increasingly larger values of $N$ (and $\hbar$) are shown in Fig. 6.5. It is clear that in the large $N$, large $\hbar$ limit, they display the typical behavior (6.29) of a non-interacting Fermi gas at zero temperature.

We will now study the reduced one-particle density matrix $C_N(x, x')$ for our mirror curves in the 't Hooft limit (6.104). For several genus one cases, the explicit kernel $\rho(x, x')$ is available, see section 3.4. It has the general form (5.3) in the appropriate variables, that we recall here with a slight change of notation:

$$\rho(\mu, \mu') = \frac{v(\mu)^{1/2} v(\mu')^{1/2}}{2\cosh\left(\frac{\mu-\mu'}{2\gamma} - \mathrm{i}\pi C\right)}, \tag{6.125}$$

Here, the variable $\mu$ is an appropriate combination of the original variables appearing in the mirror curve. The choice of $\mu$ is such that $\gamma$ does not depend on $\hbar$. The function $v(\mu)$ turns out to admit the representation

$$v(\mu) = \mathrm{e}^{-\hbar V(\mu)}, \tag{6.126}$$

where

$$V(\mu) = V_0(\mu) + \mathcal{O}(\hbar^{-2}). \tag{6.127}$$

Since we have that

$$C_N(x, x') = \frac{1}{NZ(N)} B_{N-1}(x, x'), \tag{6.128}$$

we can use the matrix model correlator (5.6) and study it in the 't Hooft limit. This is very similar to what we did at the beginning of section 5.3 for the eigenfunctions. Let us define

$$t_C(z) = \frac{\mathrm{e}^{-\mathrm{i}\pi C}\sinh(z)}{\cosh(z - \mathrm{i}\pi C)}. \tag{6.129}$$

and let us write the normalized expectation values in the matrix model as

$$\langle f(\mu_1, \ldots, \mu_N)\rangle = \frac{1}{Z_N}\frac{1}{N!}\int_{\mathbb{R}^N} \mathrm{d}\mu_1 \cdots \mathrm{d}\mu_N f(\mu_1, \ldots, \mu_N) \det_{i,j=1,\ldots,N} \rho(\mu_i, \mu_j), \tag{6.130}$$

which is just (5.7) divided by the partition function $Z(N)$. Then, we have

$$\begin{aligned}\frac{B_N(\mu, \mu')}{Z_N} &= \mathrm{e}^{2\pi\mathrm{i}CN}\rho(\mu, \mu')\left\langle \prod_{i=1}^{N} t_C\left(\frac{\mu - \mu_i}{2\gamma}\right) t_C\left(\frac{\mu' - \mu_i}{2\gamma}\right)\right\rangle \\ &= \mathrm{e}^{2\pi\mathrm{i}CN}\rho(\mu, \mu') \\ &\quad \times \exp\left[\sum_{s=1}^{\infty}\frac{1}{s!}\left\langle\left(\sum_{i=1}^{N}\log t_C\left(\frac{\mu - \mu_i}{2\gamma}\right) + \sum_{i=1}^{N}\log t_C\left(\frac{\mu' - \mu_i}{2\gamma}\right)\right)^s\right\rangle^{(c)}\right],\end{aligned} \tag{6.131}$$

where the superscript $(c)$ means that we use connected correlators in the matrix model. Let us introduce the exponentiated variable $M = \mathrm{e}^{\mu/\gamma}$, and the function

$$W(M) = \sum_{i=1}^{N}\log t_C\left(\frac{\mu - \mu_i}{2\gamma}\right). \tag{6.132}$$

We can then write

$$\begin{aligned}\frac{B_N(\mu,\mu')}{Z_N} &= \mathrm{e}^{2\pi\mathrm{i}CN}\rho(\mu,\mu')\exp\left[\sum_{s=1}^{\infty}\sum_{\ell=0}^{s}\frac{1}{(s-\ell)!\ell!}\left\langle W(M)^{s-\ell}W(M')^{\ell}\right\rangle^{(c)}\right]\\ &= \mathrm{e}^{2\pi\mathrm{i}CN}\rho(\mu,\mu')\exp\left[\sum_{n=1}^{\infty}\frac{1}{n!}\left\langle W(M)^n\right\rangle^{(c)}+\sum_{n=1}^{\infty}\frac{1}{n!}\left\langle W(M')^n\right\rangle^{(c)}\right.\\ &\qquad\left.+\sum_{m,n=1}^{\infty}\frac{1}{m!n!}\left\langle W(M)^m W(M')^n\right\rangle^{(c)}\right].\end{aligned} \tag{6.133}$$

We now define the $n$–point function as

$$\begin{aligned}W_n(M_1,...,M_n) &= \frac{\partial}{\partial M_1}\cdots\frac{\partial}{\partial M_n}\left\langle W(M_1)\cdots W(M_n)\right\rangle^{(c)}\\ &= \left\langle\prod_{k=1}^{n}\sum_{i=1}^{N}\left(\frac{1}{M_k-\mathrm{e}^{\mu_i/\gamma}}-\frac{1}{M_k-\omega\mathrm{e}^{\mu_i/\gamma}}\right)\right\rangle^{(c)},\end{aligned} \tag{6.134}$$

where we set

$$\omega = -\mathrm{e}^{2\pi\mathrm{i}C}. \tag{6.135}$$

This is precisely the $n$–point functions defined in (4.161), and they have an asymptotic expansion of the form

$$W_n(M_1,...,M_n) = \sum_{g=0}^{\infty}\hbar^{2-2g-n}W_{n,g}(M_1,...,M_n). \tag{6.136}$$

We finally obtain, to next-to-leading order in the large $N$ expansion,

$$\begin{aligned}\frac{B_N(\mu,\mu')}{Z_N} &= \mathrm{e}^{2\pi\mathrm{i}CN}\rho(\mu,\mu')\exp\left[\langle W(M)\rangle^{(c)}+\langle W(M')\rangle^{(c)}\right.\\ &\qquad\left.+\frac{1}{2}\langle W(M)^2\rangle^{(c)}+\frac{1}{2}\langle W(M')^2\rangle^{(c)}+\langle W(M)W(M')\rangle^{(c)}+\mathcal{O}(N^{-1})\right]\\ &= \rho(\mu,\mu')\exp\left[2\pi\mathrm{i}C\lambda\hbar+\hbar\int_{\infty}^{M}W_{1,0}(Z)\mathrm{d}Z+\hbar\int_{\infty}^{M'}W_{1,0}(Z)\mathrm{d}Z\right.\\ &\qquad+\frac{1}{2}\int_{\infty}^{M}\int_{\infty}^{M}W_{2,0}(Z_1,Z_2)\mathrm{d}Z_1\mathrm{d}Z_2+\frac{1}{2}\int_{\infty}^{M'}\int_{\infty}^{M'}W_{2,0}(Z_1,Z_2)\mathrm{d}Z_1\mathrm{d}Z_2\\ &\qquad\left.+\int_{\infty}^{M}\int_{\infty}^{M'}W_{2,0}(Z_1,Z_2)\mathrm{d}Z_1\mathrm{d}Z_2+\mathcal{O}(\hbar^{-1})\right].\end{aligned} \tag{6.137}$$

By using (6.128), we can obtain from the above expression the reduced density matrix $C_{N+1}(x,y)$ for many Fermi gases associated to quantum mirror curves, as well as its behavior in the semiclassical limit. The expression (6.137) involves standard

one and two-point correlation functions of the matrix model associated to the Fermi gas. These were derived in section 4.4. When $C = 0$ the resulting matrix model can be mapped to an $O(2)$ matrix model, and the functions $W_{1,0}(M)$, $W_{2,0}(M, M')$ can be explicitly calculated from the results in [104, 105]. In the next section, we will investigate this formula for the symmetric local $\mathbb{P}^1 \times \mathbb{P}^1$ case.

Let us recall that our object of interest is the distribution $\mathcal{W}_N(x, p)$ in phase space given by eq. (6.46). We want to study this quantity for the Fermi gas realization of quantum mirror curves, in the 't Hooft limit. In this limit, the Fermi energy which should be around $E_N \approx \hbar \mathcal{E}(4\pi^2\lambda)$ scales as $\hbar$, and the region in phase space where $\mathcal{W}_N(x, p)$ is non-negligible grows with $\hbar$. In order to have a "stable" limit as $\hbar$ becomes larger, it is convenient to rescale the phase space variables. This is also suggested by the study of the open string eigenfunctions for the quantum mirror curve, which requires such a scaling of the position space coordinate in the limit (6.104), as established in section 5.3. Therefore, we define the rescaled quantum distribution in phase space associated to a mirror curve as

$$\mathcal{Q}_N(x, p) = \left(\frac{\hbar}{2\pi}\right)^2 \mathcal{W}_N\left(\frac{\hbar x}{2\pi}, \frac{\hbar p}{2\pi}\right). \tag{6.138}$$

This involves the phase space coordinates appearing in the modular double theory [21]. The prefactor guarantees that the rescaled distribution is correctly normalized. The main claim of this section is that the quantum distribution (6.138) is an appropriate and precise definition of quantum geometry in the context of mirror curves. Indeed, we claim that in the limit (6.104), this distribution has constant support in the interior of the mirror curve

$$\mathcal{O}(\mathrm{e}^x, \mathrm{e}^p) = \mathrm{e}^{E_{\mathrm{DF}}}. \tag{6.139}$$

Here, $E_{\mathrm{DF}}$ is the dual Fermi energy, and it is determined by the 't Hooft parameter $\lambda$ through the equation

$$\begin{aligned} I(E_{\mathrm{DF}}) &= 4\pi^2\lambda \\ &= \hbar_{\mathrm{D}} N. \end{aligned} \tag{6.140}$$

This follows from (6.114) with $\xi_{\mathrm{D}} = 4\pi^2\lambda$. More precisely, we claim that, in the limit (6.104),

$$\mathcal{Q}_N(x, p) \approx \frac{1}{2\pi I(E_{\mathrm{DF}})} \Theta\left(\mathrm{e}^{E_{\mathrm{DF}}} - \mathcal{O}(\mathrm{e}^x, \mathrm{e}^p)\right). \tag{6.141}$$

Therefore, in this limit, the boundary of the support of $\mathcal{Q}_N(x, p)$ is the classical mirror curve. Away from the limit (6.104), the quantum distribution $\mathcal{Q}_N(x, p)$ exhibits fluctuations that make this boundary "fuzzy" in a precise, quantitative way.

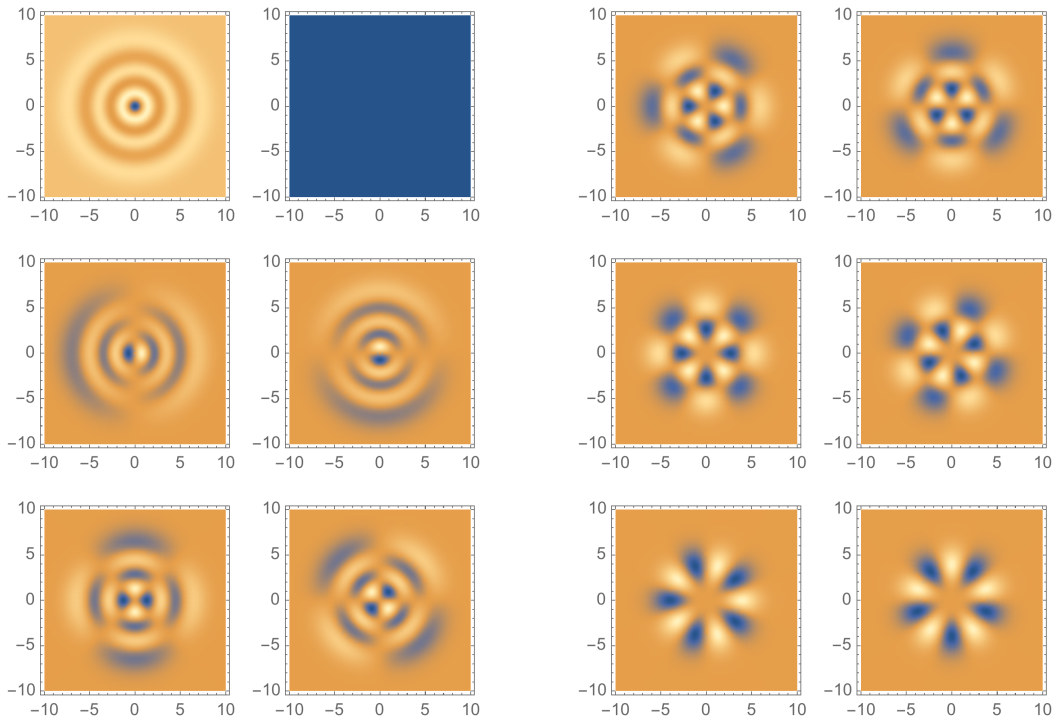

**Figure 6.6:** Density plots for the real (left) and imaginary (right) parts of $E_{5n}(x,p)$, for $n = 5,4,3$ in the left double column and $n = 2,1,0$ in the right double column. The $E_{55}(x,p)$ distribution is purely real, and corresponds to the Wigner quasi probability distribution of the $5^{\text{th}}$ state of the quantum harmonic oscillator.

The function $\mathcal{Q}_N(x,p)$ can be computed exactly for low values of $N$ and rational $\hbar/2\pi$, since in that case the kernel $\rho(\mu,\mu')$ in matrix model variables reduces to tractable functions. The canonical transformation can be performed in a similar way as in section 5.2. We performed the computation for symmetric local $\mathbb{P}^1 \times \mathbb{P}^1$, for $\hbar = 2\pi$ and $N = 1,2$. However, this is a rather tedious and case by case approach. Therefore, for a more systematic study of the functions $\mathcal{Q}_N(x,p)$, we use instead expression (6.25). After a Wigner transform, this involves the Wigner functions of the eigenstates of the operator $\rho$. Although Berry's formula (6.43) was originally derived for Hamiltonians of the form $H(x,p) = p^2/2 + V(x)$, we have explicitly verified that it correctly describes the Wigner functions associated to eigenfunctions of $\rho$. We will use however a more precise, numerical determination of these functions, obtained as follows. Let $\psi_n(x)$ denote the eigenfunctions for the harmonic oscillator,

as in (6.57). It is well-known that the mixed Wigner functions associated to this basis can be computed in terms of generalized Laguerre polynomials [164]. We have

$$\begin{aligned} E_{mn}(x,p) &\equiv \frac{1}{2\pi\hbar}\int_{-\infty}^{\infty}\psi_m^*\left(x+\frac{y}{2}\right)\psi_n\left(x-\frac{y}{2}\right)\mathrm{e}^{\frac{\mathrm{i}}{\hbar}py}\mathrm{d}y \\ &= \frac{1}{2\pi\hbar}\frac{2^{\frac{n+m}{2}+1}}{\sqrt{n!m!}}\mathrm{e}^{-z\bar{z}}\sum_{\ell=0}^{\min(m,n)}\binom{m}{\ell}\binom{n}{\ell}(-2)^{-\ell}\ell!\,z^{m-\ell}\,\bar{z}^{n-\ell}, \end{aligned} \tag{6.142}$$

where

$$z = x+\frac{\mathrm{i}}{\hbar}p, \qquad \bar{z} = x-\frac{\mathrm{i}}{\hbar}p. \tag{6.143}$$

Examples of distributions $E_{mn}(x,p)$ can be found in Fig. 6.6. We can now expand the eigenfunctions appearing in (6.25) in the basis (6.57):

$$\varphi_n(x) = \sum_{i\geq 0} v_{in}\psi_i(x), \qquad\qquad v_{in}\in\mathbb{C}. \tag{6.144}$$

Then, its Wigner transform (6.34) becomes

$$f_n(x,p) = \sum_{i,j\geq 0} v_{in}^* v_{jn} E_{ij}(x,p) = (v^\dagger E v)_{nn}. \tag{6.145}$$

In a numerical calculation of the eigenfunctions $\varphi_n(x)$ by the Rayleigh–Ritz method is in section 3.2, we determine approximate values of the coefficients $v_{ni}$ for $i = 0,1,\ldots,n_{\max}$, and this gives an approximation to the Wigner function $f_n(x,p)$. This calculation also gives numerical approximations of the energy levels $E_n$, which can be used to obtain numerical approximations for $c_n^{(N)}$ in eq. (6.26). The numerical evaluation of $\mathcal{W}_N(x,p)$ is given by

$$\mathcal{W}_N(x,p) = \sum_{n\geq 0} c_n^{(N)} f_n(x,p) = \sum_{i,j\geq 0}\left(\sum_{n\geq 0} c_n^{(N)} v_{in}^* v_{jn}\right) E_{ij}(x,p). \tag{6.146}$$

In practice, this calculation involves a double truncation in the indices $i,j$ and in the index $n$. From this we can obtain the numerical evaluation of (6.138).

Let us now compare the quantum distribution with the limiting classical geometry for symmetric local $\mathbb{P}^1\times\mathbb{P}^1$. The mirror curve is given by (6.123) and the corresponding operator is (6.124). The classical action $I(E)$ can be found by using (6.103), (5.267) and the fact that $r=2$, $B=2\pi^2/3$ for this geometry. It reads,

$$I(E) = \frac{\mathrm{e}^E}{4\pi^2}G^{2,3}_{3,3}\left(\begin{array}{c}\frac{1}{2},\frac{1}{2},\frac{1}{2}\\ 0,0,-\frac{1}{2}\end{array}\middle|\frac{\mathrm{e}^{2E}}{16}\right) - \pi. \tag{6.147}$$

The relationship between the 't Hooft parameter $\lambda$ and the modulus of the limiting curve is given by (6.140). In Fig. 6.7 and Fig. 6.8, we compare the distribution

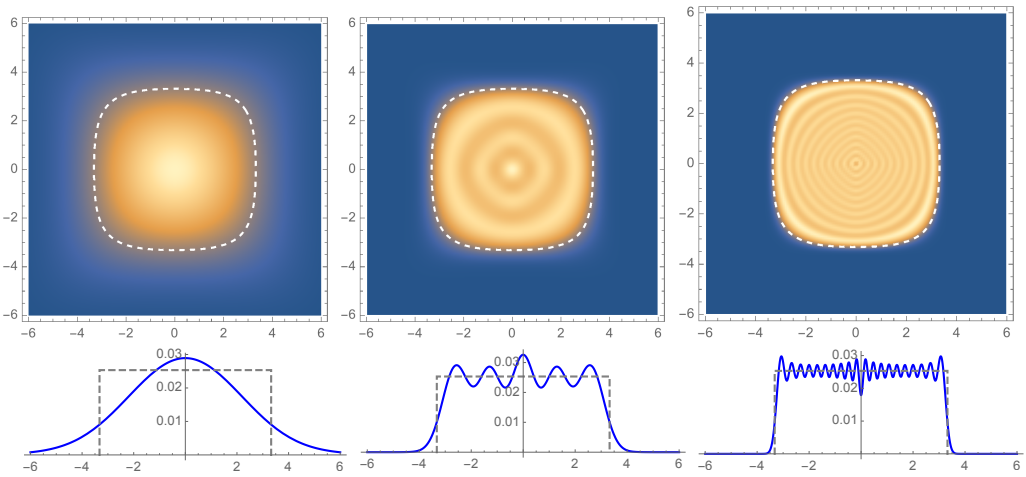

**Figure 6.7:** Top: Density plot of the quantum distribution $\mathcal{Q}_N(x,p)$ in phase space for local $\mathbb{F}_0$, compared to the classical mirror curve (6.139), which is shown as a white dashed line. In all cases, we have $N/\hbar = (2\pi)^{-1}$. On the left we show the distribution for $N = 1$, in the middle we show $N = 5$, and on the right we show $N = 20$. On the bottom, we show the restrictions of the same distributions to the slice $p = 0$, as well as the classical limit (6.141) in dashed lines.

$\mathcal{Q}_N(x,p)$ to the expected limiting behavior in (6.141), for various (increasing) values of $N$, and two fixed values of $\lambda$. It is clear that, as $N$ increases, the quantum distribution is more and more localized in the interior of the classical curve. Note that, from the point of view of quantum geometry, $N = 1$ corresponds to a very quantum regime, in which the quantum distribution is spread out in a wide region around the classical limit. The emergence of the mirror curve as a sharp boundary, as $N$, $\hbar$ increase, can be seen very clearly in the density plots of the quantum distribution shown in Fig. 6.7 and Fig. 6.8.

Although we have focused so far on the local $\mathbb{P}^1 \times \mathbb{P}^1$ geometry, we can consider other geometries of genus one, like local $\mathbb{P}^2$. In this case the mirror curve (6.92) corresponds to

$$\mathcal{O}(x,p) = \mathrm{e}^{x} + \mathrm{e}^{p} + \mathrm{e}^{-x-p}, \tag{6.148}$$

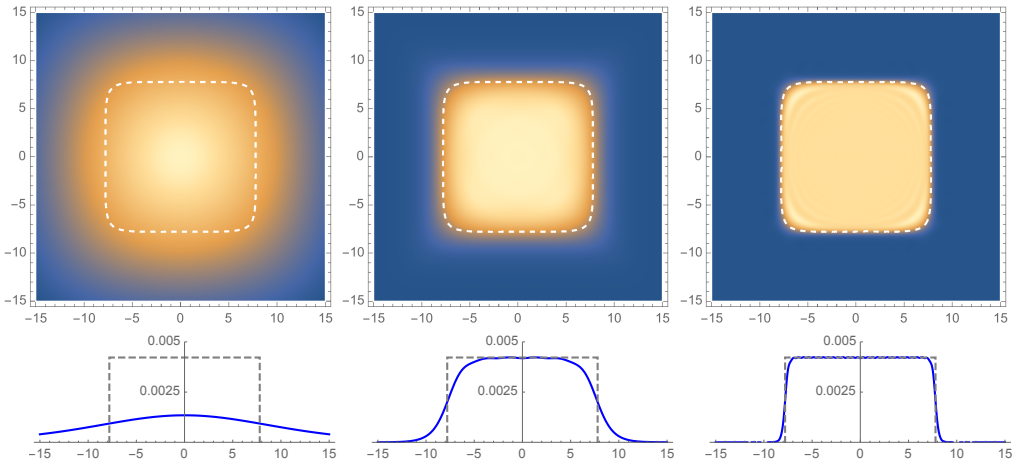


**Figure 6.8:** Same plots for $N/\hbar = 3/\pi$. On the left $N = 1$, in the middle $N = 6$, on the right $N = 30$.

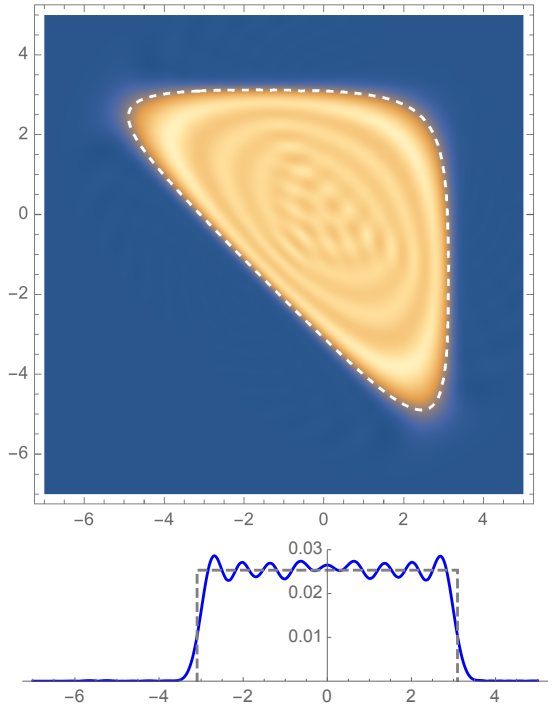


**Figure 6.9:** The same plot for local $\mathbb{P}^2$ for $N/\hbar = 1/2\pi$. Here, $N = 10$. On the bottom plot, we show the restrictions of the Wigner distribution on the slice $p = 0$, together with the classical limit in dashed lines.

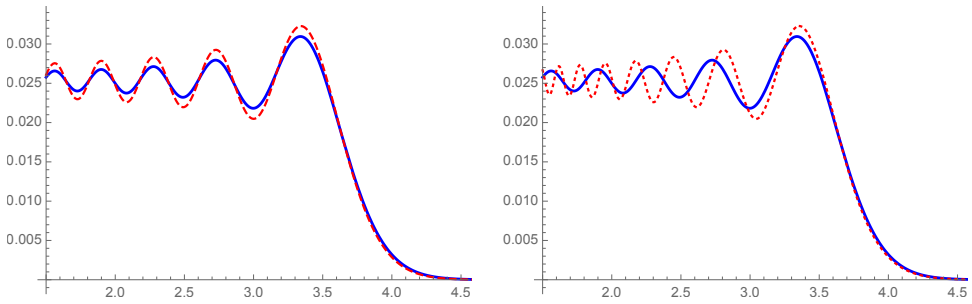


**Figure 6.10:** Comparison of $\mathcal{Q}_N(x,p)$ (in blue solid) with its semiclassical approximations, for local $\mathbb{P}^1\times\mathbb{P}^1$. On the left, the red dashed line is the expression (6.150) involving the chord area, which we analytically continue outside the classically allowed region. On the right, it is the transitional expression (6.151). We look at the slice $x=p$, and we set $N=20$, $\hbar=40\pi$.

and the classical action is given by

$$\begin{aligned} I(E) = &\frac{\sqrt{3}\Gamma\left(\frac{1}{3}\right)^3}{4\pi^2}\mathrm{e}^E\ {}_3F_2\left(\frac{1}{3},\frac{1}{3},\frac{1}{3};\frac{2}{3},\frac{4}{3};\frac{\mathrm{e}^{3E}}{27}\right)\\ &-\frac{\sqrt{3}\Gamma\left(\frac{2}{3}\right)^3}{8\pi^2}\mathrm{e}^{2E}\ {}_3F_2\left(\frac{2}{3},\frac{2}{3},\frac{2}{3};\frac{4}{3},\frac{5}{3};\frac{\mathrm{e}^{3E}}{27}\right)-\frac{2\pi}{3}. \end{aligned} \tag{6.149}$$

As we show in Fig. 6.9, where we compare the two sides of (6.141) for local $\mathbb{P}^2$, we also find in this example that the quantum distribution $\mathcal{Q}_N(x,p)$ sharpens around the classical mirror curve in the limit (6.104).

We would like to have as well a precise description of the quantum fluctuations of the distribution $\mathcal{Q}_N(x,p)$ away from the strict classical limit (6.141). It is natural to expect that the improved Balazs–Zipfel form (6.54), suitably adapted to mirror curves, provides such a description, so that

$$\mathcal{Q}_N(x,p)\approx\frac{1}{2\pi I(E_{\mathrm{DF}})}\mathcal{I}\left(-\left(\frac{3\mathcal{A}(x,p)}{2\hbar_{\mathrm{D}}}\right)^{2/3}\right), \tag{6.150}$$

where $\mathcal{A}(x,p)$ is the area of the chord defined by the classical mirror curve (6.139). We will derive this behaviour for symmetric local $\mathbb{P}^1\times\mathbb{P}^1$, but we expect this scaling form to be valid for any genus one mirror curve. We can also obtain a transitional approximation near the classical curve, as in (6.55), which gives

$$\mathcal{Q}_N(x,p)\approx\frac{1}{2\pi I(E_{\mathrm{DF}})}\mathcal{I}\left(2\frac{I(x,p)-I(E_{\mathrm{DF}}))}{\hbar^{2/3}B^{1/3}(x,p)}\right). \tag{6.151}$$

In Fig. 6.10 we compare the exact result for $\mathcal{Q}_N(x,p)$, for local $\mathbb{P}^1 \times \mathbb{P}^1$, with the improved Balazs–Zipfel form on the r.h.s. of (6.150), and with the transitional approximation (6.151), for $N = 20$ and $\hbar = 40\pi$, so that $\lambda = (2\pi)^{-1}$. As we can see, the expression (6.150) involving the full chord area gives a very good approximation deep inside the classical region. Both approximations capture with precision the shape of the quantum distribution in the vicinity of the classical mirror curve.

## 6.4 Semiclassical distribution for symmetric local $\mathbb{P}^1 \times \mathbb{P}^1$

Let us evaluate expression (6.137) for the symmetric local $\mathbb{P}^1 \times \mathbb{P}^1$ case. For this geometry, we find

$$\begin{aligned} V(\mu) &= -\frac{1}{2\pi}\mu + \frac{2}{\hbar}\log\Phi_b\left(\frac{\mu}{2\pi} - \frac{\mathrm{i}}{4}\right) - \frac{2}{\hbar}\log\Phi_b\left(\frac{\mu}{2\pi} + \frac{\mathrm{i}}{4}\right), \\ V_0(\mu) &= -\frac{\mu}{2\pi} + \frac{2}{\pi^2}\mathrm{Im}\,\mathrm{Li}_2(\mathrm{i}\mathrm{e}^{\mu}), \end{aligned} \tag{6.152}$$

and $\gamma = 1$, $C = 0$ and $b = \hbar/\pi$. The variable $\mu$ is given by $\mu = \pi\sqrt{2}\hbar^{-1}q$, where $q, P$ are related to the initial mirror curve variables $x, p$ through the linear canonical transformation $(x,p) = \left(\frac{q+P}{\sqrt{2}}, \frac{q-P}{\sqrt{2}}\right)$. Its dual variable is $v = \pi\sqrt{2}\hbar^{-1}q$. The spectral curve for the local $\mathbb{P}^1 \times \mathbb{P}^1$ matrix model in these variables can be worked out from (4.238) (see also eq. (5.107)):

$$(\mathrm{e}^{\mu} + \mathrm{e}^{-\mu})(\mathrm{e}^{\upsilon} + \mathrm{e}^{-\upsilon}) - \kappa = 0. \tag{6.153}$$

We define

$$M = \mathrm{e}^{\mu}. \tag{6.154}$$

The planar one-point function or resolvent $W_{1,0}(M)$ is obtained from the spectral curve. If we solve for $\upsilon(\mu)$ as

$$\upsilon(\mu) = \log\left(\frac{\mathrm{e}^{\mu}\kappa + 2\mathrm{i}\sqrt{\sigma(\mathrm{e}^{\mu})}}{2(1+\mathrm{e}^{2\mu})}\right), \tag{6.155}$$

where

$$\sigma(M) = M^4 - \frac{1}{4}M^2(\kappa^2 - 8) + 1, \tag{6.156}$$

then we have

$$W_{1,0}(M) = \frac{\mathrm{i}}{2\pi^2 M}\upsilon(\mu) + \frac{1}{2M}V_0'(\mu). \tag{6.157}$$

The relation between the modulus $\kappa$ and the 't Hooft coupling is given by the period (4.169), and can be written as

$$\lambda = \frac{\kappa}{16\pi^4}G^{2,3}_{3,3}\left(\begin{matrix} \frac{1}{2}, \frac{1}{2}, \frac{1}{2} \\ 0, 0, -\frac{1}{2} \end{matrix}\,\middle|\, \frac{\kappa^2}{16}\right) - \frac{1}{4\pi}. \tag{6.158}$$

This period in the complex plane precisely corresponds to the period in phase space giving $I(E)$ in (6.103):

$$I(E) = \frac{\mathrm{e}^E}{4\pi^2} G^{2,3}_{3,3}\left( \begin{matrix} \frac{1}{2}, \frac{1}{2}, \frac{1}{2} \\ 0, 0, -\frac{1}{2} \end{matrix} \middle| \frac{\mathrm{e}^{2E}}{16} \right) - \pi, \tag{6.159}$$

which can be obtained using (5.267) and the fact that $r = 2$, $B = 2\pi^2/3$ for this geometry. Therefore, we can identify $\kappa$ with the exponentiated, dual Fermi energy $\mathrm{e}^{E_{\mathrm{DF}}}$ which we define by (6.140). The elliptic modulus of the curve is

$$\tau = \mathrm{i}\frac{\mathrm{K}(16/\kappa^2)}{\mathrm{K}(1-16/\kappa^2)}. \tag{6.160}$$

For the two-point function, we can use the results of section 5.3. The planar two-point function is given by (5.119) that we recall here:

$$W_{2,0}(X_1, X_2) = \frac{1}{2\sqrt{\sigma(X_1)}\sqrt{\sigma(X_2)}} \left[ a^2 + b^2 - 2b^2 \frac{\mathrm{E}(1-\frac{a^2}{b^2})}{\mathrm{K}(1-\frac{a^2}{b^2})} \right.$$
$$\left. -(X_1^2 + X_2^2)\left( 1 - \frac{\left(\sqrt{\sigma(X_1)} - \sqrt{\sigma(X_2)}\right)^2}{(X_1^2 - X_2^2)^2} \right) \right]. \tag{6.161}$$

In this equation, $a$, $b$ are the endpoints of the cut where the eigenvalues condense, which are given in our case by

$$b = 1/a = \frac{1}{4}\left(\kappa - \sqrt{\kappa^2 - 16}\right). \tag{6.162}$$

The integrals of the planar two-point function can be written in terms of the Jacobi theta function $\vartheta_1(u)$ with modulus $\tau$ in (6.160), and the Abel–Jacobi map of the spectral curve,

$$u(X) = c_\kappa \int_\infty^X \frac{1}{\sqrt{\sigma(X')}} \mathrm{d}X', \qquad c_\kappa = \frac{\kappa}{8\mathrm{i}\mathrm{K}(1-16/\kappa^2)}. \tag{6.163}$$

These definitions are not the same as in section 5.3, and the difference arises from another choice of frame, i.e. another choice of the $\mathcal{A}$ and $\mathcal{B}$ cycles (here we chose the conifold frame). One finds, for the integrals appearing in (6.137),

$$\int_\infty^{X_1} \int_\infty^{X_2} W_{2,0}(X_1', X_2') \mathrm{d}X_1' \mathrm{d}X_2' = \log\left( -\frac{\vartheta_1(u(X_1) - u(X_2))}{X_1 - X_2} \frac{X_1 + X_2}{\vartheta_1(u(X_1) + u(X_2))} \right), \tag{6.164}$$

and

$$\int_\infty^X \int_\infty^X W_{2,0}(X_1', X_2') \mathrm{d}X_1' \mathrm{d}X_2' = \frac{1}{2} \log \left[ \left( -\frac{2c_\kappa \vartheta_1'(0)}{\vartheta_1(2u(X))} \frac{X}{\sqrt{\sigma(X)}} \right)^2 \right]. \tag{6.165}$$

The elliptic modulus of the theta functions is given by (6.160). To write down the final result, let us define

$$\mathcal{D} = \mathrm{e}^{\hbar \left( \int_\infty^a W_{1,0}(X) \mathrm{d}X - \frac{1}{2} V_0(a) \right)}. \tag{6.166}$$

Then, one has from (6.137):

$$\begin{aligned} \frac{B_N(\mu_1, \mu_2)}{Z_N} = & \frac{2c_\kappa \vartheta_1'(0) \mathcal{D}^2}{2\pi} \mathrm{e}^{\frac{\mathrm{i}\hbar}{2\pi^2} \int_a^{\mu_1} \upsilon(x) \mathrm{d}x} \mathrm{e}^{\frac{\mathrm{i}\hbar}{2\pi^2} \int_a^{\mu_2} \upsilon(x) \mathrm{d}x} \\ & \times \frac{\mathrm{e}^{\mu_1} \mathrm{e}^{\mu_2}}{\mathrm{e}^{\mu_1} - \mathrm{e}^{\mu_2}} \frac{1}{\sqrt{\sqrt{\sigma(\mathrm{e}^{\mu_1})} \vartheta_1(2u(\mathrm{e}^{\mu_1}))} \sqrt{\sqrt{\sigma(\mathrm{e}^{\mu_2})} \vartheta_1(2u(\mathrm{e}^{\mu_2}))}} \\ & \times \frac{\vartheta_1(u(\mathrm{e}^{\mu_1}) - u(\mathrm{e}^{\mu_2}))}{\vartheta_1(u(\mathrm{e}^{\mu_1}) + u(\mathrm{e}^{\mu_2}))} \left( 1 + \mathcal{O}(\hbar^{-1}) \right). \end{aligned} \tag{6.167}$$

It turns out that this expression is valid as long as the variables $M_1$, $M_2$ do not belong to the interval where the cut occurs, namely $\mathcal{C} = [a, b]$. When one of the variables is in the cut, it has to be modified as follows. The Riemann surface defined by (6.153) is a two-sheeted cover of the complex plane, and the two sheets correspond to the two sign determinations in front of the square-root when solving for $\upsilon(\mu)$. Let us define $\overline{M}_i = \exp(\bar{\mu}_i)$ as the point on the Riemann surface which corresponds to $M_i$, but on the other sheet. We have, in particular,

$$\begin{aligned} \sqrt{\sigma(\mathrm{e}^{\bar{\mu}})} &= -\sqrt{\sigma(\mathrm{e}^{\mu})}, \\ \upsilon(\bar{\mu}) &= -\upsilon(\mu), \\ u(\mathrm{e}^{\bar{\mu}}) &= 2u(\mathrm{e}^a) - u(\mathrm{e}^{\mu}). \end{aligned} \tag{6.168}$$

We now define:

$$B(\mu_1, \mu_2) = \begin{cases} \frac{B_N(\mu_1,\mu_2)}{Z_N} & \text{for } M_1, M_2 \notin \mathcal{C}, \\ \frac{B_N(\mu_1,\mu_2)}{Z_N} + \frac{B_N(\bar{\mu}_1,\mu_2)}{Z_N} & \text{for } M_1 \in \mathcal{C}, M_2 \notin \mathcal{C}, \\ \frac{B_N(\mu_1,\mu_2)}{Z_N} + \frac{B_N(\mu_1,\bar{\mu}_2)}{Z_N} & \text{for } M_1 \notin \mathcal{C}, M_2 \in \mathcal{C}, \\ \frac{B_N(\mu_1,\mu_2)}{Z_N} + \frac{B_N(\bar{\mu}_1,\mu_2)}{Z_N} + \frac{B_N(\mu_1,\bar{\mu}_2)}{Z_N} + \frac{B_N(\bar{\mu}_1,\bar{\mu}_2)}{Z_N} & \text{for } M_1, M_2 \in \mathcal{C}. \end{cases} \tag{6.169}$$

We have explicitly verified that this function gives an excellent approximation to the reduced density matrix (which can be also evaluated numerically).[1]

[1] It is not completely clear from the derivation of (6.137) from (6.131) why we need to add the different contributions in (6.169). However, we can give the following handwaving argument.

We can now use the analytic expression (6.167) and compute its Wigner transform in order to obtain $\mathcal{Q}_{N+1}(x,p)$ in the semiclassical limit:

$$\mathcal{Q}_{N+1}(x,p) \approx \frac{Z(N)}{(N+1)Z(N+1)} \frac{1}{2\pi\hbar_{\mathrm{D}}} \int_{\mathbb{R}} \mathrm{d}z\, \mathrm{e}^{\mathrm{i}(x+p)z/\hbar_{\mathrm{D}}}\, B\left(\frac{x-p}{2} - \frac{z}{2}, \frac{x-p}{2} + \frac{z}{2}\right). \tag{6.172}$$

In terms of the previous variables, we have

$$\mu = \frac{x-p}{2}, \qquad \upsilon = \frac{x+p}{2}, \tag{6.173}$$

which are the appropriate mirror curve coordinates in phase space.[2] The remaining part of the computation follows quite closely what we did in section 6.2 for the harmonic oscillator. As for that case, we consider the analogue classically allowed region. Here this is given by $M_{1,2} \in \mathcal{C}$, so $B_N(\mu,\mu')$ is the sum of four terms. As in the case of the harmonic oscillator, it is enough to use the term which leads straightforwardly to the chord construction, which is $B(\mu_1, \bar{\mu}_2)$. In exchange, we need to regularise the integration path to avoid the pole at $z=0$, as we did for the harmonic oscillator. One obtains the following expression (after rescaling $z \to 2z$):

$$\mathcal{Q}_{N+1}(x,p) \approx -\mathrm{i}\mathcal{N} \int_{\mathbb{R}+\mathrm{i}0} \mathrm{d}z\, \mathrm{e}^{2\mathrm{i}\Sigma(z)/\hbar_{\mathrm{D}}} \frac{F(z)}{\mathrm{e}^{\mu-z} - \mathrm{e}^{\mu+z}}, \tag{6.174}$$

When $M_1$ or/and $M_2$ are inside the interval $\mathcal{C}$, it means that $\mu$ or/and $\mu'$ are (6.131) are inside the interval where the $\mu_i$ condense in the 't Hooft limit. But this interval is precisely the branch cut which models the eigenvalue condensation. Therefore, there is an ambiguity to determine on which branch are the extra eigenvalue $\mu$ or/and $\mu'$ (i.e. if they are infinitesimally above or below the cut). From the expression we found, it would appear that the ambiguity is lifted by the prescription of taking the average, which means summing over the two possible branches. This is precisely what happens, for instance, when we want to evaluate the one-point function with $\mu = \log M$ inside the interval of eigenvalue condensation:

$$W_1(M) = \left\langle \sum_{i=1}^{N} \left( \frac{1}{\mathrm{e}^{\mu} - \mathrm{e}^{\mu_i}} - \frac{1}{\mathrm{e}^{\mu} - \omega \mathrm{e}^{\mu_i}} \right) \right\rangle. \tag{6.170}$$

In the 't Hooft limit, using the eigenvalue density $\rho(M)\mathrm{d}M$, this is

$$\begin{aligned} \lim_{\epsilon\to 0} \left( \int_{\mathrm{e}^a}^{M-\epsilon} + \int_{M+\epsilon}^{\mathrm{e}^b} \right) \mathrm{d}M' \rho(M') \left( \frac{1}{M-M'} - \frac{1}{M-\omega M'} \right) & \\ = \mathrm{P} \int_{\mathcal{C}} \mathrm{d}M' \rho(M') \left( \frac{1}{M-M'} - \frac{1}{M-\omega M'} \right) & \\ = W_{1,0}(M+\mathrm{i}0) + W_{1,0}(M-\mathrm{i}0), & \end{aligned} \tag{6.171}$$

in other words, the average of the function $W_{1,0}(M)$ over its two branches.

[2] Indeed, linear canonical transformations are complicated for quantum objects like eigenfunctions (they are integral transforms as in eq. (5.74)), but they are implemented by simple coordinate changes for quantum distributions. This is one of the advantages of the phase space formulation of quantum mechanics.

where

$$\begin{aligned}
\Sigma(z) &= 2\upsilon z + \int_a^{\mu-z} \upsilon(\mu')\mathrm{d}\mu' - \int_a^{\mu+z} \upsilon(\mu')\mathrm{d}\mu', \\
F(z) &= \frac{\mathrm{e}^{2\mu}}{\sqrt{\sqrt{\sigma(\mathrm{e}^{\mu-z})}\vartheta_1(2u(\mathrm{e}^{\mu-z}))}\sqrt{-\sqrt{\sigma(\mathrm{e}^{\mu+z})}\vartheta_1(4u(\mathrm{e}^a)-2u(\mathrm{e}^{\mu+z}))}} \\
&\qquad \times \frac{\vartheta_1(u(\mathrm{e}^{\mu-z})+u(\mathrm{e}^{\mu+z})-2u(\mathrm{e}^a))}{\vartheta_1(u(\mathrm{e}^{\mu-z})-u(\mathrm{e}^{\mu+z})+2u(\mathrm{e}^a))}, \\
\mathcal{N} &= \frac{2Z(N)}{(N+1)Z(N+1)} \cdot \frac{1}{2\pi\hbar_{\mathrm{D}}} \cdot \frac{2\mathrm{i}c_\kappa \vartheta_1'(0)\mathcal{D}^2}{2\pi}.
\end{aligned} \tag{6.175}$$

We can now perform the integral in (6.174) by using the uniform saddle point approximation, as in (6.69). In view of the form of $\Sigma(z)$, this will involve again Berry's chord construction. If we introduce a uniformization variable $u$ as in (6.71), the value of $\zeta$ is given by

$$\zeta = \left(\frac{3}{4}\mathcal{A}(x,p)\right)^{2/3}, \tag{6.176}$$

where $\mathcal{A}(x,p)$ is the area of the chord associated with the curve (6.139) with $\mathcal{O}(\mathrm{e}^x, \mathrm{e}^p)$ given in (6.123) (the extra factor of $1/2$ w.r.t. (6.74) is due to the fact that we have parametrized $\Sigma(z)$ with the variables $\mu$, $\upsilon$, and the volume form in these variables is $1/2$ of the volume form in the variables $x, p$). We now expand the integrand of (6.174) as in (6.76),

$$\frac{F(z(u))}{\mathrm{e}^{\mu-z(u)} - \mathrm{e}^{\mu+z(u)}} z'(u) = \frac{p_{-1}}{u} + \sum_{m\geq 0} p_m u(u^2-\zeta)^m + \sum_{m\geq 0} q_m (u^2-\zeta)^m. \tag{6.177}$$

Here, we allowed for even terms in $u$ in the r.h.s, which were not present in the harmonic oscillator case due to parity symmetry. The leading term comes from $p_{-1}$, which is given by

$$p_{-1} = -\frac{1}{2}F(0)\mathrm{e}^{-\mu} \tag{6.178}$$

and turns out to be a constant on phase space, which is equal to

$$-\frac{\mathrm{i}\mathrm{e}^{\mathrm{i}\pi\tau/2}}{4c_\kappa \vartheta_1'(0)}. \tag{6.179}$$

We finally obtain,

$$\mathcal{Q}_{N+1}(x,p) \approx -\mathcal{N}\pi \left(\frac{\mathrm{i}\mathrm{e}^{\mathrm{i}\pi\tau}}{2c_\kappa \vartheta_1'(0)}\right) \mathcal{I}\left(-\left(\frac{2}{\hbar_D}\right)^{2/3}\zeta\right). \tag{6.180}$$

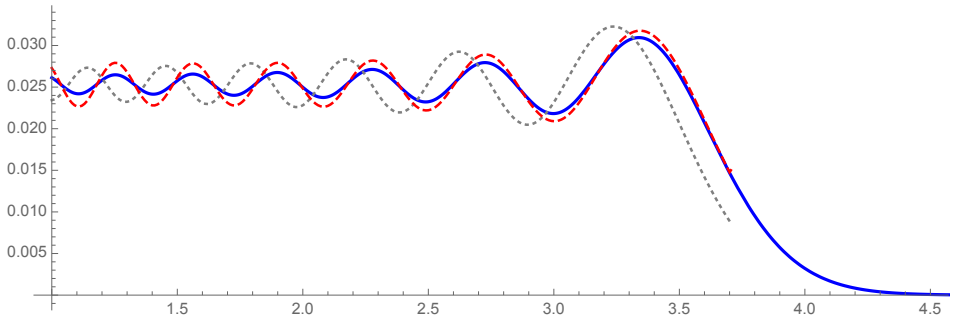


**Figure 6.11:** Comparison of $\mathcal{Q}_{N+1}(x,p)$ (in blue solid) with its large $\hbar$ approximations. The gray dotted line is expression (6.182) while the red dashed line incorporates the next-to-subleasing correction. Here we take $N = 19$, $\hbar = 40\pi$ so $\kappa \approx 27.716$, and we look at the slice $x = p$. The red dashed line reproduces the exact function with the same level of precision as in the left plot of Fig. (6.10), which uses expression (6.150) with the right chord area function. The gray dotted curve has a misalignment of order $1/N$.

The prefactor can be simplified by looking at its 't Hooft expansion. Indeed, we have

$$\begin{aligned} -\mathcal{N}\pi\left(\frac{\mathrm{i}\mathrm{e}^{\mathrm{i}\pi\tau}}{2c_\kappa\vartheta_1'(0)}\right) &= \frac{1}{2\pi\hbar_{\mathrm{D}}(N+1)}\frac{Z(N)}{Z(N+1)}\mathcal{D}^2\mathrm{e}^{\mathrm{i}\pi\tau/2} \\ &= \frac{1}{2\pi(N+1)\hbar_{\mathrm{D}}}\exp\left[2\hbar\left(\int_\infty^{\mathrm{e}^a} W_{1,0}(X)\mathrm{d}X - \frac{1}{2}V_0(a)\right) - \hbar\mathcal{F}_0'(\lambda)\right. \\ &\qquad \left. - \frac{1}{2}\mathcal{F}_0''(\lambda) + \frac{\mathrm{i}\pi\tau}{2} + O(\hbar)\right]. \end{aligned} \tag{6.181}$$

Everything in the exponential of the second line cancels due to the results of section 4.4. We finally find

$$\mathcal{Q}_{N+1}(x,p) \approx \frac{1}{2\pi\hbar_{\mathrm{D}}(N+1)}\mathcal{I}\left(-\left(\frac{3}{2\hbar_D}\mathcal{A}(x,p)\right)^{2/3}\right). \tag{6.182}$$

Since $\hbar_{\rm D} N = I(E_{\rm DF})$, this is almost exactly what we conjectured in eq. (6.150) for $N+1$ instead of $N$, except for the following fact: the spectral curve of the planar matrix model determining the classical geometry and thus chord area $\mathcal{A}(x,p)$ is still determined by the modulus $\kappa(\lambda) = \kappa\left(\frac{N}{\hbar}\right)$ through (6.158) instead of $\kappa\left(\frac{N+1}{\hbar}\right)$ as was advocated in (6.140) (recall that $\kappa = {\rm e}^{E_{\rm DF}}$). So both expressions (6.150) and (6.182) involve the same function $\mathcal{A}(x,p)$ while (6.150) computes $\mathcal{Q}_N$ and (6.182) computes $\mathcal{Q}_{N+1}$. In other words, what we find here from the leading order computation is that the conjecture (6.150) would be valid but for the curve controlled by $\lambda = \frac{N-1}{\hbar}$ instead of $\lambda = \frac{N}{\hbar}$. This would imply an order $1/N$ misalignment of the support and oscillations that we do not observe in the finite $N$ results plotted in Fig. 6.10.

This mismatch of the result (6.182) with our successful conjecture (6.150) is cured if we compute the next-to-leading correction to (6.182) in small $\hbar_{\rm D}$. This can be done exactly as for the harmonic oscillator case, and involves the $p_0$ and $q_0$ terms in the uniform saddle point approximation in (6.177). The expression we find is quite long and not very illuminating, but it can be numerically evaluated, and is found to reproduce (6.150) very closely. See Fig. 6.11. So the next-to-leading correction to (6.182) has approximately the effect of shifting $N$ by one unit.

# Chapter 7

# Concluding remarks

In this thesis, we considered three aspects of the Topological String/Spectral Theory (TS/ST) correspondence of [2, 16], which is a precise conjectural relationship between quantities appearing in the world of topological strings and enumerative invariants of toric Calabi-Yau threefolds (the TS side), and the spectral theory of difference operators arising from the quantization of mirror curves (the ST side). These three aspects are consequences or extensions of the original conjecture, which shed more light on both the TS side and the ST sides of the correspondence.

The first aspect we studied is a consequence of the TS/ST conjecture implying a relationship between convergent matrix models and topological strings. We found that in the 't Hooft limit, the free energies of our family of matrix models are the topological string free energies in the conifold frame. The 't Hooft limit in the matrix models corresponds to the genus expansion of the topological string, and, in this sense, the matrix model is a non-perturbative realization of the closed topological string partition function. We found that the weak 't Hooft coupling limit (or gaussian limit) of the matrix model corresponds to the expansion of the topological string free energies around the conifold point. But we could also obtain exact planar results for our matrix model, and test exact planar relations (like the identification of the spectral curve of the matrix model with the mirror curve of the Calabi–Yau threefold), as well as extract genus 0 enumerative invariants directly from the matrix model at strong 't Hooft coupling. We see at least two directions worth further exploration. Firstly, it would be very nice to have an algorithmic way of constructing explicit integral kernels for at least all the cases related to genus one mirror curves (e.g., what is the exact integral kernel for the local $\mathbb{F}_1$ geometry?). This would lead to explicit matrix models for all these cases, and also expand the known multi-cut matrix model family of [16] for higher genus mirror curves. Secondly, a better understanding of the large $N$ expansion of our matrix models beyond the

planar limit is highly desirable. This should follow from a set of loop equations as in the hermitian and $O(n)$ matrix model families [61, 110]. It would be very nice to derive these loop equations and show that they satisfy the topological recursion [63]. Indeed, through the BKMP theorem [57, 58, 60], this would provide a proof for the "weak" TS/ST conjecture, i.e. the relation between the matrix models and the topological string free energies in the conifold frame. Obtaining the loop equations may possibly follow from [110].

The second aspect we studied is the extension of the TS/ST correspondence to eigenfunctions. We started by studying a generalized family of eigenfunctions from the spectral theory side, in particular in a matrix model realization. We then focused on its 't Hooft limit. The computation was done for the special example of symmetric local $\mathbb{P}^1 \times \mathbb{P}^1$, and we found that the WKB resummation of the eigenfunction (which is the natural starting point to write down exact formulas) should be supplemented by the topological string wavefunction. This second contribution is the dominant one in the 't Hooft limit, but is non-perturbative in the small $\hbar$ limit: it is a natural non-perturbative completion of the WKB answer. Another point which we could gather from the study of our special case, is that the full eigenfunctions are constructed from a sum of different analytic continuations of the fundamental functions given by the WKB + topological string wavefunction. Using this knowledge, we formulated a precise conjecture for the generalized eigenfunctions. It is a one parameter extension of the TS/ST conjecture [2, 16], where the parameter is given by the position coordinate/open string modulus $x$; the extended conjecture reduces to the standard one when $x \to \infty$. This gives a precise link between the vanishing of the spectral determinant and the decaying behaviour of the generalized eigenfunction at $\infty$. We performed several numerical and analytical tests of the conjecture for various geometries, especially in the self-dual case $\hbar = 2\pi$, where the exact solution can be written down explicitly. We also discussed a link between the quantization conditions of quantum integrable systems and enhanced decay of our eigenfunctions. The generalized eigenfunctions with the most enhanced decay are a discrete subset, which we called "fully on-shell". Then, we showed that these "fully on-shell" eigenfunctions can be constructed purely from the resummed WKB wavefunction, using the modular duality structure of the underlying integrable systems. Several issues still remain in this work. Maybe the most pressing is a better understanding of the analytic continuation of the topological string wavefunction which is needed to write down exact results. Indeed, the topological string wavefunction at finite $\hbar$ is only known as a large $X = \mathrm{e}^x$ expansion around a special point on its Riemann surface. The analytic continuation to other sheets of the Riemann surface would require some kind of resummation of this expansion. A desirable result would

be for example a kind of topological vertex algorithm giving directly the expansion of the topological string wavefunction on the other sheets of the Riemann surface. If in addition we could find a good prescription for the refined topological vertex algorithm so that it gives the resummed WKB wavefunction as well, we would be in a similar situation as for the standard TS/ST conjecture: everything about the generalized eigenfunctions would be encoded in open enumerative invariants of toric Calabi–Yau threefolds, and the full eigenfunction would be algorithmically obtained from the topological vertex and its refinement. Of course, as for the standard TS/ST correspondence, the question of how to prove our extended conjecture to eigenfunctions still remains open. Finally, our extended conjecture only made use of the topological wavefunction, which is a very specialized version of the open string amplitudes (the specialization of (5.177) given by expression (5.179)). To really have a non-pertubative definition of the full open string sector, we should look for more general spectral quantities in the spectral theory side which encode the full open string amplitudes.

The third and last aspect that we studied is how the TS/ST conjecture and its interpretation in terms of a Fermi gas can help us define a sensible notion of quantum curve. We argued that this is given by a certain quantum distribution on phase space, whose support reduces to the classical mirror curve in a certain classical limit. Our main result was that this distribution can be taken as the Wigner transform of a natural quantity in many-body physics: the one-particle reduced density matrix in the gas of $N$ particles. Since our case is a gas of non-interacting fermions, this quantity is completely determined by the one particle Hamiltonian and its corresponding density matrix, which is identified with the inverse quantized mirror curve. We argued that the classical limit from the point of view of the emerging curve should correspond to the 't Hooft limit given by large $N, \hbar$ with fixed ratio, which we showed to behave as a thermodynamic and low temperature limit from the Fermi gas perspective. We formulated a conjecture for the semiclassical behaviour of the Wigner transform of the one-particle reduced density matrix, especially for its universal quantum oscillations around the classical curve. This universal oscillatory behaviour should be given by an improved version of the Balazs–Zipfel approximation [23], which we derived for the quantum harmonic oscillator at zero temperature. We also performed numerical and analytical tests of the conjecture for a couple of geometries. Several directions of study are still open. We only considered the case where the mirror curve has genus one. It would be interesting to extend our results to the higher genus cases, which are expected to involve mixed non-interacting Fermi gases containing $g_W > 1$ different types of fermions. Also, a popular statistical quantity which in other setups was found to be strongly related to the notion

of quantum geometry is the entanglement entropy. This quantity is probably also worth studying in our Fermi gas, to see if it has a counterpart on the topological string side. Finally, even at the level of standard quantum mechanics, it would be very nice to derive the improved Balazs–Zipfel approximation. We derived it for a gas of harmonic oscillators at zero temperature, but results for more general non-interacting systems and for finite temperature are, to our knowledge, lacking, even in one dimension.

During the years of this thesis, several other aspects and extensions of the TS/ST correspondence were studied by various authors. To give a more complete picture of the topic, let finish by mentioning some of the main advances in the study of this correspondence. After its initial statement in [2] for genus one mirror curves, it was extended to the higher genus cases in [16]. Many non-trivial checks were performed in [16, 82, 165]. In all these works including the present thesis, the parameter $\hbar$ was assumed to be real (as in standard quantum mechanics), but the conjecture was also tested for complex values of the parameter $\hbar$ in [81]. In parallel, exact quantization conditions for the spectral problem were conjectured in [31], only involving the topological strings in the NS limit – or resummed WKB data. These were generalized and linked to quantum integrable systems in [18, 72]. The relationship and consistency of these quantization conditions with the original TS/ST correspondence was studied in [85], and in [84, 86] using blow-up equations. These ideas were then generalized for local elliptic Calabi–Yau threefolds and their corresponding 6d superconformal gauge theories in [166, 167]. In an other direction, the TS/ST conjecture was studied in a certain limit related to 4d gauge theories and its relation to Painlevé equations in [90, 168–170]. The relation with Painlevé equations can be used in some cases to prove the TS/ST conjecture in this so called 4d limit [168]. The study of the TS/ST correspondence also led to the results in [171] solving deformed quantum mechanical systems. Still in an other direction, the TS/ST correspondence was found to have relevance in 2d electron lattice models, and could shed new light on the fractal band structures known as the Hofstadter butterfly [138, 139, 172, 173]. The TS/ST correspondence can be seen as giving a prescription for the non-perturbative completion of the NS free energy expansion. It was checked in [174] that this coincides with the non-perturbative completion that is provided by resurgence and Borel resummation. This provided insight for [175, 176] which obtained the solution of standard quantum mechanical problems using the refined holomorphic anomaly equation.

# Bibliography


[1] M. Kac, *Can one hear the shape of a drum?*, *The American Mathematical Monthly* **73** (1966) 1 [https://doi.org/10.1080/00029890.1966.11970915].

[2] A. Grassi, Y. Hatsuda and M. Marino, *Topological Strings from Quantum Mechanics*, *Annales Henri Poincare* **17** (2016) 3177 [1410.3382].

[3] M. Marino and P. Putrov, *Exact Results in ABJM Theory from Topological Strings*, *JHEP* **06** (2010) 011 [0912.3074].

[4] M. Marino and P. Putrov, *ABJM theory as a Fermi gas*, *J. Stat. Mech.* **1203** (2012) P03001 [1110.4066].

[5] Y. Hatsuda, S. Moriyama and K. Okuyama, *Instanton Effects in ABJM Theory from Fermi Gas Approach*, *JHEP* **01** (2013) 158 [1211.1251].

[6] Y. Hatsuda, M. Marino, S. Moriyama and K. Okuyama, *Non-perturbative effects and the refined topological string*, *JHEP* **09** (2014) 168 [1306.1734].

[7] S. Codesido, A. Grassi and M. Marino, *Exact results in $\mathcal{N} = 8$ Chern-Simons-matter theories and quantum geometry*, *JHEP* **07** (2015) 011 [1409.1799].

[8] J. Kallen and M. Marino, *Instanton effects and quantum spectral curves*, *Annales Henri Poincare* **17** (2016) 1037 [1308.6485].

[9] M.-x. Huang and X.-f. Wang, *Topological Strings and Quantum Spectral Problems*, *JHEP* **09** (2014) 150 [1406.6178].

[10] R. Kashaev and M. Marino, *Operators from mirror curves and the quantum dilogarithm*, *Commun. Math. Phys.* **346** (2016) 967 [1501.01014].

[11] M. Marino and S. Zakany, *Matrix models from operators and topological strings*, *Annales Henri Poincare* **17** (2016) 1075 [1502.02958].

[12] R. Kashaev, M. Marino and S. Zakany, *Matrix models from operators and topological strings, 2*, *Annales Henri Poincare* **17** (2016) 2741 [1505.02243].

[13] S. Zakany, *Matrix models for topological strings: exact results in the planar limit*, 1810.08608.

[14] I. K. Kostov, *Exact solution of the six vertex model on a random lattice*, *Nucl. Phys.* **B575** (2000) 513 [hep-th/9911023].

[15] M. Marino and S. Zakany, *Exact eigenfunctions and the open topological string*, *J. Phys.* **A50** (2017) 325401 [1606.05297].

[16] S. Codesido, A. Grassi and M. Marino, *Spectral Theory and Mirror Curves of Higher Genus*, *Annales Henri Poincare* **18** (2017) 559 [1507.02096].

[17] M. Marino and S. Zakany, *Wavefunctions, integrability, and open strings*, 1706.07402.

[18] S. Franco, Y. Hatsuda and M. Marino, *Exact quantization conditions for cluster integrable systems*, *J. Stat. Mech.* **1606** (2016) 063107 [1512.03061].

[19] S. Zakany, *Quantized mirror curves and resummed WKB*, 1711.01099.

[20] A.-K. Kashani-Poor, *Quantization condition from exact WKB for difference equations*, *JHEP* **06** (2016) 180 [1604.01690].

[21] L. D. Faddeev, *Discrete Heisenberg-Weyl group and modular group*, *Lett. Math. Phys.* **34** (1995) 249 [hep-th/9504111].

[22] M. Marino and S. Zakany, *Quantum curves as quantum distributions*, 1804.05574.

[23] N. Balazs and G. Zipfel Jr, *Quantum oscillations in the semiclassical fermion $\mu$-space density*, *Annals of Physics* **77** (1973) 139.

[24] K. Okuyama and S. Zakany, *TBA-like integral equations from quantized mirror curves*, *JHEP* **03** (2016) 101 [1512.06904].

[25] A. B. Zamolodchikov, *Painleve III and 2-d polymers*, *Nucl. Phys.* **B432** (1994) 427 [hep-th/9409108].

[26] C. A. Tracy and H. Widom, *Proofs of two conjectures related to the thermodynamic Bethe ansatz*, *Commun. Math. Phys.* **179** (1996) 667 [solv-int/9509003].

[27] Y. Hatsuda, A. Sciarappa and S. Zakany, *Exact quantization conditions for the elliptic Ruijsenaars-Schneider model*, 1809.10294.

[28] S. Ruijsenaars and H. Schneider, *A new class of integrable systems and its relation to solitons*, *Annals of Physics* **170** (1986) 370 .

[29] S. N. M. Ruijsenaars, *Complete integrability of relativistic calogero-moser systems and elliptic function identities*, *Comm. Math. Phys.* **110** (1987) 191.

[30] N. A. Nekrasov and S. L. Shatashvili, *Quantization of Integrable Systems and Four Dimensional Gauge Theories*, in *Proceedings, 16th International Congress on Mathematical Physics (ICMP09): Prague, Czech Republic, August 3-8, 2009*, pp. 265–289, 2009, 0908.4052, DOI.

[31] X. Wang, G. Zhang and M.-x. Huang, *New Exact Quantization Condition for Toric Calabi-Yau Geometries*, *Phys. Rev. Lett.* **115** (2015) 121601 [1505.05360].

[32] K. Hori, S. Katz, A. Klemm, R. Pandharipande, R. Thomas, C. Vafa et al., *Mirror symmetry*, vol. 1 of *Clay mathematics monographs*. AMS, Providence, USA, 2003.

[33] M. Vonk, *A Mini-course on topological strings*, hep-th/0504147.

[34] M. Marino, *Chern-Simons theory and topological strings*, *Rev. Mod. Phys.* **77** (2005) 675 [hep-th/0406005].

[35] M. Marino, *Les Houches lectures on matrix models and topological strings*, 2004, hep-th/0410165, http://weblib.cern.ch/abstract?CERN-PH-TH-2004-199.

[36] E. Witten, *Topological Sigma Models*, *Commun. Math. Phys.* **118** (1988) 411.

[37] E. Witten, *On the Structure of the Topological Phase of Two-dimensional Gravity*, *Nucl. Phys.* **B340** (1990) 281.

[38] K. Hori and C. Vafa, *Mirror symmetry*, hep-th/0002222.

[39] E. Witten, *Phases of N=2 theories in two-dimensions*, *Nucl. Phys.* **B403** (1993) 159 [hep-th/9301042].

[40] K. Hori, A. Iqbal and C. Vafa, *D-branes and mirror symmetry*, hep-th/0005247.

[41] E. Witten, *Chern-Simons Gauge Theory As A String Theory*, *ArXiv High Energy Physics - Theory e-prints* (1992) [hep-th/9207094].

[42] R. Gopakumar and C. Vafa, *M theory and topological strings. 1.*, hep-th/9809187.

[43] R. Gopakumar and C. Vafa, *M theory and topological strings. 2.*, hep-th/9812127.

[44] H. Ooguri and C. Vafa, *Knot invariants and topological strings*, *Nucl. Phys.* **B577** (2000) 419 [hep-th/9912123].

[45] J. M. F. Labastida, M. Marino and C. Vafa, *Knots, links and branes at large N*, *JHEP* **11** (2000) 007 [hep-th/0010102].

[46] R. Gopakumar and C. Vafa, *On the gauge theory / geometry correspondence*, *Adv. Theor. Math. Phys.* **3** (1999) 1415 [hep-th/9811131].

[47] A. Grassi, J. Kallen and M. Marino, *The topological open string wavefunction*, *Commun. Math. Phys.* **338** (2015) 533 [1304.6097].

[48] M. Aganagic, A. Klemm, M. Marino and C. Vafa, *The Topological vertex*, *Commun. Math. Phys.* **254** (2005) 425 [hep-th/0305132].

[49] V. V. Batyrev, *Dual Polyhedra and Mirror Symmetry for Calabi-Yau Hypersurfaces in Toric Varieties*, in *eprint arXiv:alg-geom/9310003*, Oct., 1993.

[50] M. Bershadsky, S. Cecotti, H. Ooguri and C. Vafa, *Kodaira-Spencer theory of gravity and exact results for quantum string amplitudes*, *Commun. Math. Phys.* **165** (1994) 311 [hep-th/9309140].

[51] B. Haghighat, A. Klemm and M. Rauch, *Integrability of the holomorphic anomaly equations*, *JHEP* **10** (2008) 097 [0809.1674].

[52] M. Aganagic, V. Bouchard and A. Klemm, *Topological Strings and (Almost) Modular Forms*, *Commun. Math. Phys.* **277** (2008) 771 [hep-th/0607100].

[53] E. Witten, *Quantum background independence in string theory*, in *Conference on Highlights of Particle and Condensed Matter Physics (SALAMFEST) Trieste, Italy, March 8-12, 1993*, pp. 0257–275, 1993, hep-th/9306122.

[54] M. Aganagic and C. Vafa, *Mirror symmetry, D-branes and counting holomorphic discs*, hep-th/0012041.

[55] M. Aganagic, A. Klemm and C. Vafa, *Disk instantons, mirror symmetry and the duality web*, *Z. Naturforsch.* **A57** (2002) 1 [hep-th/0105045].

[56] M. Marino, *Open string amplitudes and large order behavior in topological string theory*, *JHEP* **03** (2008) 060 [hep-th/0612127].

[57] V. Bouchard, A. Klemm, M. Marino and S. Pasquetti, *Remodeling the B-model*, *Commun. Math. Phys.* **287** (2009) 117 [0709.1453].

[58] B. Eynard and N. Orantin, *Computation of Open Gromov-Witten Invariants for Toric Calabi-Yau 3-Folds by Topological Recursion, a Proof of the BKMP Conjecture*, *Commun. Math. Phys.* **337** (2015) 483 [1205.1103].

[59] B. Fang, C.-C. M. Liu and Z. Zong, *All Genus Open-Closed Mirror Symmetry for Affine Toric Calabi-Yau 3-Orbifolds*, *ArXiv e-prints* (2013) [1310.4818].

[60] B. Fang, C.-C. M. Liu and Z. Zong, *On the Remodeling Conjecture for Toric Calabi-Yau 3-Orbifolds*, *ArXiv e-prints* (2016) [1604.07123].

[61] B. Eynard, *Topological expansion for the 1-Hermitian matrix model correlation functions*, *JHEP* **11** (2004) 031 [hep-th/0407261].

[62] L. Chekhov and B. Eynard, *Hermitean matrix model free energy: Feynman graph technique for all genera*, *JHEP* **03** (2006) 014 [hep-th/0504116].

[63] B. Eynard and N. Orantin, *Invariants of algebraic curves and topological expansion*, *Commun. Num. Theor. Phys.* **1** (2007) 347 [math-ph/0702045].

[64] R. Dijkgraaf and C. Vafa, *Matrix models, topological strings, and supersymmetric gauge theories*, *Nucl. Phys.* **B644** (2002) 3 [hep-th/0206255].

[65] M. Marino, *Chern-Simons theory, matrix integrals, and perturbative three manifold invariants*, *Commun. Math. Phys.* **253** (2004) 25 [hep-th/0207096].

[66] M. Aganagic, A. Klemm, M. Marino and C. Vafa, *Matrix model as a mirror of Chern-Simons theory*, *JHEP* **02** (2004) 010 [hep-th/0211098].

[67] S. H. Katz, A. Klemm and C. Vafa, *Geometric engineering of quantum field theories*, *Nucl. Phys.* **B497** (1997) 173 [hep-th/9609239].

[68] N. A. Nekrasov, *Seiberg-Witten prepotential from instanton counting*, *Adv. Theor. Math. Phys.* **7** (2003) 831 [hep-th/0206161].

[69] T. J. Hollowood, A. Iqbal and C. Vafa, *Matrix models, geometric engineering and elliptic genera*, *JHEP* **03** (2008) 069 [hep-th/0310272].

[70] A. Iqbal, C. Kozcaz and C. Vafa, *The Refined topological vertex*, *JHEP* **10** (2009) 069 [hep-th/0701156].

[71] A. Iqbal and C. Kozcaz, *Refined topological strings on local* $\mathbb{P}^2$, *JHEP* **03** (2017) 069 [1210.3016].

[72] Y. Hatsuda and M. Marino, *Exact quantization conditions for the relativistic Toda lattice*, *JHEP* **05** (2016) 133 [1511.02860].

[73] S. Kharchev, D. Lebedev and M. Semenov-Tian-Shansky, *Unitary representations of U(q) (sl(2, R)), the modular double, and the multiparticle q deformed Toda chains*, *Commun. Math. Phys.* **225** (2002) 573 [hep-th/0102180].

[74] M. Aganagic, M. C. N. Cheng, R. Dijkgraaf, D. Krefl and C. Vafa, *Quantum Geometry of Refined Topological Strings*, *JHEP* **11** (2012) 019 [1105.0630].

[75] M. Aganagic, R. Dijkgraaf, A. Klemm, M. Marino and C. Vafa, *Topological strings and integrable hierarchies*, *Commun. Math. Phys.* **261** (2006) 451 [hep-th/0312085].

[76] A. Laptev, L. Schimmer and L. A. Takhtajan, *Weyl type asymptotics and bounds for the eigenvalues of functional-difference operators for mirror curves*, 1510.00045.

[77] A. Kuroś, P. Kościk and A. Okopińska, *Determination of resonances by the optimized spectral approach*, *Journal of Physics A Mathematical General* **46** (2013) 085303 [1211.2424].

[78] Y. Hatsuda, S. Moriyama and K. Okuyama, *Exact Results on the ABJM Fermi Gas*, *JHEP* **10** (2012) 020 [1207.4283].

[79] Y. Hatsuda, S. Moriyama and K. Okuyama, *Instanton Bound States in ABJM Theory*, *JHEP* **05** (2013) 054 [1301.5184].

[80] N. Drukker, M. Marino and P. Putrov, *From weak to strong coupling in ABJM theory*, *Commun. Math. Phys.* **306** (2011) 511 [1007.3837].

[81] A. Grassi and M. Marino, *The complex side of the TS/ST correspondence*, 1708.08642.

[82] J. Gu, A. Klemm, M. Marino and J. Reuter, *Exact solutions to quantum spectral curves by topological string theory*, *JHEP* **10** (2015) 025 [1506.09176].

[83] S. Codesido, J. Gu and M. Marino, *Operators and higher genus mirror curves*, *JHEP* **02** (2017) 092 [1609.00708].

[84] A. Grassi and J. Gu, *BPS relations from spectral problems and blowup equations*, 1609.05914.

[85] K. Sun, X. Wang and M.-x. Huang, *Exact Quantization Conditions, Toric Calabi-Yau and Nonperturbative Topological String*, *JHEP* **01** (2017) 061 [1606.07330].

[86] M.-x. Huang, K. Sun and X. Wang, *Blowup Equations for Refined Topological Strings*, 1711.09884.

[87] J. Ellegaard Andersen and R. Kashaev, *A TQFT from Quantum Teichmüller Theory*, *Commun. Math. Phys.* **330** (2014) 887 [1109.6295].

[88] B. Eynard, A.-K. Kashani-Poor and O. Marchal, *A Matrix Model for the Topological String I: Deriving the Matrix model*, *Annales Henri Poincare* **15** (2014) 1867 [1003.1737].

[89] B. Eynard, A.-K. Kashani-Poor and O. Marchal, *A Matrix model for the topological string II. The spectral curve and mirror geometry*, *Annales Henri Poincare* **14** (2013) 119 [1007.2194].

[90] G. Bonelli, A. Grassi and A. Tanzini, *New results in $\mathcal{N} = 2$ theories from non-perturbative string*, *Annales Henri Poincare* **19** (2018) 743 [1704.01517].

[91] I. K. Kostov, *O(n) Vector Model on a Planar Random Lattice: Spectrum of Anomalous Dimensions*, *Mod. Phys. Lett.* **A4** (1989) 217.

[92] E. Brézin, C. Itzykson, G. Parisi and J. B. Zuber, *Planar Diagrams*, *Commun. Math. Phys.* **59** (1978) 35.

[93] D. Bessis, C. Itzykson and J. Zuber, *Quantum field theory techniques in graphical enumeration*, *Advances in Applied Mathematics* **1** (1980) 109 .

[94] D. Ghoshal and C. Vafa, *C = 1 string as the topological theory of the conifold*, *Nucl. Phys.* **B453** (1995) 121 [hep-th/9506122].

[95] M.-x. Huang and A. Klemm, *Holomorphic Anomaly in Gauge Theories and Matrix Models*, *JHEP* **09** (2007) 054 [hep-th/0605195].

[96] M. Hanada, M. Honda, Y. Honma, J. Nishimura, S. Shiba and Y. Yoshida, *Numerical studies of the ABJM theory for arbitrary N at arbitrary coupling constant*, *JHEP* **05** (2012) 121 [1202.5300].

[97] Y. Hatsuda and K. Okuyama, *Probing non-perturbative effects in M-theory*, *JHEP* **10** (2014) 158 [1407.3786].

[98] F. Rodriguez-villegas, *Modular mahler measures I*, *Topics in Number Theory* **467** (1998) .

[99] M. Kerr and C. Doran, *Algebraic K-theory of toric hypersurfaces*, *ArXiv e-prints* (2008) [0809.4669].

[100] K. Mohri, Y. Onjo and S.-K. Yang, *Closed submonodromy problems, local mirror symmetry and branes on orbifolds*, *Rev. Math. Phys.* **13** (2001) 675 [hep-th/0009072].

[101] M.-X. Huang, A. Klemm and M. Poretschkin, *Refined stable pair invariants for E-, M- and $[p,q]$-strings*, *JHEP* **11** (2013) 112 [1308.0619].

[102] A. Brini and A. Tanzini, *Exact results for topological strings on resolved Y**p,q singularities*, *Commun. Math. Phys.* **289** (2009) 205 [0804.2598].

[103] E. Witten, *Quantum field theory and the jones polynomial*, *Comm. Math. Phys.* **121** (1989) 351.

[104] B. Eynard and C. Kristjansen, *Exact solution of the O(n) model on a random lattice*, *Nucl. Phys.* **B455** (1995) 577 [hep-th/9506193].

[105] B. Eynard and C. Kristjansen, *More on the exact solution of the O(n) model on a random lattice and an investigation of the case $|n| > 2$*, *Nucl. Phys.* **B466** (1996) 463 [hep-th/9512052].

[106] F. Benini, *The Coulomb branch of the Leigh-Strassler deformation and matrix models*, *JHEP* **12** (2004) 068 [hep-th/0411057].

[107] T. J. Hollowood, *Five-dimensional gauge theories and quantum mechanical matrix models*, *JHEP* **03** (2003) 039 [hep-th/0302165].

[108] J. Hoppe, V. Kazakov and I. K. Kostov, *Dimensionally reduced SYM(4) as solvable matrix quantum mechanics*, *Nucl. Phys.* **B571** (2000) 479 [hep-th/9907058].

[109] J. Ambjørn, L. Chekhov, C. F. Kristjansen and Yu. Makeenko, *Matrix model calculations beyond the spherical limit*, *Nucl. Phys.* **B404** (1993) 127 [hep-th/9302014].

[110] G. Borot, B. Eynard and N. Orantin, *Abstract loop equations, topological recursion and new applications*, *Commun. Num. Theor. Phys.* **09** (2015) 51 [1303.5808].

[111] A. Sciarappa, *Exact relativistic Toda chain eigenfunctions from Separation of Variables and gauge theory*, *JHEP* **10** (2017) 116 [1706.05142].

[112] R. M. Kashaev and S. M. Sergeev, *Spectral equations for the modular oscillator*, 1703.06016.

[113] A. Voros, *The zeta function of the quartic oscillator*, *Nuclear Physics B* **165** (1980) 209 .

[114] A. Voros, *The return of the quartic oscillator. the complex wkb method*, *Annales de l'I.H.P. Physique théorique* **39** (1983) 211.

[115] L. A. Takhtajan, *Quantum Mechanics for mathematicians*. American Mathematical Society, 2008.

[116] P. Putrov and M. Yamazaki, *Exact ABJM Partition Function from TBA*, *Mod. Phys. Lett.* **A27** (2012) 1250200 [1207.5066].

[117] S. Garoufalidis and R. Kashaev, *Evaluation of state integrals at rational points*, *Commun. Num. Theor. Phys.* **09** (2015) 549 [1411.6062].

[118] M. Moshinsky and C. Quesne, *Linear canonical transformations and their unitary representations*, *Journal of Mathematical Physics* **12** (1971) 1772 [https://doi.org/10.1063/1.1665805].

[119] J. M. Maldacena, G. W. Moore, N. Seiberg and D. Shih, *Exact vs. semiclassical target space of the minimal string*, *JHEP* **10** (2004) 020 [hep-th/0408039].

[120] C. Kozcaz, S. Pasquetti and N. Wyllard, *A & B model approaches to surface operators and Toda theories*, *JHEP* **08** (2010) 042 [1004.2025].

[121] B. Eynard and M. Marino, *A Holomorphic and background independent partition function for matrix models and topological strings*, *J. Geom. Phys.* **61** (2011) 1181 [0810.4273].

[122] G. Borot and B. Eynard, *Geometry of Spectral Curves and All Order Dispersive Integrable System*, *ArXiv e-prints* (2011) [1110.4936].

[123] S. Gukov and P. Sulkowski, *A-polynomial, B-model, and Quantization*, *JHEP* **02** (2012) 070 [1108.0002].

[124] H. Awata, H. Fuji, H. Kanno, M. Manabe and Y. Yamada, *Localization with a Surface Operator, Irregular Conformal Blocks and Open Topological String*, *Adv. Theor. Math. Phys.* **16** (2012) 725 [1008.0574].

[125] G. Akemann, *Higher genus correlators for the Hermitian matrix model with multiple cuts*, *Nucl. Phys.* **B482** (1996) 403 [hep-th/9606004].

[126] D. Karp and S. M. Sitnik, *Asymptotic approximations for the first incomplete elliptic integral near logarithmic singularity*, *Journal of Computational and Applied Mathematics* **205** (2007) 186 [math/0604026].

[127] M. Aganagic and S. Shakirov, *Knot Homology and Refined Chern-Simons Index*, *Commun. Math. Phys.* **333** (2015) 187 [1105.5117].

[128] N. I. Akhiezer, *Elements of the Theory of Elliptic Functions*, vol. 79 of *Translations of Mathematical Monographs*. American Mathematical Society, Providence, RI, 1990.

[129] B. A. Dubrovin, *Theta functions and non-linear equations*, *Uspekhi Mat. Nauk* **36** (1981) 11.

[130] O. Babelon, D. Bernard and M. Talon, *Introduction to Classical Integrable Systems*, Cambridge Monographs on Mathematical Physics. Cambridge University Press, 2003, 10.1017/CBO9780511535024.

[131] A. B. Goncharov and R. Kenyon, *Dimers and cluster integrable systems*, *ArXiv e-prints* (2011) [1107.5588].

[132] E. K. Sklyanin, *The Quantum Toda Chain*, *Lect. Notes Phys.* **226** (1985) 196.

[133] V. Pasquier and M. Gaudin, *The periodic Toda chain and a matrix generalization of the Bessel function recursion relations*, *Journal of Physics A: Mathematical and General* **25** (1992) 5243.

[134] M. C. Gutzwiller, *The Quantum Mechanical Toda Lattice*, *Annals Phys.* **124** (1980) 347.

[135] M. C. Gutzwiller, *The Quantum Mechanical Toda Lattice. II*, *Annals Phys.* **133** (1981) 304.

[136] S. Kharchev and D. Lebedev, *Integral representation for the eigenfunctions of quantum periodic Toda chain*, *Lett. Math. Phys.* **50** (1999) 53 [hep-th/9910265].

[137] Y. Hatsuda, *Comments on Exact Quantization Conditions and Non-Perturbative Topological Strings*, 1507.04799.

[138] Y. Hatsuda, H. Katsura and Y. Tachikawa, *Hofstadter's butterfly in quantum geometry*, *New J. Phys.* **18** (2016) 103023 [1606.01894].

[139] Y. Hatsuda, Y. Sugimoto and Z. Xu, *Calabi-Yau geometry and electrons on 2d lattices*, *Phys. Rev.* **D95** (2017) 086004 [1701.01561].

[140] M. Hillery, R. O'Connell, M. Scully and E. Wigner, *Distribution functions in physics: Fundamentals*, *Physics Reports* **106** (1984) 121 .

[141] T. Curtright, D. Fairlie and C. Zachos, *A Concise Treatise on Quantum Mechanics in Phase Space*. World Scientific, 2014.

[142] J. J. Halliwell, *Correlations in the Wave Function of the Universe*, *Phys. Rev.* **D36** (1987) 3626.

[143] A. Anderson, *On Predicting Correlations From Wigner Functions*, *Phys. Rev.* **D42** (1990) 585.

[144] S. Habib, *The classical limit in quantum cosmology. 1 Quantum mechanics and the Wigner function*, *Phys. Rev.* **D42** (1990) 2566.

[145] J. B. Hartle and S. W. Hawking, *Wave Function of the Universe*, *Phys. Rev.* **D28** (1983) 2960.

[146] C. Gómez, S. Montáñez and P. Resco, *Semi-classical mechanics in phase space: The Quantum target of minimal strings*, *JHEP* **11** (2005) 049 [hep-th/0506159].

[147] J. Ambjorn and R. A. Janik, *The emergence of noncommutative target space in noncritical string theory*, *JHEP* **08** (2005) 057 [hep-th/0506197].

[148] G. W. Moore, *Geometry of the string equations*, *Commun. Math. Phys.* **133** (1990) 261.

[149] D. Berenstein, *A Toy model for the AdS / CFT correspondence*, *JHEP* **07** (2004) 018 [hep-th/0403110].

[150] H. Lin, O. Lunin and J. M. Maldacena, *Bubbling AdS space and 1/2 BPS geometries*, *JHEP* **10** (2004) 025 [hep-th/0409174].

[151] V. Balasubramanian, J. de Boer, V. Jejjala and J. Simón, *The Library of Babel: On the origin of gravitational thermodynamics*, *JHEP* **12** (2005) 006 [hep-th/0508023].

[152] K. Skenderis and M. Taylor, *Anatomy of bubbling solutions*, *JHEP* **09** (2007) 019 [0706.0216].

[153] V. Balasubramanian, B. Czech, K. Larjo and J. Simón, *Integrability versus information loss: A Simple example*, *JHEP* **11** (2006) 001 [hep-th/0602263].

[154] V. Balasubramanian, B. Czech, K. Larjo, D. Marolf and J. Simón, *Quantum geometry and gravitational entropy*, *JHEP* **12** (2007) 067 [0705.4431].

[155] M. V. Berry, *Semi-Classical Mechanics in Phase Space: A Study of Wigner's Function*, *Phil. Trans. Roy. Soc. Lond.* **A287** (1977) 237.

[156] J. W. Negele and H. Orland, *Quantum many-particle systems*. Westview, 1988.

[157] W. Krauth, *Statistical mechanics: algorithms and computations*. Oxford University Press, Oxford, 2006.

[158] D. S. Dean, P. Le Doussal, S. N. Majumdar and G. Schehr, *Noninteracting fermions at finite temperature in a d-dimensional trap: Universal correlations*, *Phys. Rev.* **A94** (2016) 063622 [1609.04366].

[159] A. Voros, *Asymptotic ħ-expansions of stationary quantum states*, *Ann. Inst. H. Poincaré A* **26** (1977) 343.

[160] N. Ripamonti, *Classical limit of the harmonic oscillator Wigner functions in the Bargmann representation*, *Journal of Physics A: Mathematical and General* **29** (1996) 5137.

[161] D. S. Dean, P. Le Doussal, S. N. Majumdar and G. Schehr, *Wigner function of noninteracting trapped fermions*, 1801.02680.

[162] K.-S. Giannopoulou and G. N. Makrakis, *An approximate series solution of the semiclassical Wigner equation*, 1705.06754.

[163] C. Chester, B. Friedman and F. Ursell, *An extension of the method of steepest descents*, in *Mathematical Proceedings of the Cambridge Philosophical Society*, vol. 53, pp. 599–611, Cambridge University Press, 1957.

[164] M. Bartlett and J. Moyal, *The exact transition probabilities of quantum-mechanical oscillators calculated by the phase-space method*, *Mathematical Proceedings of the Cambridge Philosophical Society* **45** (1949) 545.

[165] A. Grassi, *Spectral determinants and quantum theta functions*, *J. Phys.* **A49** (2016) 505401 [1604.06786].

[166] J. Gu, M.-x. Huang, A.-K. Kashani-Poor and A. Klemm, *Refined BPS invariants of 6d SCFTs from anomalies and modularity*, *JHEP* **05** (2017) 130 [1701.00764].

[167] J. Gu, B. Haghighat, K. Sun and X. Wang, *Blowup Equations for 6d SCFTs. I*, 1811.02577.

[168] G. Bonelli, A. Grassi and A. Tanzini, *Seiberg–Witten theory as a Fermi gas*, *Lett. Math. Phys.* **107** (2017) 1 [1603.01174].

[169] G. Bonelli, A. Grassi and A. Tanzini, *Quantum curves and q-deformed Painlevé equations*, 1710.11603.

[170] A. Grassi and J. Gu, *Argyres-douglas theories, painlevé ii and quantum mechanics*, 1803.02320.

[171] A. Grassi and M. Marino, *A Solvable Deformation Of Quantum Mechanics*, 1806.01407.

[172] Y. Hatsuda, *Perturbative/nonperturbative aspects of Bloch electrons in a honeycomb lattice*, *PTEP* **2018** (2018) 093A01 [1712.04012].

[173] Z. Duan, J. Gu, Y. Hatsuda and T. Sulejmanpasic, *Instantons in the Hofstadter butterfly: difference equation, resurgence and quantum mirror curves*, 1806.11092.

[174] R. Couso-Santamaría, M. Marino and R. Schiappa, *Resurgence Matches Quantization*, *J. Phys.* **A50** (2017) 145402 [1610.06782].

[175] S. Codesido and M. Marino, *Holomorphic Anomaly and Quantum Mechanics*, *J. Phys.* **A51** (2018) 055402 [1612.07687].

[176] S. Codesido, M. Marino and R. Schiappa, *Non-Perturbative Quantum Mechanics from Non-Perturbative Strings*, 1712.02603.